Regulation and role of the pro-apoptotic transcription factor C/EBP homologous protein (CHOP) in type II cells apoptosis and Idiopathic Pulmonary Fibrosis (IPF)

Inaugural Dissertation
submitted to the
Faculty of Medicine
in partial fulfilment of the requirements
for the PhD-degree of the Faculties of Veterinary Medicine and Medicine
of the Justus Liebig University Giessen

by
Oleksiy Klymenko
from
Odessa, Ukraine

Giessen, 2016

From the Department of Internal Medicine II
Director: Prof. Dr. Werner Seeger
of the Faculty of Medicine of the Justus Liebig University Giessen

First Supervisor and Committee Member: Prof. Dr. Andreas Günther
Second Supervisor and Committee Member: Prof. Dr. Reinhard Dammann
Committee Member:

Date of Doctoral Defense:

Contents

List of figures:

List of tables:

List of abbreviations:

AARE	Amino acid response element
AD	Alzheimer's disease
AECII	Alveolar epithelial type II cell
AIP	Acute interstitial pneumonia
AP-1	Activator protein 1
Apaf-1	Apoptotic protease activating factor 1
ATF4	Activating transcription factor 4
ATF5	Activating transcription factor 5
ATF6	Activating transcription factor 6
Bad	Bcl-2 agonist of cell death
Bak	Bcl-2 homologous antagonist killer
Bax	Apoptosis regulator Bax
Bcl-2	Apoptosis regulator BCL-2
BH	Bcl-2 homology (BH) domain
Bid	Bcl3-interacting domain death agonist
Bim	Bcl-2 interacting mediator of cell death
BiP	Immunoglobulin heavy-chain-binding protein
BOOP	Bronchiolitis obliterans organizing pneumonia
bp	Base pairs
BSA	Bovine serum albumin
CaMKII	Calcium/calmodulin-dependent protein kinase type II
cDNA	Complementary DNA
c-Ets-1	Erythroblastosis virus E26 oncogene homolog 1 (ets-1), or protein c-Ets-1
CFA	Cryptogenic fibrosing alveolitis
ChIP	Chromatin immunoprecipitation
CHOP	CCAAT/enhancer binding protein (EBP) homologous protein
COP	Cryptogenic organizing pneumonia
CPE	Cytopathic effect
CVD	Collagen-vascular diseases

DAPI	4',6-diamidino-2-fenylindole
DIP	Desquamative interstitial pneumonia
DMEM	Dulbecco's Modified Eagle Medium
DMSO	Dimethylsulfoxide
dNTP	Deoxynucleotide triphosphate
DOC	Downstream of CHOP
DPLD	Diffuse parenchymal lung disease
DR5	Death receptor 5
dsDNA	Double-strand DNA
ECM	Extracellular matrix
elF2α	Eukaryotic translation initiation factor 2 subunit alpha
ER	Endoplasmic reticulum
ERAD	ER-associated protein degradation
ERO1α	ER oxidoreductin 1-alpha
ERSE	ER stress response elements
FADD	FAS-associated death domain protein
FCS	Fetal calf serum
FIP	Familial interstitial pneumonia
FIPF	Familial idiopathic pulmonary fibrosis
FPF	Familial pulmonary fibrosis
FVBN	An inbred mouse strain
GADD34	Grouse arrest and DNA damage 34
GRP78	Glucose regulated protein 78
H&E	Hematoxylin and eosin
HPS	Hermansky-Pudlak syndrome
IIP	Idiopathic interstitial pneumonia
IPF	Idiopathic pulmonary fibrosis
IRE1α	Inositol-requiring enzyme 1 alpha
JNK	c-Jun N-terminal kinase
kDa	Kilo dalton
LDH	Lactate dehydrogenase
LIP	Lymphocytic interstitial pneumonia

LPS	Lipopolysaccharide
MAPK	Mitogen activated protein kinase 1
MEF	Mouse embryonic fibroblast
min	Minutes
MOI	Multiplicity of infection
NO	Nitric oxide
Noxa	Phorbol-12-myristate-13-acetate-induced protein 1
NSIP	Non-specific interstitial pneumonia
nt	Nucleotides
PAI-1	Plasminogen activator inhibitor 1
PDI	Protein disulfide isomerase
PERK	Protein kinase RNA like ER kinase
PFU	Plaque-forming unit
PGE_2	Prostaglandin E_2
PI3K	Phosphatidylinositol 4,5-bisphosphate 3-kinase
PP1	Protein phosphatase 1
RLU	Relative light unit
Puma	p53 up-regulated modulator of apoptosis
RBILD	Respiratory bronchiolitis interstitial lung disease
ROS	Reactive oxygen species
rtTA	Reverse tetracycline-controlled activator protein
SDS	Sodium dodecyl sulfate
SDS-PAGE	SDS polyacrylamide gel electrophoresis
SFTPA	Surfactant protein (SP)-A, gene
SFTPC	Surfactant protein (SP)-C, gene
SP-A	Surfactant protein A
SP-C	Surfactant protein C
$TCID_{50}$	Tissue Culture Infective Dose 50%
TEMED	N,N,N',N'-Tetramethyl-1-,2-diaminomethane
TERC	Telomerase RNA component
TERT	Telomerase reverse transcriptase
TGF-β	Transforming growth factor beta

TRB3	Tribbles homolog 3
Tu	Tunicamycin
un	untreated
UPR	Unfolded protein response
XBP-1	X-box-binding protein 1
α-SMA	alpha smooth muscle actin

Summary

Idiopathic pulmonary fibrosis (IPF) is a progressive fibrotic pulmonary disease of unknown origin with an unavoidable fatal outcome. In principle, IPF is characterized by alveolar epithelial cell damage, increased deposition of extracellular matrix (ECM) in the lung interstitium, and enhanced fibroblast/myofibroblast proliferation and activation. These processes ultimately lead to distortion of normal lung architecture and loss of respiratory function. Recent data show that Endoplasmic reticulum (ER) stress and apoptosis of alveolar epithelial cells type II (AECII) play a key role in both, sporadic and familial forms of IPF. It has been shown that an overload and accumulation of unfolded and misfolded proteins lead to ER stress. C/EBP homologous protein (CHOP) is thought to represent a key regulator of pro-apoptotic responses under ER stress. In IPF, induction and nuclear translocation of CHOP in AECII is regularly found, to a weaker extent also in yet not fibrotic areas of these lungs. Following this line, we hypothesized that ER stress-induced CHOP may significantly contribute to AECII injury and apoptosis and hence fibrosis development in IPF. The present study therefore aimed to (i) characterize the transcriptional regulation of epithelial CHOP expression *in vitro*, and (ii) to elucidate the biological role of Chop in the induction of epithelial apoptosis and lung fibrosis *in vitro* and *in vivo.*

For such purpose, the promotor of the human *CHOP* gene was extensively analyzed employing a luciferase reporter gene assay. We identified a new mechanism for the regulation of *CHOP* expression during ER stress. According to our data, Ap-1 and c-Ets-1 transcription factors are up-regulated in the lung epithelium under ER-stress conditions, interact with each other and jointly bind to the *Chop* promotor, thereby inducing the *Chop* gene expression.

Moreover, the role of Chop in the induction of epithelial apoptosis was studied using various *in vitro* and *in vivo* models. Exclusive Chop overexpression was achieved *in vitro* using an inducible ″Tetracyclin-On″ (″Tet-on″)-system in stably transfected epithelial MLE 12 cells and in isolated, primary alveolar type II cells. Both *in vitro* models revealed induction of cleaved caspase 3 and thus apoptosis in response to Chop overexpression. In addition, incubation of murine lung fibroblasts with supernatants of these stably transfected cells resulted in increased fibroblast proliferation once Chop was induced by doxycyclin application. Moreover, *in vivo* data support the results of *in vitro* studies.

Conditional Chop overexpression in AECII *in vivo* was achieved by crossing SP-C rtTA to tetO7 Chop mice. In response to oral doxycyclin feeding, Chop was induced in AECII and led to Caspase 3 cleavage and thus apoptosis of these cells. Furthermore, induction and up-regulation of Chop target genes such as *Casp11, Il1b, Il6, Ero1a, Dr5, and Gadd34* was detected on mRNA level by qPCR. In short term periods covering 8 weeks, young transgenic mice with inducible, AECII-specific Chop overexpression did yet not show a distinct fibrotic phenotype, although we could detect significant up-regulation of pro-fibrotic markers. Thus, involvement of Chop in the development of lung fibrosis requires further investigation.

Our findings demonstrate for the first time that AP-1 and c-Ets-1 play an important role in the transcriptional regulation of *CHOP* expression during ER stress. Additionally, we provide evidence that Chop expression alone is sufficient to induce apoptosis in AECII and consecutive fibroproliferation, hence suggesting a pivotal role of CHOP in the pathogenesis of pulmonary fibrosis.

Zusammenfassung

Die idiopathische pulmonale Fibrose (IPF) ist eine schwerwiegende, progressive Lungenerkrankung unbekannter Genese, die auch heute noch eine unbefriedigende Überlebenszeit aufweist. Die IPF ist durch eine chronische Schädigung und exzessive Apoptose von alveolären Typ II Zellen (AECII), durch exzessive Ablagerung von extrazellulärer Matrix im Lungeninterstitium, und durch eine gesteigerte Aktivierung und Proliferation von Fibroblasten und Myofibroblasten charakterisiert. Diese Prozesse führen durch den progressiven Ersatz der normalen Lungenstruktur durch fibrotisches Bindegewebe zu einer Zerstörung der zarten Alveolar-Struktur, und hierdurch zu der klinisch im Vordergrund stehenden Verschlechterung des Gasaustausches und der Lungendehnbarkeit (Compliance).

Neueren Untersuchungen zufolge stellt ein Endoplasmatischer Retikulum (ER)-Stress mit konsekutiver Apoptose eine Hauptursache für die Schädigung und die Apoptose der AECII bei familiären und sporadischen Formen der IPF dar. In der Vergangenheit konnte bereits gezeigt werden, dass Proteinüberladung und Anhäufung von ungefalteten und missgefalteten Proteinen im ER zu schwerem ER-Stress führt. C/EBP homologous protein (CHOP) könnte hierbei eine wichtige Rolle bei der Aktivierung von ER-Stress-induzierten Apoptose-Signalwegen spielen, und somit zu ER-Stress vermittelten Erkrankungen führen.

In IPF-Lungen ist die vermehrte Expression und nukleäre Translokation von CHOP in AECII eindeutig nachweisbar, in vermindertem Umfang auch in noch nicht fibrotisch umgebauten Arealen dieser Lungen. Wir verfolgten daher die Hypothese, dass die ER-Stress-induzierte AECII-Apoptose in IPF Lungen hauptsächlich durch CHOP vermittelt wird. Die Ziele in dieser Doktorarbeit waren daher i) die vollständige Aufklärung der transkriptionalen Regulation der epithelialen *CHOP* Expression *in vitro*, und ii) die Aufdeckung der biologischen Rolle der CHOP-Überexpression bei der Induktion von alveolär-epithelialer Apoptose und Lungenfibrose *in vitro* und *in vivo*.

In dieser Arbeit wurde der Promotor des humanen *CHOP*-Gens extensiv durch Luziferase-Reportergen-Assays analysiert, und dabei konnte ein neuer, bisher noch nicht beschriebener Mechanismus für die Regulation der *CHOP*-Expression unter ER-Stress Bedingungen identifiziert werden. So konnte gezeigt werden, dass die

Transkriptionsfaktoren Ap-1 und c-Ets-1 im Lungenepithel unter ER-Stress-Konditionen hochreguliert werden, dabei in Interaktion miteinander an den murinen *CHOP*-Promotor binden, und auf diese Weise die *Chop*-Expression induzieren.

Die Beteiligung von *Chop* in der Induktion der alveolär-epithelialen Apoptose wurde anhand vielfältiger *in vitro*- und *in vivo*-Modelle untersucht. So wurde die Überexpression von *Chop in vitro* sowohl mit einem induzierbarem ″Tetracyclin-On″ (″Tet-On″)-Expressionssystem in stabil transfizierten alveolär-epithelialen MLE12-Zellen als auch in isolierten, primären transformierten AECII direkt untersucht. Beide *in vitro*-Systeme zeigten Kaspase-3-Aktivierung und -Spaltung nach Überexpression von Chop. Zudem wurde eine Chop-abhängige, gesteigerte Proliferation von murinen Lungenfibroblasten beobachtet, nachdem diese mit Kulturüberstanden der epithelialen *in vitro* Modelle inkubiert wurden. Weiterhin wurden diese *in vitro*-Resultate durch die Ergebnisse von *in vivo*-Experimenten unterstützt. So resultierte die konditionale Chop-Überexpression in AECII in einem transgenen Maus-Modell (SP-C rtTA / tetO7 Chop) *in vivo* ebenfalls in einer Induktion von Kaspase-3-Spaltung und somit der Apoptose dieser Zellen. Zusätzlich wurde eine Induktion und Hochregulation der Chop-Targetgene *Casp11*, *Il1b*, *Il6*, *Ero1a*, *Dr5* und *Gadd34* auf Transkriptebene durch qPCR beobachtet. Im Kurzzeitexperiment von 8 Wochen zeigten diese transgenen jungen Mäuse mit konditionaler, AECII-spezifischer Überexpression von Chop (noch) keine Entwicklung von Lungenfibrose, obwohl profibrotische Gene in den Maus-Lungen signifikant hochreguliert waren. Daher sind zusätzliche Untersuchungen nötig, um die Involvierung von Chop bei der Entwicklung von Lungenfibrose zu klären.

Zusammenfassend konnte in dieser Doktorarbeit zum ersten Mal gezeigt werden, dass AP-1 und c-Ets-1 eine bedeutende Rolle in der transkriptionalen Regulation der *CHOP*-Expression während ER-Stress spielen. Zusätzlich konnte bewiesen werden, dass die alleinige Expression von Chop ausreicht um AECII in die Apoptose zu treiben und nachgeschaltet eine Fibroseantwort *in vitro* zu provozieren. Diese Ergebnisse zeigen daher eindeutig, dass CHOP eine bedeutende Rolle in der Pathogenese der Lungenfibrose spielt.

1 Introduction

1.1. Idiopathic pulmonary fibrosis

1.1.1. Characteristics of idiopathic pulmonary fibrosis

Idiopathic pulmonary fibrosis (IPF) is a chronic fibrotic progressive pulmonary disease of unknown origin, with an unavoidable fatal outcome [1]. In principle, IPF is characterized by alveolar epithelial cell damage, increased deposition of extracellular matrix (ECM) in the lung interstitium, and enhanced fibroblast/myofibroblast proliferation and activation. These processes ultimately lead to distortion of normal lung architecture and loss of respiratory function [2].

IPF is the most common subtype of idiopathic interstitial pneumonia (IIP), which composes a group of diffuse parenchymal lung diseases (DPLDs). Other types of IIP are nonspecific interstitial pneumonia (NSIP), cryptogenic organizing pneumonia (COP), acute interstitial pneumonia (AIP), respiratory bronchiolitis interstitial lung disease (RBILD), desquamative interstitial pneumonia (DIP), lymphocytic interstitial pneumonia (LIP), idiopathic lymphoid interstitial pneumonia, idiopathic pleuroparenchymal fibroelastosis [3].

IPF typically is a disease of the elderly and develops in the fifth decade of life or later. The majority of patients with IIP are over 60 years old, while children are extremely rarely affected [4]. Currently no ethnic or social factors have been associated with the disease, but it is well established that the disease has a higher incidence in men than in women [4]. The reasons for developing IPF are still not fully understood. Nevertheless, risk factors have been identified and these include smoking and other harmful environmental factors [5]. The total number of IPF patients worldwide amounts to over 5 million people, and the number of cases is steadily increasing. Prior to the authorization of the novel antifibrotic drugs, the average lifespan of patients with IPF ranged between 2.5 and 3.5 years after diagnosis. [6].

Typically patients with IPF report of dyspnea, first at exercise, later at rest, a very general symptom, which leads often to a missdiagnosis of cardiac or other lung diseases [4]. Besides dyspnea, a common symptom is the dry, non-productive cough, as well as clubbing of the fingers. [7]. In late stages of the disease patients may show signs of right

ventricular failure, as they may develop pulmonary hypertension. The initial development of symptoms is usually slow, but can aggravate during the later phases. [4].

While most cases of IPF occur sporadically, recent studies suggest that there are familial cases in which the disease is caused by heritable genetic mutations. Thus this form of the disease was called familial pulmonary fibrosis (FPF), familial interstitial pneumonia (FIP) or familial idiopathic pulmonary fibrosis (FIPF). This diagnosis can be set only if two or more members of the family were diagnosed with idiopathic interstitial pneumonia. Clinical features of familial pulmonary fibrosis are indistinguishable from usual IPF, except that the disease seems to get evident at a slightly younger age. [8] [9].

1.1.2. Histopathological changes in IPF

Histologically, IPF is described as usual interstitial pneumonia (UIP) which is characterized by areas of immature and mature fibrosis and alveolar inflammation with intervening areas of normal tissue architecture (Figure 1.1.A.). However UIP is not a unique characteristic of IPF, rather it can be encoutered in other lung diseases as lung fibrosis due to collagen-vascular diseases (CVDs), chronic hypersensitivity pneumonitis (HP), pneumoconiosis, sarcoidosis, and drug-induced lung diseases [10].

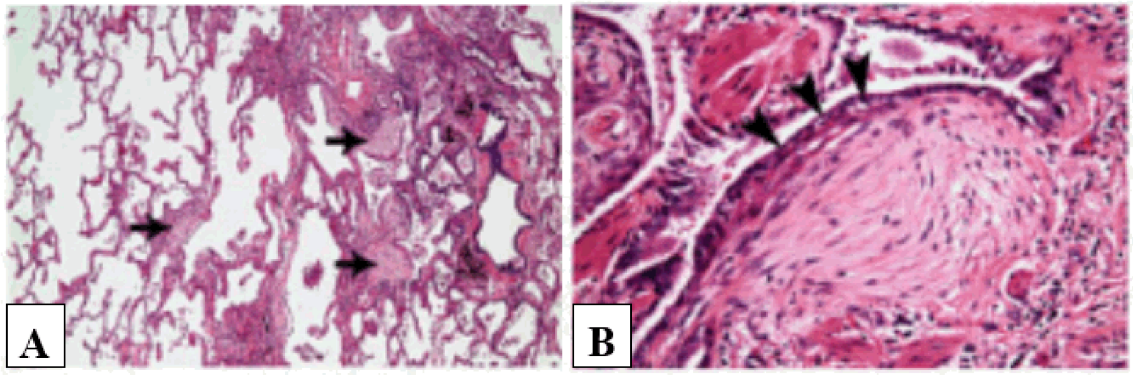

Figure 1.1. Histopathological changes in the lung in IPF.
(**A**) Low-power photomicrograph [40x, H&E stain] demonstrates temporal heterogeneity with abrupt transition between normal appearing lung (left side) and densely scarred lung parenchyma (right side). Transitional areas show multiple fibroblastic foci (arrows). (**B**) High-power photomicrograph [200x, H&E stain] shows fibroblastic focus comprised of plump spindle cells in a collagen-poor matrix bulging into an airway lined by hyperplastic epithelial cells (arrowheads) (adapted from [10]).

One of the main features of UIP is the spatial heterogeneity and the fibrotic dissemination towards the healthy areas of the lung. Particularly, changes are seen in the lower lobes of the lungs, as well as in peripheral and subpleural, peripheral and paraseptal parts of the

lungs [10]. Proliferative fibroblasts / myofibroblasts produce a variable number of clusters, these clusters are called fibrotic foci (Figure 1.1.B.). It is considered that these centers are the main sites of active disease. It was noted, that higher numbers of fibroblast foci were associated with poor prognosis [10]. Of note, in IPF lungs several studies found alveolar epithelial cell (AEC) injury with hyperplasia of type II pneumocytes (Figure 1.1.B.) as well as impaired proliferation, apoptosis of AECII, and incapacity to differentiate into type I alveolar epithelial cell [11] [12] [1].

1.1.3. Pathogenesis of IPF

The causes of IPF are still not well understood. There are two main hypotheses for the pathogenesis of IPF: an older, "inflammatory" hypothesis and more recent one focusing on "repetitive alveolar type II cells injury and abnormal wound repair" [13] [5] [1].

The inflammatory hypothesis argues that inflammation triggers fibroproliferation followed by the end-stage fibrotic scar [14]. This hypothesis proposes that inflammation of the alveolar-capillary compartment leads to the loss of alveolar type I cells, proliferation of the alveolar type II cells and stromal cells, and the deposition of extracellular matrix (ECM) [14]. However, although there are without any doubt formes of lung fibrosis, which are mediated by chronic inflammation (such as sarcoidosis or hypersensitivity pneumonia), it is still not clear whether inflammation leads to the development of the fibrotic lesions in IPF. The major counter-argument is that IPF patients in fact are placed at a higher risk for dying when put on a combination of steroids and azathioprin [15] [16] [1] [17].

Current theories suggest that IPF may be caused by repeated, prolonged damage to the alveolar compartment, followed by aberrant repair. (Figure 1.2) [4] [5]. Injury to the alveolar epithelial cells leads to fibroblast proliferation and differentiation into myofibroblasts. There is evidence that the cross talk between the alveolar epithelium and its associated mesenchyme is dysregulated in IPF leading to excessive ECM deposition [18] [19] [5].

In accordance with such hypothesis, mutations in the *SFTPA, SFTPC*, *TERC, TERT* and other genes [9] have been observed in familial forms of UIP/IPF and these genes are very tightly linked to the alveolar type II cell. These mutations are discussed more closely in the following:

First reports of pulmonary fibrosis suggested a genetic predisposition in patients with defined (systemic) clinical syndromes such as Hermansky-Pudlak-Syndrome and Dyskeratosis Congenita [20] [21] [9]. Genetic analysis of patients with these syndromes revealed mutations in *HPS* genes for Hermansky-Pudlak Syndrome [20] and *DKC, TERT* and *TERC* gene mutations for patients with Dyskeratosis Congenita [22]. These patients can develop a form of lung fibrosis which is indistinguishable from UIP/IPF.

In 2001, Nogee et al., described the first of meanwhile around 35 mutations in *SFTPC* gene. Later, mutations in the *SFTPA* gene were identified [23] [24] [25]. These reports indicate that mutations in these surfactant proteins SFTPA and SFTPC, which are almost exclusively produced by alveolar type II cells, are the underlying reason in a reasonable fraction of familial cases of IPF (percentages ranging between 5% (USA) and 45% (EU)). These mutations lead to improper protein folding followed by their accumulation in the endoplasmic reticulum which leads to activation of unfolded protein response and subsequently AECII apoptosis [24] [26] [27]. Another study suggest that expression of SFTPC mutant induces lysosome stress and epithelial cells dysfunction through macroautophagy [28].

The later proof of mutations in the *TERT* and *TERC* genes, which are responsible for maintaining an adequate telomere length and hence preventing replicative senescence in human stem cells, in ~15% of the families with IPF provided a valuable hint that cellular aging processes may also result in the development of pulmonary fibrosis [9]. Moreover, Cronkhie et al provided evidence of peripheral blood and lung epithelial cell telomere shortening in both, sporadic as well as familial, IPF patients without mutations in *TERT*/*TERC* [29], suggesting that, regardless of the TERT/TERC genotype, telomere shortening and increased cellular ageing could represent an important event in IPF. [30] [31] [9]. As mentioned above lung fibrosis is detected in the genetic disorder dyskeratosis congenital (DKC) [22]. DKC is characterized by telomere shortening [22]. Different mutations in genes regulating telomere length were identified especially genes that influence telomere or telomere associated proteins, such as DKC1, TERT, TERC. Mutation in the *DKC1* gene leads to X-linked form of DKC, whereas mutations of TERT and TERC are autosomal dominant [32].

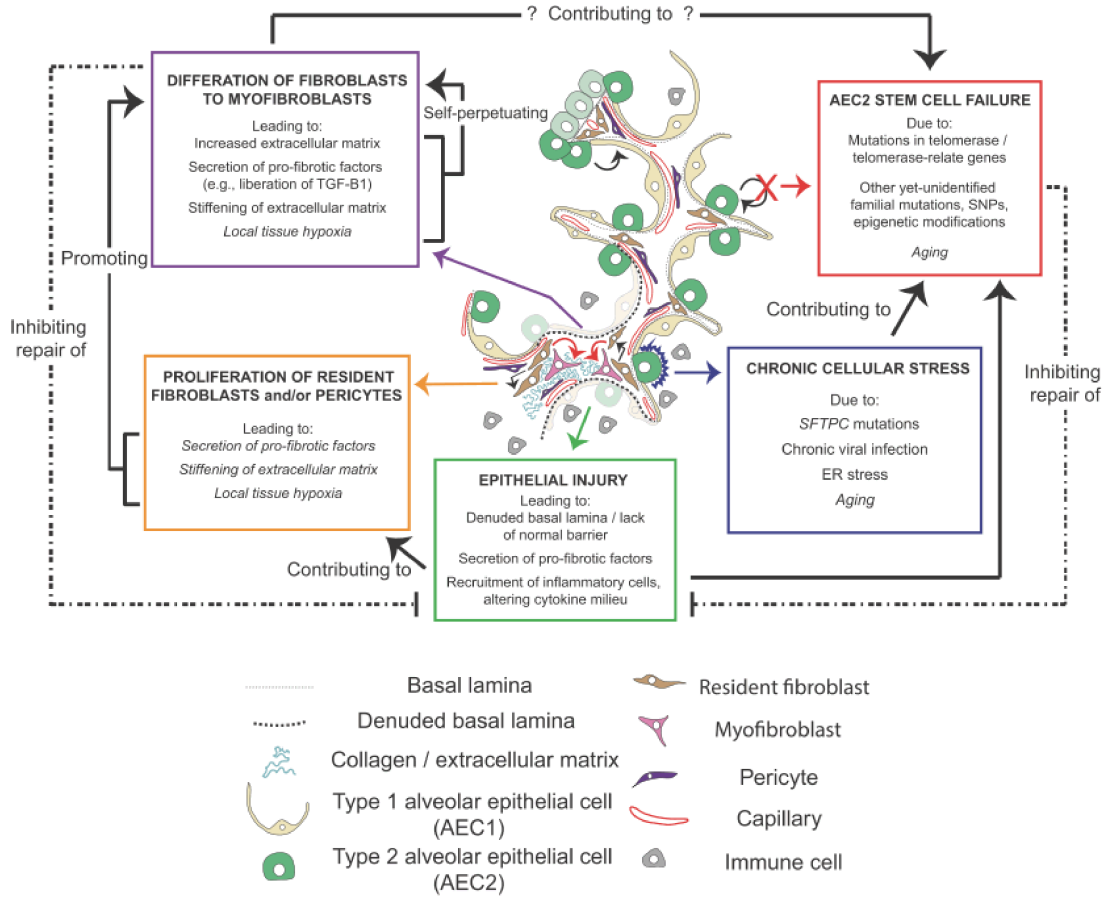

Figure 1.2. Pathways involved in the development of pulmonary fibrosis.
This figure illustrates known and hypothesized relationships between two components of the alveolar region of the lung, the epithelium and the mesenchyme. Dysregulated cross talk between these two components leads to development of the disease. An inciting factor or event that predisposes an individual to developing the disease (e.g., chronic cellular stress or epithelial injury), a host of other abnormal responses (e.g., abnormal proliferation of fibroblasts and excessive stiffening of the mesenchyme) are likely to be integral in the progression of fibrosis (adapted from [5]).

1.2. Unfolded protein response (UPR)

1.2.1. Overview

The endoplasmic reticulum (ER) is an essential organelle responsible for folding of secreted and membrane proteins and lipid and sterol biosynthesis, storage and production of glycogen and it is a major site of free calcium storage within the cell [33]. The initial stage in protein synthesis is the expansion of the polypeptide chain. Later, the polypeptide properly folds into a functional three-dimensional, structure; it is glycosylated and then passed through the secretory pathway. In normal conditions, protein folding in ER is assisted by chaperone proteins such as immunoglobulin – heavy chain binding protein

(BiP), known also as glucose regulated protein 78 (GRP78). Under stress conditions caused by factors such as calcium shortage, metabolic stress, decrease of energy reserves, increased protein synthesis or misfolding of mutant proteins an unfolded protein response (UPR) can develop, which represents a classic coping mechanism aiming to restore the cellular homeostasis [34]. The upstream signal that activates this pathway is referred to as ER stress and is defined as an imbalance between the load of resident and transit proteins in the ER and the organelle's ability to process that load. ER stress can be provoked by a variety of pathophysiological conditions such as ischemia, viral infection, increased protein synthesis (e.g. in maturating b-cells), ageing, or genetic mutations that impair resident/secretory protein folding [33].

The UPR primarily acts to improve protein folding. It contributes to the maintenance of cellular homeostasis and prevents cell death caused by the accumulation of misfolded proteins. These proteins can interfere with the basic functions of cells [35] [36]. In addition, the ERAD (ER stress associated degradation) machinery involving the proteasome is upscaled and activated [37]. If the UPR mechanisms fail, or if the ER stress is overwhelming, it results in growth arrest followed by apoptosis.

The initiation of the UPR is critically depending on the availability of GRP78. GRP78 not only binds to misfolded and unfolded proteins and helps them to fold correctly, it also regulates the transmembrane ER stress sensors protein kinase RNA like ER kinase (PERK), inositol-requiring protein 1α (IRE1α), and activating transcription factor 6 (ATF6). As long as these proteins are bound by BiP they are kept in an inactive state (Figure 1.3) [38] [39] [40] [41].

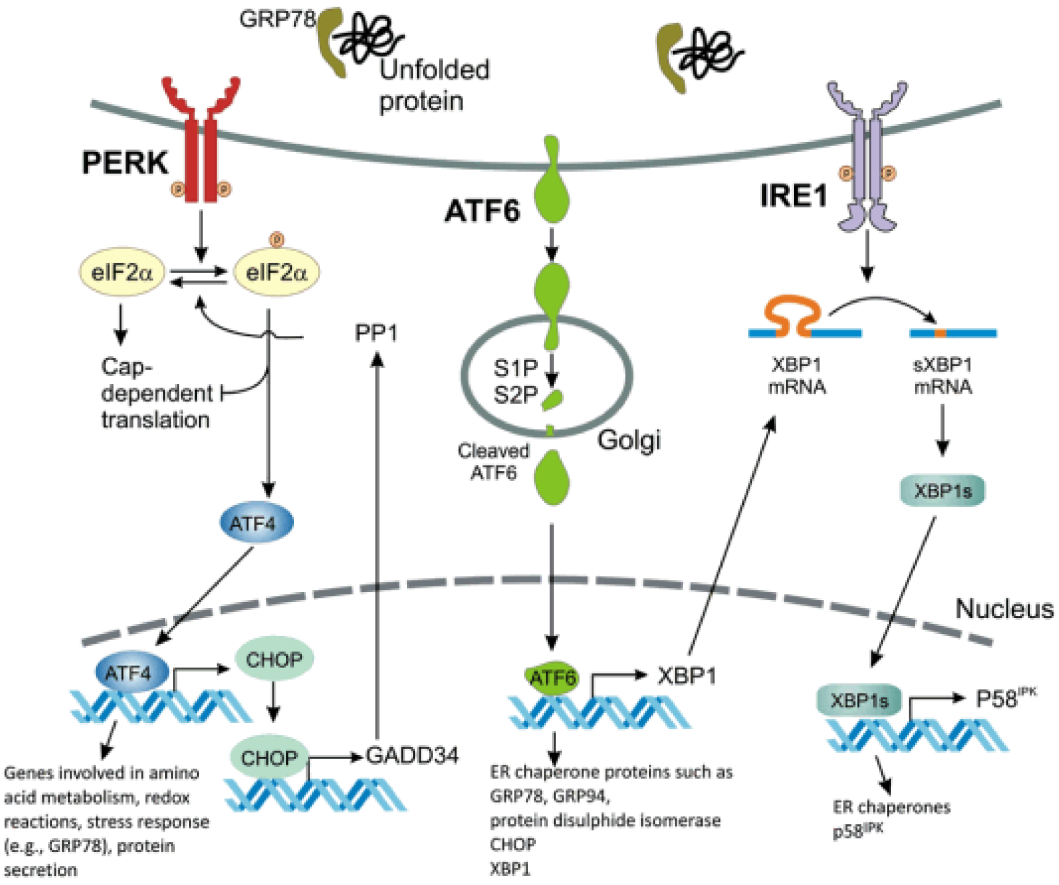

Figure. 1.3. The UPR is mediated by three ER stress sensors.
Binding of unfolded proteins to GRP78 within the ER lumen allows activation of PERK, ATF6 and IRE1. PERK dimerises and autophosphorylates. It phosphorylates eIF2α and thus general cap-dependent translation is inhibited. Cap-independent translation allows the translation of certain proteins such as ATF4 which activates CHOP transcription. One of the genes induced by CHOP is GADD34 which can dephosphorylate eIF2α. Activation of ATF6 allows its translocation to the Golgi where it undergoes cleavage by S1P and S2P proteases. Cleaved ATF6 activates XBP1 transcription. Active IRE1 is a dual kinase and endonuclease. One of its targets is XBP1 mRNA which undergoes splicing to produce an active transcription factor, XBP1s. (adapted from[42]).

BiP / GRP78 is a dominant chaperone, belonging to the family of heat shock proteins which facilitate protein folding in the ER. Properly folded proteins are liberated from BiP and transported into the Golgi apparatus. When missfolded proteins remain bound to BiP, they are retained in the ER, which may lead to their degradation. When missfolded proteins accumulate in the ER, BiP dissociates from the three key sensor molecules PERK, ATF6 and IRE1 in order to assist in protein folding. This dissociation in turn results in the activation of PERK, ATF6 and IRE1 and – through this – the activation of signaling pathways resembling the UPR [38] [40] [41]. These three pathways are described more closely in the following:

In response to BiP dissociation, PERK undergoes autophosphorylation and dimerization [43]. This active form of PERK phosphorylates and inactivates only one target – the α

subunit of eukaryotic translation initiation factor 2 (elF2α) [33]. In all eukaryotic cells, initiation of protein synthesis requires the eIF2α and phosphorylation of eIF2 α inhibits protein synthesis. eIF2α phosphorylation also controls expression of ATF4, ATF5 and C/EBP homologous protein (CHOP), genes that regulate amino acid metabolism and chaperone production and that activate glutathione [44]. ATF4's transcriptional targets include genes involved in amino acid metabolism, oxidoreductases required for disulfide bond formation in the ER and several ubiquitin ligases. In a prolonged ER stress state, ATF4- dependent induction of CHOP leads to expression of DNA damage-inducible gene 34 (GADD34), which in turn phosphorylates elF2α to, restore protein translation (Figure 1.3) [45].

Dissociation of GRP78 from transcription factor ATF6 leads to translocation of ATF6 to Golgi, where it is cleaved by site-1 and site-2 proteases to yield an active N-terminal 50 kDa domain (N-ATF6/p50ATF6) that translocates to the nucleus [40] [46]. The cleaved domain migrates to the nucleus where it binds to cis - acting ER stress response elements (ERSE) and activates the transcription of ER chaperone proteins, such as BIP, GRP94, calreticulin, calnexin and protein disulfide isomerase (PDI), ER-associated protein degradation (ERAD) components (Figure 1.3) [38]. In mammalian cells ATF6 exists in two isoforms: ATF6 α and ATF6 β. ATF6 α induces the synthesis of X-Box binding protein I (XBP-1) [38].

IRE-1 is a transmembrane protein, which has a kinase and an endonuclease activity, both being activated by ER stress. Mammals have two isoforms of IRE-1: IRE-1α and IRE-1β, which homodimerize after BiP dissociated from IRE-1. The dimerized IRE-1 RNase domain cleaves at nucleotide 26 of the intron sequence in the XBP-1 transcript. Spliced XBP-I translocates to the nucleus and binds to the ERSE and facilitates the transcription of ER associated degradation genes (ERAD) (Figure 1.3) [42].

The induction of the ERAD pathway is an important component of the ER stress response. The exact mechanisms of recognition and distortion of misfolded proteins are still not clear. However, the process was described to occur in several stages.

• recognition of misfolded proteins by PDI, BiP

• translocation of misfolded proteins from the ER to the cytoplasm via the translocon,

• ubiquitination of misfolded proteins by a sequence of enzymatic reactions, mediated by E1 (ubiquitin activating enzyme), E2 (ubiquitin conjugating enzyme) and E3 (ubiquitin ligation enzyme)

• deglycosylation

• transport to the proteasome for degradation [47]

These three sensors are activated by UPR pathways to alleviate ER stress and achieve cell protection. Unfortunately, prolonged ER stress can lead to apoptosis via the extrinsic and intrinsic pathways [42]. In the so-called "intrinsic" pathway, various noxious stimuli cause the release of cytochrome c from the mitochondria into the cytosol. Once in the cytosol, cytochrome c forms a complex, known as the apoptosome, with Apaf-1 and procaspase-9 in the presence of ATP/dATP. This results in the processing and activation of this initiator caspase [48]. In contrast, the "extrinsic" pathway utilizes death receptors such as Fas, TNFR1, DR3, DR4, or DR5 for the activation of caspases. Binding of a ligand to these cell surface receptors recruits adaptor proteins, such as FADD, to the cytoplasmic domain of the receptors, which in turn recruits the initiator procaspase-8 to form a death-inducing signaling complex that induces caspase-8 activation [49]. Once activated, the upstream initiator caspases cleave and activate downstream effector caspases such as caspase-3, -6, and -7, which in turn cleave death substrates and result in the morphological changes associated with apoptosis [50]. The extrinsic pathway can cross-talk with the intrinsic pathway through caspase-8 cleavage of the BH3-only protein Bid that activates the mitochondrial pathway to amplify the apoptotic signal [48]. Extrinsic and intrinsic pathways of apoptosis lead to influx of calcium from the ER to the cytosol and the activation of signaling cascades UPR. ER stress activates caspase-12, caspase-3 and caspase-9 mediating cell death pathways [42].

CHOP is another transcription factor involved in apoptosis induction. It is activated by all three UPR pathways through ATF4, cleaved ATF6 and spliced XBP-1 [51]. C-Jun N-terminal kinase (JNK) is also involved in UPR induced apoptosis, but the mechanism is still not fully understood [52]. An additional mechanism by which cells cope with ER stress is autophagy. Autophagy is a major catabolic process that delivers proteins, cytoplasmic components, and organelles to lysosomes for degradation and recycling. Autophagy can be activated by missfolded proteins in the ER [53]. Some studies have found a direct connection between ER stress and autophagy [54] [55]. A link between autophagy and the UPR has been further substantiated by the demonstration that the

PERK – eIF2a pathway is essential for autophagy induction after tunicamycin treatment [55]. Specifically, ATF4 and CHOP, were shown to transcriptionally regulate autophagy-related genes [55]. However, it remains unclear whether autophagy protects the cell from apoptosis or can induce cell death.

1.3. Role of CHOP in ER stress – mediated apoptosis

CHOP is believed to be the most significant mediator of ER stress-induced apoptosis [56]. Overexpression of CHOP was reported to result in cell cycle arrest and/or apoptosis. CHOP null cells were protected from ER stress-induced apoptosis, indicating the significance of this apoptotic pathway during ER stress [56]. However, the molecular mechanisms of this process are not fully understood.

As a transcriptional factor, CHOP has been shown to regulate numerous pro- and anti-apoptotic genes, including "down-stream of CHOP" (DOC) genes [57]. DOCs are a family composed of three members: DOC1, DOC4, and DOC6 [57]. DOC1 is a stress-inducible form of carbonic anhydrase VI which is predicted to increase the proton concentration and to decrease intracellular pH. DOC4 is a homolog of Tenm/Odz which might function in signaling at compartment boundaries. DOC6 is a homolog of the actin-binding proteins villin and gelsolin, and is implicated in changes in the actin cytoskeleton during apoptosis [57].

One of the most common mechanisms of CHOP-induced apoptosis is inhibition of Bcl-2 protein. This conclusion is based primarily on studies showing an inverse correlation between the expression of CHOP and Bcl-2 in fibroblasts. Inhibition of Bcl-2 as well as increased oxidative stress and apoptosis were observed in these cells [58]. It is important to note that the genetic reconstitution of Bcl-2 in CHOP-transfected cells rescued them from oxidative stress and apoptosis [58]. Additionally CHOP may interact with transcriptional repressors, thus reducing the transcription of the Bcl-2 protein [58]. In one study using thapsigargin for induction of ER stress in murine embryonic fibroblasts (MEFs) an interaction between CHOP and C/EBPβ, subsequent inhibition of Bcl-2 and increased apoptosis was encountered [59].

The Bcl-2 family of proteins, which consists of both anti- and pro-apoptotic members, controls a critical intracellular checkpoint in the intrinsic pathway of apoptosis by

regulating the release of apoptogenic factors from mitochondria [60]. Bcl-2 regulates cell survival by inhibiting BH3-specific proteins such as Bcl-2-associated death promoter (Bad), Bcl-2-like protein 11 (Bim), Phorbol-12-myristate-13-acetate-induced protein 1 (Noxa) and p53 upregulated modulator of apoptosis (Puma). These proteins are required for Bax- and Bak-mediated apoptosis and mitochondrial permeability [61]. It has been shown that especially the BH3-specific protein Bim exerts an important influence on the ER stress-induced apoptosis. Renal epithelial cells from Bim deficient mice were protected from apoptosis induced by tunicamycin. It has also been reported that ER stress increases the level of Bim through decreased proteasomal degradation and CHOP – CEBPα -mediated induction of downstream genes [62]. Bim is an important protein in ER stress-induced apoptosis in a broad range of cell types, including thymocytes, macrophages and epithelial cells from breast or kidney; however, it appears possible that different BH3-only proteins are required for this process in other tissues [62]. For example, it was found that ER-stress induced by palmitate increased Puma expression, Bax activation and apoptosis by CHOP – AP-1 complex induction [63]. Recently, it has been shown that CHOP-induced apoptosis is mediated by translocation of Bax from the cytosol to mitochondria [64]. Further investigation showed the increase of Bax in ER stress – CHOP-induced cardiomyocyte apoptosis [65].

Oxidative stress is another mechanism through which CHOP may induce apoptosis. Prolonged ER stress can lead to hyperoxidation of the ER lumen. This leads to leakage of H_2O_2 into the cytoplasm and, as a result, to the induction of cytotoxic reactive oxygen species (ROS) in the cytoplasm. Oxidation of the proteins in the ER lumen is induced by ER-oxidase 1 α (ERO1α) which is a CHOP transcriptional target [66]. Under normal conditions it promotes the formation of disulfide bonds with newly translated protein and, a partial inhibition of *ERO1α* protects cells from tunicamycin induced apoptosis. This observation lead to the suggestion that within prolonged ER stress, ERO1α may develop a hyperoxidizing environment, thereby promoting cell death [66]. In diabetes, the lack of CHOP reduces apoptosis in beta cells of the pancreas. This protection is directly related to the decrease in ERO1α, inhibition of markers of oxidative stress and antioxidant gene induction [67].

Recent studies have identified a specific molecular mechanism linking ERO1α with CHOP-induced apoptosis. Employing *in vitro* and *in vivo* studies it was shown that CHOP-induced apoptosis goes along with an activation of the pro-apoptotic cytoplasmic calcium signaling pathways [68] [69] [70]. In UPR, CHOP induced apoptosis can be

blocked by buffering of cytoplasmic calcium [68]. Cytoplasmic calcium triggers apoptosis by activating calcium-sensing kinase (CaMKII). CaMKII is a ubiquitous, multifunctional serine/threonine kinase [71]. It mediates Ca^{2+}-dependent phosphorylation of a wide range targets [71]. Activation of CaMKII leads to activations of a number of effector pathways of apoptosis [69] [70]. The role of ERO1α is supported by the fact that the CHOP induced ERO1α activates calcium channel IP13R in the ER and subsequently calcium release from the ER, which is extremely important for signaling processes induced by cytoplasmic calcium [72]. Moreover, the induction of oxidation in the ER lumen by CHOP – ERO1α is often followed by pro-apoptotic oxidative stress in the cytoplasm. In fact, one of the conditions of the CHOP – ERO1α – IP3R1 – CaMKII pathway is the induction of NADPH oxidase subunit Nox2 and generation of ROS [71].

For cells undergoing a period of prolonged ER stress it appears critical to inhibit protein translation as a key mechanism for the prevention of oxidative stress and apoptosis [73]. Under these circumstances, the target of CHOP is growth arrest and DNA damage-inducible protein (GADD34). GADD34 is member of a family of GADD genes that are induced by DNA damage, growth factor deprivation, and other forms of cell stress [74] and it has been shown to bind to the eukaryotic serine/threonine phosphatase protein phosphatase 1 (PP1) to direct eIF2α dephosphorylation *in vitro* and thus to restore protein translation [75] [45]. In this regard, renal epithelial cells from transgenic mice with mutated (loss of function) *GADD34* were protected from the otherwise pro-apoptotic consequence of tunicamycin treatment [66]. This process therefore seems to represent yet another mechanism of pro-apoptotic CHOP signaling in a state of prolonged ER stress.

Tumor necrosis factor (TNF)-related apoptosis-inducing ligand (TRAIL), a member of the TNF superfamily, is an apoptosis-inducing cytokine. TRAIL appears to specifically kill a wide variety of cancer cells in culture, but has little or no effect on normal cells. TRAIL-induced apoptosis is associated with the interaction of its ligands with two closely related membrane receptors, TRAIL-R1 (DR4) and TRAIL-R2 (DR5). This interaction - in cooperation with the adaptor molecule FADD - results in recruitment and cleavage of the initiator caspase-8 and the consecutive activation of an effector – caspase 3 [49] [50]. It has been found that CHOP up-regulates TRAIL-R2 during ER stress and that this receptor is at least partially responsible for ER stress-induced death in cultured cancer cell lines [76]. Another CHOP-induced molecule thought to induce apoptosis is Tribbles homolog 3 (TRB3). TRB3 encodes a human ortholog of *Drosophila* tribble, and TRB3-knock-down cells are resistant to ER stress-induced apoptosis [77].

Finally, the ability of CHOP to induce ER stress-associated apoptosis has recently been suggested to be dependent on the duration of the stress state. Chronic exposure resulting in mild stress could lead to a kind of adaptive response, with selective attenuation of CHOP expression through degradation of CHOP mRNA and CHOP protein in face of (still) expressed, protective downstream targets such as BiP, possibly due to long-lived mRNAs and proteins [78].

1.4. Role of ER-stress and CHOP-mediated apoptosis in non-pulmonary diseases

One crucial feature for cell survival is the ability to respond and adapt to changes in ER function. However, extensive ER stress induces apoptosis, hence turning a primarily cytoprotective mechanism into a pro-apoptotic one. Extensive data suggests that excessive apoptosis of structural parenchymal cells affects the development of many human diseases. Accordingly, CHOP has been suggested to play a pivotal role in a number of diseases, including renal dysfunction [56], diabetes [67], ethanol - induced hepatocyte injury [79], Parkinson's disease [80], experimental colitis [81], expressed atherosclerosis and heart pressure overload effects [82] [65]. Some of these diseases and the impact of CHOP on their evolution will be discussed in the following:

1.4.1. CHOP and neurodegenerative diseases

Neurodegenerative diseases are characterized by progressive neuronal dysfunction and neuronal cell death and missfolded proteins, in part due to mutations within key functional proteins, seem to play a major role in this regard. Histopathological analysis of the brain of patients with Alzheimer's disease, a classic example of a neurodegenerative disease, revealed extensive ER stress as a prominent observation and this was also observed to occur in patients with other neurodegenerative diseases such as Parkinson's disease [83] [79]. With regard to Alzheimer's disease (AD), the precise reason of which is still unknown, it is assumed that the increase of the β-amyloid (Aβ) production and accumulation is the main reason of the neurodegenerative processes. Interstingly, Aβ induces expression of CHOP in neuronal cells and the brain of animals and the expression of small interfering RNAs targeting CHOP results in increased survival of neurons which already have accumulated Aβ [84]. An increase of neuronal CHOP production was

observed in laboratory mice carrying a presenilin-1 mutation, with consecutively increased production of β-amyloid [85].

β-amyloid is produced from the amyloid precursor protein (APP) by the initial cleavage of aspartyl protease BACE1 (β -site amyloid precursor protein-cleaving enzyme 1) and subsequent cleavage by γ-secretase enzyme complex [86]. Cleavage of APP by BACE1 represents the rate-limiting step of β-amyloid production. CHOP and NF-KB activation precedes the increase of BACEI in the triple transgenic mouse model and seems to cause oxidative damage and ROS accumulation, increased levels of β-amyloid, and, ultimately, neuronal cell death. Application of CHOP-targeting siRNA in human neuroblastoma has been shown to reduce the level of 27-hydroxycholesterol (27-OHC)-induced Aβ production and to dampen the inflammatory response [87].

1.4.2. CHOP and diabetes

Type II diabetes is associated with a high demand for insulin, which is secreted exclusively by pancreatic beta-cells. Increased production of properly folded insulin therefore increases the work load of the ER and, if overwhelming, may cause ER stress. [67]. It is therefore not surprising that type II diabetes is linked to β-cell apoptosis. According to recent studies, pancreatic β-cells are extremely sensitive to ER stress and ER stress-mediated apoptosis [88] [89]. CHOP has been shown to be upregulated in type II diabetes and to contribute to the induction of apoptosis in β-cells under these conditions [90]. In a recent study it was shown that ER-stress induced H_2O_2 superoxide anion and ROS production [66]. Increase of ROS causes the activation of CHOP and TRB3 in diabetic kidneys [91]. It was also found that increased apoptosis of pancreatic β-cells in mice is linked to an increase amount of hyper-stable TRB3 linked with a reduction in β-cells function in humans [92].

1.4.3. Atherosclerosis

Atherosclerosis is a disease characterized by formation of atheroma inside blood vessels. Atheroma are structures formed by fat, cholesterol, calcium, and other substances found in the blood. In this process macrophage activation results in the excretion of proinflammatory and cytotoxic substances, including peroxynitrite, an early inducer of atherosclerosis through the ER stress pathway [93]. Studies on the regulation of ER-stress and CHOP regulation in macrophages revealed the prolonged ER stress can result in enhanced CHOP expression, release of calcium from the ER resulting in death receptor Fas activation, and macrophage apoptosis [94]. Increased macrophage apoptosis was also suggested to be favored by a concomitant decrease in the anti-apoptotic protein BAL-2.

1.4.4. Ischemic disease

Tissue ischemia is characterized by oxygen deprivation leading to glucose and endoplasmic Ca^{2+} depletion. Ischemia is also linked to ER stress. The induction of CHOP mRNA was observed in mice with brain ischemia [95]. Nitric oxide (NO) plays an important role in the pathophysiology of cerebral ischemia. NO decreases cytoplasmic Ca^{2+} and facilitates CHOP gene transcription in primary neuronal cultures [96]. Data showed that CHOP mediated cell death was involved in the transition from cardiac hypertrophy to heart failure in mice [97]. The Calnexin silenced cardiomyocytes display ER stress, as evidenced by the increase in the level of protein GRP78 and ATF6 and increasing spliced *XBP1* mRNA, *ERO1α* and *CHOP* mRNA [98].

1.5. Potential pathomechanism of ER stress in pulmonary fibrosis

The first indication that ER stress plays a role in pulmonary fibrosis came from early studies of patients with mutations in surfactant protein C gene [23]. In 2001, Nogee et al reported a mutation in the carboxy-terminal region of the surfactant protein - C (*SFTPC*) that resulted in the removal of exon 4 and its 37 amino acids (Δexon4) in an infant with nonspecific intestinal pneumonia. The mother of the child was also suffering from desquamative interstitial pneumonia [23]. Afterwards, another study on *SFTPC* mutations

found another mutation resulting in the replacement of glutamine with leucine at amino acid position 188 (L188Q) of pro-SP-C in 11 related adults and three children with UIP and nonspecific intestinal pneumonia [99]. Studies *in vitro* [100] [101] showed that mutations in the carboxy-terminal portion *SFTPC* led to incorrect processing and accumulation of the misfolded proteins in the ER. Modeling of Δexon4 and the L188Q mutation *in vitro* showed that the mutant SP-C causes ER stress and caspase 4 (12)-mediated apoptosis in AECII like cell lines such as human A549 and mouse MLE12 lung epithelial cells [27] [102] [101]. In 2003 a transgenic mouse model expressing mutations of $SFTPC^{\Delta exon4}$ under human *SFTPC* promoter was developed. These mice had abnormal lung morphogenesis resulting in fetal death with abnormal surfactant processing and accumulation of misfolded proteins in the ER [103]. Later on, another transgenic mouse model was developed which relied on the tet-on system for conditional expression of L188Q *SFTPC* mutations specifically in alveolar type II cells. Without doxycyclin, mice grew and developed normally without an apparent abnormal phenotype. In doxycyclin treated mice, however, expression of L188Q *SFTPC* resulted in a modest ER stress reaction in AECIIs in mature mice, but did not lead to overt AECII apoptosis or pulmonary fibrosis. Interestingly, treatment of these transgenic mice with low doses of bleomycin, which would not cause any significant fibrosis in wild type mice, did result in extensive AECII death, activation of the caspase 4/12 and lung fibrosis. A control experiment addressing the question if AECIIs cell death under these conditions was truly caused by ER stress was undertaken, in which wild mice were exposed to tunicamycin, which alone did only cause a modest ER-stress reaction, followed by a low dose of bleomycin. As with the transgenic expression of LI88Q SFTPC, application of tunicamycin alone induced ER stress in AECII, but apoptosis or fibrosis were not present. However, in combination with bleomycin, mice treated with tunicamycin and bleomycin showed extensive AECII apoptosis and pulmonary fibrosis [104].

Despite *SFTPC* mutations leading to ILD in childhood these mutations are rare in adults with IPF [105]. However, the disclosure of the causative role in familial cases of IPF put emphasis on the importance of the alveolar type II cell in the initiation and early pathogenesis of IPF [23]. Accordingly, elevated UPR and ER stress markers were found in the lung tissue of patients with familial IPF either carrying or not carrying the LI88Q *SFTPC* mutation, as well as patients with sporadic IPF. It was demonstrated by immunohistochemistry that the AECs lining areas of pulmonary fibrosis were expressing BiP, EDEM, XBP-1, ATF4, ATF6 and CHOP and these areas were linked with ER stress.

Thus ER stress was identified in IPF lungs even in the absence of *SFTPC* mutations [26] [27].

Similar to *SFTPC* mutations, it has been found that mutations in the gene encoding surfactant protein A2 (*SFTPA2*) were associated with FIP [25]. Wang et al. showed two different FIP families in which missense mutations in SFTPA2 were identified. One mutation was detected in replacement of valine for glycine at codon 231 (G231V) and second mutation in the *SFTPA2* gene resulted in replacement of serine for phenylalanine at codon 198 (F198S) [25]. Following overexpression of both *SFTPA2* mutated genes in A549 cells, both forms of mutant SP-A proteins were detected in ER, which led to activation of UPR. This observation provided a similar role for ER stress in *SFTPA2* mutation in induction of lung fibrosis which was observed in *SFTPC* mutations [24] [25]

It is known that ER stress and inflammation are interconnected in UPR pathways through activation of JNK, p38 mitogen-activated protein kinases and NF-KB. *In vitro* overexpression of Δexon4 *SFTPC* led to the activation of NF-KB. However, the relationship between this pathway and LI88Q *SFTPC* mutation was not found. *In vivo* expression of LI88Q *SFTPC* revealed no increased tendency to inflammation of the lungs. Although the interaction between the UPR and inflammatory signaling pathways affect tissue remodeling during fibrosis, the inflammatory effect of ER stress depends on the cause, severity, and duration of ER stress [104].

Research conducted on several groups of patients revealed that viral infections play an important role in the pathogenesis of IPF. Patients with IPF showed an increase in antibody titers to cytomegalovirus and Epstein - Barr virus [106]. Herpes antigens could also be detected in the AECs lining the areas of fibrosis in lung biopsy samples from IPF but not in control patients [107] [27] [108]. Herpesvirus causes ER stress and activates UPR [35]. It was observed that proteins of other herpes viruses (Epstein-Barr virus, cytomegalovirus, and Kaposi's sarcoma herpesvirus) have been identified in the AECIIs lining areas of fibrosis in IPF. These viral proteins can be colocalized with ER stress markers [27]. These data suggest that herpesvirus is involved in the pathogenesis of IPF. Further question is if they alone can directly induce ER stress or they aggravate an already existing ER stress response.

Cigarette smoke is usually associated with the development of both IPF [109] and FIP [110]. One study showed that exposure to cigarette smoke can activate UPR. Additionally *in vitro* studies showed that the exposure of 3T3 cells to cigarette smoke extract was

associated with PERK and activation of ATF4. This resulted in up-regulation of BiP and other ER stress associated genes [111]. Additional studies have showed that CHOP was activated by ROS in cigarette smoke in human bronchial epithelial cells [112] and this activation occurred through PERK-eIF2α pathway [113]. Other study on normal and malignant epithelial lung cells showed that the expression of UPR – related genes was induced by the exposure to cigarette smoke [114]. Many studies have shown that environmental factors related to lung fibrosis can lead to ER stress and activation of the UPR. However, it is not known if any of the listed external risk factors exert their influence through induction of ER stress.

2 Aim of the study

It is well known that dysregulation of alveolar homeostatic balance contributes to the development of chronic fibrotic interstitial lung diseases, such as IPF. Endoplasmic reticulum stress plays a role in the dysregulation of apoptosis in alveolar type II cells. ER stress is the most potent inducer of C/EBP homologous protein (CHOP) expression and CHOP is known as a pro-apoptotic factor. CHOP-mediated apoptosis contributes to the pathogenesis of a number of ER stress-related diseases. Little is known about regulation of CHOP expression in lung epithelial cells. Furthermore, our previous studies showed that CHOP is up-regulated specifically in alveolar type II cells. Thus, I hypothesize that ER stress-induced apoptosis is mediated by CHOP and this is the major factor responsible for AECII injury and apoptosis in IPF.

In this context, the research focus is:

1. To analyse the transcriptional regulation of epithelial CHOP expression *in vitro.*
2. To elucidate the biological role of Chop overexpression in induction of epithelial apoptosis and lung fibrosis *in vitro* and *in vivo*

3 Materials and methods

3.1 Materials

3.1.1 Reagents

Name	Company
2-(4,2-hydroxyethyl)-piperazinyl-1-	Sigma Aldrich, Germany
2-amino-2-hydroxymethyl-1,3-propanediol (Tris)	Roth, Germany
2-Mercapto-ethanol	Sigma Aldrich, Germany
4-[3-(4-iodophenyl)-2-(4-nitrophenyl)-2H-5-tet-razolio]-1,3-benzene (WST-1)	Roche, Germany
Acetic acid	Sigma-Aldrich, Germany
Acrylamide solution, Rotiphorese® Gel 30	Roth, Germany
Agarose	Roth, Germany
Albumine, Bovine Serum Fraktion V (BSA)	Roth, Germany
Ammonium Persulfate (APS)	Roth, Germany
Ampicillin sodium	Sigma Aldrich, Germany
Bacto Agar	BD, Sparks, USA
Bacto-Yeast extract	BD, Sparks, USA
Bacto-Trypton	BD, Sparks, USA
Beads for ChIP	Millipore, Germany
BJ5183 cells	Agilent Technologies, USA
Bovine serum albumin (BSA) 10mg/ml solution	New England BioLabs, USA
Bromphenol Blue	Sigma Aldrich, Germany
Calcium chloride	Sigma-Aldrich, Germany
Chloroform	Merck, Germany
Chloroform	Merck, Germany
Cytotoxicity Detection Kit (LDH)	Roche, Germany
D-(+)-Glucose	Roth, Germany
Dimethyl Sulfoxide (DMSO)	Sigma Aldrich, Germany
Dispase	BD Bioscience, USA

DMEM medium	Gibco, Germany
DMEM-F12 Medium	Gibco, Germany
DNA ladder	Eurogentee, Belgium
Dnase	Fermentas, Germany
DNeasy blood and tissue kit	Qiagen, Germany
Dulbecco's Phosphate Buffered Saline (PBS)	PAA, Austria
Ethanol 99,5%	Roth, Germany
Ethansulfonate (HEPES)	Roth, Germany
Ethidium bromide	Sigma-Aldrich, Germany
Ethylenediamine-tetraacetic Acid (EDTA)	Sigma Aldrich, Germany
Fetal Calf Serum (FCS)	Roth, Germany
Formaldehyde 37,8%	Sigma Aldrich, Germany
Gel extraction kit	Qiagen, Germany
Geneticin/G418	Roth, Germany
Glycergel® Mounting Medium	Dako, Denmark
Glycerol	Roth, Germany
Glycine 99%	Roth, Germany
Hot Start DNA polymerase	Merck, Germany
HotStar high fidelity DNA Polymerase	Qiagen, Germany
HotStar Taq DNA Polymerase	Qiagen, Germany
Hydrobeta-estradiole	Sigma Aldrich, Germany
Hydrochloric Acid (HCl) 32%	Sigma Aldrich, Germany
Hydrocortisone	Sigma Aldrich, Germany
Hygromycin	Roth, Germany
Insulin, Transferrin, Sodium Selenite (ITS)	PAN Biotech, Germany
iQ™ SYBR® Green Supermix	Bio-Rad, USA
Isoamyl alcohol	Sigma Aldrich, Germany
Isopropanol	Sigma-Aldrich, Germany
Kanamycin	Roth, Germany
KH_2PO_4	Merck, Germany
L-Glutamine	Gibco, Germany
Luciferase Assay Kit	Promega, Germany

Magnesiumchloride (anhydrous)	Sigma-Aldrich, Germany
Matrigel™ Growth Factor Reduced	BD Biosciences, Germany
Methanol 99,9%	Roth, Germany
Milk powder	Roth, Germany
N,N,N',N'-tetramethyl-1,2-diaminomethane (TEMED)	Sigma Aldrich, Germany
Na_2HPO_4 x $2H_2O$	Merck, Germany
Na-deoxycholate	Merck, Germany
NP-40	Sigma Aldrich, Germany
Nucleotide Mix (dNTPs)	Qiagen, Germany
Oligo(dT) Primer	Roche, Germany
Omniscript RT Kit	Qiagen, Germany
Opti-MEM medium	Invitrogen, Germany
PageRuler™ Prestained Protein Ladder	Thermo Scientific, USA
Paraffin, Paraplast Plus®	Sigma Aldrich, Germany
PCR purification kit	Qiagen, Germany
Penicillin/Streptomycin	PAA, Austria
Phenol	Roth, Germany
Phosphatase Inhibitor Cocktail Set III™	Calbiochem, Germany
Pierce® BCA Protein Assay Kit	Thermo Scientific, USA
Pierce® ECL Plus Western Blotting Substrate	Thermo Scientific, USA
Plasmid isolation Mini and Maxi kit	Qiagen, Germany
PMSF (phenylmethylsulfonyl fluoride)	Thermo Scientific, USA
Potassium Chloride (KCl)	Merck, Germany
Potassium phosphate monobasic	Sigma-Aldrich, Germany
Protease Inhibitor Cocktail Set I™	Calbiochem, Germany
Protein A agarose/Salmone Sperm DNA	Millipore, Germany
Proteinase K	PEQLAB Biotechnologie, Germany
QIAshredder	Qiagen, Germany
QuikChange® II Site-Directed Mutagenesis Kit	Stratagene, Germany
Reporter Lysis Buffer	Promega, Germany
Restore™ Western Blot Stripping Buffer	Thermo Scientific, USA

Restriction endonucleases	New England BioLabs, USA
RNase A	Thermo Scientific, USA
RNase Inhibitor	Roche, Germany
RNase-free Water	Qiagen, Germany
RNeasy Mini Kit	Qiagen, Germany
Skim Milk Powder	Fluka, Germany
SmartLadder	Eurogentec, Belgium
Sodium Chloride (NaCl)	Sigma Aldrich, Germany
Sodium Citrate Tribasic Dihydrate	Sigma Aldrich, Germany
Sodium Dodecyl Sulfate (SDS)	Sigma Aldrich, Germany
Sodium Hydroxide (NaOH)	Sigma Aldrich, Germany
Sodium phosphate (monobasic, anhydrous)	Sigma-Aldrich, Germany
Staurosporine	Calbiochem, Germany
Streptavidin coated magnetic beads	Invitrogen, Germany
T4 DNA ligase	New England BioLabs, USA
T4 DNA ligase buffer	New England BioLabs, USA
TOP 10, competent cells	Invitrogen, Germany
Triton-X-100	Sigma Aldrich, Germany
Trypsin/EDTA	PAA, Austria
Tunicamycin	Calbiochem, Germany
TurboFect	Thermo Scientific, USA
Tween-20	Sigma Aldrich, Germany
XL10 cells	Agilent Technologies, USA
β-Galactosidase Assay Kit	Promega, Germany

3.1.2 Equipment

Name	**Company**
Agarose-gel electrophoresis chambers	Kreutz Labortechnik, Germany
Analytical Balance	Mettler Toledo, Switzerland

Bacteria culture incubator	Heraeus, Germany
Cell culture centrifuge, Universal 30RF	Hettich, Germany
Cell Culture Hood HERAsafe	Hereaus, Germany
Cell Culture Incubator, HERAcell 150i	Thermo Scientific, Germany
Cell Scrapers	Costar, USA
Ceramic beads	PeqLab, Germany
Electrophoresis Chambers	Bio-Rad, UK
Falcon Roller	CAT, Germany
Falcon tubes	Greiner, Germany
Falcons filters: 70µm; 40µm; 10µm	BD Falcon, USA
Filter Tips: 10; 100; 1000µl	Eppendorf, Germany
Filter units 0.22 µm syringe-driven	Millipore, USA
Fluorescence microscope	Carl Zeiss, Germany
Fridge +4°C	Bosch, Germany
Freezer -20 °C	Bosch, Germany
Frezer -80°C	Bosch, Germany
Gel Doc XR+	Biorad, Hercules, USA
Glass bottles: 250, 500, 1000 ml	Roth, Germany
Glass Pipettes	Greiner, Germany
Heating block VLM EC2	VLM, Bielefeld, Germany
Heating Oven, FunctionLine	Hereaus, Germany
iCycler IQ™ Thermocycler	Bio-Rad, USA
Light Microscope, Axiovert 25	Carl Zeiss, Germany
Magnetic Stirrer	Heidolph, Germany
Mini spin centrifuge	Eppendorf, Germany
Multifuge centrifuge	Eppendorf, Germany
Multipipette	Eppendorf, Germany
NanoDrop	PeqLab, Germany
NanoZoomer	Hamamatsu, Germany
Neubauer Chamber	Optik Labor, Germany
PCR-thermocycler	Bio-Rad, Germany
Petri Dish	Sarstedt, Germany

pH-meters	MettlerToledo, Germany
Pipet tips: P10, P20, P100, P200, P1000	Biozym, Germany
Pipetboy	Eppendorf, Germany
Pipets	Eppendorf, Germany
Power Supply, Consort	Roth, Germany
Precellys Homogeniser	PeqLab, Germany
PVDF Transfer Membrane, Hybond™-P	GE Healthcare, UK
Semi Dry Blot (Trans-Blot SD)	Bio-Rad, USA
Serological pipette: 10ml	BD Falcon, USA
Sonorex	Bandelin, Germany
SpectraFluor Plus	Tecan, Germany
Syringes	Braun, Germany
Tissue Culture Dish 100mm	Greiner, Germany
Tissue culture plates: 6, 24, 48 well	BD Falcon, USA
Vortex machine	VWR, Germany
Water bath	Medingen, Germany
Western blot unit	Bio-Rad, Germany
Whatmann paper	GE Healthcare, UK

3.2 Methods

3.2.1. Human tissues

The study was approved by the local research ethics committee, and written consent was obtained from all participants (No. 31/93, 29/01, and No. 111/08: European IPF Registry). Lung tissue samples were obtained from two healthy patients (mean age 40 ± 4 years; one female, one male).

3.2.2. Animal experiments

All animal experimentation as described in this thesis were performed according to the Helsinki convention for the use and care of animals and was approved by the Justus-Liebig-University`s Committee on Animal Investigations (V54-19c 20/15 h02, Gi 20/10-Nr. A53/2012). The animal experiments including genetically modified mice (mice with conditional AECII-specific overexpression of Chop) were approved by the local authorities [Regierungspräsidium Gießen], GI 20/10-Nr. 12/2009). 8 weeks old male and female mice (FVBN strain) with a weight between 18-20g were used in all experiments. Mice were obtained from Charles River Laboratories, Sulzfeld, Germany. All experimental protocols involving animals were performed by Dr. Ingrid Henneke and Stefanie Hezel.

3.2.2.1. Generation of transgenic animals and induction of the transgene

For generation of transgenic mice with conditional overexpression of CHOP in AECII, the bidirectional pBI-L vector from Clontech was used. This vector allows the simultaneous expression of the gene of interest and luciferase from the bidirectional tetracycline responsive promoter *P*bi-1. The mouse *Chop* gene was previously cloned into the pBI-L vector and then kindly provided by Dr. M. Hühn.

After cloning, DNA fragments containing bacterial Amp^r resistant cassette and Col E1 ori were removed from created pBI-L-CHOP-Tet construct by restriction endonucleases. The linearized pBI-L-CHOP-Tet construct was then injected into oocytes by Dr. P Moreira, (EMBL Mouse Biology Unit, Italy). 3 positive founders were identified by PCR screening and bred to homozygosity (two males and one female founder). After that,

homozygous transgenic mice were crossbred with homozygous transactivator SP-C rtTA mice. For induction of transgene expression, homozygous Chop transgenic mice were fed with doxycyclin enriched nutriment and phenotyped after 4 and 8 weeks. AECII specific transgene induction was evaluated using qPCR (chapter 3.2.7) and Western blotting analysis (chapter 3.2.10) of lung homogenate and immunohistochemistry (chapter 3.2.11).

Mice number	Time point	Dox	Founder
164	4 weeks	Dox -	Female
130	4 weeks	Dox +	1st Male
134	4 weeks	Dox +	1st Male
145	4 weeks	Dox +	Female
146	4 weeks	Dox +	Female
161	4 weeks	Dox +	2nd Male
172	4 weeks	Dox +	2nd Male
174	4 weeks	Dox +	2nd Male
99	8 weeks	Dox -	1st Male
101	8 weeks	Dox -	1st Male
110	8 weeks	Dox -	1st Male
97	8 weeks	Dox +	1st Male
98	8 weeks	Dox +	1st Male
102	8 weeks	Dox +	1st Male
113	8 weeks	Dox +	2nd Male
120	8 weeks	Dox +	2nd Male
123	8 weeks	Dox +	2nd Male
124	8 weeks	Dox +	2nd Male
131	8 weeks	Dox +	1st Male
132	8 weeks	Dox +	1st Male
148	8 weeks	Dox +	Female
149	8 weeks	Dox +	Female
150	8 weeks	Dox +	Female
175	8 weeks	Dox +	2nd Male
176	8 weeks	Dox +	2nd Male

Table 1. List and characteristics of transgenic mice used for analysis.

3.2.3. Cell lines and culturing conditions

The human and mouse lung epithelial cell lines (A549 and MLE-12 respectively) were obtained from ATCC, Manassas, USA. The human embryonic epithelial kidney 293T cell line (HEK293T) was kindly provided by Dr. Sven Becker, Max Planck Institute for Lung Research, Bad Nauheim, Germany. The mouse lung fibroblast (Mlg) was a kind gift of Prof. Saverio Bellusci, Department of Internal Medicine, Justus Liebig University, Giessen, Germany. All cells were grown in 10 cm^2 tissue culture plates in full medium based on growth medium DMEM-F12 for A549 and MLE12, DMEM for HEK293T and Mlg, at 37°C, 5% CO_2.

DMEM-F12 medium for A549 cell line

Component	Final Concentration
FCS	10% (v/v)
L-Glutamine	2 mM
MEM Vitamins	1% (v/v)
MEM Non-essential	1% (v/v)
Penicillin	100 U/ml
Streptomycin	100 µg/ml

DMEM-F12 medium for MLE12 cell line

Component	Final Concentration
Hydrocortisone	10 nM
Hydrobeta estradiole	10 nM
ITS	5% (v/v)
HEPES	10 mM
L-Glutamine	2 mM
FCS	2% (v/v)
Penicillin	100 U/ml
Streptomycin	100 µg/ml

DMEM medium for HEK293T and Mlg cell line

Component	Final Concentration
FCS	10% (v/v)
L-Glutamine	2 mM
Penicillin	100 U/ml
Streptomycin	100 µg/ml

When cells had reached a confluence of 80-90%, they were passaged to a new plate. In order to detach from culture plate, cells were washed with PBS and incubated with 2 ml of trypsin for 2-5 min at 37°C. After that, 2 ml of culture medium containing FCS was added to neutralize trypsin. For maintaining the culture, the cells were diluted 1:10 and plated on new culture dishes.

For *in vitro* experiments, cells were seeded on 6-, 12- or 96-well plates and cultured in the medium for 16h. Transfections as well as treatment of cells with chemicals were performed when cells reached 60-70% of confluency.

3.2.3.1. Isolation of alveolar epithelial type II cells (AECII)

Primary murine alveolar epithelial type II cells (AECII) were isolated from the lungs of C57BL/6 mice as described [115]. Stefanie Hezel performed all steps with handling and killing of mice. Animals were anesthetized by intraperitoneal injection of a mixture of ketamine, xylazine and heparin (in the ratio 2:2:1). The abdominal cavity was opened and the renal artery was severed to exsanguinate the mouse. The lungs were perfused with 10ml of saline, until visually cleared of blood. Dispase, followed by 0.5 ml of 1% low-melting-point agarose in DMEM medium, was injected into lungs via the trachea (with a Vasofix® Safety cannula from Braun). Agarose solution was allowed to solidify for 2 min. Then lungs were separated from the trachea and other connective tissues. The isolated organ was incubated in 2 ml of dispase for 45 min at room temperature. After this time, lungs were dissected in 7 ml of Plus Medium. Lungs were chopped; the resulting crude cell mixture was incubated for 10 min at room temperature with gentle shaking. This was followed by subsequent washing with Plus Medium and filtration through 70 µm, 40 µm and 10 µm Nitex filters. The resulting filtrate was centrifuged at 130×g at 4°C for 10 min and resuspended in 2 mL of ER Lysis Buffer. The lysis reaction was stopped

by adding Minus Medium + 10% FCS followed by centrifugation at 130×g at 4°C for 10 min. Obtained cells were counted with Trypan Blue. The following antibodies (BD Bioscience) were then added to the cell suspension in 5 ml of Minus media + 10% FCS: anti-CD16/32 at 0.75 µl/million cells, anti-CD45 at 0.9 µl/million cells, anti CD-31 at 0.4 µl/million cells. The mix was then incubated at 37°C for 30 min, followed by centrifugation and resuspension in Minus media (216 µl/million cells). Streptavidin coated magnetic beads were prepared by washing three times in PBS and beads suspension (11 µl/milion cells) was added to the cells. The mix was incubated at room temperature for 30 min and then placed on a magnetic separator for 15 min. The cell suspension was carefully aspirated from beads, transferred to a new tube and centrifuged as described above. The isolated AECII were then resuspended in Minus medium. The AECII were plated on wells of a 6-well-plate ($1x10^6$/well) coated with matrigel (BD Bioscience, Germany). Cells were cultured in BEGM (Lonza) medium supplemented with CS-FBS (HyClone) and hKGF (PreproTech). In this study, AECII cells were cultured up to 5 days. All cultures were maintained in humidified atmosphere with 5% CO_2 at 37°C.

Minus Medium	**Plus Medium**	**ER (Erythrocyte) Lysis Buffer**
500 ml DMEM 10 mM HEPES 100 U/l Penicillin 100 µg/ml Streptomycin	Minus Medium supplemented with 0,04 mg/ml DNase	8,29g NH_4Cl 1g $KHCO_3$ 0,037g $Na_2EDTA \times H_2O$ Add 1000 ml dest. H_2O pH 7,4

3.2.4. Isolation of genomic DNA

Genomic DNA from human lung tissue was generally isolated with use of the “QIAgen DNeasy Blood and Tissue Kit” following the instructions of the manual. Genomic DNA from lung tissue was provided as a pellet in 70 % (v/v) ethanol and spinned down, dried at air and resuspended in 200 µl water before further use.

3.2.5. RNA isolation

Total RNA was isolated from exponentially growing cells and animal lung tissues according to the manufacturer's instructions using the "RNeasy® Plus Mini Kit (Qiagen)". The concentration and quality of the isolated RNA were determined by applying of 2µl of the sample to NanoDrop® spectrophotometer and by measuring its absorbance at 260 nm and 280 nm. RNA samples were stored at -80°C until further use.

3.2.6. Reverse transcription

In order to synthesize cDNA from isolated total RNA, reverse transcription (RT) was performed using Omniscript® Reverse Transcription Kit (Qiagen) and Oligo dT primers (Applied Biosystem) according to manufacturer's instructions. 2 µg of total RNA per sample was used. For annealing of Oligo dT primers to RNA, samples were incubated at room temperature for 10 min. Thereafter, cDNA was synthesized at 37°C for 65 min and newly synthesized cDNA was stored at -20°C.

Reverse Transcriptase reaction mix:

Component	Volume (20 µl)	Final concentration
10×RT Buffer	2 µl	1×
RNase inhibitor (20U/ µl)	0,5 µl	0,5 U
5mM dNTP mix	2 µl	0,5 mM
50µM Oligo d(T)	0,5 µl	1,25 µM
Omniscript™ RT (4U/ul)	1 µl	2 U
RNA	up to 2 µg	
Water	up to 20 µl	

3.2.7. Quantitative polymerase chain reaction (qPCR)

qPCR is used for simultaneous quantification and amplification of specific cDNA sequences. The procedure follows the common PCR strategy, but after each round of amplification, the DNA is quantified. Quantification is performed by the incorporation of a fluorescent reporter dye – SYBR® Green I – which directly binds to dsDNA. The

incorporated dye produces a signal that is proportional to the DNA concentration. Quantification of cDNA was performed according to the manufacturer's instructions provided with a SYBR® Green PCR Supermix Kit (Bio-Rad).

PCR reaction mix was prepared as follows:

Component	Volume (20µl)	Final concentration
iQ™ SYBR® Green Supermix	10µl	1×
Forward primer * (10pmol/µl)	0,5µl	0,25 nM
Reverse primer * (10pmol/µl)	0,5µl	0,25 nM
cDNA template	1µl	25-50 µg
Water	8µl	

* All primer sequences are listed in Table 1

The qPCRs were performed using a Bio-Rad iCycler with MyiQ detection system. The amplification and quantification of cDNA was performed according to the following program:

Step		Time	Temperature
Polymerase activation	1×	3 min	95°C
Denaturation	35 cycles	15 sec	95°C
Annealing *		30 sec	59-60°C
Melting curve analysis	70 cycles	10 sec/step	0,5°C increment

*Annealing temperatures varied depending on the primers used in the experiment.

The primers for qPCR were designed using the online program GeneFISHER (http://bibiserv.techfak.unibielefeld.de/genefisher2). As endogenous reference, gene *Actb* was used for all qPCR reactions. The relative transcript abundance of a gene was represented as ΔCt values (ΔCt = Ct target – Ct reference). Relative changes in transcript levels were displayed as fold induction ($2^{(-\Delta Ct)}$).

Gene name	Forward primer (5'-3')	Reverse primer (5'-3')
Casp11	ACTGTCCAGGTCTACGAGAC	CCGGAAGCAGGAAATGATTC
Chop	CCTAGCTTGGCTGACAGAG	GTCAGGCGGTCGATTTCC
Col1a1	GAGCGGAGAGATCTGGATCG	GTGGCTACGCTGTTCTTGC
Dr5	CTAGGCCTCTGGATAGGACTC	GGAGTCAAAGGGCACTATGTC
Ero1α	TGGAATTAAGTCTGCGAGCTAC	GACACTCCATATCCTCCAAGG
Gadd34	CCAGGACAAGATGATCTTAGAG	CAGCAGAAGCTTGGTAAGTC
Il1	GGACCCATATGAGCTGAAAGC	ACTCCACTTTGATCTTGACTTC
Pai1	CCTGGTGCTGGTGAATGC	CTGGTCATGTTGCCCTTC
Acta2	ATCCGACACTGCTGACAGAG	ACGCTCGGCAGTCAC
Xbp1 spliced	GCTTTTACGGGAGATAACTC	GCCTGAACCTGCTGCG
Actb	CTACAGCTTCACCACCACAG	CTCGTTGCCAATAGTGATGAC

Table 2. List of primers used for qPCR

3.2.8. Protein isolation

3.2.8.1. Protein isolation from cells

Cells were harvested at indicated time points by detaching from plate surface using ice cold proteolytic enzyme 1× trypsin. Then cells were transferred to a 15ml falcon tube and collected by centrifugation. After that, cell pellets were washed with ice cold PBS and shock-frozen in liquid nitrogen. In order to get raw protein extract, 100 µl of lysis buffer containing PMSF was applied to a cell pellet from a well of a 6-well-plate, followed by repeated shock freezing in liquid nitrogen and thawing (3 times) in liquid nitrogen. After 3rd time freezing and thawing, samples were incubated on ice for 1 h, and afterwards centrifuged for 10 min at 13000×g at 4°C to get clear extract. Supernatants were transferred to new tubes and stored at -20°C for further experiments.

3.2.8.2. Protein isolation from lung tissue

Protein extracts from murine lung tissue were isolated by using Precellys® homogenizator (Bertin Technology). Pieces of murine lung tissue were put into homogenization vials containing 1,4 mm and 2,8 mm ceramic beads and 1 ml of lysis buffer, followed by homogenization for 2 times, for 20 sec at the speed of 5000 rpm. To get clear extracts, samples were centrifuged at 13000×g at 4°C for 10 min. Supernatants were stored at -20°C.

Protein extraction buffer

Component	Final concentration
Tris-HCl pH 7.5,	50 mM
EDTA pH 8.0	5 mM
NaCl	150 mM
Triton-X-100	1% (w/v)
Na-deoxycholate	0.5% (w/v)
Water	up to 1l

3.2.8.3. Protein quantification

Protein concentrations of tissue and cell extracts were determined spectrophotometrically using the Pierce® BCA Protein Assay Kit (Thermo Scientific) and a microtiter plate reader (SpectraFluor Plus, Tecan) according to the manufacturer's instructions. Bicinchoninic Acid (BCA) protein assay is based on the color detection and quantification of total protein compared to a protein standard. BCA reaction forms an intense purple chelate-complex with Cu^{+} ions. The protein reduces alkaline Cu^{2+} to Cu^{+} in a concentration-dependent manner. BCA is a highly specific chromogenic reagent for Cu^{+}, thereby forming the purple complex with an absorbance maximum at 562 nm. Because of this property, the resulted absorbance at 562 nm is directly proportional to the protein concentration. The dye binds primarily to sulfur (from cysteine), aromatic amino acids residues and the peptide bounds. 20 µl of protein sample were mixed with 200 µl of BCA reagent in a well of a 96-well plate, followed by incubation at 37°C for 30 min. Different dilutions in the range 7,8 µg/ml to 1,5 mg/ml of bovine serum albumin were used as a standard, and were prepared and mixed with the BCA reagent in the same ratio as the

sample of unknown concentration. Finally, purple-colored complexes of the samples and standards were quantified by measuring the absorbance at 562 nm.

3.2.9. SDS-polyacrylamide gel electrophoresis

Protein extracts were separated by SDS-polyacrylamide gel electrophoresis (SDS-PAGE). Before loading onto the gel, protein was mixed with 4× loading buffer, and denaturated by heating for 10 min at 98°C. Thereafter, samples were shortly vortexed and collected by brief centrifugation. Separation of proteins was performed in the gel consisting of 4 % stacking gel and different concentrations of resolving gel – depending on the size of the target protein. Electrophoresis was carried out in 1× SDS-running buffer at 100 V.

Loading buffer (4×)

Component	Final concentration
SDS	5% (w/v)
Tris/HCl, pH 6,8	156 mM
Glycerol	40% (v/v)
Bromophenol blue	0,01% (w/v)
2-mercaptoethanol	5% (v/v)
Water	up to 100 ml

SDS-PAGE	Resolving gel (10ml)			Stacking gel (10ml)
	9%	10%	15%	4%
Acylamide/Bisacrylamide (30%/0,8%)	3ml	3,33ml	5ml	1,33ml
Dist.H_2O	3,53ml	3,20ml	1,53ml	6,57ml
10% SDS	100µl	100µl	100µl	100µl
1,125M Tris, pH 8,8	3,33ml	3,33ml	3,33ml	--
0.625M Tris, pH6.8	--	--	--	2ml
10%APS	50µl	50µl	50µl	100µl
TEMED	10µl	10µl	10µl	10µl

SDS-running buffer (1×)

Component	Final concentration
Tris	25 mM
Glycine	192 mM
SDS	0,1% (w/v)
Water	up to 1l

3.2.10. Protein blotting

3.2.10.1. Western blotting

Western blotting was performed in order to visualize and detect specific proteins separated by SDS-PAGE. Proteins separated by SDS-PAGE were transferred onto a 0,45 µm polyvinylidene fluoride (PVDF) membrane in a semi-dry blotting chamber. Transfer was performed with transfer buffer at 75 mA for 1,5 h.

Transfer buffer

Component	Final concentration
Tris	20 mM
Glycine	159 mM
Methanol	20% (v/v)
Water	up to 1l

3.2.10.2. Protein detection

The membranes were blocked with 5% (w/v) non fat dry milk in 1% TBST buffer at room temperature for 90 min, followed by incubation with primary antibody dissolved in 5% (w/v) Skim milk solution (Table 2) at 4°C overnight. The membranes were washed 3 times for 15 min in TBST buffer and were incubated for 2h at room temperature with HRP-conjugated secondary antibody (Dako), and finally washed for 4 times for 20 min with TBST buffer. Proteins on the membrane were detected using the Pierce® ECL Plus chemiluminescent detection system (Thermo Scientific), and emitted signals were detected with a chemiluminescence imager (Intas ChemoStar, Intas, Germany). In order to re-probe membranes with β-actin antibodies, membranes were stripped in Restore™

Western Blot Stripping Buffer for 1h at room temperature after which subsequent protein detection was performed as described above.

TBST buffer, pH 7,5

Component	Final concentration
Tris	50 mM
NaCl	50 mM
Tween-20	0,1% (v/v)
Water	up to 1l

Name	Source	Dilution	Company
AP-1	Rabbit	1:1000	Abcam
ATF4	Rabbit	1:6000	Aviva Systems Biology
ATF6	Rabbit	1:1000	Abcam
c-Ets-1	Rabbit	1:1000	Santa Cruz
cleaved Caspase 3	Rabbit	1:500	Cell Signaling
CHOP	Rabbit	1:1000	Santa Cruz
DR5	Rabbit	1:500	Abcam
GADD34	Rabbit	1:300	Santa Cruz
β-actin	Rabbit	1:10000	Abcam

Table 3. List of primary antibodies used in Western Blot.

3.2.10.3. Densitometry

Band densities of respective proteins in immunoblot were measured using ImageJ software (version 1.46, NIH). The band densities were normalized to β-actin.

3.2.11. Immunofluorescence

In order to localize and detect the expression of proteins in lung tissue, immunofluorescence analysis was performed. Paraffin-embedded, formalin-fixed lung tissue was sectioned (3 μm – sections) and used for immunofluorescence staining. Sections were deparaffinized by incubation at 60°C for 1h at air, followed by washing in xylene for 10 min. Sections were then rehydrated in alcohol baths with declining concentrations of ethanol (99.6% > 96% > 80% > 70% > 50%, each bath for 3 min) and kept in distilled water until further use. Antigen retrieval was performed by incubating the sections in a 1% trypsin solution for 10 min at room temperature, and then washed 3 times for 5 min with 1 × PBS. After that, sections were blocked in 5% (w/v) BSA for 1h at room temperature and then incubated with primary antibodies (antibodies used in immunofluorescence analysis are listed in Table 3) overnight at 4°C. After 3 washes for 10 min in PBS, sections were incubated for 40 min with fluorochrome-conjugated secondary antibodies (Invitrogen) in the dark at room temperature. Finally, sections were stained with DAPI (4',6-diamidyno-2-fenyloindol) for indicating the nuclei. Control sections were performed by omitting the primary antibody. Visualization of protein expression was performed using a Zeiss (Germany) fluorescence microscope.

PBS 10×, pH 7,4

Component	Final concentration
NaCl	1,37 M
KCl	26,8 mM
$Na_2HPO_4x2H_2O$	64,6 mM
KH_2PO_4	14,7 mM
Water	up to 1l

Name	Source	Dilution	Company
ABCA3	Mouse	1:500	Seven Hills Bioreagents
CHOP	Rabbit	1:100	Santa Cruz
cleaved Caspase-3	Rabbit	1:500	Cell Signaling

Table 4. List of primary antibodies used in immunofluorescence studies.

3.2.12.Cloning

3.2.12.1. Cloning of DNA fragments into plasmids

For cloning of the mouse full length *Chop* cDNA into pAdTrack-CMV-vector (Addgene), and *Mzf-1, Sp-1, Ap-1, c-Ets-1* cDNAs into the pCMV-3Tag-4a-vector (Agilent Technologies), reverse transcription was performed using RNA extracts from mouse lung tissue in order to synthesize complementary DNA (cDNA). Then the full-length cDNA's for mentioned genes were amplified using gene-specific primers (Table 4) and HotStar-HighFidelity Polymerase (Qiagen) according to the manufacturer's instruction. The *Chop* gene was cloned into the pAdTrack-CMV-vector together with the *Kozak* sequence and its *STOP* codon sequence.

The DNA fragments of the human *CHOP* promoter as well as of the human *ACTB* promoter were amplified from genomic DNA using gene-specific primers (Table 5) and the HotStarTaq DNA Polymerase (Qiagen) according to manufacturer's instruction, and then cloned into the pGL4.14-plasmid [luc2/hygro] (Promega). For deletion analysis, small DNA sequences from the 4th fragment of the human CHOP promoter were cloned using the whole DNA sequence of the 4th fragment as template, and with use of gene-specific primers (Table 6) and HotStarTaq DNA Polymerase (Qiagen). Finally, PCR-generated DNA sequences of the 4th fragment were cloned into the pGL4.14-plasmid.

After amplification, PCR products were in general purified using the PCR purification kit (Qiagen), followed by digestion with restrictions enzymes (for projected cloning) and separation by agarose gel electrophoresis. Digested DNA fragments were gel-purified using the commercially available "QIAquick Gel Extraction Kit" (Qiagen) according to the manufacturer's instruction.

Gene	Restriction enzyme	Primers (5'→3')
Chop	SalI	**F**-CTTGATGTCGAC*GCCACC***ATG**GCAGCTGAGTCCCTGC
	HindIII	**R**-GGTCATAAGCTT*TCA*TGCTTGGTGCAGGCTGAC
Sp-1	EcoRI	**F**-CTTGATGAATTC**ATG**AGCGACCAAGATCACTC
	XhoI	**R**-GGTCATCTCGAGGAAACCATTGCCACTGATATTAAT
c-Ets-1	BamHI	**F**-CTTGATGGATCC**ATG**AAGGCGGCCGTCGATC
	SalI	**R**-GGTCATGTCGACGTCAGCATCCGGCTTTACAT

Ap-1	BamHI	**F**-CTTGATGGATCC**ATG**ACTGCAAAGATGGAAACGA
	XhoI	**R**-GGTCATCTCGAGAAACGTTTGCAACTGCTGCG
Mzf-1	EcoRI	**F**-CTTGATGAATTC**ATG**AGACCCACTGTGCTGGGCTCC
	XhoI	**R**-GGTCATCTCGAGCTCAGTGCTGTGGACACGCTGGT

Table 5. List of primers used for cloning of genes.

Fragment name	Restriction enzyme	Primers (5'→3')
1st fragment	KpnI	**F**-CTTGATGGTACCCGGCTAATTTTTGTATTTTTAGTA
	HindIII	**R**-GGTCATAAGCTTGACCTCGGGAGCGCCTG
2nd fragment	KpnI	**F**-CTTGATGGTACCTCCCCTGCGCGTGCGCG
	HindIII	**R**-GGTCATAAGCTTGCCGACCTCGGGAGCTG
3rd fragment	KpnI	**F**-CTTGATGGTACCCGGCTAATTTTTGTATTTTTAGTA
	HindIII	**R**-GGTCATAAGCTTCACCGAGGGTGGTGGGAG
4th fragment	KpnI	**F**-CTTGATGGTACCTCCCCGCCCCCCTTTCCT
	HindIII	**R**-GGTCATAAGCTTGCCCCGCCCCGTGCCT
5th fragment	KpnI	**F**-CTTGATGGTACCCAAGTCACATGACCTCTGCC
	HindIII	**R**-GGTCATAAGCTTGGTGTGCTGATGCGCGCCT
Actin promotor	KpnI	**F**-CTTGATGGTACCGAAAGGGTGACAAGGACAGG
	HindIII	**R**-GGTCATAAGCTTTACCCCCTCTCCCCTCCTT

Table 6. List of primers used for cloning of human *CHOP* promoter.

	Fragment name	Restriction enzyme	Primers (5'→3')
Forward	4.1 fragment - ΔSP-C	KpnI	**F-** CTTGATGGTACCCCTTTCCTCCCCTCCCCC
		HindIII	**R-** GGTCATAAGCTTGCCCCGCCCCGTGCCT
	4.2 fragment - ΔSP-1/MZF-1	KpnI	**F-** CTTGATGGTACCCCCGCTACACTCCCCTC
		HindIII	**R-** GGTCATAAGCTTGCCCCGCCCCGTGCCT

	4.3 fragment - ΔSP-1/MZF-1/MZF-1	KpnI	**F-** CTTGATGGTACCGCGCGCATGACTCACCCA
		HindIII	**R-** GGTCATAAGCTTGCCCCGCCCCGTGCCT
	4.4 fragment - ΔSP-1/MZF-1/MZF-1/AP-1	KpnI	**F-** CTTGATGGTACCCCTCCTCCGTGAAGCCTC
		HindIII	**R-** GGTCATAAGCTTGCCCCGCCCCGTGCCT
	4.5 fragment - ΔSP-1/MZF-1/MZF-1/AP-1/c-Ets-1	KpnI	**F-** CTTGATGGTACCTCCGACACTACGTCGACCC
		HindIII	**R-** GGTCATAAGCTTGCCCCGCCCCGTGCCT
Reverse	4.6 fragment - ΔSP-1	KpnI	**F-** CTTGATGGTACCTCCCCGCCCCCCTTTCCT
		HindIII	**R-** GGTCATAAGCTTGTCCCTCGCATCCGCCA
	4.7 fragment - ΔSP-1/c-Ets-1	KpnI	**F-** CTTGATGGTACCTCCCCGCCCCCCTTTCCT
		HindIII	**R-** GGTCATAAGCTTGGCTTTGGGTCACGAGGC
	4.8 fragment - ΔSP-1/c-Ets-1/AP-1	KpnI	**F-** CTTGATGGTACCTCCCCGCCCCCCTTTCCT
		HindIII	**R-** GGTCATAAGCTTGCGCGCCGCGGAGGG
	4.9 fragment - ΔSP-1/c-Ets-1/AP-1/MZF-1	KpnI	**F-** CTTGATGGTACCTCCCCGCCCCCCTTTCCT
		HindIII	**R-** GGTCATAAGCTTGGAGTGTAGCGGGGGGG
	4.10 fragment - ΔSP-1/c-Ets-1/AP-1/MZF-1/MZF-1	KpnI	**F-** CTTGATGGTACCTCCCCGCCCCCCTTTCCTCC
		HindIII	**R-** GGTCATAAGCTTAGGGGCGGGGGGAAAGGAGG

Table 7. List of primers used for amplification of very small DNA fragments of the 4th fragment of the human *CHOP* promotor (For "deletion analysis" of the 4th fragment).

Legend: Restriction site; *Kozak* – sequence; **Start codon**; *Stop codon*; **F** – forward primer; **R** – reverse primer

3.2.12.2. Ligation of DNA fragments into vectors

The purified DNA fragments were ligated into the linearized plasmids by using the NEB T4 DNA ligase in a molar ratio of roughly 1:3. The ligation reaction was incubated overnight at 16°C and then transformed into competent cells of *E. coli*.

Components	Volume/concentration
DNA fragment	100 ng
Linearized plasmid	50 ng
10 × ligase buffer	1µl
T4 DNA ligase	1U
H_2O	up to 10 µl

3.2.12.3. Heat shock transformation and amplification of plasmids

The transformation of TOP10 *E. coli* cells was performed by the heat shock method. The ligation mixture or the plasmid DNA was gently mixed with one aliquot of the competent cells and incubated at 4°C for 30 min. Then the mixture was heated immediately to 42°C for 2 min and cooled on ice for 2 min. Thereafter, the bacterial cells were cultured in 1 ml Luria Bertani medium (LB) medium without antibiotics at 37°C for 1.5h. An aliquot of 100 µl was spread over an ampicillin (100µg/ml) containing agar dish and incubated overnight at 37°C.

Luria Bertani medium (LB) medium

Components	Final concentration
Tryptone	10 g/l
Yeast extract	5 g/l
NaCl	10 g/l
pH	7.3

After overnight incubation, individual bacterial colonies were picked from the plate on the following day and inoculated in LB medium containing the appropriate antibiotics. The bacterial tubes were shaken overnight at 37°C at 222 rpm. Plasmids were subsequently isolated using a mini or maxi plasmid isolation kit (Qiagen).

In order to evaluate the efficiency of cloning, an aliquot of purified plasmids was sent to GATC-Biotech for sequencing. The primers used for sequencing are listed in Table 7. The sequences were then compared to the expected insert sequence obtained from the NCBI (NCBI gene/NCBI-Blast)

Vector	Primers (5'→3')
pCMV-3Tag-4a	**F**-GTCTATATAAGCAGAGCTG
pGL4.14 [luc2/hygro]	**F**-CTAGCAAAATAGGCTGTCCC
pAdTrack-CMV	**R**-GTGGTATGGCTGATTATGATCAG

Table 8. List of primers used for sequencing.

3.2.13. Agarose gel electrophoresis

In order to separate and analyze DNA-fragments, the agarose gel electrophoresis technique was used. DNA was analyzed in 1.5% (w/v) agarose gels. Agarose was mixed with 1×TAE buffer and 0,5 µg/ml ethidium bromide. The DNA samples were mixed with 5×DNA loading buffer and loaded onto the gel. The gel was then run in 1×TAE buffer at 100 V. The size of separated DNA was determined with use of a DNA molecular weight standard (SmartLadder, Eurogentech). The DNA was visualized by UV light in a Biorad Gel Doc XR+ gel imager.

1× TAE

Component	Final concentration
Tris-acetate, pH 8,0	40 mM
EDTA, pH 8,0	1 mM

5× DNA loading buffer

Component	Final concentration
Bromophenol blue	0.01% (w/v)
Glycerol	40 % (w/v)

3.2.14. Epithelial cell lines with conditional, stable overexpression of transgenes

3.2.14.1. Stable transfection of cell lines and selection of double-transgenic cells

The pTet-on plasmid (containing rtTA) and the pBI-L-vector were purchased from Clontech (Clontech Laboratories Inc). The pBI-L vector allows the expression of both the gene of interest and luciferase from a bidirectional tetracycline responsive promoter. The mouse *Chop* gene was already cloned into the pBI-L vector by Dr. Martin Hühn. All procedures for creating of stable, double-transgenic cell lines were performed according to Clontech guidelines.

Prior to transfection, pTet-on vector was linearized with *HindIII* and purified with PCR purification kit (Qiagen) according to manufacturer's instructions. MLE12 cells were seeded in 6-well plates in full-growth DMEM/F12 media, as described in chapter 3.2.3 and allowed to grow for 24 h. Cells were transfected with 2 µg of the *linearized* Tet-on vector containing a rtTA (reverse tetracycline-controlled activator protein) element and a neomycin resistance gene. Transfection was carried out using TurboFect reagent (Thermo Scientific) as described in chapter 3.2.16. After 32 h post-transfection, growth DMEM/F12 medium was replaced with medium containing 500 µg/ml of G418/geneticin (Roche) and left for additional 48 h.

Stably transfected cell lines were established by limit dilution method. After transfection, MLE12 cells were plated onto 96-well plates in volume of 100 µl at a density of approximately 5000 cells per well. After 2–3 weeks with changing of the culture media every 3-4 days, resistant cells to the G418 grew. If cells were able to grow out in the wells in the presence of G418/geneticin, the cells were regarded as a transgenic cell lines and were referred to as MLE12/Tet-on cells.

In order to check efficiency of stable transfection, all antibiotic (G418) resistant clones were transiently transfected with 2 µg of the pBI-L-empty vector using the TurboFect reagent (Thermo Scientific) (chapter 3.2.16). After 24 h of transfection cells were treated with 1 µg/ml of doxycyclin (Sigma Aldrich) or left untreated, and incubated for additional 24 h. Thereafter, cells were harvested, and the activity of reporter gene *luciferase* was determined (see below, chapter 3.2.14.2). Only luciferase-positive clones were used for second round of stable transfection.

Using the same method of transfection described above, MLE12/Tet-on cells were co-transfected either with pBI-L-empty-vector or the pBI-L-CHOP together with the *linear hygromycin marker* (Clontech Laboratories Inc.) in a ratio 1:15. Before transfection, these plasmids were linearized with *AatII* and purified by PCR purification kit (Qiagen), as described before. The *linear hygromycin marker* is a DNA fragment containing the hygromycin resistance gene for the selection of stably transfected cells. Multiple cell clones of stably co-transfected MLE12/Tet-on cells were selected by adding 100 µg/ml of the G418 (Roche) and 100 µg/ml of the hygromycin (InvivoGen) to the medium. Selection process was performed for 2-3 weeks after co-transfection. Finally, obtained cell clones were named MLE12/pBI-L-CHOP or MLE12/pBI-L-EV cells, respectively.

3.2.14.2. Identification of stably transfected cells using a reporter gene-luciferase assay

The pBI-L vector contains the bidirectional tet-responsive promotor (P_{bi-1}), which allows to express a gene of interest and the *Luciferase* gene at the same time.

In order to identify MLE12/pBI-L-CHOP or MLE12/pBI-L-EV cells in which *Chop* or *Luciferase* expression was effectively regulated by doxycyclin, all antibiotics (G418 and hygromycin) resistant clones were treated with 1 µg/ml of doxycyclin (Sigma Aldrich) or left untreated. After 24 h of treatment, the cells were harvested, and the activity of the reporter gene Luciferase was detected using the "Luciferase Reporter Assay System" (Promega) as described in chapter 3.2.19. If the luciferase activity of the cells was low without doxycyclin induction, but high with doxycyclin induction, the clonal population was considered to be stably transfected MLE12/pBI-L-*Chop* or MLE12/pBI-L-EV cells in which transgene expression was effectively regulated by doxycyclin. These clones were used in subsequent experiments.

3.2.15. Viral techniques

3.2.15.1. Vectors used for homologous recombination in bacteria

The *in vitro*-studies with use of adenoviral overexpression systems were approved by the local authorities ([Regierungspräsidium Gießen], No.: IV44-53r 30.03 UGI 106.13.02). For creating of adenoviruses, two vectors were used. The first adenoviral plasmid was

pAdEasy-1 (Addgene), which contains all Ad5 (genome of adenovirus, generation 5) sequences except nucleotides 1–3,533 (encoding the E1 genes) and nucleotides 28,130–30,820 (encoding E3 gene). The second vector was pAdTrack-CMV (Addgene) which is used for expression of transgenes. It contains a CMV promotor and a polylinker for insertion of exogenous transgenes. This site is surrounded by adenoviral sequences (‘‘arms’’) that allow the homologous recombination with pAdEasy-1. The left arm contains Ad5 nucleotides 34,931–35,935, which mediate the homologous recombination with pAdEasy-vectors in *E. coli*, and contains inverted terminal repeat (ITR) and packaging signal sequences (nucleotides 1–480 of Ad5), which are required for viral production in mammalian cells. The right arm contains again Ad5 nucleotides 3,534–5,790, which mediate homologous recombination with the pAdEasy-vector. *PacI* restriction sites are surrounding both arms. The pAdTrack-CMV-plasmid also contains a *kanamycin* resistance gene as well as the *GFP* gene under control of independent CMV promotor.

3.2.15.2. Generation of recombinant adenoviral plasmids by homologous recombination in *E. coli*.

Cloning of the mouse *Chop* gene into pAdTrack-CMV was performed as described in chapter 3.2.12.

Before co-transformation, either pAdTrack-CMV-EV or pAdTrack-CMV-CHOP were linearized with *PmeI.* To create either pAd-EV or pAd-CHOP, 1 µg of the linearized pAdTrack-CMV-EV or pAdTrack-CMV-*Chop* was co-transformed with 100 ng of the supercoiled circular pAdEasy-1-plasmid into *E. coli* BJ5183 cells (Agilent Technologies), as described in chapter 3.2.12.3. 16h after transformation, 20 kanamycin-resistant clones were picked up and inoculated in LB medium containing 50µg/ml of kanamycin, and incubated for additional 16h at 37°C. Plasmids were isolated and purified by using phenol/chloroform/isoamyl alcohol (25:24:1) extraction and ethanol precipitation. Clones were first screened by analyzing their supercoiled sizes on agarose gels, by comparing them with pAdEasy-1 controls; and candidate clones were then digested with *BamHI* and *PacI* restriction endonucleases to verify proper recombination. Afterwards, plasmid-DNA of the positive clones was transformed into *E. coli* XL-10 Gold cells (Agilent Technologies), and propagated overnight at 37°C in 100 ml of LB media

containing 50µg/ml of kanamycin. After that, plasmids were isolated using maxi-plasmid purification kit (Qiagen).

3.2.15.3. Production of adenoviruses in mammalian cells

Transfection of mammalian cells was performed using the transfection reagent TurboFect as described in chapter 3.2.16. Approximately 1.5×10^6 HEK293T- "packaging cells" were plated in 25 cm^2-flasks, and reached after 24h 50–70% confluency. Before transfection procedure, 4 µg of recombinant adenoviral vector pAd-EV and pAd-CHOP was digested with *PacI* and ethanol precipitated. Both linearized adenoviral vectors pAd-EV and pAd-CHOP were then used for transfection of each 25- cm^2 flask. Transfected cells were monitored for GFP expression, and collected during 20 days after transfection by scraping cells from flasks and pelleting them along with any floating cells in the culture supernatants. In order to get viral particles, cells were destroyed by three cycles of freezing at -80°C and rapid thawing at 37°C. Afterwards, whole viral lysate was used to infect 10×10^6 HEK 293T cells in a 75 cm^2 flask, two flasks were used for each viruses. Five days later, viruses were harvested as described above and proceeded to 3rd round of infection, where 35 of 75 cm^2 flasks were infected. The efficiency of such infections could be conveniently followed with GFP; after three to four days, cells were harvested and viruses were isolated as described above. Cell lysate containing either Ad-EV or Ad-CHOP were used for determination of viral titer and infection of AECII.

3.2.15.4. Tissue culture infectious dose 50 ($TCID_{50}$)

The $TCID_{50}$ method is based on the development of CPE (cytopathic effect) in HEK293T cells using end-point dilutions to estimate the titer.

HEK 293T cells were plated in 96-well-plates to reach 5×10^3 cell density one day before infection, and left for 16h to adhere in a humidified atmosphere at 37°C and 5% CO_2. Virus titrations were performed by applying virus-dilutions onto cells, which grew in 96-well-plates in medium containing the diluted viruses. Titrations were carried out from 10^{-3} to 10^{-10} fold dilutions. 10^{-6} and 10^{-7} dilutions were necessary to determine the endpoint for Ad-EV and Ad-CHOP. The efficiency of virus titrations were monitored with GFP

expression, after five days of infection. The titer was expressed as the log10 TCID50/ml and PFU/ml.

3.2.16. Transient transfection

Cells were transiently transfected using TurboFect reagent (Thermo Scientific) according to the manufacturer's instruction on 6- or 12-well plates. Transfections were performed, when cells reached 60-70% confluency. On the day of transfection, plasmid DNA was diluted with serum-free DMEM-F12 or DMEM (depends on cell line) without use of antibiotics. After that, transfection reagent was added to the mixture and incubated for 30 min at room temperature in order to form the complex between plasmid DNA and cationic transfection reagent, which in turn was added onto cells. After 6 h, the transfection mixture was replaced with complete DMEM-F12 or DMEM medium. Cells were harvested and analyzed for gene and protein expression after a given time point.

3.2.17. Cytotoxicity assay

The "Cytotoxicity Detection Kit" (Roche) contains a colorimetric assay for the quantification of cell death and cell lysis, based on the measurement of lactate dehydrogenase (LDH) activity released from the cytosol of damaged cells into the cell-culture medium. The relative LDH release is directly proportional to the cell death level in an experimental setting. LDH assay was performed according to manufacturer's instructions. Experiments were performed on 12-well plates, each well with a volume of 1 ml. As a positive control, cells were treated for 5 min with 500 µl of 2% Triton-X-100 in full medium. For measuring cell death, 500 µl of cell supernatants were transferred into new tubes and centrifuged at 1000×g for 5 min. Subsequently, the reaction mix from the kit was added, and the absorbance at 490 nm was measured by an ELISA-plate reader (SpectraFluor Plus, Tecan). The raw data were analyzed according to the formula stated below and presented as a % of relative LDH release into the medium.

$$\frac{{}^{\text{Absorbance}}\,\text{Medium} - {}^{\text{Absorbance}}\,\text{Blank}}{{}^{\text{Absorbance}}\,\text{Medium} + \text{Triton-}\times 100 - {}^{\text{Absorbance}}\,\text{Blank}} \times 100\% = \text{LDH relative release}$$

For each sample, two biological replicates were employed and three independent experiments had been performed.

3.2.18. Measurement of fibroblast proliferation after incubation with supernatants of Chop overexpressing epithelial cells.

WST-1 (4- [3- (4- iodophenyl)- 2- (4-nitrophenyl)- 2H- 5-tetrazolio]- 1,3-benzene disulphonate) is a colorimetric reagent that quantifies mitochondrial dehydrogenase activity and thus reflects cell viability. Cell proliferation, measurements for WST-1 assay (Roche) was performed according to manufacturer's instructions. Briefly, MLE12/pBI-L-CHOP or MLE12/pBI-L-EV cells were grown in 12-well plates in complete medium containing 100 µg/ml G418 and hygromycin. At 60% confluency, cells were treated for 6h, 12h, 24h and 48h with 1 µg/ml of the doxycyclin (Sigma Aldrich) or left untreated. Thereafter, supernatants of Chop overexpressing MLE 12 cells were used for lung fibroblast – proliferation experiments.

Meanwhile, approximately $5x10^3$/ml Mlg cells (mouse lung fibroblast cell line) were seeded in 96-well plates. Then, 100 µl of culture supernatant from MLE12/pBI-L-CHOP-overexpressing MLE 12 cells or MLE12/pBI-L-EV-expressing MLE 12 cells were transferred to Mlg cells and incubated for an additional 24h. After that, WST-1 reagent was added to Mlg cells and re-incubated for 2h in the dark at 37°C and 5% CO_2. The absorbance of each well was then determined by an ELISA reader (Tecan) at 450 nm. A triplicate of untreated cells was taken as blank. The average absorbance of blank should range between 0.1-0.2. The sample absorbance was calculated as:

Sample absorbance = Absorbance measured – Average absorbance of blank.

3.2.19. Luciferase and β-galactosidase assay

The Luciferase assay system is used to study gene expression and other cellular events coupled to gene expression, such as receptor activity, intracellular signal transduction, mRNA processing, protein folding and protein-protein interactions. The β-Galactosidase assay is used to determine the efficiency of transfection and the normalization of luciferase activity.

Luciferase assay (Promega) and β-Galactosidase assay (Promega) were done according to the manufacturer's instruction. Briefly, after transfection and treatment with chemicals at appropriate time points, cells were washed with ice-cold PBS and "Reporter lysis buffer" (Promega) was applied, 200 µl per well of a 12-well plate. For lysis of cells, one cycle of freezing at -80°C overnight and thawing on ice was performed. Then cells were scraped and centrifuged for 10 min at 13000×g at 4°C, in order to get clear extract. To measure luciferase and β-galactosidase activity, 20 µl and 50 µl of clear extract were used, respectively. Luciferase-activity was then measured by using a luminometer (SpectraFluor Plus, Tecan); and β-galactosidase activity was determined by absorbance at 420 nm using the spectrophotometer (SpectraFluor Plus, Tecan). Results of luciferase activity were normalized against β-galactosidase activity.

3.2.20. Site-directed mutagenesis

Single point mutations were introduced into the *AP-1* and *c-Ets-1* consensus sequences of the human *CHOP* promoter to inactivate their binding activity in the pGL4-Hygro-4th fragment-promoter construct containing these both consensus sequences using the "QuickChange Site-Directed Mutagenesis Kit" (Stratagene) according to the manufacturer's instructions. To produce a double-mutant pGL4-Hygro-4th fragment of the human *CHOP* promotor, the plasmid containing the 4th fragment with mutated *AP-1* binding site was used as a template. Primers which were used for site directed mutagenesis are listed in table 8. Successful insertion of the mutations into the *AP-1* and *c-Ets-1* consensus sequences of the *CHOP* promoter were confirmed by sequencing.

Primer name	Forward Primer (5'→3')	Reverse Primer (5'→3')
ΔAP-1	CGCGGCGCGCA**g**GACTCACCCAC	GTGGGTGAGTC**c**TGCGCGCCGCG
Δc-Ets-1	CAAAGCCACTTC**t**GGGTCCGACACT	AGTGTCGGACCC**a**GAAGTGGCTTTG

Table 9. List of primers used for site directed mutagenesis (lowercase letters represent mutations)

3.2.21. Chromatin immunoprecipitation (ChIP)

Chromatin immunoprecipitation was performed on 10×10^6 MLE 12 cells. Cells were cross-linked with 1% (w/v) formaldehyde (Sigma) for 10 min, and subsequently stopped by adding 125 mM glycine (Roche) for 5 min. Cells were then washed three times with ice-cold PBS and lysed for 10 min with "L1 lysis buffer". After that, cell lysates were centrifuged at 13000×g at 4°C for 10 min. Pellets were subsequently lysed for 5 min with "L2 nuclear resuspension buffer". Obtained nuclear extracts were stored at -80°C or proceeded for sonication. Nuclear extracts were sonicated using a Sonorex sonicator (Bandeling). One part from the chromatin solution was used as an input. The remaining was diluted 1:9 with dilution buffer, and incubated overnight with 200 µl of Protein A agarose beads conjugated with salmon sperm DNA (Millipore), with rotation. Afterwards, diluted chromatin was centrifuged at 1000×g at 4°C for 3 min, in order to remove the beads, and transferred into new tubes. Chromatin was then incubated with 2 µg of irrelevant IgG (Santa Cruz Biotechnology), or antibody for AP-1 (Abcam) or c-Ets-1 (Abcam) overnight, with rotation at 8 rpm/min, followed by incubation with 30 µl of the Protein A agarose beads conjugated with salmon sperm DNA (Millipore). In order to remove nonspecific binding, the beads were washed in low salt washing buffer, high salt washing buffer, LiCl-washing buffer and then with TE buffer. Finally, chromatin was eluted with 200 µl of DNA-elution buffer supplemented with 1 mg/ml of RNaseA (Thermo Scientific) for 1 hour at 37°C, with shaking at 900 rpm. Thereafter, chromatin was incubated in elution buffer containing 10 mg/ml Proteinase K (Peqlab) for 2 hours at 56°C with shaking, at 900 rpm. The crosslinking was reversed overnight at 65°C after addition of NaCl to a final concentration of 200 mM. The DNA was then purified with phenol, chloroform and isoamyl alcohol (25:24:1). DNA was dissolved in 30 µl TE buffer and stored at -20°C for further experiments. Before proceeding with PCR, eluted DNA was diluted 1:4. PCR was performed using HotStar Taq DNA Polymerase (Qiagen) with the primers indicated in table 9. PCR conditions were as follows: Hot Start: 95°C for 20 min, denaturation: 94°C for 30 sec, annealing: 60°C for 30 sec, elongation: 70°C for 1 min, for 40 cycles. PCR products were subsequently analyzed by 1,5% agarose gel electrophoresis. *Gapdh*-PCR was employed as a negative control.

For simultaneous analysis of ChIP-CoIP experiments, beads were washed three times with TE buffer, followed by mixing with 20 µl of SDS-loading-buffer, and analyzed by immunoblotting as described in chapters 3.2.9; 3.2.10.

L1 lysis buffer:

Component	Final concentration
Tris-HCl, pH 8.0,	50 mM
EDTA, pH 8.0	2 mM
NP-40	0.1 % (w/v)
Glycerol	10% (w/v)
PMSF	1 mM
Protease inhibitor cocktail	1 mM
Phosphatase inhibitor cocktail	1×
DTT	2 mM

L2 nuclear resuspension buffer:

Component	Final concentration
Tris-HCl, pH 8.0,	50 mM
EDTA, pH 8.0	5 mM
SDS	1% (w/v)
PMSF	1 mM
Protease inhibitor cocktail	1 mM
Phosphatase inhibitor cocktail	1×
DTT	2 mM

Dilution buffer:

Component	Final concentration
Tris-HCl, pH 8.0,	50 mM
EDTA, pH 8.0	5 mM
NP-40	0.5 % (w/v)
NaCl	200 mM
PMSF	1 mM
Protease inhibitor cocktail	1 mM
Phosphatase inhibitor cocktail	1×

Low salt washing buffer:

Component	Final concentration
Tris-HCl, pH 8.0,	20 mM
EDTA, pH 8.0	2 mM
NP-40	1% (w/v)
SDS	0.1% (w/v)
NaCl	150 mM
PMSF	1 mM

High salt washing buffer:

Component	Final concentration
Tris-HCl, pH 8.0,	20 mM
EDTA, pH 8.0	2 mM
NP-40	1 % (w/v)
SDS	0.1 % (w/v)
NaCl	500 mM
PMSF	1 mM

LiCl washing buffer:

Component	Final concentration
Tris-HCl, pH 8.0,	10 mM
EDTA, pH 8.0	1 mM
NP-40	1 % (w/v)
Na-deoxycholate	1 % (w/v)
LiCl	250 mM
PMSF	1 mM

DNA elution buffer:

Component	Final concentration
Tris-HCl, pH 8.0	10 mM
EDTA, pH 8.0	1 mM
$NaHCO_3$	100 mM
SDS	1% (w/v)

TE buffer:

Component	Final concentration
Tris-HCl, pH 8.0,	10 mM
EDTA, pH 8.0	1 mM

Primer name	Forward Primer (5'→3')	Reverse Primer (5'→3')	PCR product size
4th fragment (*Chop* promoter), full length	TCCCCGCCCCCCTTTCCT	GCCCCGCCCCGTGCCT	222 bp.
Gapdh	ATGGTTGCCACTGGGGATCT	TGCCAAAGCCTAGGGGAAGA	174 bp.

Table 10. List of primers used for ChIP-PCR

3.2.22. Bioinformatic analysis of *CHOP* promoter

The genomic sequence of the 5' upstream flanking region of the human and mouse *Chop* gene were retrieved from Ensemble (http://www.ensembl.org) (Accession No. ENSG00000175197; No. ENSMUSG00000025408 respectively). Sequence analysis seeking for putative transcription factor-binding sites was performed using databases MatInspektor (Genomatix): (https://www.genomatix.de/online_help/help_matinspector/matinspector_help.html) and TFSEARCH: (www.cbrc.jp/research/db/TFSEARCH.html). Sequence alignments were performed using a Blast/NCBI: http://blast.ncbi.nlm.nih.gov/Blast.cgi).

3.2.23. Statistical analysis

Data were analyzed by GraphPad Prism 5.02 software using student's t-test. Each experiment was performed in duplicate or triplicate, dependent on the style of experiment. Significance is indicated by *p<0.05, **p<0.01, ***p<0.001, n.s. = not significant, and data are expressed as mean ± SD.

4 Results

4.1. Promoter analysis of human *CHOP* gene

4.1.1. *In silico* analysis of the *CHOP* gene promoter

To investigate the transcriptional regulation of the *CHOP* gene in the lung on molecular level, an *in silico* analysis was performed for both the human and the murine *Chop* gene. For this purpose, the genomic sequence of the upstream flanking regions were retrieved from Ensemble (Accession No. ENSG00000175197; No. ENSMUSG00000025408 respectively). Consequently, the TFSEARCH and MatInspektor (Genomatix) software were used to identify putative transcriptional factor binding sites, with scores > 90% considered as positive (Figure 4.1; Appendix: 6.1.1.). The *in silico* analysis of the 2700 kb to +1 bp 5'-flanking region of the human *CHOP* gene clearly indicated 31 putative *cis*-regulatory transcription factor binding sites of 17 different transcription factors together with the well-known amino acid response elements (AARE) at bp. -310 and -778 bp. and the endoplasmic reticulum stress elements (ERSE) at bp. -93 and -103 bp. Six putative stimulating protein (Sp1) binding elements were identified at bp. positions -111, -299, -1883, -2190, -2490, and -2535, one for avian erythroblastosis virus E26 oncogene homolog 1 (c-Ets-1) at bp. -199, one for activator protein (AP-1 or c-Jun) at bp. -240, three myeloid zinc finger 1 (MZF-1) binding sites at positions bp. -259, -274, and -2605, two viral myb oncogene (v-Myb) binding sites at bp. -420 and -429, two GATA family of transcription factors (GATA1 and 2) binding sites at bp. -439 and -1402, two DNA-binding protein Ikaros (Lyf-1) binding sites at bp. -710, and -1025, one homeobox protein Nkx-2.5 binding site at bp. -736, two runt related transcription factor 1 (oncogene AML-1) binding sites at bp. -812 and -1557, one binding site for heat shock factor 2 (HSF2) at bp. -862, one for fork head box protein D3 (FOXD3 or HFH-2) at bp. -978, one for C/EBP regulatory element at bp. -1670, one for T-cell acute lymphocytic leukemia protein 1 (Tal1) at bp. -1742, and two putative regulatory elements for members of the transcription factor STAT family at bp. -1957 and -2284 (see Figure 4.1).

Both, the human and the mouse *Chop* promoter were shown to have a TATA element (box) 31 bp. (Appendix: 6.1.1. and 6.1.2. respectively).

In order to show similarity between human and mouse *Chop* promoters, a sequence alignment was performed using a BLAST/NCBI analysis. According to the sequence

alignment depicted in 6.1.4. of the appendix, human and mouse *Chop* promoters revealed a high extent of homology and, at least for the first 500 bp. of the flanking region of the promoter sequence, a comparable pattern of putative transcription factor binding sites (Suppl. Figure 1). However, according to the Ensemble database, only the human *CHOP* promoter contained the full DNA sequence, whereas the one for the murine sequence was incomplete in this database.

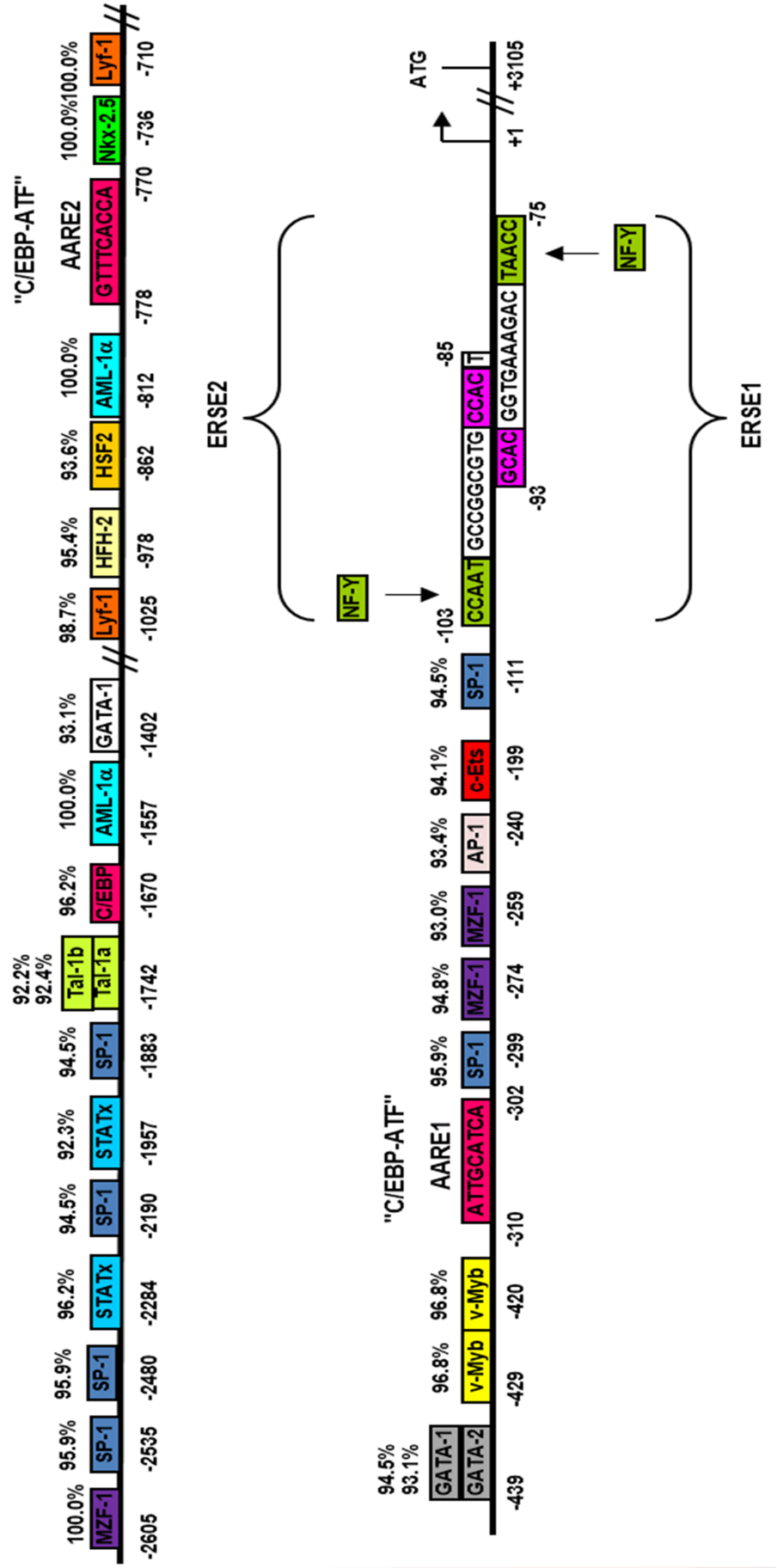

Figure 4.1. Schematic illustration of the 5' flanking region of the human *CHOP* gene. TFSEARCH and MatInspektor software were used to identify putative transcriptional factor binding sites in the human *CHOP* promoter. The transcriptional initiation site (bent arrow) and translational site (ATG) are shown. High scoring transcription factor binding sites in the 2.6 kb. 5' flanking region of the human *CHOP* gene are illustrated, those scoring >90% were considered as the positives. Definitions for the abbreviations are written in the text above.

4.1.2. CHOP is induced by tunicamycin in different epithelial cell lines

Before starting the promoter analysis, we had to consider the time course for induction of the *CHOP* gene. CHOP is expressed at very low levels in both dividing and post-mitotic cells [116] [117]. In order to induce *CHOP* expression, tunicamycin was chosen as a widely accepted, chemical inducer of ER-stress. Tunicamycin is an antibiotic, which blocks N-glycosylation of proteins in the ER, subsequently leading to aggregation of misfolded proteins in the ER and induction of the UPR [47].

The human alveolar epithelial cell type II (AEC2)-like cell line A549, originally derived from a lung cancer patient, and the murine AECII-like MLE 12 cell line, originally obtained from SV40-transformed AEC2s, were used. As a non lung cell comparator line, we also used human embryonic kidney cell (HEK293T) line. Cells were treated with 2 µg of tunicamycin (Tu) or DMSO as solvent control for 15 min, 30 min, 1h, 2h, and 5h. After these time points, cells were harvested for analysis of CHOP expression on protein level.

As shown in Figure 4.2, CHOP protein level was equally increased after 2h of treatment of the cells with tunicamycin in all three cell lines, whereas the solvent control DMSO alone did not increase the protein level of CHOP. Based on this result, treatment of cells with 2 µg of Tu for 2h was used for all promoter analysis experiments.

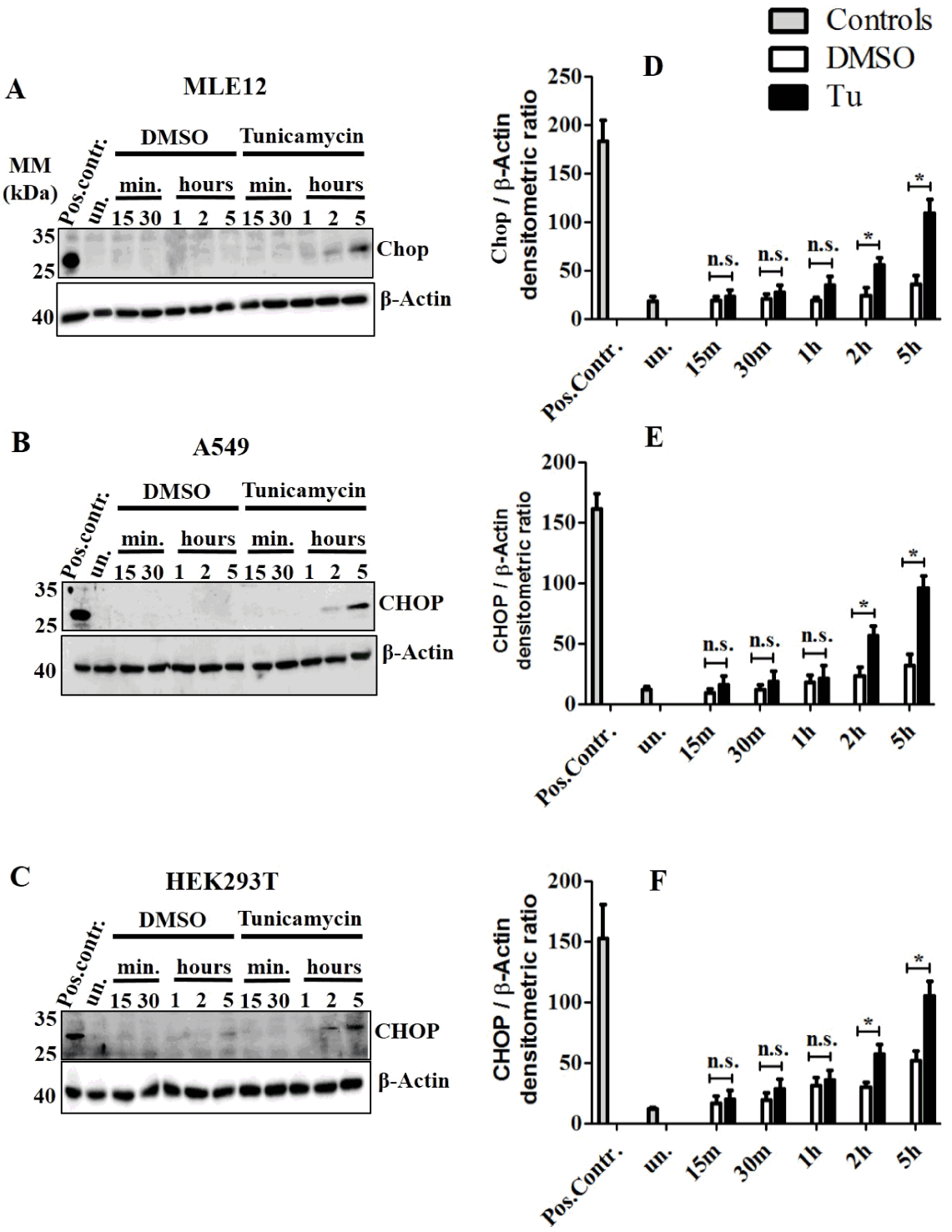

Figure 4.2. CHOP is induced by tunicamycin in different epithelial cell lines.
(**A,B,C**) MLE 12, A549, HEK293T cell lines were treated with 2 μg of tunicamycin for different time points. After each time point, cells were harvested for protein isolation and western blot was performed using antibodies against CHOP and β-Actin (internal control). (**D,E,F**) Densitometric quantification of immunoblots for MLE 12, A549, HEK293T cell lines, respectively. Pos.contr. – positive control, appropriate cell line treated with 1 μg of tunicamycin for 24h. un. – untreated cells. Statistical significance was assured by Student's t-test. Significance levels is *$p<0.05$. n.s. – non significant, N=3.

4.1.3. Reporter gene assays to identify relevant response elements in the human *CHOP* promoter

To investigate the transcriptional regulation of the human *CHOP* gene, five different fragments of genomic DNA were amplified per PCR from human donor lungs and, amplified PCR products were checked by sequencing (data not shown). Figure 4.3. demonstrates a schematic structure of the five amplified fragments with their respective regulatory elements. We were particularly interested in the 4th and 5th fragment, as these did not include the ERSE and AARE elements.

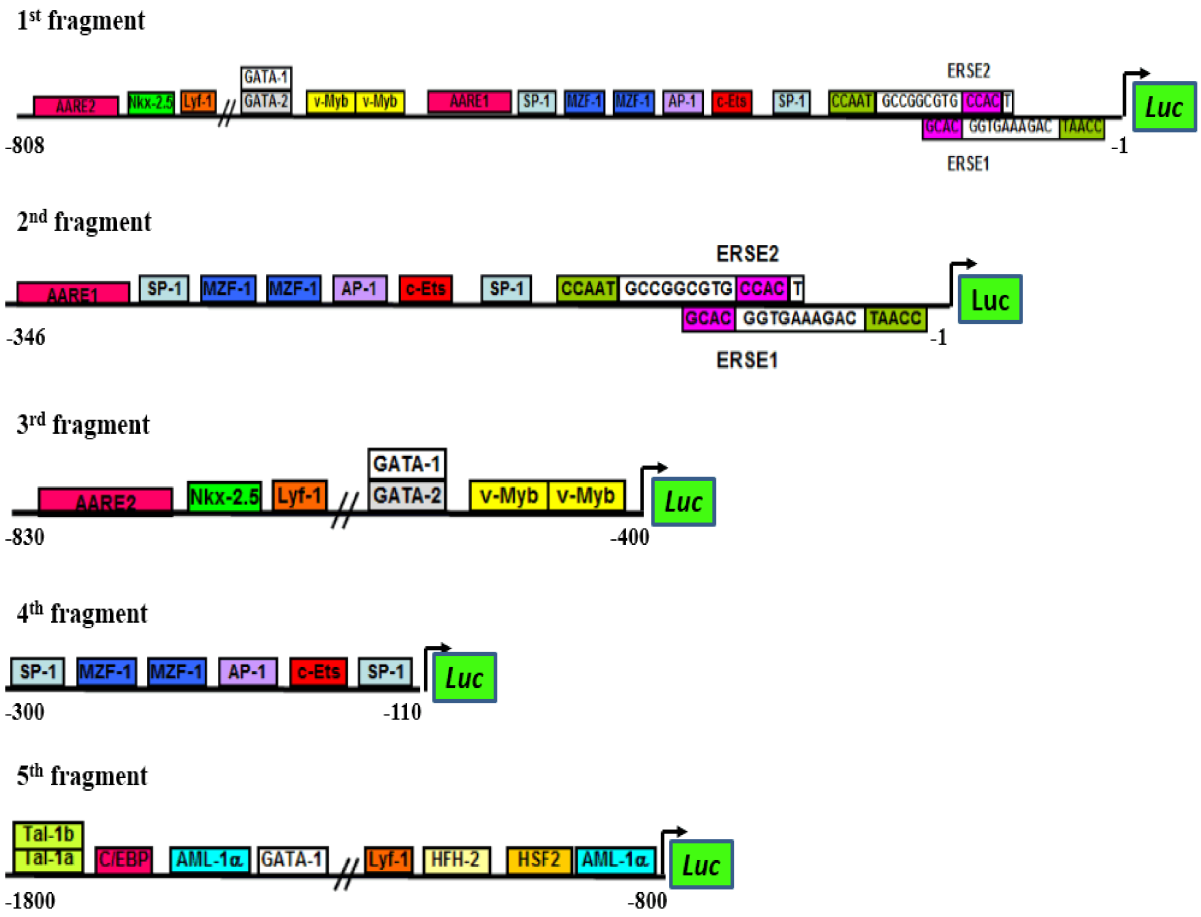

Figure 4.3. Schematic illustration of *CHOP* promoter fragments used in the luciferase reporter assay analysis.
2 kb of human *CHOP* promoter was divided into 5 fragments using a PCR amplification. 1st fragment (nt. -1 - -808) containing ERSE1 and 2 as well as AARE1 and 2, 2nd fragment (nt. -1 - -346) containing ERSE1 and 2, and AARE1, 3rd fragment (nt. -400 - -830) with AARE2, 4th fragment (nt. -110 - -300) and 5th fragment (nt. -800 - -1800). All five promoter fragments were cloned into pGL4-Hygro vector upstream of the *Luciferase* reporter gene.

In addition, a *β-Actin* promoter fragment (nt. -1 - -1000), which does not contain any of those transcription binding sites found in the human *CHOP* promoter, was used as a

negative control. All five genomic DNA fragments containing the human *CHOP* promoter region and *β-Actin* promoter control fragment were cloned into pGL4-Hygro vector (Promega) upstream of the start codon of the *Luciferase* reporter gene. Transcription activity of these promoter – luciferase constructs was studied by transient transfection of A549 and MLE 12 cell lines, respectively. In order to check if the activity of the human *CHOP* promoter is regulated in a lung specific manner, I also transfected the HEK293T cell line with mentioned above constructs and analyzed them employing a Luciferase Reporter Assay System (Promega).

All reporter plasmids and pGL4-Hygro empty vector were transiently transfected together with a vector containing a *β-Galactosidase* gene as internal control into A549, MLE12 and HEK293T cells (as described in chapter 3.2.16). 24 hours post transfection, cells were treated with tunicamycin as a ER stress inducer agent and DMSO as solvent control for 2h or left untreated. Then cells were harvested for determination of luciferase activity and β-galactosidase (as described in chapter 3.2.19).

The transcriptional activity of the reporter plasmids is presented in Figure 4.4. Transfection of the cells with 1st (-1 - -808) and 2nd (-1 - -346) fragment resulted in a much higher promoter activity as compared to the pGL4-Hygro (empty) vector or the *β-Actin* promoter fragment in response to tunicamycin treatment. In contrast, the 3rd (-400 - -830) and the 5th (-800 - -1800) fragment displayed a rather weak promoter activity under these conditions, whereas the 4th (-110 - -300) fragment, which does not contain any ERSE and AARE elements, also showed a significant increase in promoter activity in response to tunicamycin versus DMSO treatment and in comparison to the empty vector or the *β-Actin* promoter fragment control (Figure 4.4.).

Together, these results suggest that some of the transcriptional binding sites, which are located in the 4th (-110 - -300) fragment of the human *CHOP* promoter, greatly contributed to the induction of the *Luciferase* and may play a significant role in the transcriptional regulation of the human *CHOP* gene. As the regulatory profile was superimposable in lung cells versus kidney cell lines (compare A, B and C part of Figure 4.4.), the transcriptional control of the human *CHOP* promoter does not seem to be lung specific. For the same reason the MLE 12 cell line was used for all other consecutive experiments employing lung epithelial cell lines.

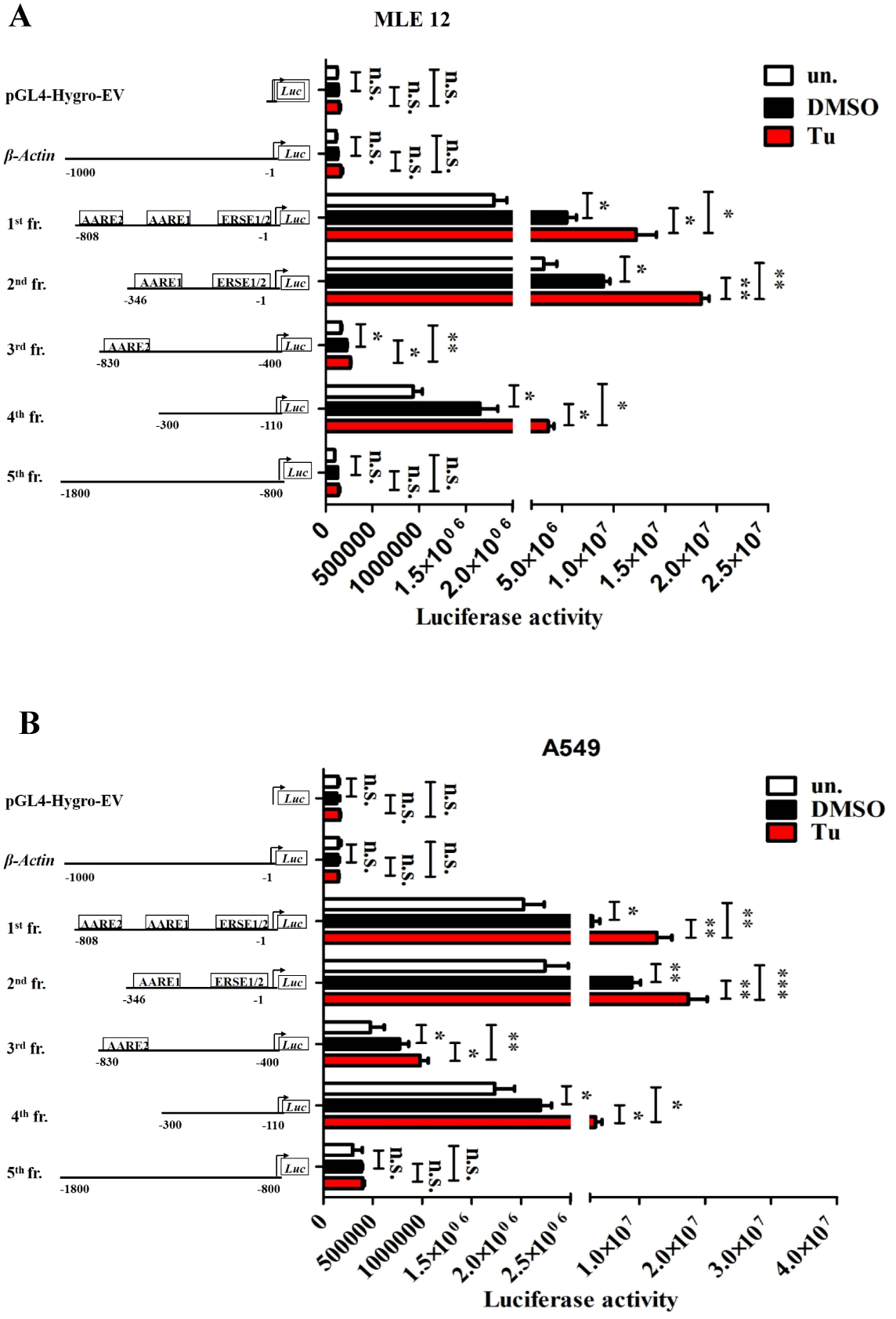
A
MLE 12
un.
DMSO
Tu
pGL4-Hygro-EV
β-Actin
-1000
-1
1st fr.
AARE2
AARE1
ERSE1/2
-808
2nd fr.
-346
3rd fr.
-830
-400
4th fr.
-300
-110
5th fr.
-1800
-800
Luc
n.s.
*
**
0
500000
1000000
1.5×10^6
2.0×10^6
5.0×10^6
1.0×10^7
1.5×10^7
2.0×10^7
2.5×10^7
Luciferase activity
B
A549
un.
DMSO
Tu
pGL4-Hygro-EV
β-Actin
1st fr.
2nd fr.
3rd fr.
4th fr.
5th fr.
n.s.
*
**
0
500000
1000000
1.5×10^6
2.0×10^6
2.5×10^6
1.0×10^7
2.0×10^7
3.0×10^7
4.0×10^7
Luciferase activity

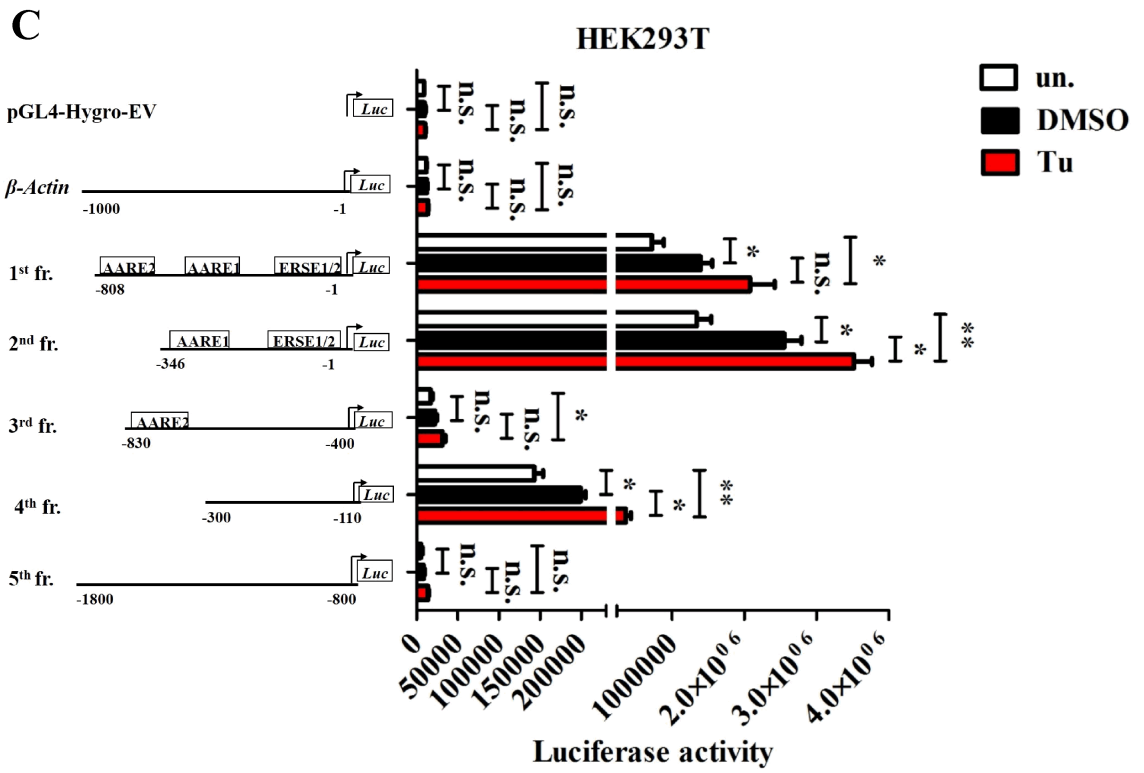

Figure 4.4. Mapping of the endogenous response elements in the human *CHOP* promoter.

Reporter plasmids containing either one of the 5 fragments of human *CHOP* promoter or the *β-Actin* promoter fragment or pGL4-Hygro empty vector (EV) were transiently transfected together with a vector containing a *β-Galactosidase* gene into MLE 12 (**A**), A549 (**B**), and HEK293T (**C**) cells, respectively. 24h post-transfection cells were treated with 2 µg of tunicamycin for 2h. After 2h incubation with tunicamycin, cells were harvested for measuring of luciferase and β-galactosidase activity. Results are presented as corrected luciferase activity, using β-galactosidase activity as reference. Statistical significance was assured by Student's t-test. Significance levels is *p<0.05, **p<0.01, ***p<0.001. n.s. – non significant, N=3.

4.1.4. AP-1 and c-Ets-1 are potential regulatory elements of the human *CHOP* gene

For identification of the potential transcription binding site in the above mentioned 4th fragment, we performed a deletion analysis of the 4th fragment of the human *CHOP* promoter. For that purpose, different constructs were amplified by PCR and cloned into pGL4-Hygro luciferase reporter vector. Figure 4.5.A depicts the different fragments that have been generated. In every genetic construct, one of the transcription binding site was deleted in forward from 5' to 3' direction (constructs 4.1 – 4.5) and reverse from 3' to 5' direction (constructs 4.6 - 4.10).

All genetic constructs and pGL4-Hygro empty vector were again transiently transfected together with a vector containing a *β-Galactosidase* gene as internal control into MLE 12 cells (as described in chapter 3.2.16). 24 h post-transfection cells, were treated with tunicamycin for induction of ER stress for 2h, DMSO was used as a solvent control. After incubation with tunicamycin, luciferase activity was measured (as described in chapter 3.2.19).

Luciferase activity of the different constructs is presented in Figure 4.5. Based on the analysis of luciferase activity, it's visible that constructs 4.1-4.4 lacking the two *MZFs, SP-1, AP-1* in forward direction and construct 4.6 lacking the *SP-1* in reverse direction, were not responsible for induction of luciferase. However, construct 4.5, which was lacking the *c-Ets-1* binding site in forward direction, did not show any luciferase activity in comparison with the full length version of the 4th fragment. From these data we concluded that the *c-Ets-1* site would be essential for induction of the *CHOP* gene *in vitro*. In contrast to the weak promoter activity of construct 4.5. containing the *c-Ets-1* site deletion in forward direction, deletion of the *c-Ets-1* in reverse direction (see construct 4.7 in Fig. 4.5) did only result in a marginal decline in luciferase activity in response to tunicamycin treatment as compared to full length fragment 4 or fragment 4.6. containing *c-Ets-1*. Even more striking, when *AP-1* (and *c-Ets-1*) binding sites were deleted in reverse direction (construct 4.8), complete suppression of luciferase activity was detected, suggesting that the *AP-1* site may be of importance for the activation of the *CHOP* gene *in vitro* as well.

Our interpretation of these results was, that *AP-1* and *c-Ets-1* transcription binding sites are both important for the activation of luciferase activity and therefore for the transcriptional control of the human *CHOP* gene *in vitro*. Furthermore, because we could observe differences in the luciferase activity in constructs 4.4 – 4.5 and 4.7 – 4.8, we hypothesized that these two transcription factors support each other or even physically interact with each other, and bind to the 4th fragment of the human *CHOP* promoter under ER stress conditions.

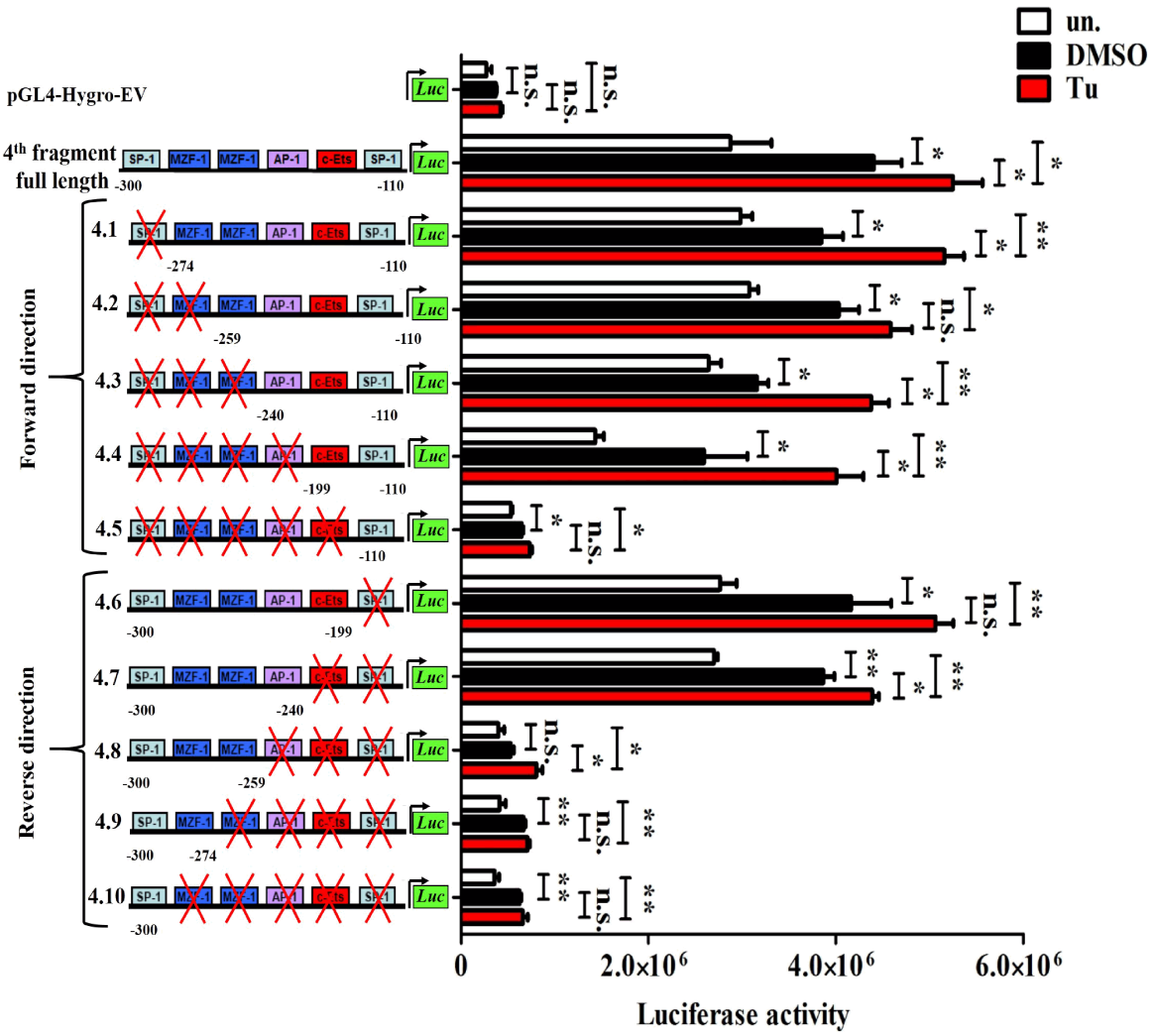

Figure 4.5. AP-1 and c-Ets-1 are potential regulatory elements of human *CHOP* gene.

Deletion analysis of the 4th fragment of human *CHOP* promoter. Deleted fragments were created by PCR amplification using 4th fragment as a template and then cloned upstream of the *Luciferase* gene. In every genetic construct, one of the transcription the binding site was deleted in forward from 5' to 3' direction (constructs 4.1 – 4.5) and reverse from 3' to 5' direction (constructs 4.6 - 4.10). Reporter plasmids containing different fragments or pGL4-Hygro empty vector (EV) were transiently transfected together with a vector containing a *β-Galactosidase* gene into MLE 12 cells. 24h post transfection, cells were treated with 2 µg of tunicamycin for 2h. After 2h incubation with tunicamycin, cells were harvested for measuring of luciferase activity using Luciferase Reporter Assay System. Results are presented as a luciferase activity. Statistical significance was assured by Student's t-test. Significance levels is *p<0.05, **p<0.01. n.s. – non significant, N=3.

4.1.5. The transcription factors Ap-1 and c-Ets-1 are up-regulated during ER stress.

Drawn against the experimental data as shown above, and the putative role of *AP-1* and *c-Ets-1* in the transcriptional control of the human *CHOP* promoter, we checked the expression status of AP-1 and c-Ets-1 as well as other UPR markers such as Atf4, Atf6 and Xbp-1 in response to the induction of ER stress by tunicamycin in MLE 12 cells.

For such purpose, MLE 12 cells were treated with 2 µg tunicamycin for different time points and harvested for protein analysis. Western Blot analysis was done for Atf4, Atf6, c-Ets-1 and Ap-1 (as described in chapter 3.2.10). Due to lack of a good antibody to detect the spliced form of Xbp-1, the alternative splicing of *Xbp-1* was assessed on mRNA level using specific primers which recognized only spliced form of mouse *Xbp-1* (as described in chapter 3.2.7).

Under these conditions, Ap-1 and c-Ets-1, as well as all other UPR markers, were significantly up-regulated on protein level after 1h, and *Xbp-1* was alternatively spliced on mRNA level after 2h in response to tunicamycin versus solvent (DMSO) treatment (see Figure 4.6.).

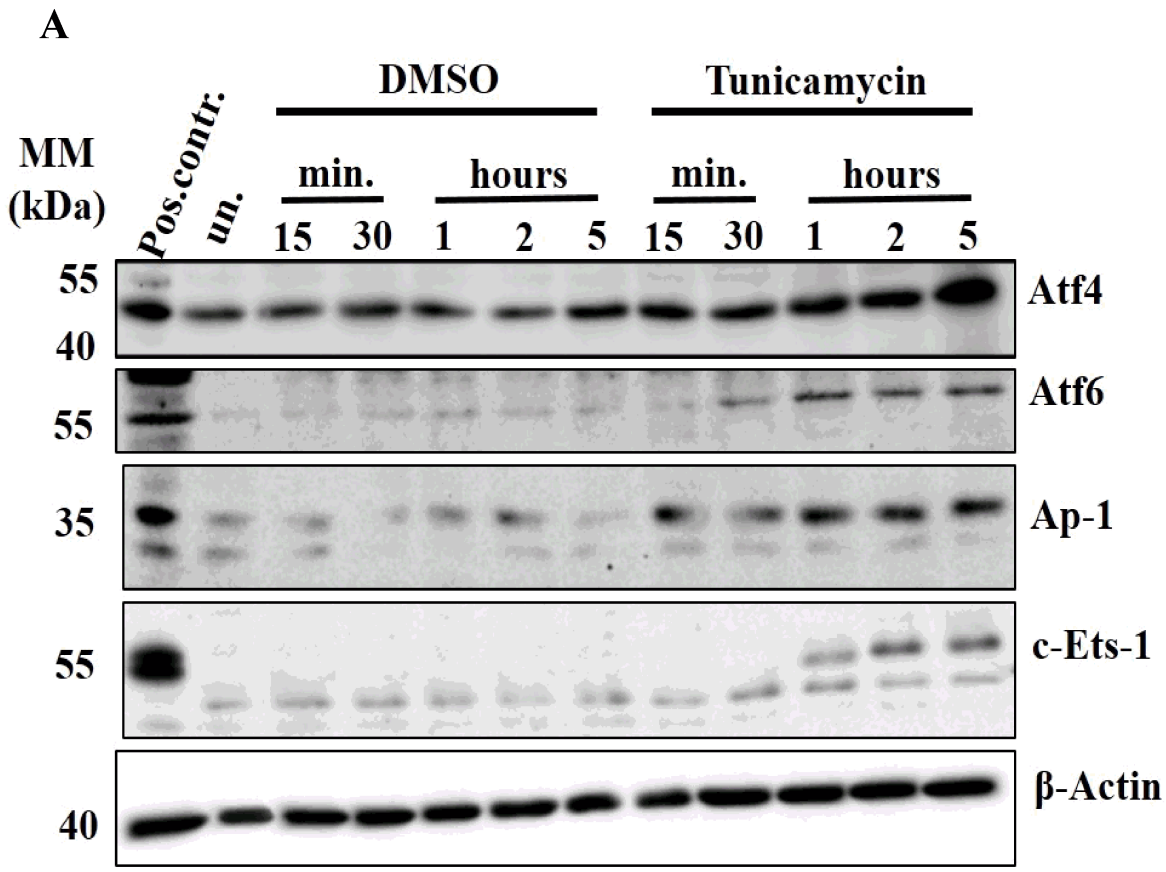

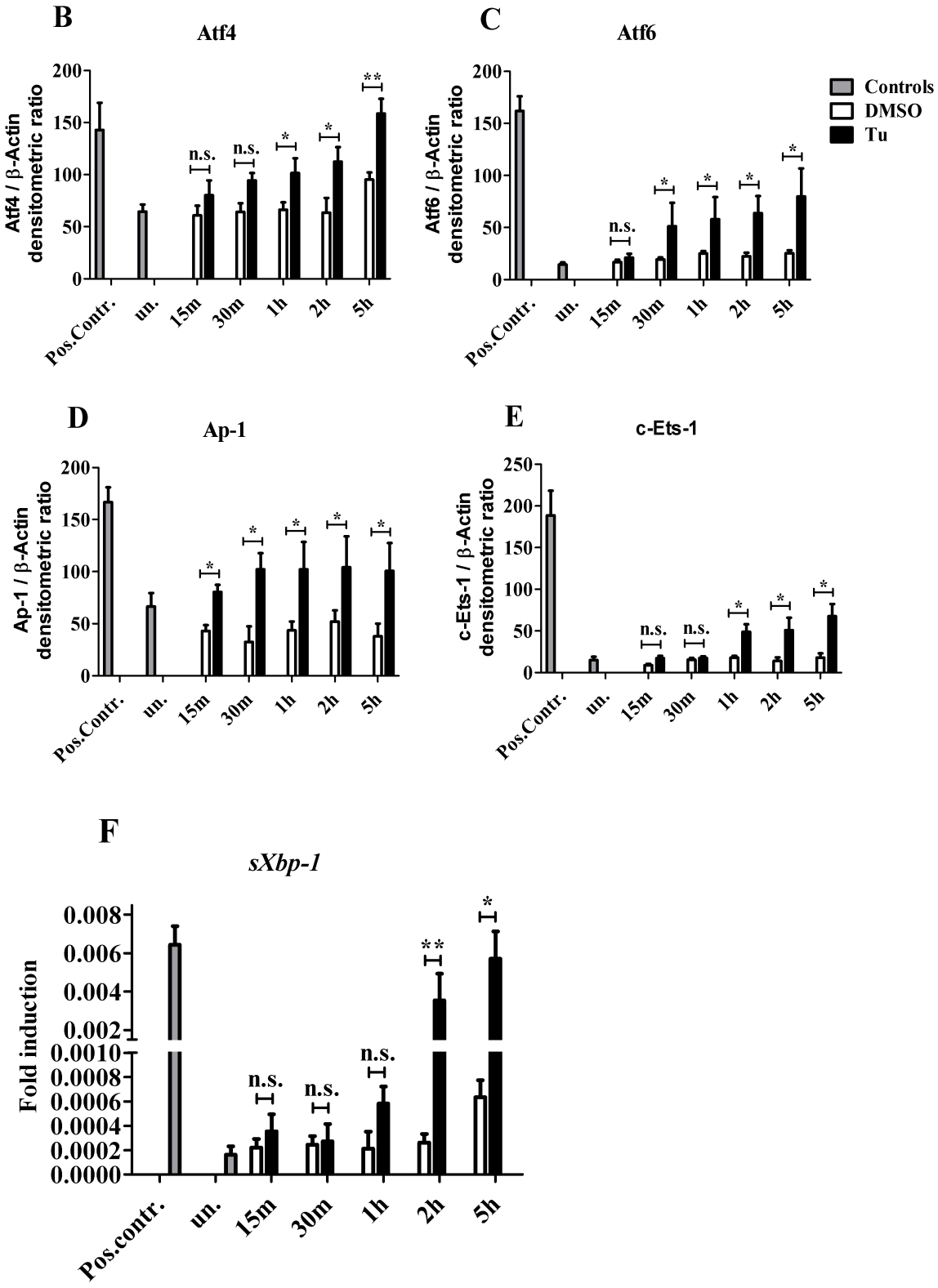

Figure 4.6. Ap-1 and c-Ets-1 are up-regulated during ER stress.

(A) MLE 12 cells were treated with 2 µg tunicamycin for 15 min, 30 min, 1h, 2h, 5h. Western blotting was performed using anti-ATF4, ATF6, AP-1, c-Ets-1 and β-Actin (internal control) antibodies as indicated. **(B,C,D,E)** Densitomeric quantification of immunoblots for Atf4, Atf6, Ap-1 and c-Ets-1, respectively. **(F)** Expression of spliced *Xbp-1* mRNA in MLE 12 cells treated with tunicamycin. Pos.Contr. – positive control, MLE 12 cells treated with 1 µg of tunicamycin for 24h. un. – untreated, MLE 12 cells kept in

culture for 5h. Statistical significance was assured by Student's t-test. Significance levels is *p<0.05, **p<0.01. n.s. – non significant, N=3.

4.1.6. Impact of *AP-1* and *c-Ets-1* binding to the *CHOP* promoter regulation

To investigate the functional role of the *AP-1* and *c-Ets-1* binding motifs, as well as to prove hypothesis of interaction between these two transcriptional factors, two different experiments were performed:

In the first type of experiments, the binding activity of transcription factors which were found in 4th fragment of human *CHOP* promoter, was analyzed using luciferase reporter gene assays. For that, each transcription factor found in the 4th fragment of human *CHOP* promoter was cloned into pCMV-3Tag-4a expression vector, up-stream of c-myc-tag. After that, these constructs containing the single transcription factor were co-transfected together with the 4th fragment-*CHOP* – Luc promoter construct, and the control *β-Galactosidase* reporter gene construct, into MLE 12 cells. Additionally, both, Ap-1 and c-Ets-1 transcription factors were co-transfected together with 4th fragment-*CHOP* – Luc promoter construct and *β-Galactosidase* reporter gene construct (as described in chapter 3.2.16). As a negative control, the c-myc-tag-empty vector was co-transfected together with the pGL4-Hygro-empty vector, and the plasmid containing the *β-Galactosidase* reporter gene. 24 hours post-transfection, cells were treated with tunicamycin with a final concentration 2 μg for two hours, and were then analyzed by reporter luciferase assay (as described in chapter 3.2.19).

As shown in Figure 4.7., overexpression of all transcription factors modestly induced luciferase activity under ER stress conditions in comparison with empty vectors and co-transfections of the 4th fragment and c-myc-tag empty vector alone. Even more, when both Ap-1 and c-Ets-1 transcription factors were co-transfected together with the 4th fragment *CHOP* – Luc promoter construct, the highest level of luciferase activity was observed (Figure 4.7.).

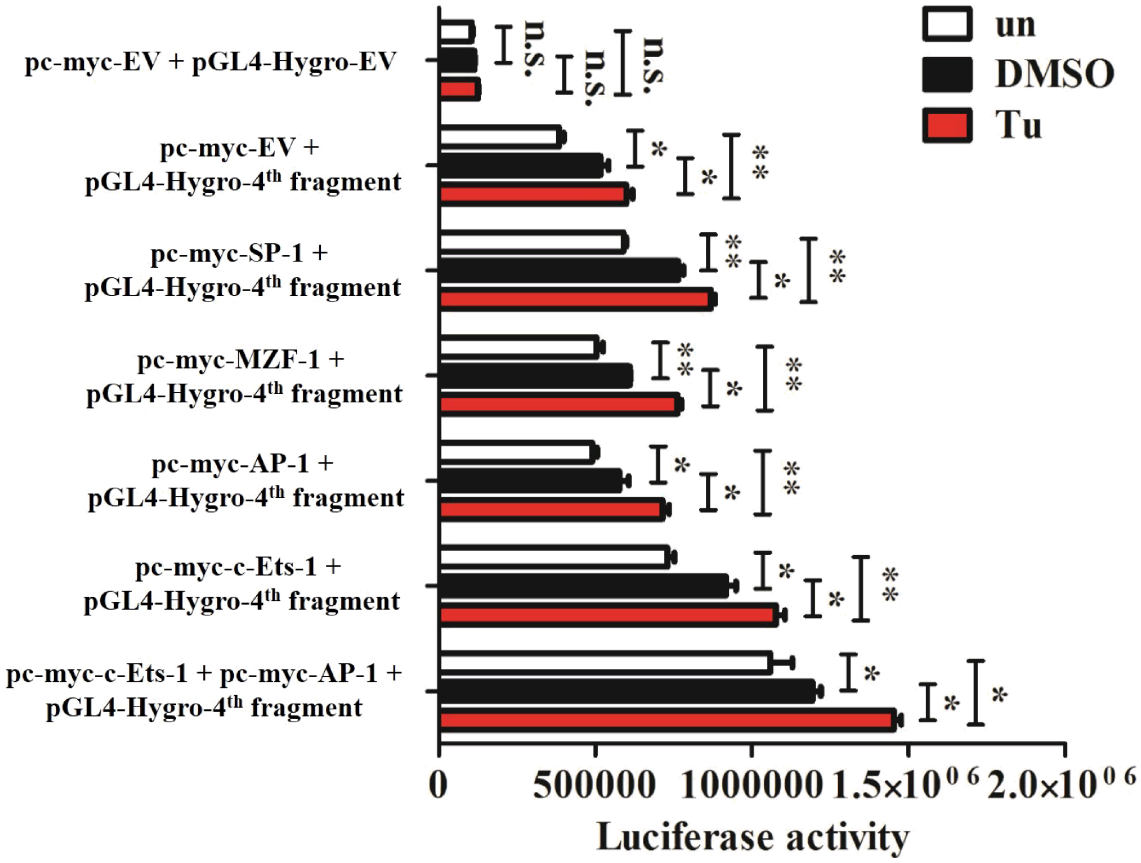

Figure 4.7. AP-1 and c-Ets-1 regulate the human *CHOP* promoter *in vitro*.
Effects of active forms of Sp-1, Mzf-1, Ap-1 and c-Ets-1 on *CHOP* promoter activity were assessed after co-transfection of 4th fragment of human *CHOP*-Luc with expression plasmids pCMV-3tag-4a(c-myc-tag)-SP-1, MZF-1, AP-1 and c-Ets-1 + *β-Galactosidase* plasmid or co-transfection CHOP-Luc + pCMV-3tag-4a(c-myc-tag)-AP-1 + pCMV-3tag-4a(c-myc-tag)-c-Ets-1 + *β-Galactosidase* plasmid into MLE 12 cells. 24h post-transfection, cells were treated with 2 µg tunicamycin for 2h, then collected for measuring of luciferase activity. Statistical significance was assured by Student's t-test. Significance levels is *p<0.05, **p<0.01. n.s. – non significant, N=3.

It is generally known that the essential nucleosides in the consensus transcription factor binding sequences are thymine (5'-a**t**gactcaccca-3') for AP-1 and cytosine (5'-acttc**c**gggtcc-3') for c-Ets-1. Making use of this knowledge and employing the QuickChange site directed mutagenesis kit, we generated constructs, in which thymine was exchanged to guanine in the *AP-1* binding site of the 4th *CHOP* promotor fragment (construct pΔAP-1), in which cytosine was mutated to thymine in the *c-Ets-1* binding site (construct pΔc-Ets-1), or in which both of these sites were mutated (construct pΔAP1 + pΔc-Ets-1) (as described in chapter 3.2.20). Then these mutated constructs versus the wild-type 4th fragment of the *CHOP* promoter construct or pGL4-Hygro empty vector were transfected together with a *β-Galactosidase* reporter gene construct into MLE 12 cells and analyzed by transient reporter assay to compare the activities of the mutants in

the presence or absence of tunicamycin as ER-stress inducing agent (as described in chapter 3.2.16 and 3.2.19)

As can be taken from Figure 4.8., the mutation in the *AP-1* and *c-Ets-1* binding sites (constructs pΔAP1 and pΔc-Ets-1, respectively) resulted in a partial decrease in the *Luciferase* activity reflecting the transcriptional activity. However, when the double-mutant, in which the binding sites of both, *AP-1* and *c-Ets-1*, were mutated (construct "pΔAP1-pΔc-Ets-1"), the promoter activity was greatly reduced and, in fact, almost reached baseline activity as noted employing the pGL4-Hygro empty vector and the 4th wild-type *CHOP* promoter fragment.

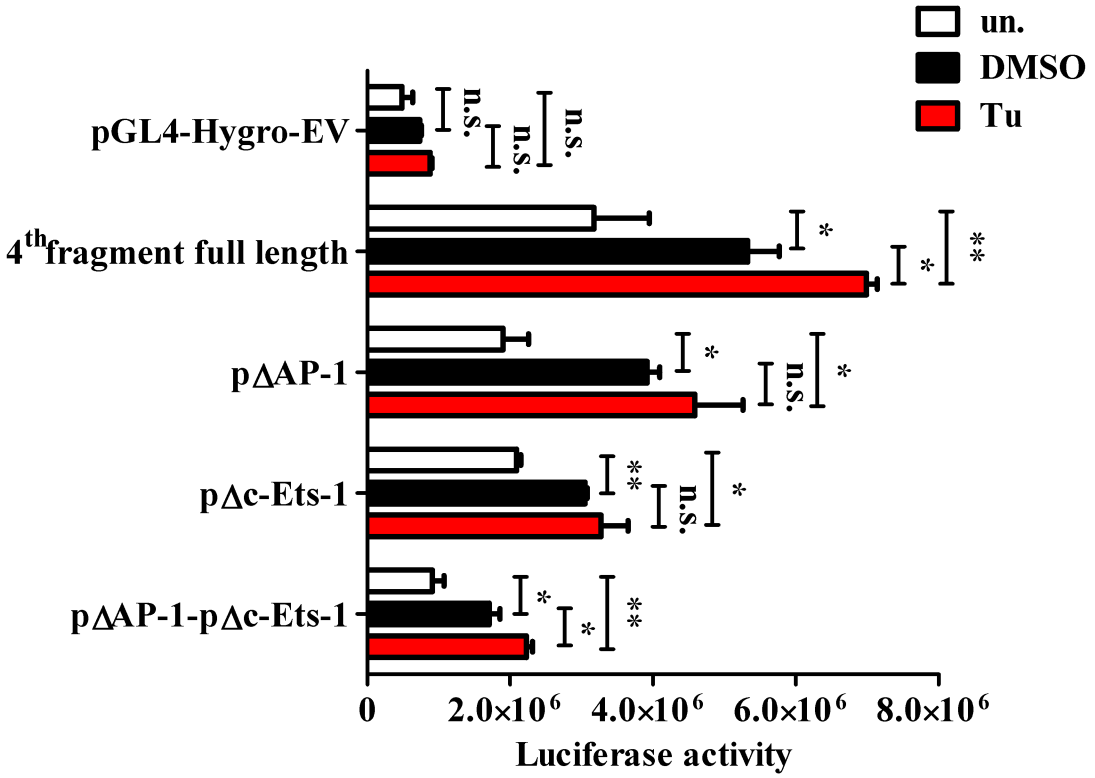

Figure 4.8. Mutational analysis of *CHOP* promoter-luciferase constructs.
Employing the 4th fragment of the *CHOP* promotor, binding sites for *AP-1* (pΔAP-1), or *c-Ets-1* (pΔc-Ets-1) or both (pΔAP-1- pΔc-Ets-1) were site-directed mutated to block transcription factor binding. These fragments, or the wild type 4th fragment of the *CHOP* promotor (4th fragment full length) or the empty vector (pGL4-Hygro-EV) were then transiently transfected together with a *β-Galactosidase* gene into MLE 12 cells. 24h post-transfection, cells were treated with 2 µg tunicamycin for 2h, then collected for measuring of luciferase activity. Statistical significance was assured by Student's t-test. Significance levels is *p<0.05, **p<0.01. n.s. – non significant, N=3.

Collectively, all these results suggest that the *AP-1* and *c-Ets-1* transcription binding sites are indeed important for the regulation of the activity of the human *CHOP* promoter under ER stress conditions. It also appeared that simultaneous action of the AP-1 and c-Ets-1 transcription factors is crucial for induction of *Luciferase* reporter gene activity / *CHOP*

promotor activation. In addition, these two experiments add further proof to the concept of an interaction of the AP-1 and c-Ets-1 transcription factors under ER-stress conditions.

4.1.7. Direct proof of binding of Ap-1 and c-Ets-1 to the 4th fragment of the murine *Chop* promoter *in vitro*

To examine whether or not Ap-1 and c-Ets-1 bind to the 4th fragment of the *Chop* promotor under ER-stress conditions, chromatin immunoprecipitation was performed upon tunicamycin treatment of MLE 12 cells. For that purpose, MLE 12 cells were treated with tunicamycin and DMSO for 2h or left untreated. Then, in order to fix DNA-protein interaction, cells were treated with formaldehyde and ChIP was undertaken as described in the methods section (Chapter 3.2.21). As shown in Figure 4.9., transcription factor Ap-1 indeed binds to the *Ap-1* binding site (lane 12), and transcription factor c-Ets-1 indeed binds to the *c-Ets-1* binding site (lane 13) in the 4th fragment of the murine *Chop* promoter in response to the induction of ER-stress by tunicamycin. In contrast, no binding of Ap-1 and c-Ets-1 to the *Ap-1* and *c-Ets-1* sites was observed in untreated cells, respectively (lanes 4 and 5; Figure 4.9.) and DMSO treatment resulted in a rather weak binding of *Ap-1* and *c-Ets-1* to their respective binding sites (Figure 4.9.; lanes 7 and 9). Negative control primers, designed to amplify a region of *Gapdh* promotor fragment, did not show any enrichment in the Ap-1 and c-Ets-1 ChIP under unstressed and stressed conditions. (Figure 4.9.).

Collectively, the results of these ChIP experiments indicate that Ap-1 and c-Ets-1 truly bind to the *Chop* gene under ER stress conditions.

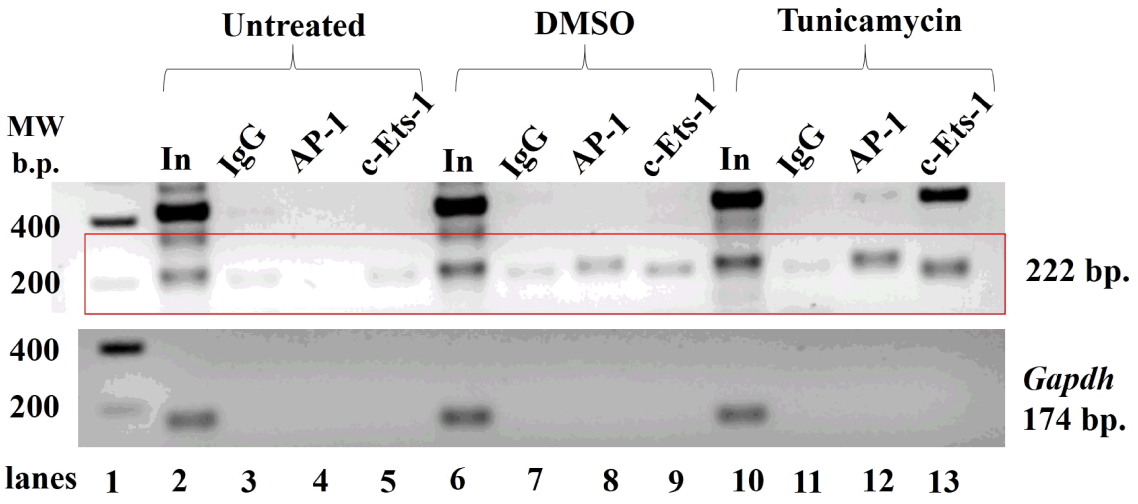

Figure 4.9. Binding of Ap-1 and c-Ets-1 to the 4th fragment of murine *Chop* promoter *in vitro.*
Chromatin immunoprecipitation assays were done on untreated MLE 12 cells ("untreated"; lanes 2-5), on cells treated with DMSO as a solvent control ("DMSO", lanes 6-9), and cells treated with 2 µg of tunicamycin ("Tunicamycin", lanes 10-13). The extracted chromatin was immunoprecipitated with anti-AP-1, anti-c-Ets-1 antibodies or with a non-specific IgG as control as indicated. Recovered DNA was amplified by PCR using primers covering the region of the 4th fragment of murine *Chop* promoter from nucleotides -300 to -110. Amplification by PCR of *Gapdh* by PCR was performed as a negative control for ChIP experiment. Control amplifications were done on pre-immunoprecipitated (''In'') chromatin.

4.1.8. c-Ets-1 interacts with Ap-1 during ER stress *in vitro*

In order to examine the possibility that c-Ets-1 not only binds to its respective binding site in the 4th fragment of the *CHOP* promoter, but also interacts with AP-1, the protein-protein interaction between Ap-1 and c-Ets-1 was analyzed.

As a first step, the classical CoIP approach was applied, which, however, did not produce a meaningful result (not shown in detail, possibly due to a low affinity between the two transcription factors). Therefore, MLE 12 cells were treated for 2h with 2 µg of tunicamycin and then treated with formaldehyde for covalent cross-linking. The nuclear extract was then subjected to immunoprecipitation. Prior to analysis of interaction by SDS gel electrophoresis and western blotting using specific antibodies for AP-1 and c-Ets-1, samples were boiled at 100 °C for 20 min in order to reverse the cross-linked protein complex (as described in chapter 3.2.21).

Under ER stress conditions, c-Ets-1 was co-precipitated with Ap-1 (Figure 4.10 lanes 11 – 12). Control reactions, untreated or DMSO treated cells did not yield detectable co-precipitation for c-Ets-1 and Ap-1 (Figure 4.10.; lanes 2 – 4 and 6 – 8, respectively). Additionally, in samples which were subjected to immunoprecipitation, we could detect the heavy chain of mouse IgG migrating at 55 kDa.

As can be taken from Figure 4.10., Ap-1 appears to form a specific complex with c-Ets-1 especially during ER stress *in vitro*.

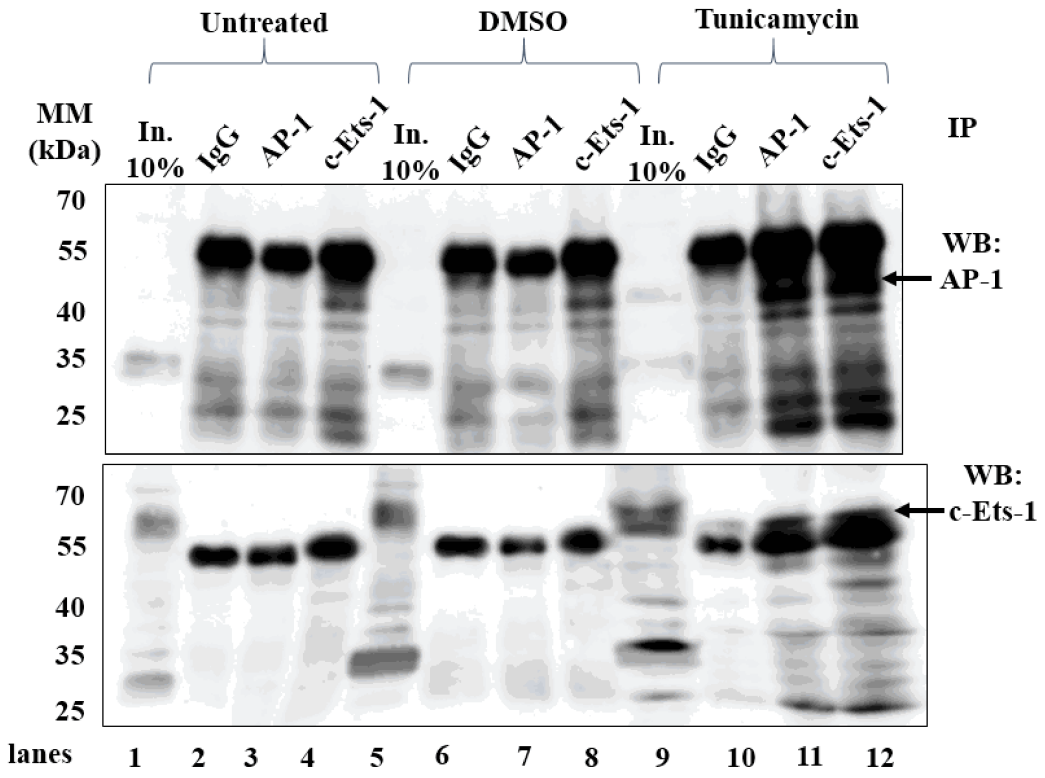

Figure 4.10. c-Ets-1 interacts with Ap-1 during ER stress *in vitro*. Covalent cross-linking, co-immunoprecipitation analysis to examine c-Ets-1 and AP-1 interaction is presented. MLE 12 cells were treated with 2 µg of tunicamycin for 2h, then treated with 1% of formaldehyde, nuclear extracts were subjected to immunoprecipitation and analyzed by western blotting. Immunoprecipitations were done with anti-AP-1 (lanes 3, 7, 11) or anti-c-Ets-1 (lanes 4, 8, 12) antibodies as indicated; IgG (lanes 2, 6, 10) was used as a negative control. Western blotting was done with anti-AP-1 or anti-c-Ets-1 antibodies. 10% of Input (In.) was used as a positive control. Arrows show interaction partner.

4.1.9. Ap-1 and c-Ets-1 overexpression induces endogenous *Chop* expression *in vitro*

To further confirm the involvement of Ap-1 and c-Ets-1 transcription factors in the transcriptional control of the *Chop* gene *in vitro*, Ap-1 and c-Ets-1 were transiently overexpressed alone and together in MLE 12 cells, and time-dependent *Chop* expression was analyzed.

To perform this experiment, MLE 12 cells were transiently transfected with 2 µg of pCMV-3Tag-4a(c-myc-tag)-AP-1 or pCMV-3Tag-4a(c-myc-tag)-c-Ets-1 or 1 µg of each vector (as described in chapter 3.2.16). Cells were harvested for protein analysis after 12h, 24h, 48h post-transfection (as described in chapter 3.2.8 and 3.2.10). Our data indeed suggest that expression of Chop on protein level (Figure 4.11.) was increased in a time-

dependent manner in response to single and simultaneous overexpression of Ap-1 and c-Ets-1 in MLE 12 cells *in vitro*. More interestingly, Chop expression appeared to be even higher in case of combined Ap-1 and c-Ets-1 overexpression (Figure 4.11.), although this did not reach statistical significance.. These results further suggest that synergistic interaction of Ap-1 and c-Ets-1 during ER-stress plays a significant role in the transcriptional control of *Chop*.

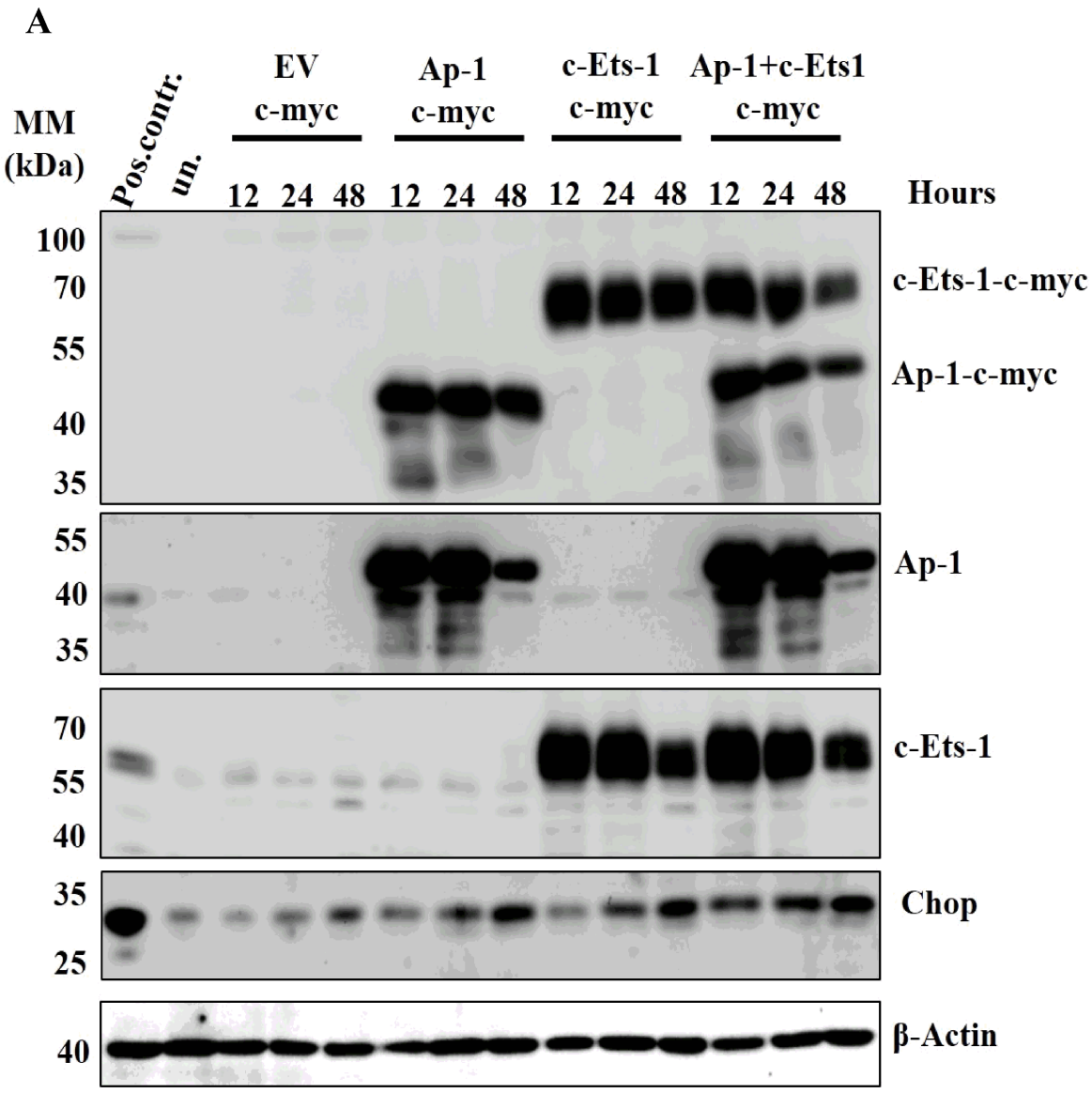

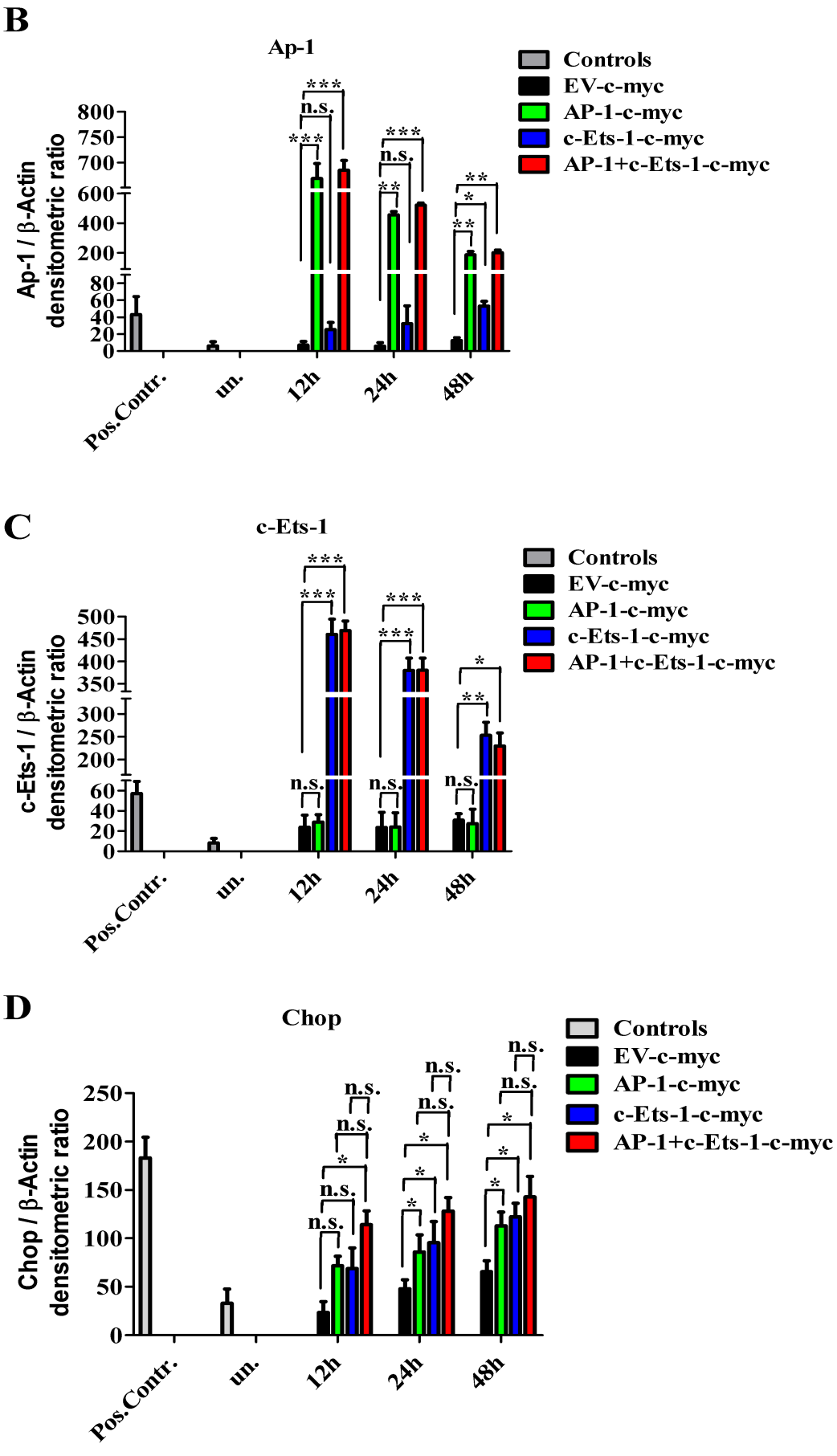
B
Ap-1
Ap-1 / β-Actin densitometric ratio
Controls
EV-c-myc
AP-1-c-myc
c-Ets-1-c-myc
AP-1+c-Ets-1-c-myc
Pos.Contr.
un.
12h
24h
48h
C
c-Ets-1
c-Ets-1 / β-Actin densitometric ratio
D
Chop
Chop / β-Actin densitometric ratio
n.s.

Figure 4.11. Ap-1 and c-Ets-1 overexpression induces *Chop* expression *in vitro*.
(A) Effect of overexpressing Ap-1 and c-Ets-1 protein on *Chop* expression. MLE 12 cells were transiently transfected with 2 µg of pCMV-3Tag-4a(c-myc-tag)-AP-1, pCMV-3Tag-4a(c-myc-tag)-c-Ets-1 pCMV-3Tag-4a(c-myc-tag)-EV as a vector control or 1 µg of pCMV-3Tag-4a(c-myc-tag)-AP-1 and pCMV-3Tag-4a(c-myc-tag)-c-Ets-1were co-transfected. Western blotting was performed using anti-c-myc, AP-1, c-Ets-1, CHOP and β-Actin (internal control) as indicated. **(B,C,D)** Densitometric quantification for Ap-1, c-Ets-1 and Chop respectively. Pos.Contr. – positive control, MLE 12 cells treated with 1 µg of tunicamycin for 24h. un. – untransfected MLE 12 cells kept in culture for 48h. Statistical significance was assured by Student's t-test. Significance levels is *p<0.05, **p<0.01, ***p<0.001. n.s. – non significant, N=3.

4.2. Effect of Chop overexpression on apoptosis of epithelial cells *in vitro*.

4.2.1. Creation of stably transfected, Dox-inducible MLE12/pBI-L-EV and MLE12/pBI-L-CHOP cell lines.

The Tet-on system consists of two critical components: the regulatory plasmid (pTet-on) and the response plasmid (pTRE) [118]. pTet-on expresses rtTA from the strong immediate early promoter of cytomegalovirus, which is used to develop stable Tet-on cell lines. A vector that contains a gene of interest under the control of a TRE, has been transfected into the stable Tet-on cell lines, and the rtTA binds then to TRE to activate the transcription of the target gene in the presence of Tet or its derivatives (such as doxycyclin, Dox). Therefore, in order to obtain stable Tet-inducible Chop expression cell lines, the plasmid pTet-on (containing rtTA) and the plasmid pBI-L-Chop (containing TRE and *Chop* gene) should be transfected together into cells.

As a first step in creating double, stably transfected cell lines, MLE 12 cells were therefore transfected with pTet-on (chapter 3.2.14.1.). After clone selection, G418 resistant clones were transiently transfected with pBI-L-empty vector and treated with 1 µg/ml Dox. 24h post-treatment with Dox, cells were analyzed for luciferase activity as described in chapter 3.2.14.2 and 3.2.19. Figure 4.12.A depicts the luciferase activity of four MLE 12 cell clones which were stably transfected with pTet-on. Comparing the luciferase activity of clones treated with doxycyclin or left untreated, luciferase activity of three clones was found to be higher than that of the Dox-untreated cells (clone 10, 20, 29; Figure 4.12.A); one clone (23) did not show any luciferase activity. However, only in the case of clones 20 and 29 the luciferase activity was significantly higher than in the untreated cells (Figure 4.12.A), indicating effective up-regulation by Dox. They showed low luciferase expression in the absence of Dox and high expression in its presence. Clone 29, which

showed the highest expression level in response to Dox-application, was named as a MLE12/Tet-on and used for the second round of stable transfection.

In this second step, MLE12/Tet-on cells were transfected with either a pBI-L-empty vector (EV) or the pBI-L-CHOP (chapter 3.2.14.1.) vector. G418 and hygromycin resistant clones of MLE12/Tet-on cells transfected with pBI-L-EV or pBI-L-CHOP were picked for analysis of luciferase activity.

Luciferase activity of MLE12/Tet-on cell line stably transfected with pBI-L-EV or pBI-L-CHOP is depicted on Figure 4.12.B and Figure 4.12.C, respectively. In case of empty vector (Figure 4.12.B), clones 6 and 40 revealed higher luciferase activity, and clone 6 was used for all further experiments and named MLE12/pBI-L-EV. For pBI-L-CHOP, clone 13, which showed the highest luciferase activity (Figure 4.12.C), was selected, named accordingly and used in subsequent experiments.

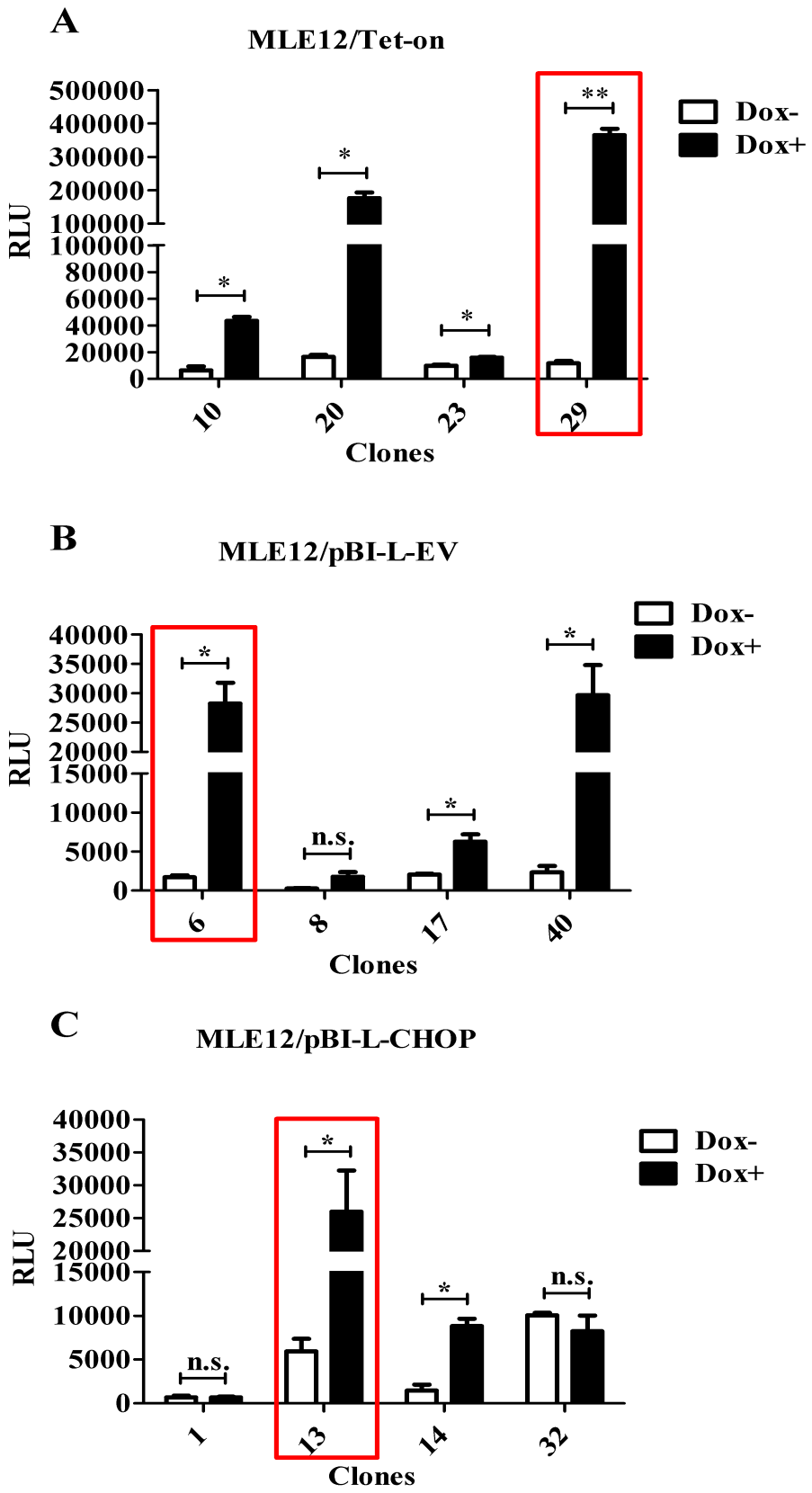

Figure 4.12. Creation of stably transfected, Dox-inducible MLE12/pBI-L-EV and MLE12/pBI-L-CHOP cell lines.

(A) Luciferase activities of different MLE 12/pTet-on clone cells. MLE 12 cells were stably transfected with pTet-on vector. After clone selection, clones were transiently transfected with pBI-L empty vector

(EV). 24h post-transfection, clones were treated with 1µg/ml of Dox for 24h. Then luciferase activity was measured. **(B, C)** Luciferase activities of different MLE 12/pBI-L-EV and MLE 12/pBI-L-CHOP clone cells. MLE 12/pTet-on cells were stably transfected with pBI-L-EV and pBI-L-CHOP. After clone selection, cells were treated with 1µg/ml of Dox for 24h and luciferase activity was measured. Statistical significance was assured by Student's t-test. Significance levels is *p<0.05. n.s. – non significant, N=2. Red rectangles: clones used in the consecutive experiments

4.2.2. Time-dependent Chop overexpression in MLE12/pBI-L-CHOP cell line

In order to check efficiency of Chop overexpression in the MLE 12/pBI-L-CHOP and the MLE12/pBI-L-EV cell line, cells were treated with Dox for 6, 12, 24, 48 hours. After these time points, cells were harvested for analysis of *Chop* expression on mRNA and protein level (as described in chapter 3.2.7 and 3.2.10). Following Dox induction for 48 h, the level of *Chop* mRNA as well as protein (Figure 4.13.A and 4.13.B, C, respectively) was found to be greater in MLE 12/pBI-L-CHOP than in the untreated cells and MLE 12/pBI-L-EV.

This indicates that MLE12/pBI-L-CHOP cells expresses low levels of *Chop* mRNA and protein in the absence of Dox and high levels in its presence. Furthermore, MLE12/pBI-L-EV do not show *Chop* expression on mRNA and protein level (Figure 4.13.A and 4.13.B,C respectively) in both, absence and presence of Dox. It also appears important to conclude that overexpression of the pBI-L vector components does not induce *Chop* expression per se and the Tet system does not appear to be leaky.

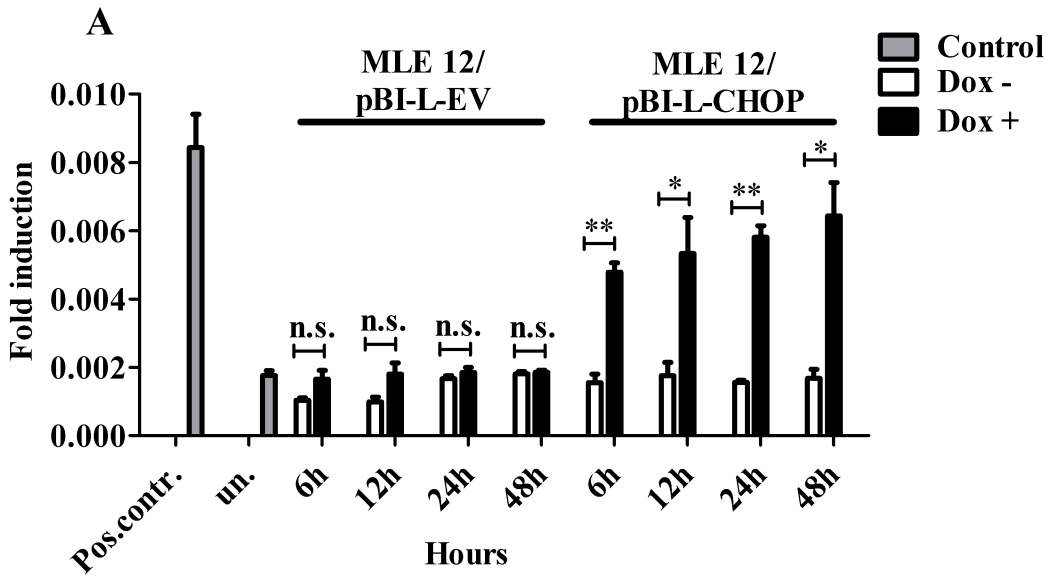

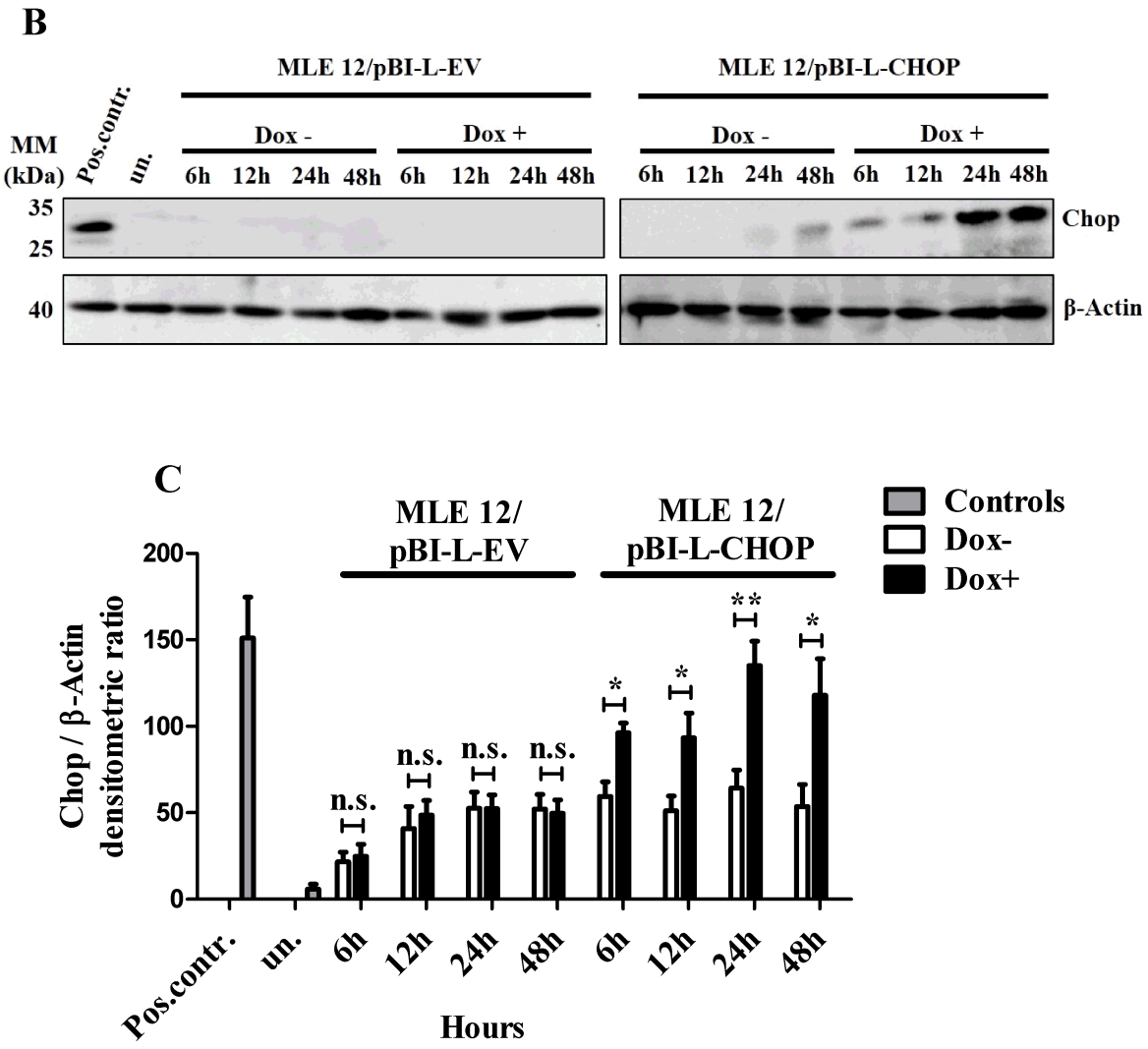

Figure 4.13. Time-dependent *Chop* overexpression in MLE12/pBI-L-CHOP cell line. Stably transfected MLE12/pBI-L-EV and MLE12/pBI-L-CHOP cells were treated with 1 μg/ml Dox for 6, 12, 24, 48 hours, after each time point cells were harvested for mRNA and protein isolation and quantification. **(A)** Expression of *Chop* mRNA detected by real-time PCR. **(B)** Western blot and **(C)** densitometric quantification of Chop expression detected on protein level using anti-CHOP and β-Actin (internal control) antibodies as indicated. Pos.contr. – positive control, MLE 12 cells treated with 1 μg of tunicamycin for 24h. un. – untransfected MLE 12 cells were used as a negative control. Statistical significance was assured by Student's t-test. Significance levels is *$p<0.05$, **$p<0.01$. n.s. – non-significant, N=3.

4.2.3. Chop overexpression in stably transfected MLE 12 cells causes apoptosis

One of the aims of this study was to clarify if Chop induces apoptosis *in vitro.* Therefore, cleaved caspase 3 as well as overall cell death by LDH release were examined in response to Chop overexpression in MLE 12 stably transfected cells. For such purpose, MLE12/pBI-L-EV and MLE12/pBI-L-CHOP cells were treated with 1 μg/ml Dox for 6, 12, 24, 48 hours. After each time point cells were harvested for analysis of cleaved caspase 3 by western blotting (as described in chapter 3.2.8). Additionally, culture supernatants were assayed for cell death by measurement of lactate dehydrogenase activity (as described in chapter 3.2.17).

Cleaved caspase 3 could be weakly detected after 6 h incubation of MLE12/pBI-L-CHOP with Dox, and reached a maximum at 48 h (Figure 4.14.A, B). It was undetectable in untreated conditions (Figure 4.14.A,B) or MLE12/pBI-L-EV cells (Figure 4.14.A, B). Furthermore, activity of lactate dehydrogenase was significantly higher in MLE12/pBI-L-CHOP treated with Dox (Figure 4.14.C) as compared to Dox-untreated cells or the MLE12/pBI-L-EV cells (Figure 4.14.C).

Together, the results suggest that Chop overexpression *in vitro* leads to the activation of apoptosis in the AECII – like, MLE 12 cells.

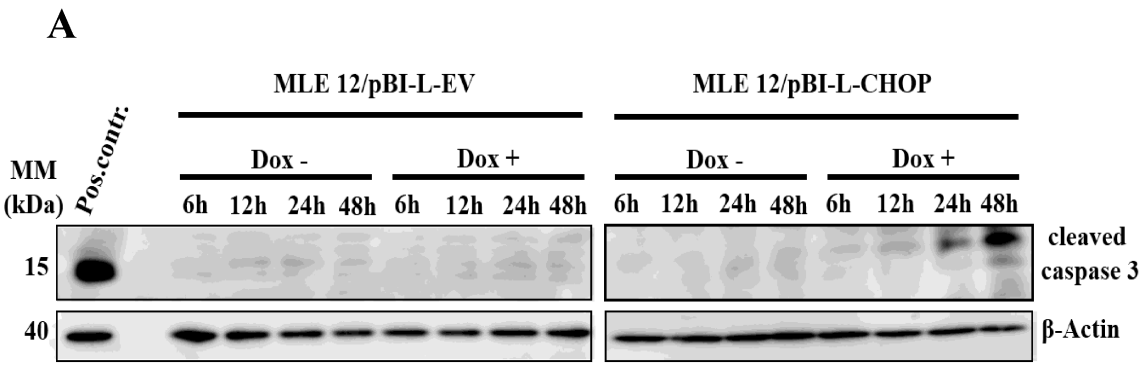

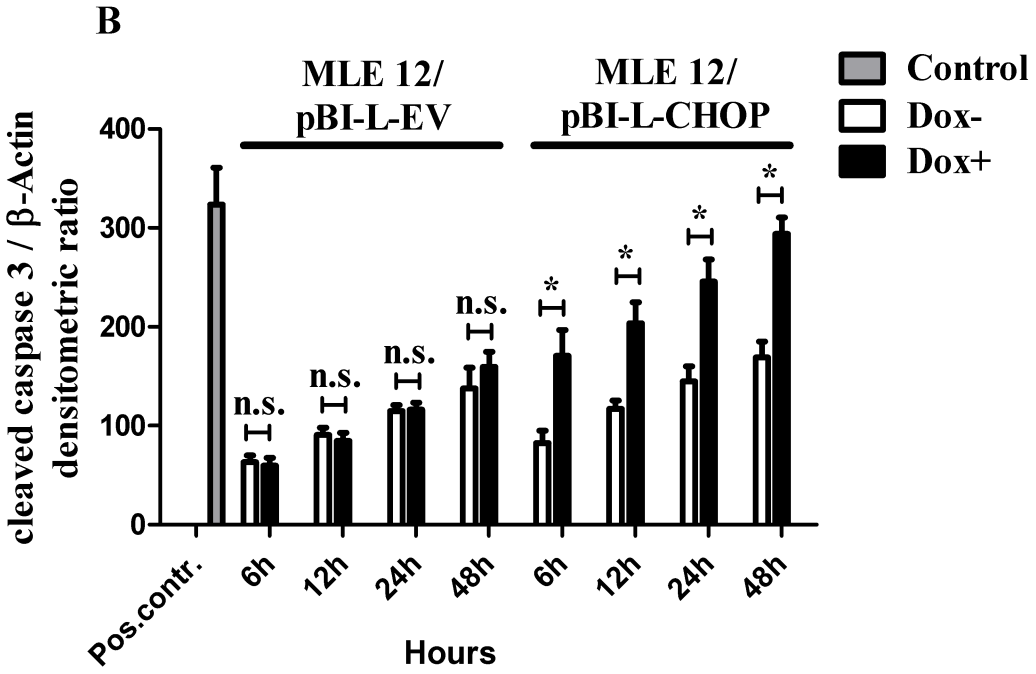
B
MLE 12/
pBI-L-EV
MLE 12/
pBI-L-CHOP
Control
Dox-
Dox+
cleaved caspase 3 / β-Actin
densitometric ratio
400
300
200
100
0
n.s.
n.s.
n.s.
n.s.
*
*
*
*
Pos.contr.
6h
12h
24h
48h
6h
12h
24h
48h
Hours

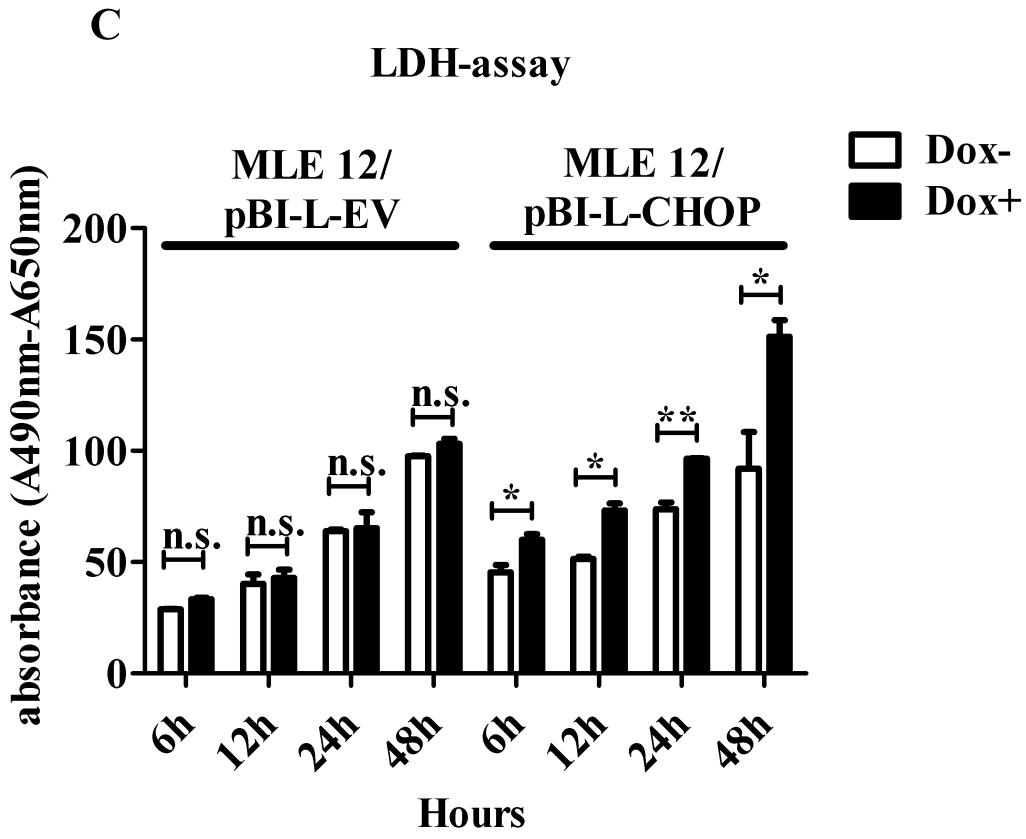
C
LDH-assay
MLE 12/
pBI-L-EV
MLE 12/
pBI-L-CHOP
Dox-
Dox+
absorbance (A490nm-A650nm)
200
150
100
50
0
n.s.
n.s.
n.s.
n.s.
*
*
**
*
6h
12h
24h
48h
6h
12h
24h
48h
Hours

Figure 4.14. Chop overexpression *in vitro* induces apoptosis in stably transfected MLE 12 cell line.

Stably transfected MLE12/pBI-L-EV and MLE12/pBI-L-CHOP cells treated with 1 µg/ml Dox for 6, 12, 24, 48 hours, after each time point cells were harvested and medium was collected for apoptosis quantification. **(A)** Western blot analysis and **(B)** densitometric quantification showed induction of apoptosis via activation of cleaved caspase 3 in response to Chop overexpression. **(C)** Constant increase of cell death detected by LDH activity assay after Dox treatment. Pos.contr. – MLE 12 cells treated with 1 µg/ml of Staurosporine for 8h. Statistical significance was assured by Student's t-test. Significance levels is *p<0.05, **p<0.01. n.s. – non significant, N=3.

4.2.4. Induction of Dr5 and Gadd34 in response to Chop expression *in vitro*

To further characterize the signaling response elicited by Chop overexpression and to verify that known downstream targets of Chop are induced under the experimental conditions used herein, the regulation of Dr5 and Gadd34 was analyzed in the stably *Chop* transfected MLE 12 cells. For this purpose, MLE12/pBI-L-EV and MLE12/pBI-L-CHOP cells were treated with 1 µg/ml Dox for 6, 12, 24, 48 hours. After appropriate time points, cells were harvested for analysis of Dr5 and Gadd34 expression on protein level (as described in chapter 3.2.10).

Expression of Gadd34 and Dr5 was increased in a time-dependent fashion in stably transfected MLE12/pBI-L-CHOP cells, with a maximum level of expression 48h following Dox treatment (Figure 4.15.; A,B,C). In contrast, Gadd34 and Dr5 were not found to be induced in MLE 12/pBI-L-EV under Dox treatment (Figure 4.15.; A,B,C).

These results proof that stable overexpression of Chop in MLE 12 cells results downstream in activating of Chop-target genes and in apoptosis induction.

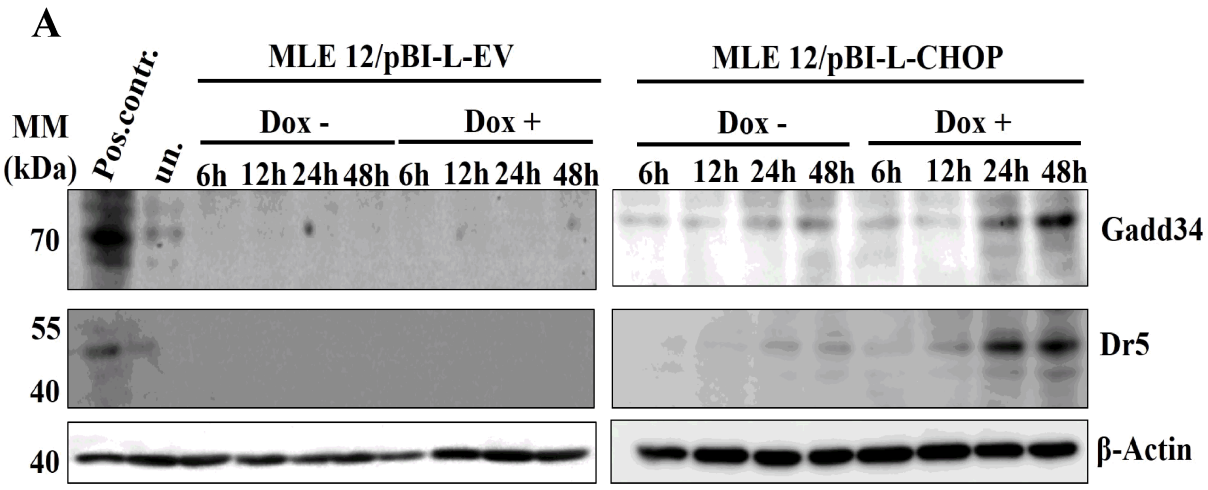

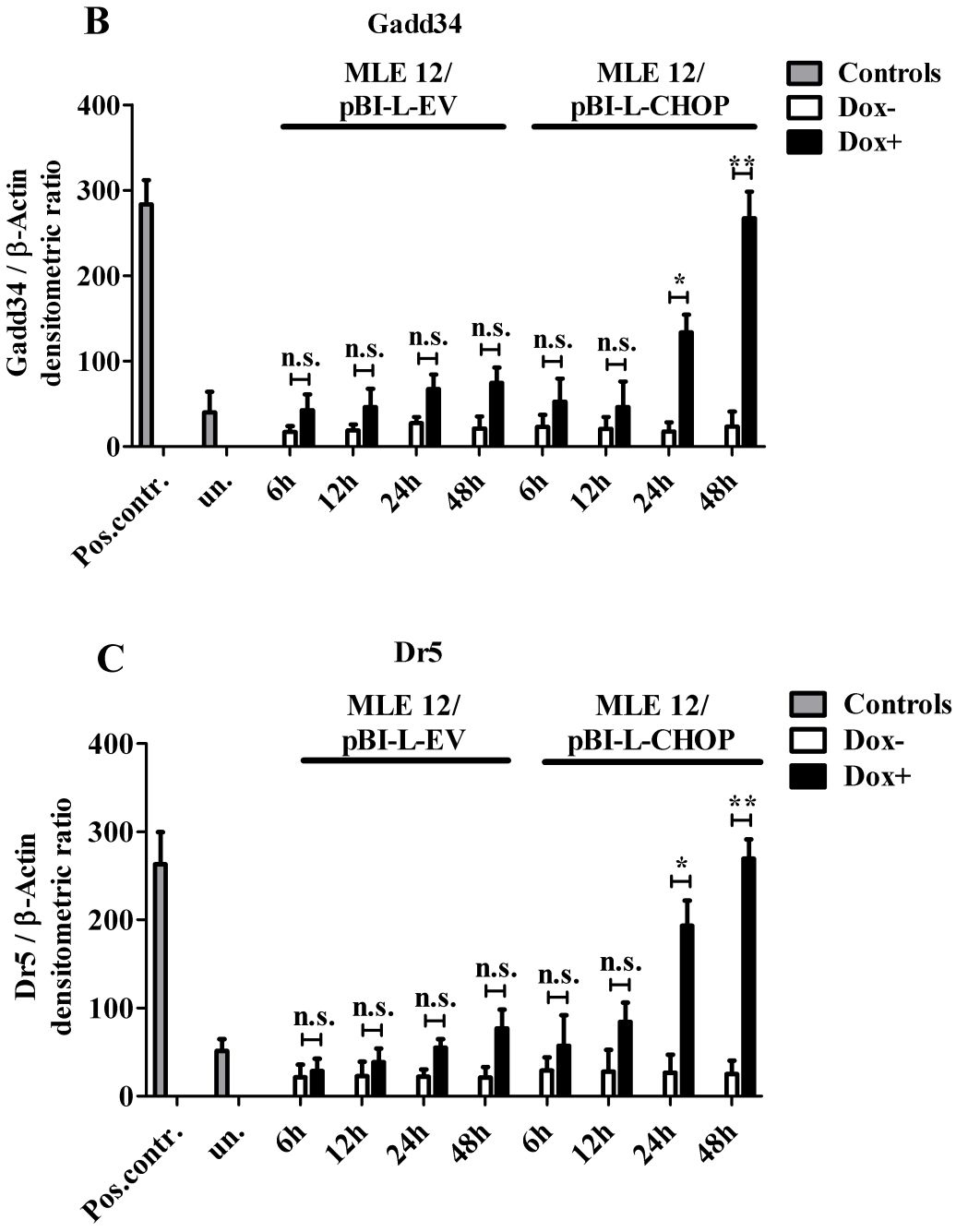

Figure 4.15. Induction of Dr5 and Gadd34 in response to Chop expression.
Stably transfected MLE12/pBI-L-EV and MLE12/pBI-L-CHOP cells were treated with 1 µg/ml Dox for 6, 12, 24, 48 hours; after each time point, cells were harvested for protein analysis. **(A)** Western blot and **(B, C)** densitometric quantification of Gadd34 and Dr5 expression detected on protein level using anti-GADD34, DR5 and β-Actin (internal control) antibody as indicated. Pos.contr. – positive control, MLE 12 cells treated with 1 µg of tunicamycin for 24h. un. – untransfected MLE 12 cells were used as a negative control. Statistical significance was assured by Student's t-test. Significance levels is *$p<0.05$, **$p<0.01$. n.s. – non significant, N=3.

4.3. Effect of Chop overexpression on apoptosis in primary alveolar epithelial type II cells and fibroblast proliferation *in vitro*

4.3.1. Overexpression of Chop in alveolar type II cells results in induction of apoptosis

In order to confirm the data presented above in primary alveolar type II cells (AECII), an adenoviral gene transfer model was implemented. For such purpose, freshly isolated mouse AECII were infected with adenoviruses containing an empty vector backbone (Ad-EV) or the *Chop* gene (Ad-CHOP) at a MOI 10 (10 millions of viruses per cell) or left uninfected for 24, 48, 72, 96 hours. After each time point, AECIIs were collected for protein isolation, and analysis of Chop expression and amount of cleaved caspase 3 by western blotting (as described in chapter 3.2.10). For quantification of total cell death, media from cultured and infected AECIIs was collected and LDH assay was performed (as described in chapter 3.2.17).

As shown in Figure 4.16.A and, B, AECII expressed Chop on protein level after transduction with Ad-CHOP already after 24h of incubation. On the other hand, uninfected or cells infected with Ad-EV did not show any Chop expression, hence indicating that primary AECII do not express Chop in absence of any stimulus and that the adenoviral transfection model used does also not induce a maladaptive ER stress response per se. Furthermore, cleaved caspase 3 and low levels of Chop were already detected after 24h of Chop overexpression in AECII indicating a rather rapid, apoptotic response of the AECII to Chop induction (Figure 4.16.A,C). Accordingly, the LDH was found to be significantly increased 24h after transfection and in response to Chop overexpression (Figure 4.16.D).

Taken together, we conclude that the causal relationship between Chop induction and epithelial apoptosis, as established in MLE12 cells in response to stable transfection, can fully reconfirmed in these experiments based on adenoviral transfection of *Chop* in primary AECII.

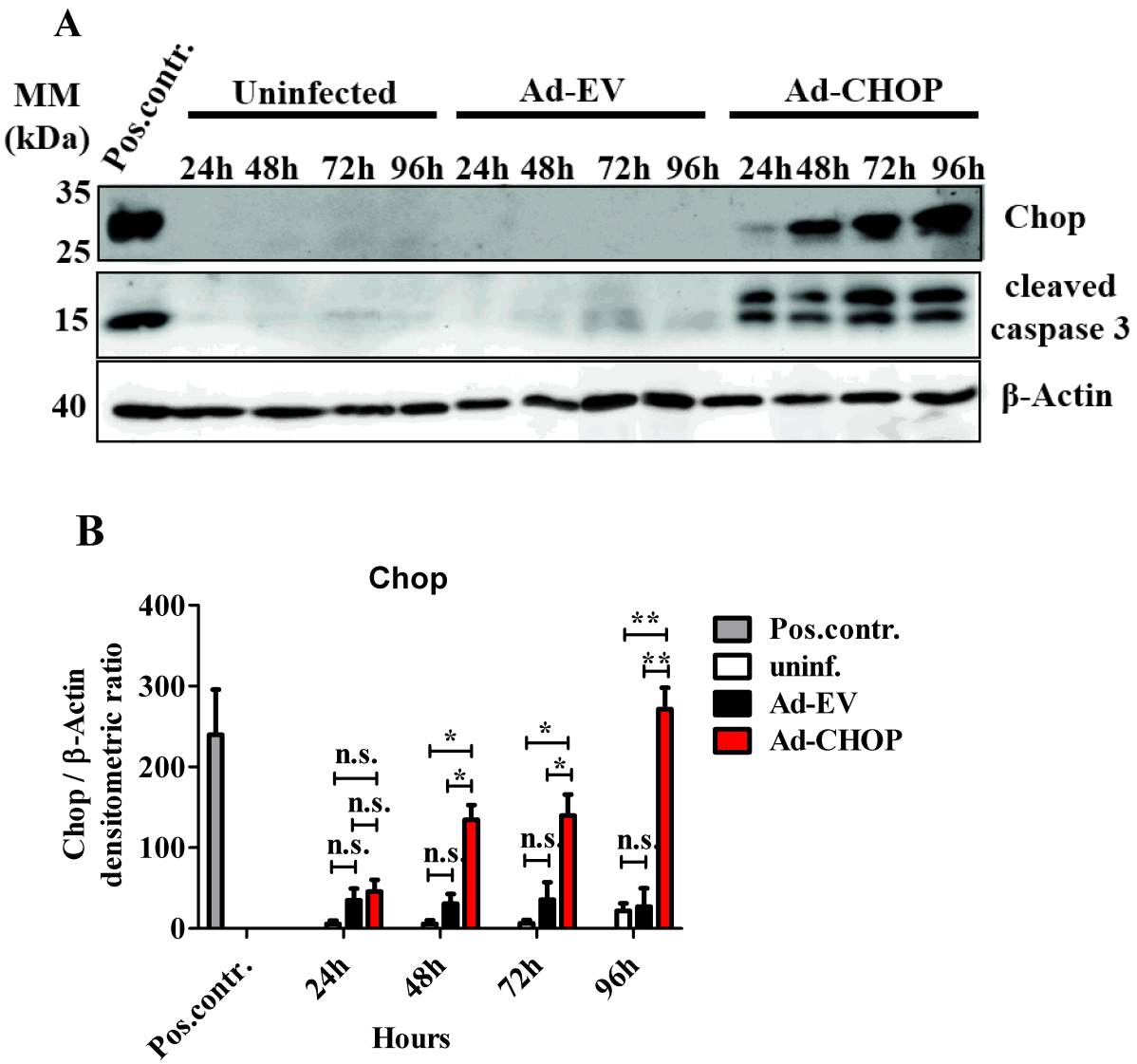
A
MM
(kDa)
Pos.contr.
Uninfected
Ad-EV
Ad-CHOP
24h 48h 72h 96h 24h 48h 72h 96h 24h 48h 72h 96h
35
25
15
40
Chop
cleaved
caspase 3
β-Actin
B
Chop
Chop / β-Actin
densitometric ratio
400
300
200
100
0
n.s.
*
**
Pos.contr.
uninf.
Ad-EV
Ad-CHOP
Pos.contr.
24h
48h
72h
96h
Hours

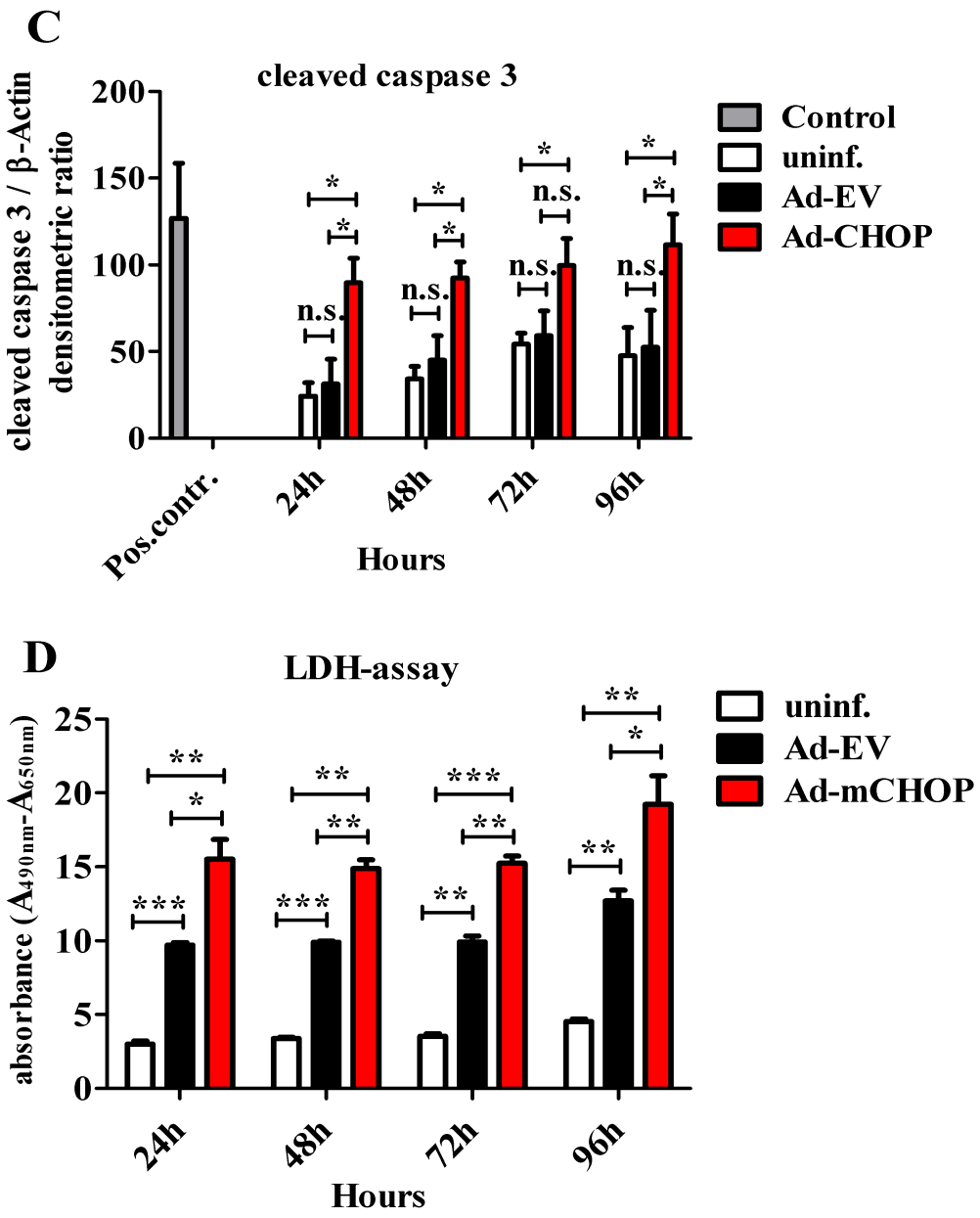

Figure 4.16. Overexpression of Chop *in vitro* activates caspase 3 cleavage in alveolar type II cells.

AECIIs were infected with AD-EV and AD-CHOP at a MOI 10 or left uninfected and incubated for 24h, 48h, 72h, 96h. **(A)** Western blotting was performed using anti-CHOP, cleaved caspase 3 and β-Actin (internal control) antibody as indicated, **(B, C)** Densitometric quantification for Chop and cleaved caspase 3. **(D)** LDH assay representing AECII cell death in response to Chop overexpression. Pos.contr. – positive control, MLE 12 cells treated with either 1 µg of tunicamycin for 24h for Chop blot or with 1 µg of Staurosporine for 8h for cleaved caspase 3 blot. Statistical significance was assured by Student's t-test. Significance levels is *p<0.05, **p<0.01, ***p<0.001. n.s. – non significant, N=2.

4.4. Chop overexpression *in vitro* leads to fibroblast proliferation

Taking into consideration that intensive fibroblast proliferation and collagen deposition is a hallmark of lung fibrosis, it appeared logical to extend the above illustrated experiments by assessing the pro-proliferative signal of Chop transfected AECII or MLE 12 supernatants on cultured lung fibroblasts. To answer this question, MLE 12/pBI-L-CHOP and MLE 12/pBI-L-EV cells were treated with 1 μg/ml of Dox for 6, 12, 24, 48 hours. Likewise, freshly isolated AECII were infected with Ad-CHOP and Ad-EV at a MOI 10 or left uninfected for 24, 48, 72, 96 hours. After each time point, conditioned media from MLE 12 and AECII were then applied on murine lung fibroblasts. Fibroblast proliferation was measured by WST-1 assay (as described in chapter 3.2.18).

As shown on Figure 4.17., conditioned media from both, stably Chop overexpressing MLE 12 cells (Figure 4.17.A) and adenoviral *Chop* transfected AECII (Figure 4.17.B) induced mouse lung fibroblast proliferation, whereas conditional media from empty vector control experiments did not cause such increase in proliferation (Figure 4.17.A,B).

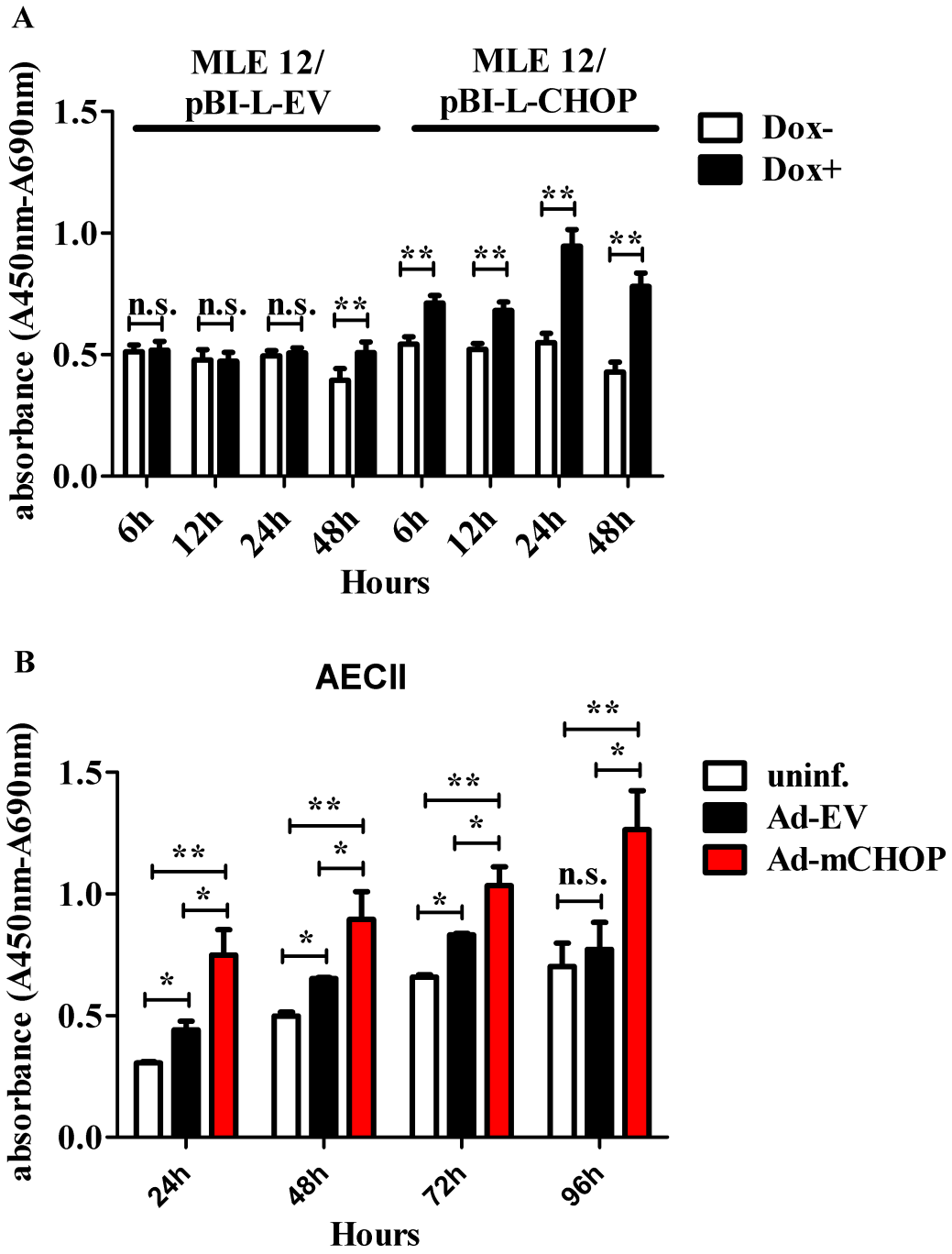

Figure 4.17. Chop overexpression *in vitro* leads to fibroblast proliferation.
(A, B) Lung fibroblast proliferation was measured by water-soluble tetrazolium salt (WST)-1 assay. **(A)** MLE 12/pBI-L-EV and MLE 12/pBI-L-CHOP cells were treated with 1 µg/ml of Dox for 6, 12, 24, 48 hours. **(B)** AECIIs were infected with Ad-EV and Ad-CHOP at a MOI 10 or left uninfected for 24h, 48h, 72h, 96h. Conditioned media from either Chop overexpression cells or empty vector or uninfected AECII were applied to an equal number of Mlg fibroblasts and their proliferation was measured. Statistical significance was assured by Student's t-test. Significance levels is *p<0.05, **p<0.01. n.s. – non significant, N=2.

4.5. Effect of Chop overexpression on apoptosis of AECII *in vivo*

4.5.1. Characterization of *Chop* transgenic mice

In order to prove that the causal relationship between alveolar epithelial induction of Chop and activation of apoptosis would also be observable under *in vivo* conditions, transgenic mice with AECII-specific, conditional overexpression of Chop were generated (as described in chapter 3.2.2.1).

Chop double transgenic mice (SP-C rtTA / tetO7 CHOP) were phenotyped after feeding them with doxycycline (Dox+) for 4 and 8 weeks. The mRNA and protein expression of *Chop* was analyzed in the lung homogenates of *Chop* transgenic mice (as described in chapter 3.2.7 and 3.2.10). Efficiency of *Chop* overexpression was compared to FVBN background mice and transgenic mice not fed with Dox (Dox-) (characteristic and genetic background of each mouse used for the analysis is described in Table 1, chapter 3.2.2.1.). As shown in Figure 4.18.A, C, D, *Chop* was robustly overexpressed already after 4 weeks feeding with Dox on the mRNA and the protein level in some (e.g. #145,#146,#172) but not all Dox-treated, double transgenic mice. Chop was also robustly overexpressed after 8 weeks feeding with Dox, and *Chop* expression was detectable on the mRNA (Figure 4.19.A) and the protein level (Figure 4.18.C and D) in mice #97, 98, 102, 113, 132, 148, 148, 150, 175, compared with FVBN background and Dox- mice (# 99 and 110). In Dox- mouse #101 at 8 weeks time point, *Chop* was detected on the mRNA level (Figure 4.19. A) and on the protein level (Figure 4.19.C and D), and this may be due to aberrant, Dox-independent activation of the transgene. Although we could detect Chop overexpression after 4 and 8 week time points, we could not observe statistical significance comparing two groups Dox- versus Dox+, neither after 4 weeks (Figure 4.18.B, E) nor 8 weeks time points (Figure 4.19.B, E). This is because of different level of Chop expression in each mouse.

In order to check the cell-specific localization of Chop expression, immunofluorescence (IF) analysis was performed employing a Chop antibody and an Abca3 antibody as a specific AECII marker (as described in chapter 3.2.11).

As can be taken from Figure 4.18., Chop was overexpressed specifically in AECII after feeding for 4 (Figure 4.20.G-I,j,k,l) and 8 (Figure 4.20.G-q,r,s,t) weeks with Dox, whereas no Chop expression could be detected in AECII of FVBN background (Figure 4.20.G-

a,b,c,d) or transgenic mice not fed with Dox for 4 (Figure 4.20.G-e,f,g,h) or 8 weeks (Figure 4.18.G-m,n,o,p).

Taking together, all these results indicate that *Chop* transgenic mice were successfully created, and Chop is overexpressed specifically in AECII after 4 and 8 weeks feeding with Dox.

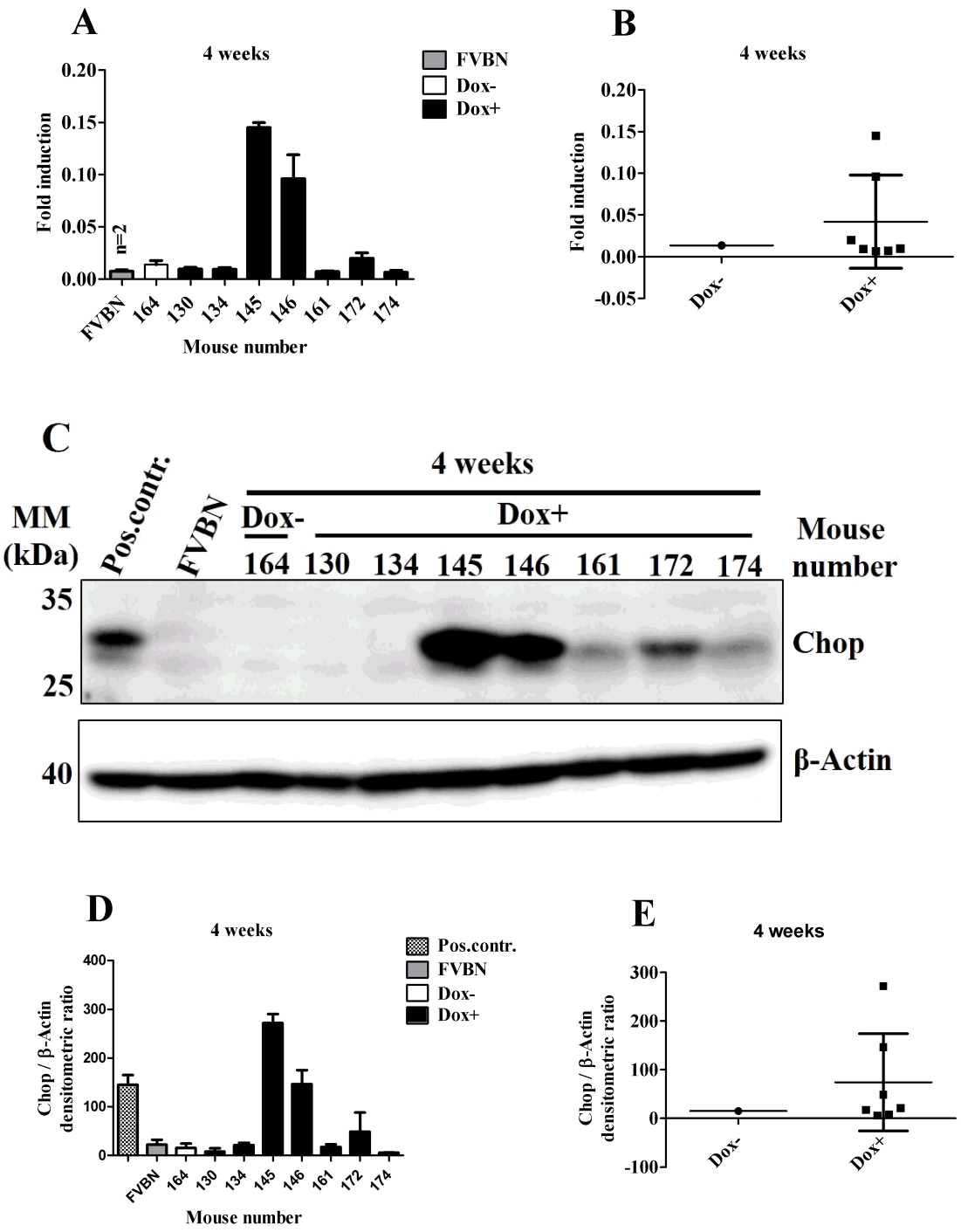

Figure 4.18. Chop overexpression *in vivo* in AECII of *Chop* transgenic mice at 4 weeks time point.

(A, B) Expression of *Chop* mRNA detected by real-time PCR in lung homogenate of *Chop* transgenic mice (SP-C rtTA / tetO7 CHOP) fed (Dox+) or unfed (Dox-) with Dox for 4 weeks. **(C)** Chop expression was analyzed by Western blot in lung homogenates from control and Dox induced mice using anti-CHOP and β-Actin (internal control) antibody as indicated. **(D, E)** Densitometric analysis of Chop expression, normalized to internal control. Pos.contr. – positive control, MLE 12 cells treated with 1 µg of tunicamycin for 24h. **(B, E)** Statistical comparison of two groups Dox- versus Dox+ by Student's t-test for Chop overexpression on mRNA and protein level, respectively, n.s. – non significant.

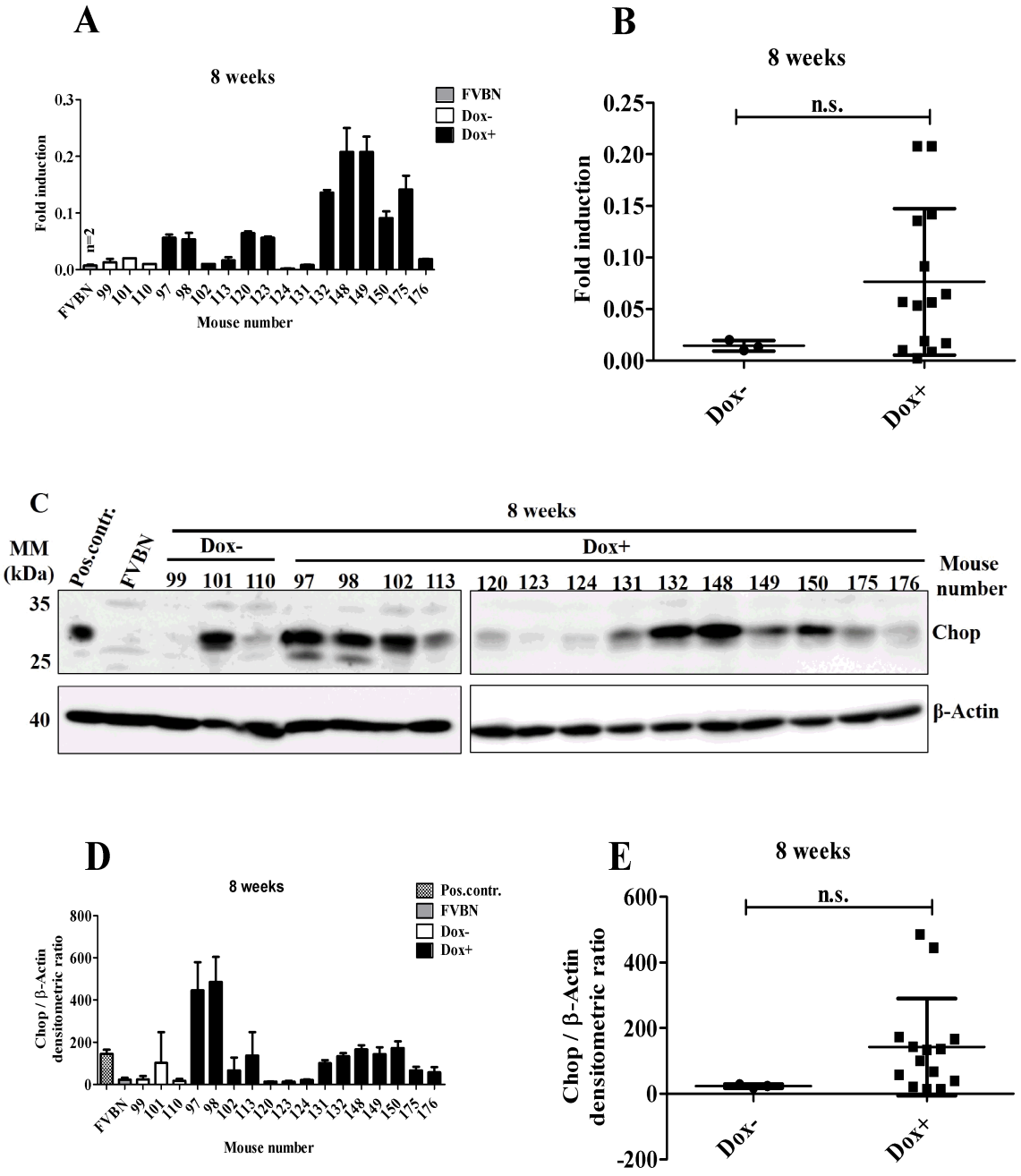

Figure 4.19. Chop overexpression *in vivo* in AECII of *Chop* transgenic mice at 8 weeks time point.
(A, B) Expression of *Chop* mRNA detected by real-time PCR in lung homogenate of *Chop* transgenic mice (SP-C rtTA / tetO7 CHOP) fed (Dox+) or unfed (Dox-) with Dox for 8 weeks. **(C)** Chop expression was analyzed by Western blot in lung homogenates from control and Dox induced mice using anti-CHOP and β-Actin (internal control) antibody as indicated. **(D, E)** Densitometric analysis of Chop expression, normalized to internal control. Pos.contr. – positive control, MLE 12 cells treated with 1 µg of tunicamycin for 24h. **(B, E)** Statistical comparison of two groups Dox- versus Dox+ by Student's t-test for Chop overexpression on mRNA and protein level, respectively, n.s. – non significant.

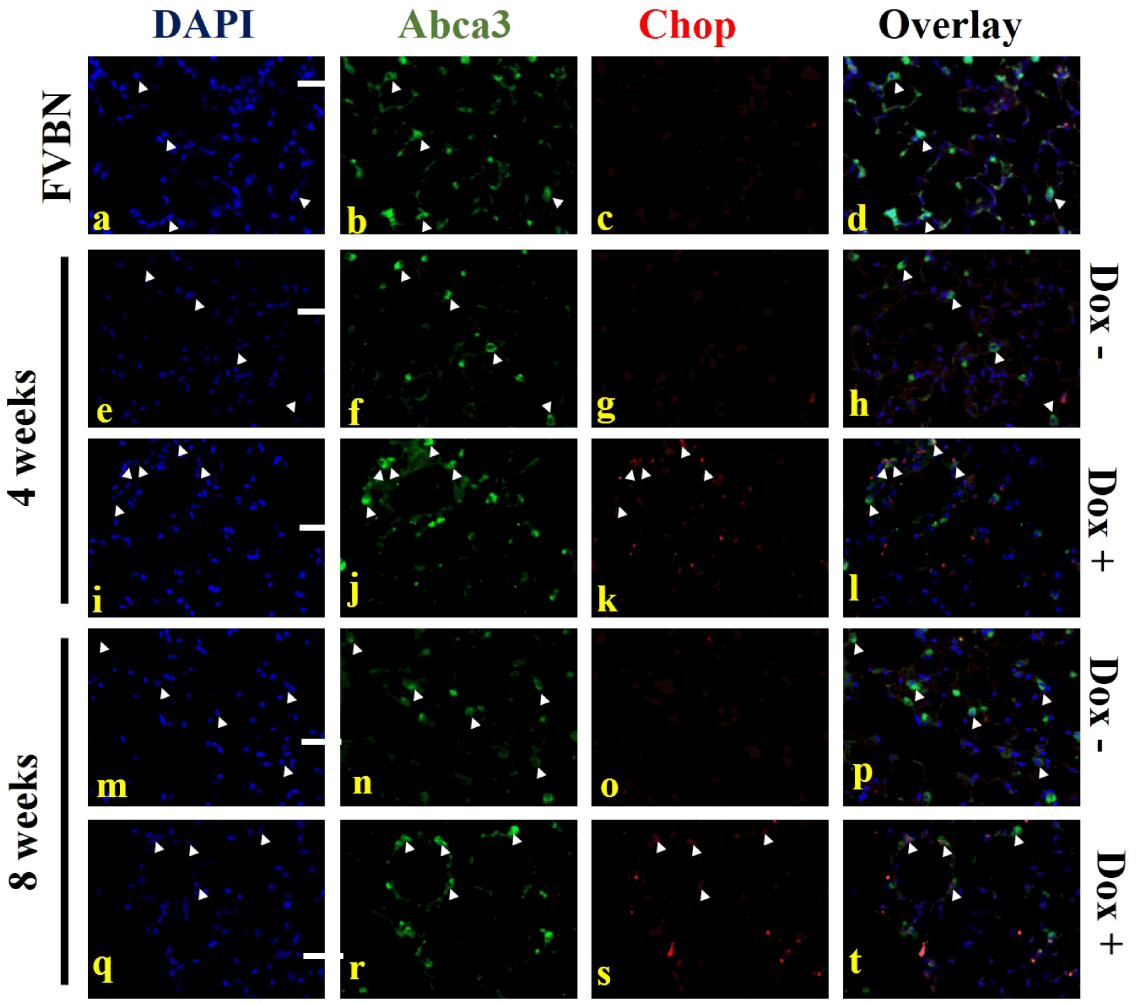

Figure 4.20. Localization of Chop in AECII of *Chop* transgenic mice.
Representative immunofluorescence analysis. Co-localization of Chop and Abca3 in AECII in lung sections from *Chop* transgenic mice at 4 weeks (e-l) (Dox- #164; Dox+ #145), 8 weeks (m-t) (Dox- #99; Dox+ #98) time points in comparison to FVBN background control mouse (a-d). Scale = 100 µm, original magnification:×200. Arrowheads represent alveolar type II cells expressing Chop and Abca3.

4.5.2. Investigation of effect of Chop overexpression on apoptosis *in vivo*

As the *Chop* transgenic mice indeed showed AECII specific overexpression of Chop in response to Dox treatment, we looked for a putative induction of apoptosis in these mice *in vivo*. To this end, lung homogenates from transgenic mice (SP-R rtTA / tetO7 CHOP) either fed with Dox (Dox+) or not (Dox-) for 4 and 8 weeks were investigated for the regulation of cleaved caspase 3 on protein level (as described in chapter 3.2.10).

Figures 4.21.A and D represent western blot analysis for cleaved caspase 3 for 4 and 8 weeks, respectively. After 4 weeks of Dox treatment, mice # 145 and 146, who had already shown significant upregulation of Chop as detailed above, also revealed a significant increase in cleaved caspase 3 as compared to Dox- mouse #164. Likewise, cleaved caspase 3 was detected after 8 weeks of dox feeding in mice # 97, 98, 148 and 150 as compared with dox - mice # 99, 101 and 110. Again, as with the Chop expression per se, not all Dox-fed transgenic mice showed a significant increase in cleaved caspase 3, and such behaviors pretty much reflected what had been seen with regard to Chop induction (Figure 4.18, A-E, 4.19 A-E and 4.20). Due to the variance in the groups and different level of Chop expression we could not show a significant difference by comparison of Dox- versus Dox+ for 4 and 8 week time point (Figure 4.21.C, F, respectively).

Furthermore, in order to check cellular localization of cleaved caspase 3 on lung sections of these mice, IF analysis was performed employing antibodies recognizing exclusively the cleaved form of caspase ,3 and Abca3 as AECII marker (as described in chapter 3.2.11). As shown in Figure 4.21.G-i,j,k,l for 4 week Dox treated mice and Figure 4.21.G-q,r,s,t for 8 week Dox treated mice, co-localization of cleaved caspase 3 alongside with Abca3 in AECII was observed for the Dox-treated versus the FVBN background (Figure 4.21.G-a,b,c,d) or versus Dox-untreated mice after 4 (Figure 4.21.G-e,f,g,h) and 8 weeks (Figure 4.21.G-m,n,o,p).

Together, the results suggest that also under *in vivo* conditions, expression of Chop in AECII goes along with increased apoptosis of alveolar epithelial type II cells.

Due to different level of Chop expression (Figure 4.18. and 4.19.) and cleaved caspase 3 (Figure 4.21.) in the transgenic mouse model, for further downstream analysis, we used only mice in which Chop was highly overexpressed mouse # 145, 146 at 4 weeks time point, and mouse # 97, 98, 132, 148, 150 at 8 in Dox-induced conditions.

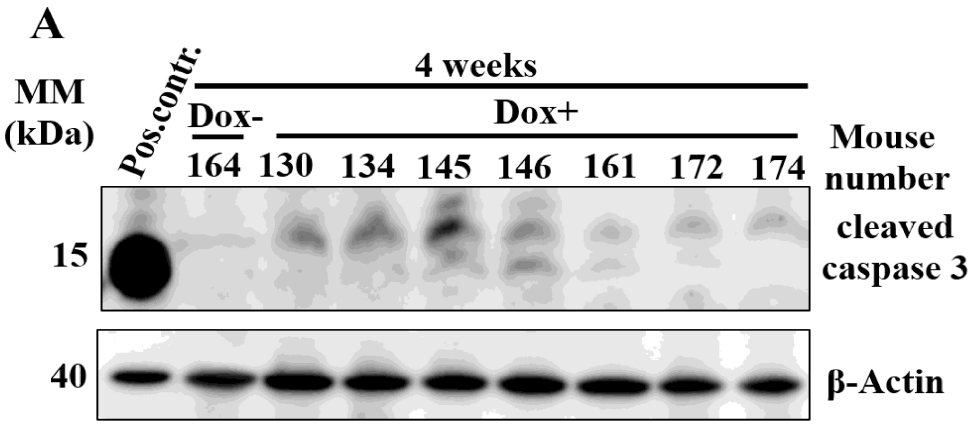
A
MM (kDa)
Pos.contr.
4 weeks
Dox-
Dox+
164 130 134 145 146 161 172 174
Mouse number
15
cleaved caspase 3
40
β-Actin

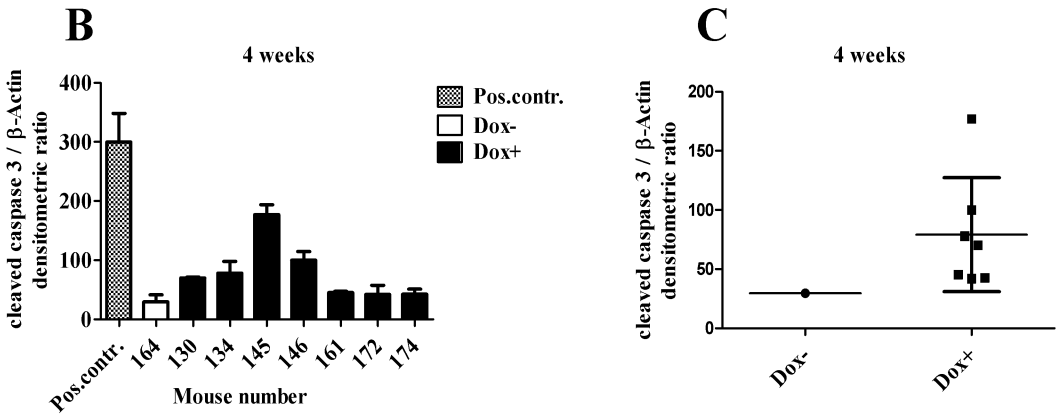
B
4 weeks
cleaved caspase 3 / β-Actin densitometric ratio
400
300
200
100
0
Pos.contr.
Dox-
Dox+
Pos.contr. 164 130 134 145 146 161 172 174
Mouse number
C
4 weeks
cleaved caspase 3 / β-Actin densitometric ratio
200
150
100
50
0
Dox-
Dox+

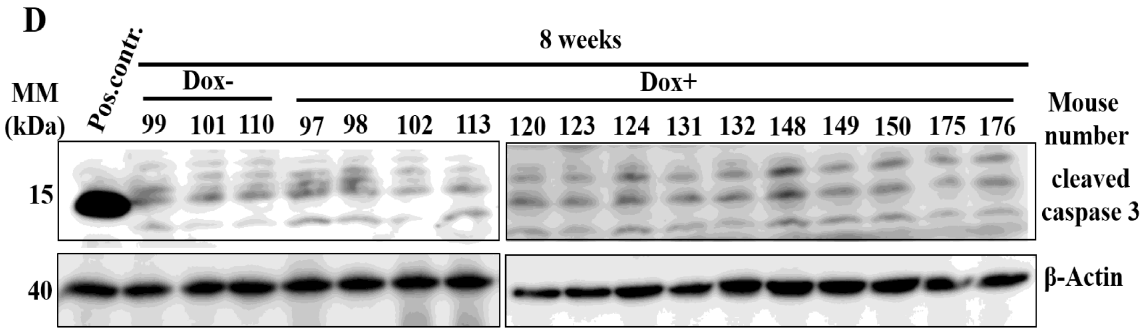
D
MM (kDa)
Pos.contr.
8 weeks
Dox-
Dox+
99 101 110 97 98 102 113 120 123 124 131 132 148 149 150 175 176
Mouse number
15
cleaved caspase 3
40
β-Actin

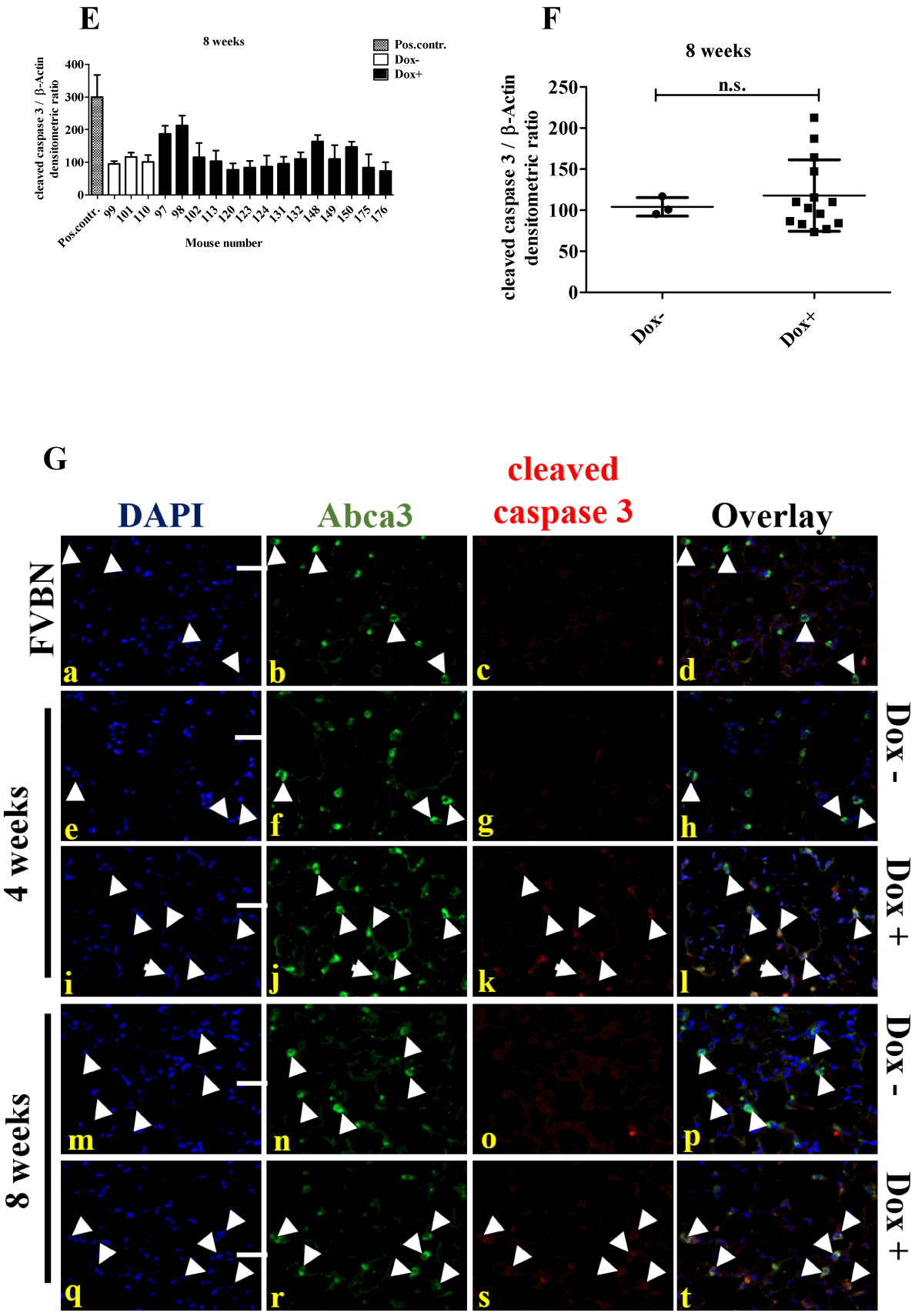

Figure 4.21. Investigation of effect of Chop overexpression on apoptosis *in vivo*.
Chop transgenic mice were Dox treated (Dox+) or left untreated (Dox-) for 4 and 8 weeks. Thereafter, lung homogenate and lung sections were prepared. **(A, D)** Western blotting was performed using anti- cleaved caspase 3 and β-Actin (internal control) antibody as indicated. **(B, E)** Densitometric analysis of cleaved

caspase 3 expression, normalized to internal control. Pos.contr. – positive control, MLE 12 cells treated with 1 µg of Staurosporine for 8h. **(C, F)** Statistical comparison of two groups Dox- versus Dox+ by Student's t-test, 4 weeks and 8 weeks time points, respectively, n.s. – non significant.
(G) Representative immunofluorescence analysis. Co-localization of cleaved caspase 3 and Abca3 in AECII in lung sections from *Chop* transgenic mice at 4 weeks (e-l) (Dox- #164; Dox+ #145), 8 weeks (m-t) (Dox- #99; Dox+ #98) time points, and FVBN background control mouse (a-d). Scale = 100 µm, original magnification: ×200. Arrowheads represent alveolar type II cells expressing caspase 3 and Abca3.

4.5.3. Investigation of effect of AECII specific Chop overexpression *in vivo* on induction of expression of downstream target genes

In addition to the question of induction of AECII apoptosis in response to Chop overexpression, the expression of typical Chop downstream targets was investigated.

Expression status of inflammatory genes *Il6* and *Il1,* as well as *Casp11,* through which *Il1* is induced, were checked. *Dr5* is a Chop target gene and is involved in induction of the extrinsic pathway of apoptosis. *Ero1α* is up-regulated in response to Chop overexpression and is involved in the oxidative stress-response. Furthermore, it is known that *Gadd34* is induced by Chop and involved in maintaining the ER stress response (detailed information about all these genes, see chapter 1.3.).

As mentioned above, Chop transgenic mice were fed with Dox or left untreated with Dox for 4 and 8 weeks, after which lung homogenates were analyzed for expression of *Il6, Il1, Casp11, Dr5, Ero1α* and *Gadd34* on mRNA level by qPCR (as described in chapter 3.2.7). Downstream target genes were analyzed exclusively in those mice in which Chop was highly overexpressed on mRNA and protein level in dependency of the Dox feeding.

As described in chapter 4.5.2., mice in which Chop was highly overexpressed at 4 and 8 weeks in Dox-induced conditions were used for further analysis.

As compared to the non Dox treated transgenic mice, all genes were up-regulated in Dox-fed transgenic mice in response to Chop overexpression *in vivo* mainly in later time point at 8 weeks (Figure 4.22.). *Il6* was expressed after 4 and 8 weeks in Dox-induced conditions whereas *Il1* was significantly up-regulated only in mouse #97 at 8 week time point (Figure 4.22.C and A respectively). In addition, *Casp11* was induced in mice # 97, 98, 132 at 8 weeks time point (Figure 4.22.I). *Dr5* and *Gadd34* were up-regulated in Dox-induced mice at 8 weeks time point (Figure 4.22.G, E). Furthermore, *Ero1α* was induced in response to Chop overexpression already after 4 weeks feeding with Dox, and expression was significantly higher at 8 weeks time point (Figure 4.22.K).

Figures 4.22. B, D, F, H, J, L, represent statistical comparison between Dox- and Dox+ for *Il1, Il6, Gadd34, Dr5, Casp11* and *Ero1α*, respectively. As discussed before, due to the variance in expression level of each mouse we could not show a statistical significance between two groups.

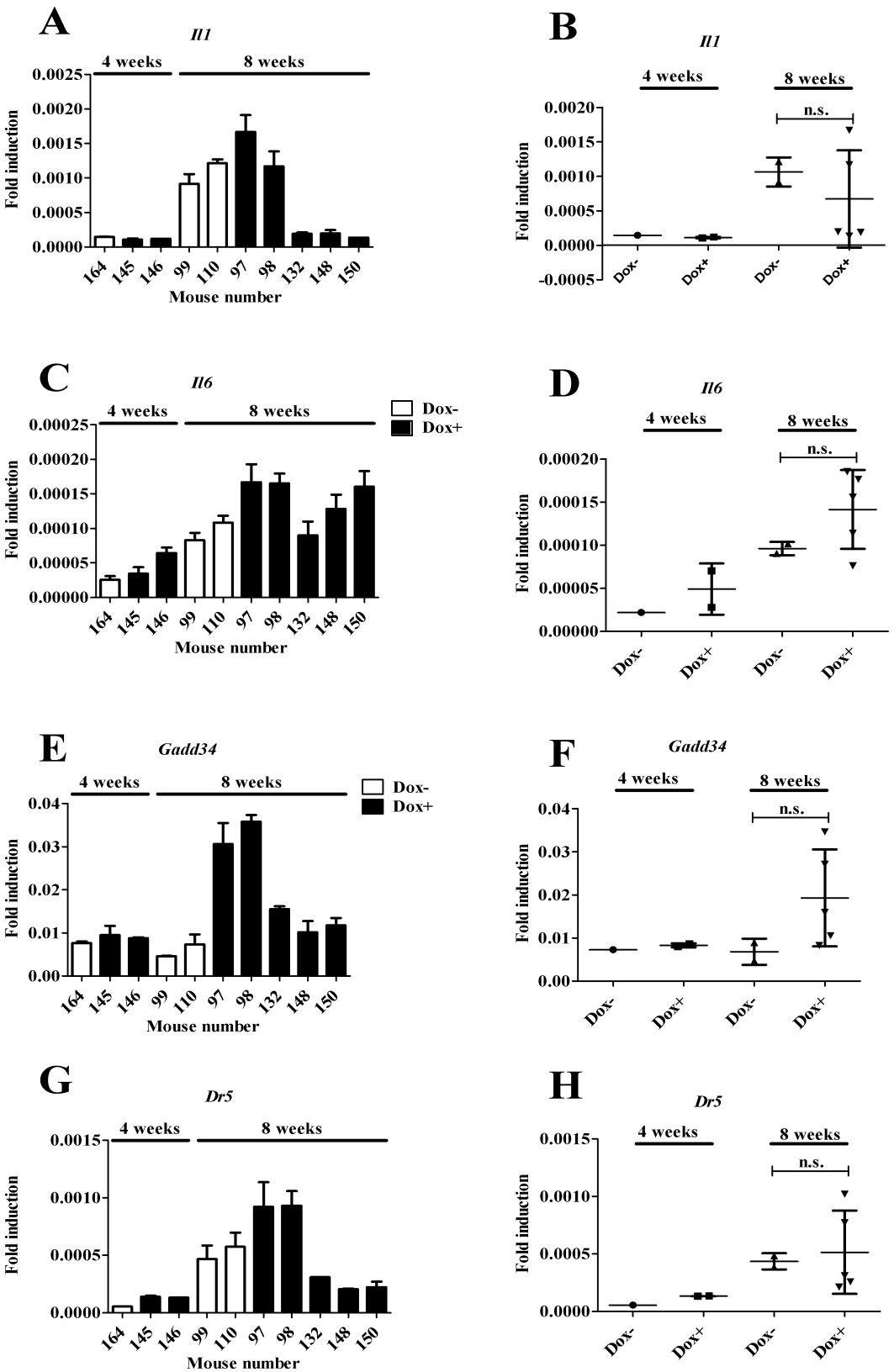
A
Il1
4 weeks
8 weeks
Fold induction
Mouse number
164 145 146 99 110 97 98 132 148 150
B
Il1
n.s.
Dox-
Dox+
C
Il6
Dox-
Dox+
D
Il6
E
Gadd34
F
Gadd34
G
Dr5
H
Dr5

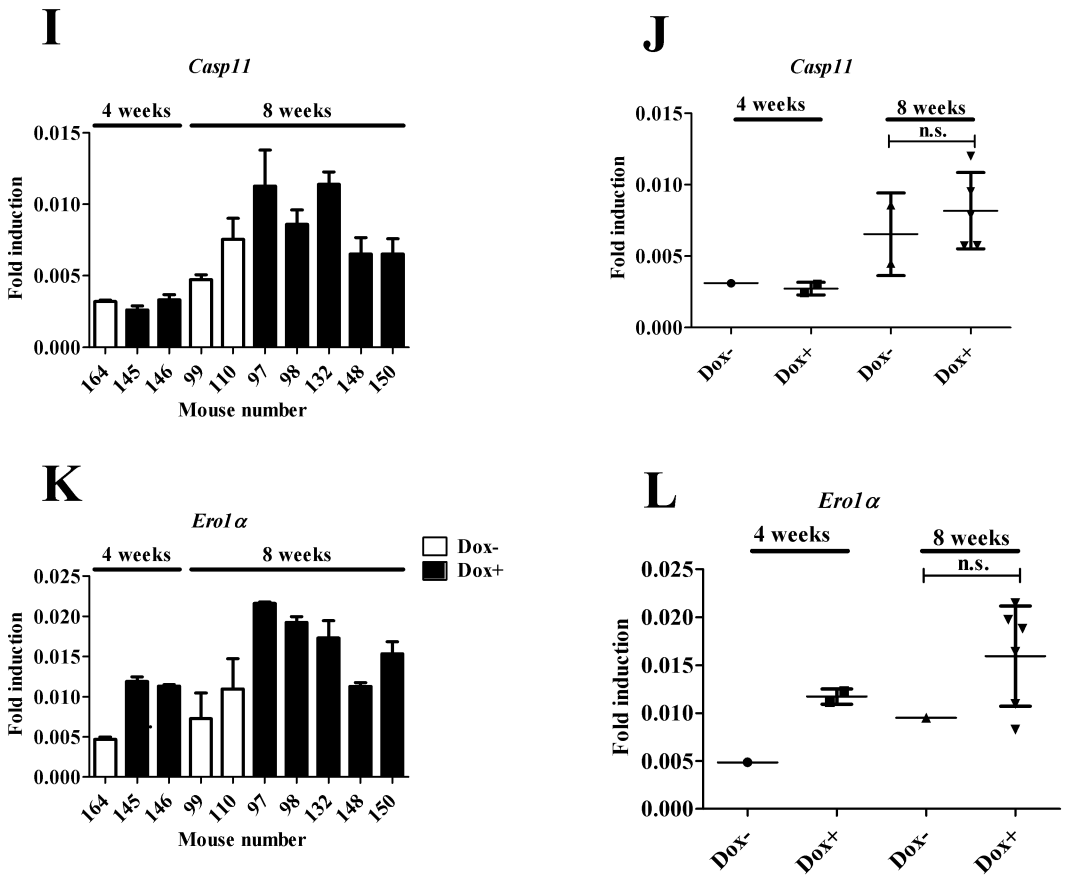

Figure 4.22. Investigation of effect of AECII specific Chop overexpression *in vivo* on induction of expression of downstream target genes.
(A, C, E, G, I, K) Expression of *Il1, Il6, Gadd34, Dr5, Casp11, Ero1α* mRNA in lung homogenate from mice fed (Dox+) or unfed (Dox-) during 4 and 8 weeks.
(B, D, F, H, J, L) Statistical comparison of two groups Dox- versus Dox+ by Student's t-test, 4 weeks and 8 weeks time points, n.s. – non significant.

4.5.4. Expression of Chop up to 8 weeks did not result in development of lung fibrosis *in vivo*

In order to answer one key question of this study whether Chop overexpression leads to induction of lung injury and fibrosis, H&E staining of lung sections was performed. Histologic lung phenotype from *Chop* transgenic mice was normal after 4 and 8 weeks feeding with Dox (Figure 4.23.). There were no differences between Dox-treated mice at 4 weeks (Figure 4.23A, B-c,h) and 8 weeks (Figure 4.23A, B-e,j) versus Dox-untreated, mice at 4 weeks (Figure 4.23A, B-b,g) and 8 weeks (Figure 4.23A, B-d,i) animals, as well as their FVBN background control mice (Figure 4.23A, B-a,f) were not observed. The only observation was a slight, but inconsistent, increase in cellularity in some of the Dox treated mice (Figure 4.23)

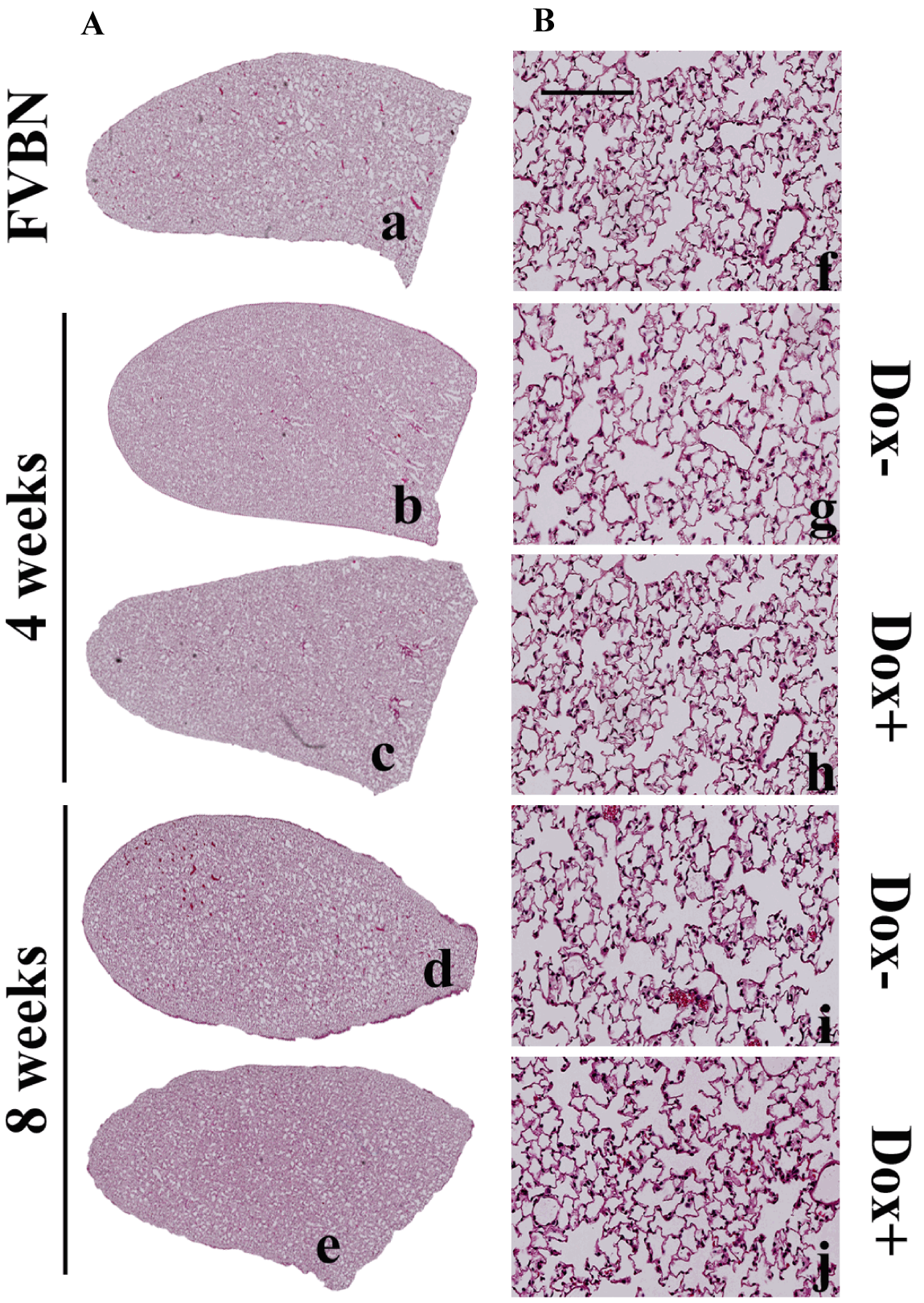

Figure 4.23. Expression of Chop did not lead to development of lung fibrosis *in vivo*. **(A)** Representative H&E stainings of complete mouse lungs of *Chop* transgenic mice in Dox induced (Dox+) conditions at 4 (c) and 8 (e) weeks, and Dox uninduced conditions at 4 (b) and 8 (d) weeks, and their FVBN background control mice. **(B)** Representative 20× magnification pictures of H&E stained lungs of *Chop* transgenic mice, 4 weeks Dox+ (h) and Dox- (g), 8 weeks Dox+ (j) and Dox- (i), and their FVBN background control mice (f). Scale 100 µm.

4.5.5. Investigation of effect of Chop induction on expression of pro-fibrotic factors in transgenic mice

Although Chop overexpression *in vivo* did not induce lung injury and fibrosis, we asked, whether we can detect up-regulation of pro-fibrotic proteins in the induced *Chop* transgenic mice.

Lung homogenate from Dox- and Dox+ *Chop* transgenic mice was analyzed for expression status of pro-fibrotic factors *Col1a1, Acta2* and *Pai1* on mRNA level (as described in chapter 3.2.7), and as described in chapter 4.5.2., mice in which Chop was highly overexpressed at 4 and 8 weeks in Dox-induced conditions were used for the analysis.

All analyzed genes were up-regulated on mRNA level. However, *Acta2* was up-regulated only at 8 week time point in Dox induced conditions (Figure 4.24.C), whereas *Col1a1* and *Pai1* were up-regulated already after 4 weeks and highly expressed after 8 weeks feeding time with Dox (Figure 4.24.A and E respectively). By comparing of Dox- and Dox+ at 4 and 8 week time points, we could not observe a significant difference between two groups for *Col1a1*, *Acta2* and *Pai1* (Figure 4.24.B, C, E, respectively).

These results suggest that Chop may be involved in the induction of lung fibrosis at later time points, such as 6 or 9 month in the Dox induced conditions. However, this study will have to be performed in future.

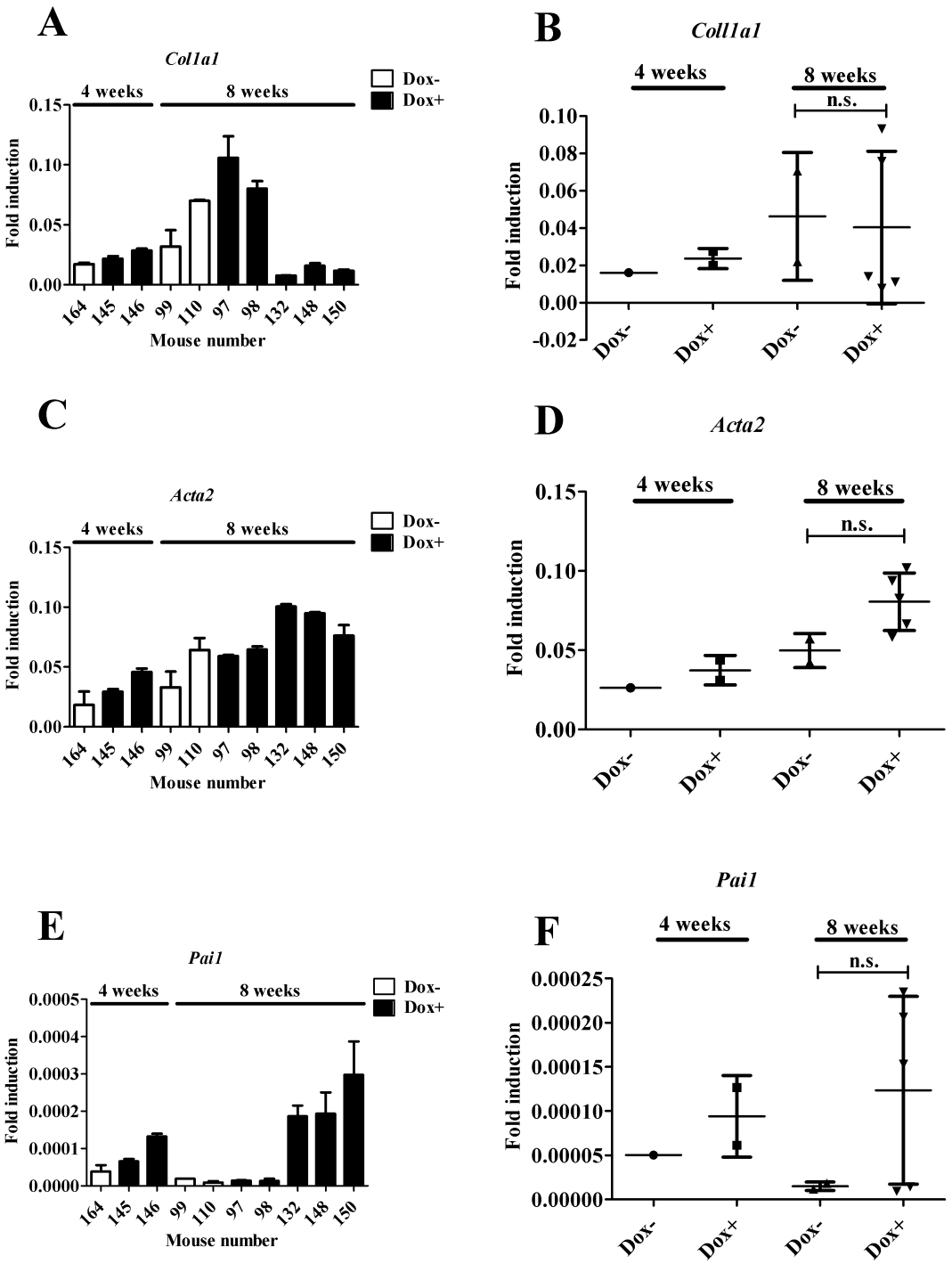

Figure 4.24. Investigation of effect of Chop induction on expression of pro-fibrotic factors in transgenic mice.

(A, C, E) Expression of *Col1a1, Acta2* and *Pai1* mRNA in lung homogenate from mice fed (Dox+) or unfed (Dox-) during 4 and 8 weeks.

(B, D, F) Statistical comparison of two groups Dox- versus Dox+ by Student's t-test, 4 weeks and 8 weeks time points, n.s. – non significant.

5 Discussion

5.1. New molecular mechanism of *CHOP* transcriptional activation

5.1.1. Multiple pathways in *CHOP* gene induction

CHOP encodes a nuclear pro-apoptotic basic region leucine zipper transcription factor belonging to the CCAAT/enhancer-binding protein (C/EBP) transcription factor family, which is markedly induced by a variety of cellular stresses [56] [57] [117]. CHOP was first identified as being expressed in response to growth arrest and DNA damage [119]. The expression of CHOP was subsequently shown to be induced by many other cellular stresses such as amino acid deprivation [120] [121], growth inhibition by prostaglandin A2 [122], hypoxia [123], acute phase response [124], endoplasmic reticulum stress [125], glucose deprivation [116], cysteine conjugates [126], as well as tunicamycin [127] [123] and calcium ionophore treatment [128].

Multiple transcription factors are involved in the activation of the *CHOP* gene in response to different stress stimuli. *CHOP* can be induced by SP-1 in response to paclitaxel treatment [129], by ATF2 due to amino acid starvation [130], by ATF5 in human hepatoma, in HepG2 cells after amino acid limitation, by arsenite or cadmium exposure [131], and by p53 during DNA damage [132]. However, in all these situations, the induction of the *CHOP* gene was linked to the activation of the endoplasmic reticulum stress (ER) stress response resulting from the accumulation of missfolded proteins, which induces the unfolded protein response (UPR) [125] [56] [76] [133]. Several components of the UPR have been identified. First, IRE-1α and β, which have RNA endonuclease activity, induce alternative splicing of the *XBP1* transcript, the translocation of which encodes a potent transcription factor, that induces genes involved in the ERAD pathway. [38] [134]. Second, the 90 kDa ATF6 transcription factor is proteolytically cleaved to p50ATF6, and migrates to the nucleus to serve as a transcription factor for ER chaperones, in order to maintain correct folding of unfolded and missfolded proteins. [135] [38]. Another important protein involved in UPR is PERK, an ER transmembrane protein like IRE-1 and ATF6, and its target gene ATF4 [136]. Previous studies described that *CHOP* is induced by ATF4, ATF6, and the spliced form of XBP-1 under ER stress conditions [137] [134] [135].

Several publications reported the up-regulation of CHOP during ER stress on mRNA and protein level in pathological conditions such as atherosclerosis [82] [65], diabetes [89], and neurodegenerative diseases [80]. Other publications described up-regulation of UPR markers such as XBP-1, EDEM, GRP78 in idiopathic pulmonary fibrosis [26] [104]. We showed the co-localization of UPR markers with CHOP and cleaved caspase 3 in alveolar type II cells in idiopathic pulmonary fibrosis. [27]. Furthermore, our group also focused on the role of ATF4, ATF6 and XBP-1 transcription factors in induction of AECII apoptosis [138]. Atf4, Atf6 and Xbp-1 were overexpressed *in vitro* in MLE 12 as well as *in vivo* using a transgenic mouse model. Overexpression of Atf4, Atf6 and Xbp-1 in MLE 12 *in vitro* and in transgenic mice *in vivo* did not cause the induction of endogenous *Chop* expression and subsequent apoptosis [138]. This led us to hypothesize that the *CHOP* promoter contains other yet unidentified transcription factors binding sites, which are operative and of relevance for the transcriptional control of the *CHOP* gene during ER stress.

To dissect the molecular structure of the human *CHOP* distal and proximal promoter regions, a bioinformatic approach was employed to search for transcription factor binding sites. According to this analysis, we identified already known and highly conserved transcription factor binding regions downstream of nucleotides -103, -778 and -310, containing putative endoplasmic reticulum stress response elements (ERSE1 and 2) [51] and amino acid response elements (AARE1 and 2) [130], respectively (Figure 4.1.). Additionally, bioinformatic analysis of the *CHOP* promoter showed approximately 31 putative *cis*-regulatory transcription factor binding sites of 17 different transcription factors (Figure 4.1). In summary, the human *CHOP* promoter is mainly characterized by the occurrence of four putative transcription binding elements AARE1/2 and ERSE1/2, a variety of distinct binding sites for AP-1, GATA-1, GATA-2, MZF-1, c-Ets-1, C/EBPs, Myb, STATx, Tal-1a/b, Lyf-1 transcription factors, and six *cis*-regulatory elements for SP-1 (Figure 4.1), suggesting their possible involvement in the regulation of human *CHOP* gene expression.

Previous studies described that AARE elements in the *CHOP* promoter are bound by ATF2 in response to amino acid starvation [129], by ATF4 and ATF6 during ER stress [139] [135], and by ATF5 after arsenite treatment [131]. In other publications, it was reported that ERSE1/2 are as important in regulation of the binding of ATF6 and XBP-1

transcription factors to the human *CHOP* promoter after induction of ER stress [137] [134] [135].

Our *in silico* promoter analysis correlated well with the published literature. Using a reporter gene assay, we showed that a promoter fragment containing two AARE and two ERSE elements (Figure 4.4. fragment 1), and a fragment containing one AARE and two ERSE elements (Figure 4.4. fragment 2), induced luciferase expression in response to tunicamycin treatment in human and mouse epithelial type II - like cell lines A549 and MLE 12, as well as in renal HEK293T cells. However, a promoter fragment containing one AARE element did not show any luciferase activity (Figure 4.4. fragment 3), confirming previously published results that the two AARE elements have to act together in order to induce *CHOP* gene expression [120]. However, the fourth fragment containing the *AP-1*, *c-Ets-1* together with two *SP-1* and *MZF-1* transcription factor binding sites induced luciferase expression in all three cell lines (Figure 4.4.A, B and C, fragment 4). Therefore, the nucleotides essential for transcriptional activity of *CHOP* during ER stress located in the fourth fragment, region -300 - -110 nt., had to be further investigated.

5.1.2. *CHOP* is a potential target gene of AP-1 and c-Ets-1 transcription factors during ER stress

In the present study, deletion analysis of the fourth fragment of the human *CHOP* promoter using a reporter gene assay revealed that *AP-1* and *c-Ets-1* transcription factor binding sites seem to play a role in the induction of the *CHOP* gene during ER stress (Figure 4.5.).

Some authors have suggested that AP-1 is up-regulated under ER stress conditions and that it is induced by IRE-1 via MAPK-dependent signaling pathways in different experimental models [52] [140] [141] [142]. Others have described that c-Ets-1 can be induced by spliced XBP-1 through the PI3K/Akt pathway [143] [144]. Our data favorably fit to these previous observations. We detected up-regulation of Ap-1 and c-Ets-1, as well as of the other UPR markers Atf4 and Atf6 on protein level, as well as of *sXbp1* on mRNA level, after induction of ER stress by tunicamycin in a time-dependent manner (Figure 4.6.)

In a recent study by Guyton et al. it was shown that *CHOP* is activated in response to oxidative stress and arsenite treatment in HeLa (human cervical carcinoma) cells.

However, in their work, the authors did not show the induction of the *CHOP* gene by AP-1 in response to ER stress or the correlation between oxidative stress and ER stress [145]. Additional studies described the induction of *CHOP* gene by c-Ets-1 in COS (CV-1 in Origin with SV40 genes) cells [146]. However, in this paper, the authors checked the efficiency of binding of c-Ets-1 to the *CHOP* promotor in isolated nuclear extracts and without any further experimental challenge [146].

Our results support the hypothesis that Ap-1 and c-Ets-1 transcription factors bind the *Chop* promoter in MLE 12 lung epithelial cells under ER stress conditions. Employing a *Luciferase* reporter gene assay, the region -300 - -110 nt. of the human *CHOP* promoter induced luciferase expression in human A549, mouse MLE 12 lung epithelial cells and in kidney epithelial HEK293T cells in response to tunicamycin treatment in comparison to solvent control (Figure 4.4. 4th fragment). These results were confirmed by ChIP assay (Figure 4.9.). Here, Ap-1 and c-Ets-1 transcription factors were found to bind to the *Chop* promoter after treatment of cells with tunicamycin, but not in untreated or DMSO treated cells (Figure 4.9.).

5.1.3. AP-1 and c-Ets-1 transcription factors induce *CHOP* gene expression via interaction during ER stress

The herein described deletion analysis of the region -300 - -110 nt. of the *CHOP* promoter revealed that *Ap-1* and *c-Ets-1* transcription factor binding sites are responsible for the induction of luciferase expression and hence *Chop* induction in MLE 12 cells after induction of ER stress *in vitro* (Figure 4.5.). Furthermore, and to our surprise, deletion analysis of fourth fragment of the human *CHOP* promoter also showed that these two transcription factor binding sites seem to act synchronously in inducing luciferase expression *in vitro* (Figure 4.5.). Based on our results, we hypothesized that, during ER stress, AP-1 and c-Ets-1 physically interact with each other in order to induce *CHOP* gene expression. In support of this hypothesis, one previous report showed that AP-1 and c-Ets-1 interact with each other in order to mediate basal activity of glutathione S-transferase expression through binding to the regulatory element EpRE in response to treatment of HepG2 (hepatocyte perpetual cell line) cells with phorbol 12-myristate 13-acetate (PMA) [147] [148]. Others reported the direct physical interaction between c-Ets-1 and AP-1 proteins both *in vitro* and in activated human T cells [149]. Logan et al. found that tissue inhibitor of metalloproteinases-1 (TIMP-1) is regulated by AP-1 and c-Ets-1

transcription factors. In this study, the authors showed that c-Ets-1 was not able to activate the expression of TIMP-1 alone, but would enhance the transcription in cooperation with AP-1 [150]. Nevertheless, no direct evidence has yet been provided concerning the cooperation of AP-1 and c-Ets-1 in activating of the *CHOP* during ER stress.

In this report, we now present evidence that not only AP-1 affects *CHOP* gene expression, but also that it requires the cooperative interaction between AP-1 and c-Ets-1 under ER stress conditions. Such interpretation stems from the observation that optimal induction of CHOP during ER stress requires both *AP-1* and *c-Ets-1* signaling. We demonstrated that the *Chop* promoter contains both *Ap-1* and *c-Ets-1* transcription factor binding sites as shown by ChIP analysis, and that Ap-1 and c-Ets-1 interact with each other, and act synchronously in binding and activating the *Chop* promoter. Finally, we added proof for such hypothesis by showing that mutation of *AP-1* or *c-Ets-1* transcription binding site caused a significant reduction of luciferase and hence promoter activity, and that simultaneous mutation of both binding sites resulted in even more reduction of luciferase activity compared with the wild-type promoter (Figure 4.8.). Forth, simultaneous overexpression of Ap-1 and c-Ets-1 transcription factors together with the *CHOP* promoter-luciferase reporter construct revealed binding to the promoter by AP-1 and c-Ets-1 and subsequently activation of the *Luciferase* gene (Figure 4.7.). Finally, overexpression of both transcription factors *in vitro* in MLE 12 cells revealed induction of endogenous *Chop* gene expression (Figure 4.11.). In summary, our data support the concept that concomitant overexpression of Ap-1 and c-Ets-1 regulate the level of *Chop* mRNA by enhancing the transcriptional activity of the *Chop* gene. These findings improve our understanding of the transcriptional control of the *Chop* gene and explain how signaling potentially apart from the conventional UPR (PERK, IRE-1, ATF6) could switch a primarily cytoprotective response into an apoptotic one. With this regard, AP-1 and c-Ets-1 offer as novel players which may modify the UPR accordingly.

5.2. Chop is involved in induction of alveolar epithelial apoptosis and fibroblast proliferation

5.2.1. Chop induces apoptosis in alveolar type II cells (AECII)

CHOP was originally isolated as a gene induced primarily due to DNA-damaging agents; subsequently, it became clear that *CHOP* is induced in response to endoplasmic reticulum stress [119] [56]. Gain-of-function and loss-of-function experiments have shown that CHOP acts as an inducer of cell cycle arrest and apoptosis during ER stress [151] [152] [56]. Some investigators have hypothesized that CHOP may also be involved in the initiation or execution of apoptosis in response to toxic agents that kill cells by cell death, although the precise details of this action are not well understood [153] [154] [155] [74] [156]. In more detail, it was shown that treatment of leukemic cell lines with the topoisomerase inhibitor etoposide, an inducer of CHOP expression, resulted in apoptotic DNA fragmentation at the time when CHOP expression first increases [154]. Mice deficient for the *Chop* gene do not show a similar epithelial apoptosis in response to treatment with tunicamycin, an inducer of endoplasmic stress, in comparison with wild type mice [56], thus indicating a requirement for CHOP in mediating tunicamycin-induced epithelial apoptosis [56]. On the opposite, overexpression of CHOP has been linked to the induction of programmed cell death in growth-factor dependent 32D myeloid precursor cells, providing additional evidence for a causal link between CHOP expression and apoptosis [153]. Finally, CHOP also seems to play a role in macrophage apoptosis induced by a combination of ER stress inducing agents and pattern recognition receptor (PRR) ligands, a deletion of CHOP blocked apoptosis [157] [158].

Apoptosis of AECII is a prominent feature in both, experimental and human lung fibrosis [159] [160] [161] [162]. Although the specific role of apoptosis in lung fibrosis remains an open question, elucidation of this mechanism is worthy of attention [163] [164] [165]. In this regard, we suggest that ER stress may be an important mode in inducing of AECII apoptosis leading to lung fibrosis.

Although the common relationship between AECII apoptosis and induction of lung fibrosis has been proven experimentally in the past [166], the precise role of CHOP in this context is not well settled. In previous studies, it was reported that markers of UPR activation such as ATF6, CHOP, BiP and XBP-1 are elevated in AECII of patients with IPF [167] [26] [27]. Moreover, AECII isolated from IPF lungs showed increased levels

of active phosphorylated IRE1α and spliced *XBP1* [166]. In additional, Korfei et al. performed a comparative proteome analysis of lung tissue from patients with sporadic IPF and human donor lungs using two-dimensional gel electrophoresis and MALDI-TOF-MS. In this study, an increased expression of UPR markers, heat-shock proteins and DNA damage stress markers was observed in IPF lungs [168]. In a more recent study by Korfei et al., by employing competitive proteome analysis, up-regulation of ER stress markers and down-regulation of anti-apoptotic and anti-fibrotic proteins was observed in peripheral lung tissue from patients with IPF as well as with fibrotic non-specific interstitial pneumonia (NSIP) [169]. In addition, UPR markers were detected in Hermansky-Pudlak syndrome interstitial pneumonia (HPSIP) in which AECIIs are also injured and lung fibrosis develops with grade similarity to human IPF [170] [166] [171].

In view of the proposed role of CHOP in ER stress-induced apoptosis, we examined its role by overexpression of Chop, *in vitro,* in MLE 12 cell line and in primary murine AECII and, *in vivo,* using transgenic mice with AECII specific overexpression of Chop. Based on our study, Chop overexpression induced cleavage of caspase 3 in MLE 12 and in freshly isolated primary type II cells *in vitro* (Figure 4.14 and 4.16.). Furthermore, by using a LDH assay, we could detect cell death in both of these models in response to Chop overexpression in a time-dependent manner. Additionally, by using a conditional transgenic mouse model, we detected up-regulation of cleaved caspase 3 in AECII after feeding of mice with doxycyclin for 4 and 8 weeks time points (Figure 4.21.), although the overall level of cleaved caspase 3 appeared not too high.

Chop regulates the expression of Gadd34, which negatively regulates the phosphorylation of eIF2α. Enhanced phosphorylation of eIF2α reduces protein translation [172]. In this study, we observed an up-regulation of Gadd34 in response to Chop overexpression on protein level *in vitro* in a time-dependent manner (Figure 4.15.), and on mRNA level in the transgenic mouse model *in vivo* (Figure 4.22.). However, we could not detect significant protein level of phosphorylated and unphosphorylated eIF2α (data not shown). Gadd34 may have pro-apoptotic effects that are independent of its role as a component of an eIF2α-dephosphorylation complex [173] [174].

Recently, it was found that DR5 was up-regulated in the lung tissue samples of IPF patients, and induction of DR5 was specifically detected in AECIIs [175]. In this study, we observed induction of Dr5 in response to Chop overexpression on protein level *in vitro* (Figure 4.15.), and on mRNA level *in vivo* in lung homogenate from *Chop* transgenic

animals (Figure 4.22.). It has been found that Chop up-regulates the Dr5 during ER stress [76].

Furthermore, CHOP can also directly regulate death effectors such as Bcl-2, which is one of the key determinants of cell death or survival [58]. Overexpression of CHOP leads to a decrease in Bcl-2 protein, whereas overexpression of Bcl2 blocks CHOP induced apoptosis [58] [152]. In addition, overexpression of CHOP leads to translocation of Bax protein from the cytosol to the mitochondria [176]. Thus, the CHOP-mediated death signal is finally transmitted to the mitochondria, leading to activation of caspase-3 [56]. It has been reported that a significant up-regulation of pro-apoptotic proteins p53, Bax and caspase 3 was found in alveolar epithelial cells of IPF lungs, whereas the anti-apoptotic protein Bcl-2 was downregulated [162]. In the present study, we could neither detect an increased level of Bax expression nor a down-regulation of the Bcl-2 protein in our *in vitro* and *in vivo* models (data not shown).

5.2.2. Chop may contribute to oxidative stress in alveolar type II cells

Many studies have claimed that oxidative stress and/or oxidative signaling may play a major role in the pathogenesis of pulmonary fibrosis [177] [178] [179] [180]. Oxidative stress has been proposed previously as a mechanism for the alveolar epithelial cell injury in IPF [181]. It was reported that alveolar inflammatory cells represent the cellular source of reactive oxygen species (ROS) generation that induce AEC death in IPF [181] [182]. However, in more recent studies it was shown that structural cells of the lung, in particular activated myofibroblasts, produce significant amounts of extracellular ROS being sufficient to induce apoptosis of adjacent epithelial cells [183]. Moreover, the commonly used murine model of bleomycin-induced pulmonary fibrosis is characterized by an early induction of ROS-dependent AEC apoptosis, which can be inhibited by caspase inhibitors [184]. In addition, it was reported that the level of nonenzymatic low-molecular-weight antioxidants such as uric acid, ascorbic acid, retinol, and alpha-tocopherol was increased in the bronchoalveolar lavage fluids from patients with IPF, but that, despite of the upregulation of these low molecular weight antioxidants and also of Nrf2, a master switch of the antioxidant response, still there was ongoing oxidative stress, indicating that the compensatory increases in antioxidants were not sufficient to counterbalance the oxidative stress [185].

In several larger series, it was reported that oxidative stress and ER stress occur concurrently under some pathophysiological conditions, and that there is a cross-talk between these stress responses [186] which contribute also to the evolution of fibrosis of different organs [180] [187] [188]. To this end, cigarette smoke induces ER stress in bronchial epithelial cells via generation of ROS [112] [113]. In line with this, expression of CHOP by cigarette smoke is inhibited by application of antioxidants [112] [113]. Moreover, the induction of the UPR by ROS can result in the activation of Nrf2. The authors have suggested that PERK phosphorylates Nrf2, which represents an alternative mechanism to activate this transcription factor [189].

In the present study, we showed that overexpression of Chop *in vivo* induces expression of *Ero1α* on mRNA level (Figure 4.22.). It is known that the ERO1α is a transcriptional target of CHOP [66]. Recently, in a study employing mammalian cells, it was found that Ero1α contributes significantly to the levels of ROS generation in ER stress conditions [190]. Activation of ERO1α by CHOP might thus contribute to the CHOP dependent accumulation of ROS in ER stressed cells, and may thus contribute to the severe stress level and the reaction to undergo apoptosis in these cells [58].

5.2.3. Chop might contribute to pulmonary inflammation

Not too long ago, inflammation was considered as a primary pathway for development of IPF [14]. According to this older hypothesis, inflammation of the terminal respiratory unit including alveolar-capillary components and basement membrane would result in a loss of alveolar type I cells, proliferation of the alveolar type II cells and stromal cells, and the deposition of ECM [14]. According to many reports, the expression of cytokines such as TGFβ [191] [192], IL-1β [193] [194], IL-6 [195] and others [1] are highly unregulated in IPF.

It is known that ER stress induces inflammation through JNK, p38 mitogen-activated protein kinases and NF-kB [196]. According to many reports, CHOP is up-regulated in response to LPS treatment and subsequently induces lung inflammation via induction of caspase 11 and IL-1β [64] [197] [198] [199] [200]. Additional research showed that CHOP induces IL-6 in B-cells of LPS-treated mice [201]. It was also suggested that Chop plays a crucial role in the development of bleomycin-induced pulmonary fibrosis through induction of caspase 11 and IL-1β [202].

Our regarding the effect of Chop overexpression *in vivo* on expression of *Casp11, Il-1β* and *Il-6* mRNA levels (Figure 4.22.) is currently inconclusive however further studies will more precisely characterize the inflammatory response elicited by Chop.

5.2.4. Epithelial Chop expression favors proliferation of lung fibroblasts

It is well known that lung fibroblast are highly proliferative in IPF and that the myofibroblast is the pivotal mesenchymal cell type being responsible for the expansion of the mesenchymal cell pool and the greatly increased ECM deposition in IPF lungs [203]. This cell type thereafter contributes enormously to the histological and pathological pattern of UIP/IPF [203] [204].

In the present study, we showed that epithelial apoptosis induced by Chop overexpression in MLE 12 cells and freshly isolated primarily AECII would result in a change of the supernatant's composition which in turn induce proliferation of lung fibroblasts (Figure 4.17.A and 4.17.B respectively). The epithelial cell injury and apoptosis therefore seems to result in activation of fibroblasts and the deposition of extracellular matrix, hence the pro-fibrotic and pathologic changes observed in IPF lungs [205] [206]. Many studies have reported that alveolar epithelial cells are the main source of transforming growth factor (TGF)-β [207] [208] [209]. Xu et al suggest that the release of TGF-β by injured epithelial cells and its activation by the epithelial integrin $\alpha_v\beta_{6,}$ which may signal to fibroblast, convert them into αSMA-expressing myofibroblasts [207]. Another cytokine, which is produced and released on a high level by AECs in IPF, is platelet-derived growth factor (PDGF) [208] which can similar contribute to lung fibrosis by promoting fibroblast proliferation [209]. Other growth factors such as TNF-α and Endothelin-1 are expressed and secreted by hyperplastic AECII and act as potent inducers of fibroblast-to-myofibroblast differentiation [1] [210]. In addition to these various profibrotic mediators, which can induce differentiation of fibroblasts into myofibroblasts, it is of interest to mention prostaglandin E_2 (PGE_2). PGE_2 is synthesized by alveolar epithelial cells [211], fibroblasts [212], and alveolar macrophages [213]. This molecule originally has been shown as an inhibitor of fibroblast proliferation [214] and their differentiation into myofibroblasts [215]. Garrison et al showed that PGE_2 is able to reverse myofibroblast differentiation, by the ligation of the E-prostanoid 4 and, especially, the E-prostanoid 2 receptors and generation of the second messenger cAMP [216]. Several publications

suggest the explanation of an additional mechanism how damage of AECII can lead to the loss of control exerted by AECII on fibroblast proliferation and collagen synthesis. AECIIs are an important source of prostaglandin E_2, which has been shown to inhibit multiple aspects of the fibroproliferative response, including fibroblast chemotaxis, proliferation and collagen synthesis [217] [218]. A loss of AECII due to apoptosis could decrease intra-alveolar levels of this antifibrotic mediator. Recently, it has been shown that prostaglandin E_2 deficiency results in increased AEC, but reduced fibroblast sensitivity to apoptosis in IPF [219]. Furthermore, it has been published that injured AEC release a number of profibrotic molecules, such as tissue factor, factor VII and factor X, which are all able to activate mesenchymal cells [220, 221]. It is important to notice, that these different mechanisms mentioned above are not mutually distinctive, and may all potentially drive potent fibroproliferative responses.

5.2.5. Is epithelial Chop a major factor inducing lung fibrosis?

A main goal of this study was to investigate whether Chop overexpression *in vivo* induces alveolar epithelial injury and lung fibrosis. Although we could observe activation of cleaved caspase 3 *in vivo* (Figure 4.21.) in response to Chop overexpression for 8 weeks, we could not detect any significant change in lung structure in transgenic mice (Figure 4.23.).

According to a number of studies, there is evidence that ER stress is involved in development of fibrosis in other organs apart from the lung. In detail, such relationship has been observed in cardiac fibrosis [222] [223], inflammatory bowel disease [224] [225], renal [226] [227] [228] [229] [230] and liver fibrosis [231] [232].

In the context of this thesis, it is interesting to mention the extraordinary impact of Chop on the development of these fibrotic diseases. For example, in one paper it was strongly suggested that ER stress is activated in cardiac myocytes after treatment with isoproterenol which is a well-established model for *in vivo* study of an acute hyperadrenergic state. It led to increase of Chop expression in those myocytes being responsible for triggering apoptosis. In this research paper, the authors claimed that cardiac fibrosis indeed is mediated by ER stress [222]. As an additional example, Tamaki et al. found that Chop plays an important role in hepatocyte apoptosis and subsequent liver fibrosis due to cholestasis. In this study, decreased levels of TGF-β1 and αSMA,

alongside with a subsequently reduced collagen deposition was observed in Chop deficient mice after bile duct ligation [222]. These results were confirmed in models of lipid-induced hepatocyte cell death [231] and methionine – choline deficient diet [232]. Together they are determining the important role of Chop in liver injury and liver apoptosis.

As was mentioned above, CHOP was up-regulated in IPF where it was found to be expressed specifically in AECII [26] [27]. Despite the fact, that we could successfully overexpress Chop in AECII *in vivo* and induce at least a certain degree of AECII apoptosis, we could not observe any significant change in the lung structure after 8 weeks of feeding of transgenic mice with doxycyclin. Several reasons may be found to explain this obvious discrepancy between the expected and the observed phenotype. IPF is an age-dependent disease [233] [5], with a pick of cases beyond 60 years of age. Such observation is well in line with the fact that almost all chronic diseases with tissue fibrosis increase with age [233] [234] [235]. As underling reason, there is emerging evidence that GRP78 expression is reduced in the renal tubular cells in kidneys of aged mice. Thereafter, renal tubular cells develop apoptosis through caspase 12 activation, and thus aged mice develop more easily kidney fibrosis [227]. Furthermore, Torres-Gonzalez et al. found that aged mice develop fibrosis faster as compared to younger mice after infection with herpesviruses [236]. Additionally, aged mice developed ER stress and apoptosis in the AEC population faster than younger mice after infection with herpesviruses [236]. There are also few studies suggesting that Chop is up-regulated, whereas ER chaperones are down-regulated in aged mice [235] [237]. Additionally, Puzianowska-Kuznicka has reported that level of CHOP expression as well as epithelial apoptosis are higher in aged hepatocytes [238].

Our possible explanation for the observed phenotype therefore may be that the aged epithelium reacts differentially to Chop exposure as compared to non-aged epithelium, and that the level of epithelial apoptosis may be higher in aged AECII.

There are few mechanisms, which lead to apoptosis of AECII in aged lungs. Increased level of oxidative stress was observed in the aged AECII [239]. ROS are known to induce cellular senescence [240] and are elevated in experimental models of lung injury and fibrosis [241] [242]. Together with ROS formation, the aging process contains abundant characteristics that might affect the ER stress response (e.g., increased disturbance in calcium homeostasis, misfolding and aggregation of proteins, and impairment in global

protein synthesis) [238]. All these age-related changes imply that aged cells might be more vulnerable to ER stressors, leading to apoptosis. An additional possible mechanism, which can induce an apoptosis in the aged AECII, is telomere shortening. Telomerase can maintain the precursor function of AECII, and telomerase deficiency can contribute significantly to the impairment of their reparative capacity [243] [244]. Telomere shortening can cause DNA damage that leads to cell death, and defective telomere maintenance is a main mechanism for cellular apoptosis [245]. Telomeres activity has been demonstrated to be inversely associated with AECs apoptosis both in a bleomycin-induced model and in patients with IPF [244].

5.3. Conclusion and future perspectives

Idiopathic pulmonary fibrosis (IPF) is a progressive fibrotic pulmonary disease of unknown origin with a finally fatal outcome. Recent data show that ER stress and apoptosis of AECII play a central role in this disease. C/EBP homologous protein (CHOP) is a key regulator of maladaptive ER stress responses. ER stress is the most potent inducer of CHOP expression and CHOP is known as a pro-apoptotic factor. Recently, we showed that CHOP is expressed specifically in AECII in IPF, whereas it was not detectable in other cell types in the IPF lung. For this reason, we focused our attention on CHOP regulation in ER stress and apoptosis in AECII.

We hypothesized that the ER stress-induced apoptosis pathway mediated by CHOP is a major driver of AECII apoptosis in IPF. We therefore asked for the transcriptional control of the *CHOP* gene and discovered a new regulatory mechanism of *CHOP* expression. In detail, AP-1 and c-Ets-1 transcription factors were found to be up-regulated during ER stress, to bind to the human *CHOP* promotor under ER stress, and to subsequently induce expression of the *CHOP* gene *in vitro*. Furthermore, we also found that AP-1 and c-Ets-1 transcription factors physically interact with each other and induce *CHOP* gene expression *in vitro*. Our current observation needs to be explained in conditional knockout experiments showing that AP-1 and c-Ets-1 are truly the decisive factors during epithelial apoptosis and lung fibrosis *in vivo*.

Based on these observations, we also investigated the putative role of Chop in inducing epithelial apoptosis and lung fibrosis. We herein provide evidence that CHOP indeed induces apoptosis in AECII *in vitro* and *in vivo* and that expression of Chop alone, without a concomitant orchestrating UPR response, is enough to induce epithelial apoptosis.

Moreover, our results provide evidence that Chop is involved in lung fibroblast proliferation, thus again underscoring the significance of epithelial apoptosis for induction of lung fibrosis. Although we were not able to induce lung fibrosis after 8 weeks of transgene expression in young mice, we do believe that, once mice are aged or are contracted with exogenous hits, they most likely will develop lung fibrosis.

In conclusion, for the first time, we can show that *CHOP* can be induced by transcription factors other than the conventional UPR during ER stress. Furthermore, we demonstrated that epithelial Chop overexpression induces apoptosis of alveolar type II cells and fibroblast proliferation. We therefore speculate that epithelial CHOP plays a key role in pulmonary fibrosis.

6 Appendix

6.1. *In silico* analysis of the human and mouse *CHOP* gene promoter

6.1.1. Sequence of human *CHOP* promoter

-2686 AAGCACTGAGGGGAGGGCGGTGAGGAAGGCAGAAGTCTGGCAGTGAGAGGGAGAAGCGGC
MZF-1
-2626 GGGGGCAGGTGAGGGCGGGGGAGTGGGGATGGGGCCGGGGAAAGGGGCCGAGAGGACGCG
SP-1
-2566 GAGGGGGCAGAGGGTAGGGACGGGAGGGGGAGGGGCAGGGTGGGGGGGGCCGGGCCCCGC
SP-1
-2506 ACTCACCGCGGCCCATGGTTCGGCCGGCCCCGCCCTGCGCAGTCGCGGCCCAGAGGGTGA
-2446 GTGGGAGGGGGTGGGAGGAGGGTCGGTGGAGCCCGAGCCTCCGGTACGGCCCCGGCCGGT
-2386 CCTAGCAGGAAGCGCCGCTGCCGCCGCCGCGGATCACCGAGCGGCCTCCCGCGCATGCGC
STATx
-2326 CATGGGGGCCAGGGGCAGCCCTGGGGATTCCGTTCCCAGAAGGCACTGCGCAGGCTGCTG
-2266 CCGCTGCCGCCGCCGCCGTCGCTGCCGCAGCCGCCGCCGCAGGAGCCGCCGCCTCCGCCG
SP-1
-2206 CTGCCCGGACGGGAGAGGGGCGGGGCCGGGCCCCCGCCCAGCGGACAGCGACGAGCCAAC
-2146 TGGAGGGGCTGCAGTGCGCATGCGGGAGCGCGCCTACCCCTCCCCCACAACCCCCCATTA
-2086 ATCCCCAAGAGAACAAACACCCCACGCGGCCCCCCCGCCCTCCGCGGAAGGATCTGCGCC
-2026 TCTTCCCAGGCCACTGGTGGCCAATCCCAGCCCTCCTCAGGGAGGGGCCCCTTCCAAAGC
STATx
-1966 CACAGTCTGTTGCGGGAACCAGGAATGCCAGGTCCGGGAGGGGCCAGGCCCCGAAAGATG
SP-1
-1906 AAAGTCGCGACTTGCCCTGCCCCGCCCCAAAGGCTTCCCGGGTAGTGTGCTGGGACTTGA
-1846 CCCGCCTCCCCAGGTCAACATGTCACAACACGACCTCAGCCTGTCAAGTCACATGACCTC
Tal-1a/b
-1786 TGCCTGTCACTGACAACCTGGTCTGTCTTTAGGCCAGGGGAGACCATCTGGTCCACCCTC
C/EBP
-1726 CACACTACCCCCATTTTCAGAGAGGAAATGGAGGTGTGGAGCAGCGGAGCAGCCTAACCA
-1666 AAGACCTGTCATTGCCACACCACTCCAGTCACAACCGGCCTTGTGACAGTTTCTACTTAA
AML-1α
-1606 ACTCTGGCTGCCCCCATGAGGGTATGACAGGATATGTAACAGGCCACCACATGGCCTCTG
-1546 TTTTCAAGGCACAAGAAAAATACTTTGCATTCTGGGTGGTGCGTTTTACTTTTGGTCAAG
-1486 TTGCCTCCAAGTTCATGGTTCTCATTTTACCTTCACAACTTTTATCTTTAATTTACAAAC
GATA-1
-1426 AAGGACGGTAAGATCCCTTGGCAAGTGATGGGGAGTTGAGTCTAAAATCGCGGCTCCGGT
-1366 CTCCCCAGTCCAGGGCAGTCCTGCGCTGAAGTGCACTCACACGTCCCGGGATGAGACTCC
-1306 GCTGTAAATCTCGACCCGAACACCTAGGAGGCAGGCCTGTGCCGCGCTCCTCACACAGGG
-1246 AGTCACAGGACTTGCTGTCTGGTACAGCAAGAGAGGGTCTTGGAGAAAGCCATAGGAGTA
-1186 CCGTGGGGGAAAATAGGTGGCCAAACAGAATCGGGTCCACTGGGCAAAATACATGACTTC
-1126 TGGCAGGCTGAGGGCTTACCAACTACAAGGTAAAAGTCAAGGGCGCTGTTCTGAGAGAAG
Lyf-1
-1066 CGGAAAATGACTACCAAGGGATTCCAGTACCTCGGCCCCTTTGGGAGATTTACGGGGCT
HFH-2
-1006 AGAACAGGAGACCACCCCCGTTTTTTTGTTTGTTTGTTTTGTTTTTTGTTTTTGGTGAAA
-946 CGTAGTCTCGCTCTGTCACCCAGGCTGGAGTGCAGTGGCGCGATCTCGGTCACTGCAACA
HSF2
-886 TCCGCCTCCAGGGTTCAAGCGATTCTTCTGCCTCTGCCTCCAGAGTAGCTGGGATTACAG
AML-1α
AARE2
-826 GCGCGCATCACCACACCCGGCTAATTTTTGTATTTTTAGTAGAGACGGGGTTTCACCATG
Nkx-2.5
Lyf-1
-766 TTGGTCAGGCTGATCTCGAACTCCTGACCTCAAGTGATCCGCTCTCCTCAGCCTCCCAAA
-706 GTGCTGGGATTACAGGCGTAAGCCACTGAGCCCGGCCAGGAGACCTCTTTAAGAAGACTC
-646 GAGATGTCGACAATCCCAGTGGATGGATACCAACTTTAAAAAGAAAAGTTCAAAAGGCCT
-586 ATGTGCCCATTAGCTGGGAGGGGCCAAGAAATATGGGAGTCCCTTATAGTGGGGGTAAAA
-526 CGGCGGGTAAAGCTAGGTGGGCGGAACAGCAGCTTCTGGGGGAGACAAGCGGCAAAGAGG
GATA1/2
v-Myb
v-Myb
-466 CTCACGACCGACTAGGGGCGACCAAGGCTGATAGCCGTTGGGGCCGTTGGGCGCCGGGAG
-406 CTGGCGCCCCGCCCTCTCTCCTCTCCCCCACCCTCCGCACCTCCCACCACCCTCGGTGTC
AARE1
SP-1
-346 CCCTGCGCGTGCGCGTGCAGACACCGGTTGCCAAACATTGCATCATCCCCGCCCCCTTTT
MZF-1
MZF-1
AP-1
-286 CCTCCCCTCCCCCCCCGCTACACTCCCCTCCGCGCGCGCGCATGACTCACCCACCTCCTC
c-Ets-1
-226 CGTGAAGCCTCGTGACCCAAAGCCACTTCCGGGTCCGACACTACGTCGACCCCCTAGCGA

```
                                                                                                SP-1
-166 GAGGGAGCGACGGGGGCGGTGCCGCGGGGCTCCTGAGTGGCGGATGCGAGGGACGGGGCG
          NF-Y   ERSE                          NF-Y
-106 GGGCCAATGCCGGCGTGCCACTTTCTGATTGGTAGGTTTTGGGGTCCCGCCCCTGAGAGG
                      TATA                                    +1
-46 AGGGCAAGGCCATGGTAAAAGATTACAGCCAGGCGCTCCCGAGGTCAGAGACTTAAGTCT
+14 AAGGCACTGAGCGTATCATGTTAAAGATGAGCGGGTGGCAGCGACAGAGCCAAAATCAGA
+74 GCTGGAACCTGAGGAGAGAGGCGAGTACTGATTCCCATCTACCTTTTACCCTCCCGTCTC
+134 CTCAAAGTTGGGGCGTCCGCTCTTTAGGATCGGCCTCACTCCTCCACAGTGAAGTTAGGG
+194 ACCGTCCGAGAGAGGAATGGGGAGAGTCCCTTATTCTGGGGTGGTGCTTACAAACCCCTA
+254 TTGCTTCGGACGACGGCGTCTCTCCACCCCTGCCCGGAGCCGGAACACGGGCCCTGCTCT
+314 GTGCTGCTGGGCAAAGGGACCTCGGTTGCCCTTGGGAAATTCATTCTTTCCCGTAGCCAA
+374 CTTCAGGCCTCATCGTTAGGCCTGTCCGCGGGGAGGCAGGTCAGCAGGACACACCCCCGC
+434 TCTAAGACTGGGTGACCATCGCTCAGGCCGTTTCCGCCGCTTCGCCACCAGCGGGCCTTC
+494 TCCCTACCCCACCCCCAATTCTGTCTCAGTCTCAGTGCCTCTGGTGTCAGCATGGCCACC
+554 TTGGTAGCTGGGGCTACTGGACCCTGCAGCGGATAGGGGAACCTTGAGGAGACACAAGCC
+614 TTTGGGAGGGGTGCCGATGGACAGGGAGTGGTGTGTTTTCCTTTTGCCGTAGAGGTCTCT
+674 GGGCCTCCTGCACAAGAGAGCAGCCTGGATCTCTTAAGTGTAGGAGGCCATTTGGGGTCT
+734 CCCCAGGGTATTGTCCTTCCCTCGGGATTAGTCCCTGCCTCTTTAACCCGGTCCTGTCTC
+794 CCAGCTAATCTCTGTGTAACCATTGCATCAGGCCAGCCCCGTTTGGCTCTGCAGCCTTCT
+854 GACCTGAGGCTCTACTGCTGATGAAAGCCAAGTCCCACACACTGGAAGGCAAGGGAGGGT
+914 TCCCCAGGGAGGACAGCCCTGCAGAGAAATACTTCGGGCAATATTGCATCTCTAGCCCCT
+974 AGGGATCAGCAGCTGCCACTCTGCTTCTGCCCCTTCCCTATAAGAGAGACTGGGGGGAGT
+1034 TTATCCATTCATTCTTAACAAATACTTAATGAGGACCTACTGTGTGCCACACAGTTTGGG
+1094 GCTCAGGGTACATCCTTGAGCAAGAGGAAAAAATCATCTCAGTGGGAGGCCTACAGTAAA
+1154 CAAAATATAAGTGCCACGGAGAAAGCTAAAGCAGAGAAAGGAATGGAGAATGTTCAGGAT
+1214 GGAGGTCAGAGTGTTACATCAGGTGGTCAGGAATTACCTTAGGTAATTCCTCCACTCAAA
+1274 ACCCTTCAGTGACTTCCATGACATGAAATAGGAAGTCATTGGAGGGTTTGAGCAGAGGAA
+1334 TGACCTGTTTTAAAAGGCTCACTCAGGCTGCTGTATGGTGAATAGAGTTGCGGAGGGGTG
+1394 GCAAGAGAAGAAATGGGAAGACCTTCTGCAGTCAGAAAGTTTCTGCAGTAATTTAGAGAT
+1454 GGTAGTGAATTGATCTAGATTGGAAACAATGGAATTAGAAGTGTTTAGATTCTTCTAAGC
+1514 AAAGGTTTTAAAAACTCATTTTTAAAGAATGAGTTAAGGGCCGGGCATGGTGGCTCACAC
+1574 CTGTAATCCCAGCACTTTGGGAGACCAGAGGTGGGTGGATCACCTGAGGTCAGGAGTTCA
+1634 AGACCAGCCTGGCCAACATGGTGAAATCCCATCTTTACTAAAAATACAAAAATTAGCCGG
+1694 GCATGGCAGTGCATGCCTGTAATCCCAGCTACTCCGGAGGCTGAAGCAGGAGAATCGCTT
+1754 GAACCCAGCAGGCGGAGGTTGCAGTGAGCCGATTGCGCCACTGCCTTCCAGCCTGGGCAA
+1814 AAAGAGTGAGACCCGTCTCAGAAAAAAAAGGAATGAGTTAAAATTTGCTAGTACTTTGGAT
+1874 TGCAGGGTGTGAGAGAAGAGGAATGAAGGATGATACCAAGGTTTTTAGCTTAAGCAACTA
+1934 GAGTTGTCATCTGAGATGGGGATGACCTTGGAAGGGGAAAATCAGCAAGAGTTTGCCTTT
+1994 GCACATAGTCTTAGGTGCCTATTAGACATTGAAAAAGAAATGGCAAGTAGGCAGTAGACA
+2054 GCAGAGTCTGAAGTTCTGGAAGAGGTCCAGACTGGAAATGTACATTTGGAGGATGTCAGC
+2114 CCTGTGGGAATGGAGTTAGGAAAATGCTATGATTTGTTCCCTTCCCTGTAGTTTAGTTTT
+2174 TACCCTGGCAGATTTGAGGCCTGCTTTGGATTTAGAGAAAGCTGAGTTGGCCAGGACTTT
+2234 ACTATTATGTAACCAGGACTACAAATGTCAGCAACTAAAAATAAAGAAAGTCAGGCCCTC
+2294 TTCTGCCCTTCGAAATGGCTACAGGGACCAAGTATGCATACCCCACAAGACCAGAAGTAA
+2354 GGAAGGACCAGTAGGAGGCTGGAGGTAAAAGAAAAATAAGGGCCCAGCACGGTAGCTCAT
+2414 GCCTATAATCCCAGCACTTTGGGAAGCGATGGATCACAAGGTTAAGAGATGGAGACCATC
+2474 CTGGCCAACATAGTGAAACCCTATCTCTGCTAAAAACACAAAAATTAGCTGGGCGTGGTG
+2534 GCACGCGCCTGTAGTCCCAGCTACTCGGGAGGCCGAGGCAGAAGAATCACTTGAACCGAG
+2594 GAGGCAGAGGTTGCAGTGAGCCGAGATCGCACCACTGCACTTCAGCCTGGCAACAGAGCA
+2654 AGACTTGGTCTCAAAAAAAAAAAAAGAAAGAAAAAAAGAAAAAGAAAAGTAAGTTGCCTC
+2714 TCCCCCTTCCAAAAATGGCTGACATTTCTCTTTGTTGCCCACAGTGTTCAAGAAGGAAGT
+2774 GTATCTTCATACATCACCACACCTGAAAGCAGGTAAACTTAACCTACCCTTTTCCAAAAA
+2834 TTTTAAACGGCAGGACAGTAAATATTTTAGATGTTAAAAGTCCTATAGTCTCTAGCGTGA
+2894 CTCTTCATCTCTGCCACTGTAGCACCAAAGCAGCCATAAACAATATGTAAATAAACAGAT
+2954 GTGGCTGTATTCCAGTACAACTTTACCTACAAAAACAGGCATCAGACCAGCTTGCCAACT
+3014 TGTGGCATAGACTGTTTGCTACATGGAGCTTGTTCCAGCCACTCCCCATTATCCTGCAGA
                                          +3105
+3074 TGTGCTTTTCCAGACTGATCCAACTGCAGAGATGGCAGCTGAGTCATTGCCTTTCTCCTT
     CGGGACACTGTCCAGCTGGGAGCTGGAAGCCTGGTATGAGGACCTGCAAGAGGTCCTGTC///////
```

6.1.2. Sequence of mouse *Chop* promoter

```
-663 ACTATCAAGGAACTCAGTCTTTGGGACGCATTAGAAGGCTAAAAGAGGAGGAGAGCTCTT
-603 AAAAGATTCGAGGAGATGTCAATCCAGGTGAACAAATTGGAAACTTTAAAGAGGTTCCAG
-543 AGCCCCGGTGCCCATTAGCTGGGAGGGGCCAGGGAAAATGGGAGCCTTTCATGGAGGAGT
                                                GATA1/2  v-Myb      v-Myb
-483 AAGTTAAAGGTGATGGGAGGTGGGCAGACAAGTTCAGGAAGGACAGCCGTTGGGGCCGTT
-423 GGACACTGGGAGCTGGCGCTCCGCCCTCTTTCCTCTCTCCCCCATAGCCCCCCTCCCGCA
                                                                AARE1
-363 CCTCCCACCACCATCGACGTCCCCTGCGCGTGCGCGCGCGGACACCGGTTGCCAAACATT
           SP-1                                  MZF-1          AP-1
```

-303 GCATCATCCCCGCCCCCCCATCCCCTCCCTCGCCGCGCTCTCCTCCGCGCGCGCGCATGA
c-Ets-1
-243 CTCACTCACCTCCTCCGCGAAGCCGCGTGACCCAAAGCCACTTCCGGGTCCGAGACAACG
-183 TAGACTCTCAAGCCAGAGGGCGCGATGGGGGTGGGGCCGTGAGACTCCTGAGTGGCGGAT
SP-1 NF-Y ERSE NF-Y
-123 GTAAGGGATGAGGCGGAGCCAGTGCCAGCGTGCCGCTTTCTGATTGGTAGGCTCCTGGAC
TATA
-63 CCTGCCCCCCCCCCCAGGAGGGGCCGGACAGCATAAAGGATACTCGCTCTCCGCTCTTGAG
+1
-3 GTCAGTTATCTTGAGCCTAACACGTCGATTATATCATGTTGAAGATGAGCGGGTGGCAGC
+57 GACAGAGCCAGAATAACAGCCGGAACCTGAGGAGAGAGGCGAGTACTGGCTCCGTCTAAC
+117 CCTTACCTTCCCATCCTGGCCAGCATAGCTATTTTATAAAGTTGGAGACAACTGTTCTGG
+177 AGGATGTAGCCCCACCCCTTCCACTGTAAGCTTGTAGACTGGGAAGGGTGAAGGCCGGGA
+237 ATCCCTGATTCAGGAATGGTGCTTACAGGCCCTCTCTTGCATTGGGCGATTGCATTCCCG
+297 TTCCCTTGTCTCGAGTTGGTCCCCACTCTGCAGAGGGACTCCGGTTGCCTTCGGGAACTT
+357 GTCTCTGTAGTGCGAACTGCGGGCCAGCTTAGGCCTGGGCAGTTCGCAGGAAAGGCGGGG
+417 CAGCAGGACACACCCCCAAAGTCGGGGACTCTGGCTGTCTCAGCCTTTTCTTCACCAGCC
+477 TCATTCCCCCCAACTCTTTCAAGCTGAAGCGCCTCAGTCAAGGGGCCAACATGGCCACGT
+537 TAGTAGCTGACTCTCAAGTTCAAGAGAACGCGAAGACTGACAGATCTTTGCGAGTGGGGG
+597 TGCTGGTGGGAGGAGCATAGATGGGTTTTTCCCTTTTCCCCAGAGGTTTCTAGGTTTCCA
+657 TACAAGAGAGCAGCCTGGATCTCTTTAACTATGGGAAATTATTTGGGATCTCTCCAGGGT
+717 CTTCTGCTTCTCCCAGGGCTGATTGATCTCTGCTTCTTTCCTCAGTCCCGTCTCCTAACT
+777 AAACTGTGTAACCATTGCGTCAGGCCAGCCCACTGTTTGTCTCTGCACCCTCAGGCCTGG
+837 GGCTCCTCTGCTGATGAAAGCCAGGTCCCACACACTGGAAGACCAAGGGAGTTTTCCCTA
+897 GAGGACAACCCTGCAGAGAAACACTCAGGGCAATATTGCATCTGCAGTCCCCAGAGACAG
+957 CCAGCTCCGCTCTGCCTTTAGGCTCAGTGGGCTTAATTCTCTATAAGGGAACTTGGGGGA
+1017 GGGGCTTTTTCCCCATTCATTCCTAACAAATGCCTAATAAGCACCCACTATGTACCAAGT
+1077 ATCTGGGGACCCAGGGTATATTAGGAGCAAAAGATAAAACTGTTCTCAATAAAACTTACA
+1137 TTTCAGTATAAAGCAAAAGGGAAAAAAAAAACAAAAGCAGGGCAGAATAGTTCAGGGCGG
+1197 TGACTAGAGGTTGTCATCAGAAGCCAAGCCTGTGAGCCAAGCCCCGGTGTTAGAGCTTTA
+1257 TAGAAGGGAGAGGCTGAGCAACAGAGTTAAGATAAGCATGCCATGCCGGTATCTTTAGGA
+1317 ACAGGACTAGAGTAAGCAGGAGAGGGTGATGAAAGGAAACTCAAGCAGCCGGTCTCATAG
+1377 AGCCTTGCAAGCACCCTCATGATGCTAATCTTTAACAATCATGAAACAGGAAGCCATTGG
+1437 GGGATCTGAGCAGAGGAATGATCATAGCACATGCATTTAATTCCAGCACTCAGAGAGGCA
+1497 GATCTCTGAGCTCCAGGCCAGCCAGGGCTACATTATGAGACCCTGACTCAAAATAAATAC
+1557 AAAAACAAAGGGTTAGGTATGTAGCTCAATAGTACACTGCTTGCCTGGTATGTAGAGGAC
+1617 CCTAGGTCAACCCACAGCCGTGAAAATAAAGTAAAAGACAAGAATAGAAACAGGAGGTCT
+1677 CAGCTGAACATAGTGGCACAGCCTTTAATCCCAGCACTTGAAAGGCAGGCAGATCTAAAT
+1737 TCAAAGCCAGAGAGTCTACAAAGCAAGTTCCAGGACAGCAAAAGCTACATAGTGAGACCC
+1797 TGTCTAAAAGAGAAAGAAAGGAAAGGAAAGGAAGAAAGAAAGGAGAGATTTCAAAGAGGC
+1857 TTCCAAAATAATCCAGGGAAAGAAATGTATGGTAAATTTATATCTGGAGCCAGGCAGTGG
+1917 TGGTGCACGCCTTTAATCCCAGCATTTGGGAGACAGAGACAGGCGGATTTCTGAATTCGA
+1977 GGCCAGCCTTGTCCACAGTGAGTTCCAGGACAGCCAAGGCTACACAGAGAAACCCTGTCA
+2037 AGAAAAACCAAAAAAATAAATAAATGAAAAATAAAAAATTGCATCTGGAAATAATGTAGT
+2097 AATGAGAAATACTTAGGTTTGGGGTACTTTTAAAGTTGTCAGTGCTTTAGGCTGAGCTGT
+2157 GGTATCTGAGAAAGGGGCATCAAGGATACCAAAGTTTTTGGCTTTCAGCACCTAGAGTTG
+2217 CCATTTAGTAAGAACTATACAGCCTTGGTAGGAAAGGCCTTTCATGTAAGCTGAACGCCT
+2277 GCTCAACACTGCCAAGGAGCTGGAGATCCCAGAGCAGGTCTGCACTGAGGCTGCCAGTGG
+2337 GGGGATGGAATCTGAGCAAGCACTGCTGAGTTTACTCTTCCTTCCCTCTAGTTCTGTCTC
+2397 CCTTTGGCGGACTTGAGGTCTATCTGGGATTTAGAGAAAACTTAGTTGGCCAGGACTTTG
+2457 CTATTATGTAATCAAGACGGCAAATGTCAGCAACTAAAAATAAAGTTAAGCCTGCCTCTG
+2517 TCCTTGGAGTTGGCTTCAGGGACACACACGCTGCAAGACACACGCCTGTGTGTGTGTGTG
+2577 TATTACAAGAGAAGAAATGGCTTCAGGGACACACCCGCTGCAAGACACACACACCTCTGT
+2637 ATGTGTGTGTGTGTATTACAAGAGAAGAACTGGAGCCTGGTCTGCAGAGTTGTTGAGTTC
+2697 CAGAATTCCAGGATGCCCAGGGATGCACAAAGAAACCATCTCACAACCCATTTTAGAAAG
+2757 GATCTAGAAAAGGGCTAGGAGGAGTTAGAAAGGATCTAGAGAGGGGCTAGGAGGAGTTAG
+2817 AAAGGATCTAGAGAGGGGCTAGGAGGAGTTAGAAAGGATCTAGAGAAGGGCTAGGAGGAG
+2877 GCTGGAGGTAAAGGACTGTTTTTTCCTTTTCTCCACAGTGTTCCAGAAGGAAGTGCATCT
+2937 TCATACACCACCACACCTGAAAGCAGGTAATCTTGGCCACCCTCTCAGTCAGCTGCGAAT
+2997 GCTGCTCATGTTGCTTTGCTGGGGGAGAGTTAGACAAGGCCTTCATCTGAACAAGCTTTT
+3057 GCTGTCAGACCATGTCTTTCTCTGACCCCATAATGTTGTTTGAGAGCTGGCTTTCGAAGT
+3117 CAGCCTCAACAATGGCAATTGGTTTGTCTTCCCAACTCTCAGTCCACACCAAGATTAGAC
+3177 CCAAAGGACCTTTTGCCCAAGCTTCCCACACGAGAGAAAAAAAGAGTACAAATGGCCTGG
+3237 TAATTGCCCCTGGAAATTACCAGTAGTGTTCCCAAGAGAGTTGAATACTTTTACTGTAAT
+3297 CCTGTAAGAATATATATGTATAGCCAAGCCCAGTGACTGTTCCTCTCTCAGAACTTGAGA
+3357 GGATCCTGAAGTTATCTGTAGTAAATCCTTCTCAATAAAGGGTATGTTCTATCAGGTGTA
+3417 GTGGTGCATACCTTTAGTCCCAGCACTTGGGAGGCAGAGGAAGGTAAATGTCTGAGTCAA
+3477 AGCCAGCCTATTTTGCAGAGTGAGTTCCAGGGAAGCCAGAACTATATATACAGAGAAACC
+3537 CTTTCTTGAAAATACACCCCCCACCCTCCAAGTTTTGTTTCCAGGAGCTAGAGAGATGAC
+3597 TCAGTGGTTAAGAGCACGTGCTCTTCTTGTAGAGGATCTAGTCTAACTCCCAGTACCCAA
+3657 ATGGCAGTTCAAAACCATCTATGACTCTAGTTCCCAGGGAATCCATTCCCTCTTGTGGCC
+3717 TCCATGTCTACCAGGAACACACACACAGCACACATTCAGGCACTCACTTATATATGCATA
+3777 GATAATAAAATAAATATATCTTTGGGAAAAAAAAAAAGATATTTAAGGTTAGGTAGCCAG
+3837 CCTGGATTAAGCTTGGTAGTGACCAGCATATAAATGAAAACAAAACAAAAAGTTGGAAAG
+3897 CTGTGTGGGGGTGGTGCATACTTTTAATCCCAGCCTTCAGGAGGCTGAGGCAGGTTGATC
+3957 TCTGAGGCCAGTGTGAGTTCTAGGACAGGCAGGGCTACACAGAGAGACCCTGTCTTGAAC
+4017 AAACACCAAAAAGAATGGCAATGAGAGCCCGGAGAAAGCCTATCAGTTCCACACCCATGC
+4077 TGCCTGTGTGCCGTACCTGAGTCAGGTTTCCAGCAGCCACAGAAGGTGGCTCACATGGCC

+4137 TGGACCTCCAGCTCCAGGAGAGCCAATGAATGCTGCTGGCCCCCAGACACTGAATTACAT
+4197 CCGTTTCAGGGTCCTGGCCATGGTGTGCATGTGATCATCTGGACAACTTTTGAGAGTTGG
+4257 ATCTGGCAGGGTCAAAGTCAAGGCTGCTAGGCTTGAGAGGCAGCCATCTCCCCATCCCGA
+4317 CACACCATCATTAGTGTGTGTGCAGGTCAGAGAACAACTTGTGCGAGTTGACTCTTCACC
+4377 TCCACCCTCTGCCAATGTAGCCTTCAAGGAGTGACAACCCATGCCCTTACCTATCGTGCA
+4437 AGACCAGTAAATTTTAAATTCTACGTGTTAGAAAAGGGACAAGGTCAGCTCACCGACTGT
+4544
+4497 GGTGAATGGAATGTATGTCCTTTCCAGAACCTGGTCCACGTGCAGTC*ATG*GCAGCTGAGT
CCCTGCCTTTCACCTTGGAGACGGTGTCCAGCTGGGAGCTGGAAGCCTGGTATGAGGATC//////

Supplementary sequence 1 and 2: **Sequences of the human and mouse *CHOP* gene promoter are represent respectively.**

TFSEARCH and MatInspektor software were used to identify putative transcriptional factor binding sites in the human and mouse *CHOP* promotor. The translational site (ATG) is shown. High scoring transcription factor binding sites in the 2.6 kb. And 0.5 kb 5' flanking region of the human and mouse *CHOP* gene are illustrated respectively, those scoring >90 were considered as a positive. Definitions for the abbreviations are written in the text (chapter 4.1.1.).

6.1.3. Schematic illustration of the 5' flanking region of the mouse *Chop* gene

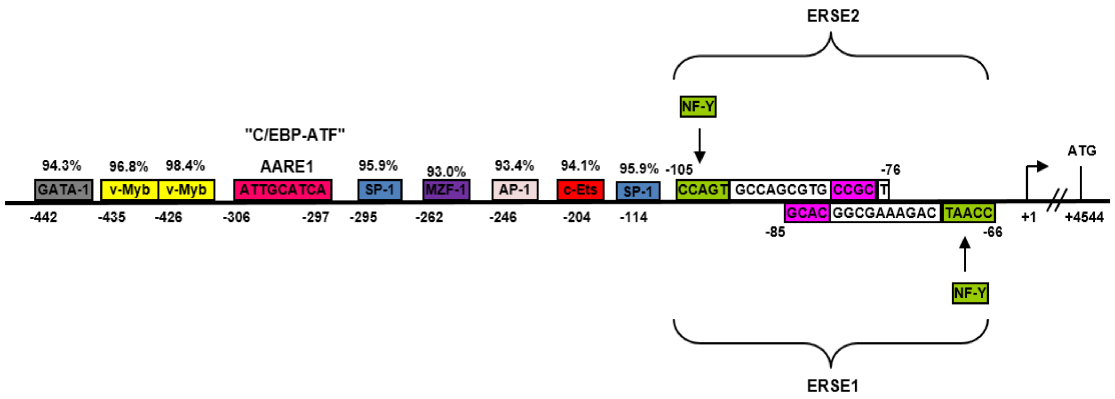

Supplementary figure 1: TFSEARCH and MatInspektor software were used to identify putative transcriptional factor binding sites in the mouse *Chop* promotor. The transcriptional initiation site (bent arrow) and translational site (ATG) are shown. High scoring transcription factor binding sites in the 0.5 kb. 5' flanking region of the mouse *Chop* gene are illustrated, those scoring >90 were considered as a positive. Definitions for the abbreviations are written in the text (chapter 4.1.1.).

6.1.4. BLAST analysis of human and mouse *CHOP* promoter

```
Human   GTGGGCGAAGCACTGAGGGGAGGGCGGTGAGGAAGGCAGAAGTCTGGCAGTGAGAG-GGA -2633
Mouse   GTGGGCGAAGCACTGAAGGGAGCGAGGTCAGGAAGGCAGAAGTCAGGCACTTTGGGAGGA -2235
        ***************** ***** * *** *************** **** *  * * ***
                                    MZF-1
Human   GAAGCGGCGGGGGCAGGTGAGGGCGGGGGAGTGGGGATGGGGCCGGGGAAAGGGGCCGAG -2574
Mouse   GAAATGGCGGGGGCAGGTGAGGGTGCGGGGCTGTGGATGGGGCCAGGGAAAGGGGCCGAA -2175
        ***  ****************** * ***  ** ********** **************
```

```
                                                                                                SP-1
Human   AGGACGCGGAGGGGGCAGAGGGTAGGGACGGGAGGGG-------------GAGGGGCAGG -2514
Mouse   AGGACGCGGAGGGGGCAGAGGGTAGGGACAGAAGGGGAGGAGAGAGAAGGGAGGGGGAGG -2115
        ***************************** * *****              ****** ***

                                                                        SP-1
Human   GTGGGGGGGGCCGGGCCCCGCACTCACCGCGGCCCATGGTTCGGCCGGCCCCGCCCTGCG -2467
Mouse   GGCGGGGGGGCCGGGCCCCGCACTCACCGCGGCCCATGGTTCGGCTGGCCCCGCCCTGCG -2055
        *  ****************************************** **************

Human   CAGTCGCGGCCCAGAGGGTGAGTGGGAGGGGGTGGGAGGAGGGTCGGTGGAGCCCGAGCC -2407
Mouse   CAGTCGCGGCCCAGAGGGTGAGTGGGAGGGGGTGGGAGGTGGGTCGGTGGAGCCCGAGCC -1995
        ************************************ ********************

Human   TCCGGTACGGCCCCGGCCGGTCCTAGCAGGAAGCGCCGCTGCCGCCGCCGC---GGATCA -2347
Mouse   TCCGGTACGGCCCCGGCCGGTCTTAGCAGGAAGCGCCGCCGCCGCCGCCGCGGATCA -1935
        ********************** *************** ***********   ******

                                                                  STATx
Human   CCGAGCGGCCTCCCGCGCATGCGCCATGGGGGCCAGGGGCAGCCCTGGGGATTCCGTTCC -2290
Mouse   CCGAGCGGCCTCCCGCGCATGCGCCATAGGGGCCAGGGGCAGCCCTGGGGATTCCGTTCC -1875
        **************************** ******************************

Human   CAGAAGGCACTGCGCAGGCTGCTGCCGCTGCCGCCGCCGCCGTCGCTGCCGCAGCCGCCG -2230
Mouse   CAGAAGGCACCGCGCAGGCTGCTACCGCCGCCGCCGCCGTCGCTGCCGCCGCCACCGCCGCAG -1815
        ********** ************ **** ******* *** * *** *** * ***** *

                                                    SP-1
Human   CCGCAGGAGCCGCCGCCTCCGCCGCTGCCCGGACGGGAGAGGGGCGGGGCCGGGCCCCCG -2170
Mouse   CCGCCG---CCGCCGCCGCCGCCGCTGCCCGGACGGGAGAGGGGCGGGGCCGGGCCCCCG -1755
        **** *   ******** ****************************************

Human   CCCAGCGGACAGCGACGAGCCAACTGGAGGGGCTGCAGTGCGCATGCGGGAGCGCGCCTA -2110
Mouse   CCCAGCGGACAGCAGCGAGCCAACAGGAGGGGACGCAGTGCGCATGCGGGAGCGCGCCTA -1698
        *************  ********* *******  *************************

Human   CCCCTCCCCCACAACCCCCCATTAATCCCCAAGAGAACAAACACCCCACGCGGCCCCCCC -2050
Mouse   CCCCTCCCCCACAACCCCCCATTAATCCCCAAGAGAACAAACACCCCACGCGGCCCCCCC -1638
        ************************************************************

Human   ------GCCCTCCGCGGAAGGATCTGCGCCTCTTCCCAGGCCACTGGTGGCCAATCCCAG -1990
Mouse   CCACCCGCCCTCCGCGGAAGGATCTGGGCCTCTTCCCAGGCCACTGGTGGCCAATCCCAG -1578
              ******************** *********************************

                                                    STATx
Human   CCCTCCTCAGGGAGGGGCCCCTTCCAAAGCCACAGTCTGTTGCGGGAACCAGGAATGCCA -1936
Mouse   TCCTCCCTCGGGAGGGGCCCCTTCCGAAGCCACAATCTGTTGGGGGAGTCAGGAATGTCA -1518
         *****   ***************** ******** ******* ****  ******** **

                                                                SP-1
Human   GGTCCGGGAGGGGCCAGGCCCCGAAAGATGAAAGTCGCGACTTGCCCTGCCCCGCCCCAA -1876
Mouse   GGTCCGGGAGGGGCCAG-CCCTAAAAGATGAAAGTCGCGACTTGCCCTGCCCCGCCCCAA -1458
        ****************** ***  ************************************

Human   AGGCTTCCCGGGTAGTGTGCTGGGACTTGACCCGCCTCCCCAGGTCAACATGTCACAACA -1816
Mouse   AGGCTTCCCGGGTAGTGTGCAGAGACTTGACCCGCCTCTCCAGGTCAACATGTCACAACA -1399
        ******************** * *************** *********************

Human   CGACCTCAGCCTGTCAAGTCACATGACCTCTGCCTGTCACTGACAACCTGGTCTGTCTTT -1756
Mouse   CGACCTCAGCCTGTCAAGTCACATGACCTCTGCCTGTCACTGACAACCTGGTCTGTCTTT -1339
        ************************************************************

                Tal-1a/b
Human   AGGCCAGGGGAGACCATCTGGTCCACCCTCCACACTACCCCCATTTTCAGA-GAGGAAAT -1696
Mouse   AGGCCAGGAGAGACCATCTGGTCCAACCCACCCCCCACCTCTACTAACAGAAGGGGAAAT -1279
        ******** ***************** **  * * * *** * * *  **** * ******

                        C/EBP
Human   GGAGGTGTGGAGCAGCGGAGCAGCCTAACCAAAGACCTGTCATTGCCACACCACTCCAGT -1637
Mouse   GAAGGTCTGGAGCGAAGGAGCAGTCTGGCCAAGGACCTGTCACCGTCGCACCA-TCCAAT -1219
        * **** ******   ******* **  **** *********  * * ***** **** *

Human   CACAACCGGCCTTGTGACAGTTTCTACTTAAACTCTGGCT-GCCCC-CATGAGGGTATGA -1577
Mouse   AGCAACCGGTCTTGGTTCAGTTTCTACTTAAACTCTGGCTTGCCCCTCTTGAGTCTACGA -1160
          ******* ****   ********************** ***** * ****  ** **

                        AML-1α
Human   CAGGATATGTAACAGGCCACCACATGGCCTCTGTTTTCAAGGCACAAGAAAAATACTTTG -1519
Mouse   CAGACTATGTAATAGGCCACCACATGGCCTCTGTTTTCATGGCACAAAAAAAAAAAAATA -1100
        ***  ******* ************************** ******* ***** *   *

Human   CATTCTGGGTGGTGCGTTTTACTTTTGGTCAAGTTGCCTCCAAGTTCATGGTTCTCATTT -1459
Mouse   CGTTTTGCAAGATGT-TTTTACTTTTACTCAAGTTTTCTCCA----CAGAGCTGCT-TTT -1040
        * ** **   * **  **********  *******  *****    **  * *    ***

                                                                GATA-1
Human   TACCTTCACAACTTTTATCTTTAATTTACAAACAAGGACGGTAAGATCCCTTGGCAAGTG -1399
Mouse   TACCTTTATCGT-----TGTTTAATTTACAAATGAGTAAGGTAGAATCCTTGGACAAATT -986
```

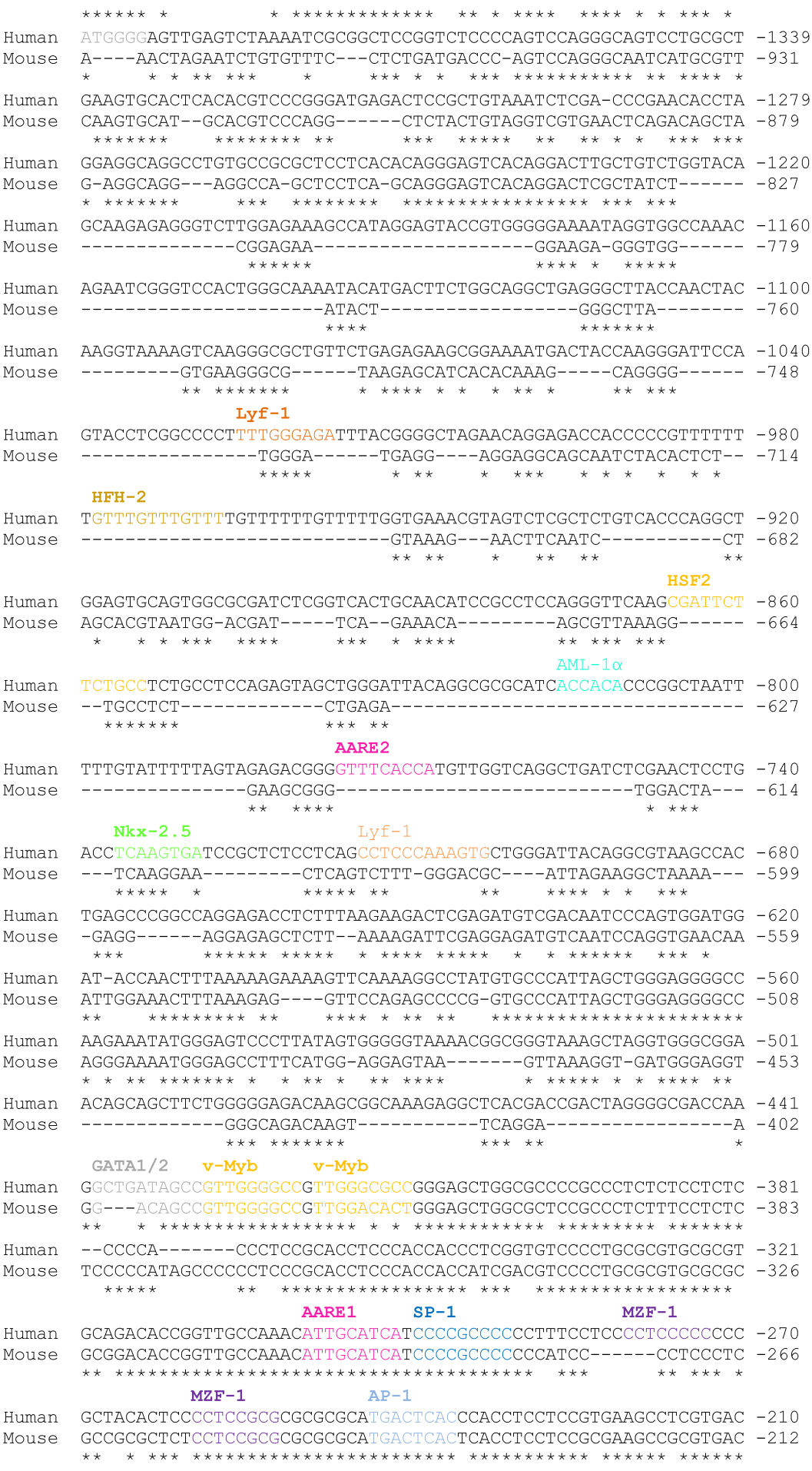
Lyf-1
HFH-2
HSF2
AML-1α
AARE2
Nkx-2.5
Lyf-1
GATA1/2
v-Myb
v-Myb
AARE1
SP-1
MZF-1
MZF-1
AP-1

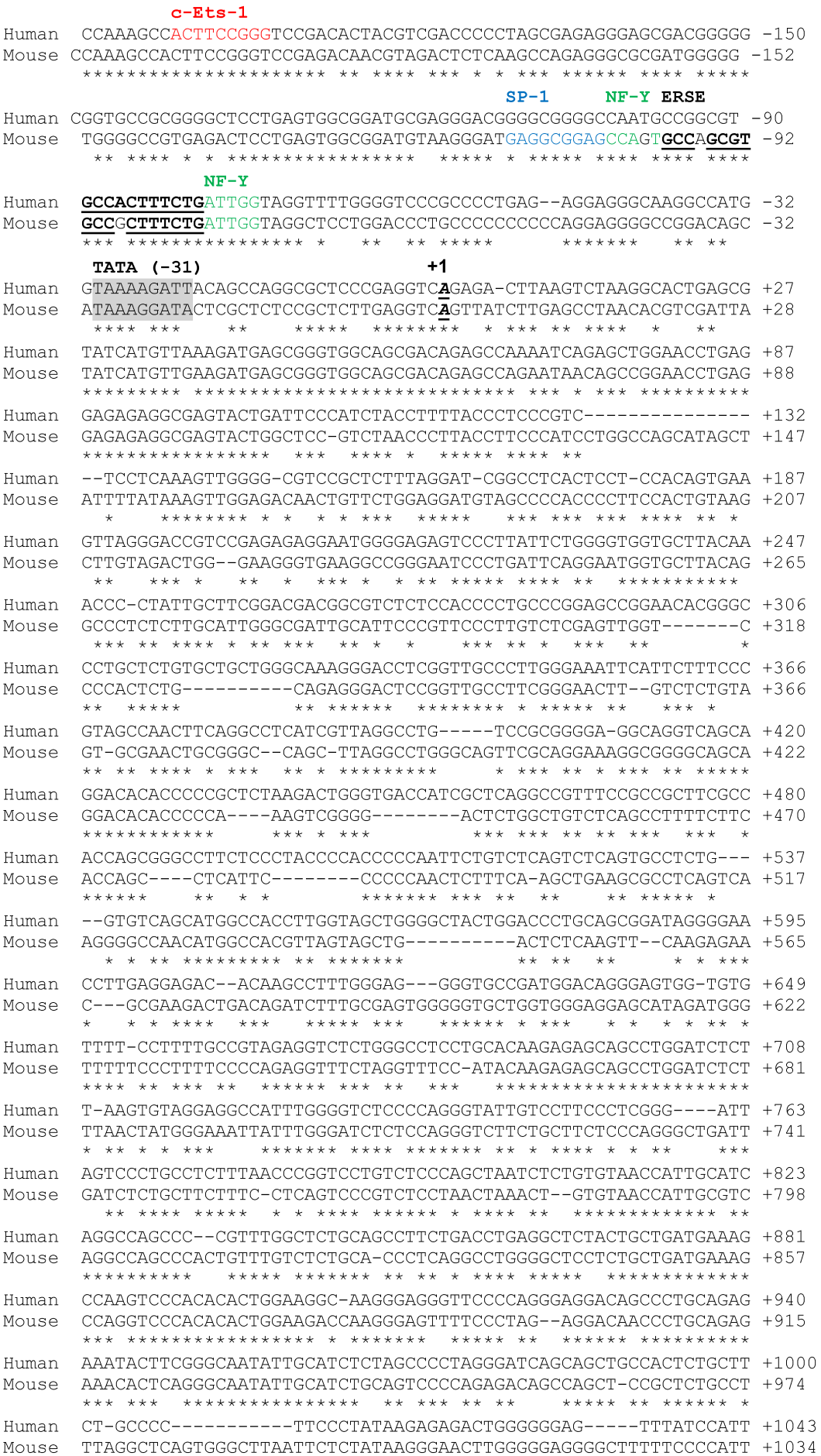
c-Ets-1
SP-1
NF-Y
ERSE
NF-Y
TATA (-31)
+1

```
         * * * *           *** ******* **   ******  *     ***  *****
Human   CATTCTTAACAAATACTTAATGAGGACCTACTGTGTGCCACACAGTTTGGGGCTCAGGGT +1103
Mouse   CATTCCTAACAAATGCCTAATAAGCACCCACTATGTACCAAGTATCTGGGGACCCAGGGT +1094
        ***** ******** * **** ** *** *** *** ***   *  * *** * ******
Human   ACATCCTTGAGCAAGAGGAAAAAATCATCTCAGTGGGAGGCCTACAGT---AAACAAAAT +1160
Mouse   ATATTAG-GAGCAAAAGATAAAACTGTTCTCAAT--AAAACTTACATTTCAGTATAAAGC +1151
        * **    ****** **  **** *  ***** *   *  * **** *     * ***
Human   ATAAGTGCCACGGAGAAAGCTAAAGCAG---AGAA-AG-----------GAATGGAGAAT +1205
Mouse   AAAAGGG--AAAAAAAAAACAAAAGCAGGGCAGAATAGTTCAGGGCGGTGACTAGAGGTT +1209
        * *** *  *   * *** * *******   **** **          ** * ***  *
Human   GT--TCAGGA--------TG-GAG------------GTCAGAGTGTTACATCAGG----- +1237
Mouse   GTCATCAGAAGCCAAGCCTGTGAGCCAAGCCCCGGTGTTAGAGCTTTATAGAAGGGAGAG +1269
        **  **** *        ** ***           ** ****  *** *  ***
Human   --TG---------GTCAGGA-----AT----------TACCTT----------------- +1254
Mouse   GCTGAGCAACAGAGTTAAGATAAGCATGCCATGCCGGTATCTTTAGGAACAGGACTAGAG +1329
          **         ** * **     **          ** ***
Human   ---------------------AGGTAATTCCTCCA------CTCA--AAACCCTTCAGTG +1285
Mouse   TAAGCAGGAGAGGGTGATGAAAGGAAACTCAAGCAGCCGGTCTCATAGAGCCTTGCAAGC +1389
                           *** ** **   **      ****   * ** * **
Human   ACTTCCATGA-----------------CATGAAATAGGAAGTCATTGGAGGGTTTGAGCA +1328
Mouse   ACCCTCATGATGCTAATCTTTAACAATCATGAAACAGGAAGCCATTGGGGGATCTGAGCA +1449
        **   *****                 ******* ****** ****** ** * ******
Human   GAGGAATGACC---------TGT-TTTAA--------------AAGGC---TCACT----- +1357
Mouse   GAGGAATGATCATAGCACATGCATTTAATTCCAGCACTCAGAGAGGCAGATCTCTGAGCT +1509
        ********* *        **  *****              ****   ** **
Human   -CAGGCT-------GCTGTATGGTGA---------------------------ATAGAG +1375
Mouse   CCAGGCCAGCCAGGGCTACATTATGAGACCCTGACTCAAAATAAATACAAAAACAAAGGG +1569
         *****        ***  **  ***                          * ** *
Human   TT-------------------------------------GCGGAGG------GGT----- +1387
Mouse   TTAGGTATGTAGCTCAATAGTACACTGCTTGCCTGGTATGTAGAGGACCCTAGGTCAACC +1629
        **                                  *  ****      ***
Human   ------------------------GGCAAGAGAAGAAATGGGAAGACCTT-CTG----CA +1418
Mouse   CACAGCCGTGAAAATAAAGTAAAAGACAAGAATAGAAACAGGAGGTCTCAGCTGAACATA +1689
                               * *****  *****  *** * *    ***     *
Human   GTCAGAAAGTTTCTG----CAGTAATTTAGAGAT-GGTAG---TGAATT--GATCTAGAT +1468
Mouse   GTGGCACAGCCTTTAATCCCAGCACTTGAAAGGCAGGCAGATCTAAATTCAAAGCCAGAG +1749
        **   * **  * *     *** * ** * **   ** **   * ****   * * ***
Human   TG-----GAAACAA----TGGAAT--TAGAAG-----TGTTTAGATTCT-TCTAA----- +1506
Mouse   AGTCTACAAAGCAAGTTCCAGGACAGCAAAAGCTACATAGTGAGACCCTGTCTAAAAGAG +1809
         *      ** ***      * *    * ***     *  * ***  ** *****
Human   ------------------------------GCAAAGGTTTTAAAAA--CTC-----ATTTT +1530
Mouse   AAAGAAAGGAAAGGAAAGGAAGAAAGAAAGGAGAGATTTCAAAGAGGCTTCCAAAATAAT +1869
                                     * * ** *** *** *  **      **  *
Human   T-----AAAGAA--------TGAGTTAA------GGGCCGGGCA-TGGTGGCTCACACCT +1570
Mouse   CCAGGGAAAGAAATGTATGGTAAATTTATATCTGGAGCCAGGCAGTGGTGGTGCACGCCT +1929
              ******        * * ** *      * *** **** ******  *** ***
Human   GTAATCCCAGCACTTTGGGAGACCAGAGGTGGGTGGATC-----ACCTGAGGTCAG---- +1621
Mouse   TTAATCCCAGCA-TTTGGGAGAC-AGAGACAGGCGGATTTCTGAATTCGAGGCCAGCCTT +1987
         *********** ********** ****   ** ****      *   **** ***
Human   ---------GAGTTCAAGACCAGCCTGGCCAACATGGTGAAATCCCATC----------- +1661
Mouse   GTCCACAGTGAGTTCCAGGACAGCCAAGGCTACACAGAGAAACCCTGTCAAGAAAAACCA +2047
                ****** **  *****  * * ***  * **** **  **
Human   ----------TTTACTAAAAATACAAAAATT--AGCCGGGCATG--GCAGT--------- +1698
Mouse   AAAAAATAAATAAATGAAAAATA-AAAAATTGCATCTGGAAATAATGTAGTAATGAGAAA +2106
                  *  *  ******* *******  * * **  **   * ***
Human   ------------GCATGCCTGTAA------------TCCCAGCTA--CTCCGGAGGCTGA +1732
Mouse   TACTTAGGTTTGGGGTACTTTTAAAGTTGTCAGTGCTTTAGGCTGAGCTGTGGTATCTGA +2166
                     *  * * * ***           *    ***   **  **   ****
Human   AGCAGGAGAATCG-------------CTTGAACC--CAGCAGGCGGAGGTTGC-----AG +1772
Mouse   GAAAGGGGCATCAAGGATACCAAAGTTTTTGGCTTTCAGCACCTAGAG-TTGCCATTTAG +2225
           *** * ***             **   *   *****    *** ****     **
Human   TGAGCCGATTGCGCCACT------------GCCTTCCA------------GCCTGGGCAA +1800
Mouse   TAAG--AACTATACAGCCTTGGTAGGAAAGGCCTTTCATGTAAGCTGAACGCCTGCTCAA +2283
        * **   * *   *  *             ***** **             *****  ***
Human   -------AAAGAGT--GAGACCC--------GTCT-CA--------------GAAAAAAA +1828
Mouse   CACTGCCAAGGAGCTGGAGATCCCAGAGCAGGTCTGCACTGAGGCTGCCAGTGGGGGGAT +2343
                ** ***   **** **        **** **               *     *
Human   GGAAT--GAGTTAA--------AATTTGCT-------------AGTACTTT--------- +1856
Mouse   GGAATCTGAGCAAGCACTGCTGAGTTTACTCTTCCTTCCCTCTAGTTCTGTCTCCCTTTG +2403
        *****  ***  *          * *** **              *** ** *
```

```
Human  --GGATTGCAGG---GTGTGAGA---GAAGAGGAATGA-------AGGA----------- +1890
Mouse  GCGGACTTGAGGTCTATCTGGGATTTAGAGAAAACTTAGTTGGCCAGGACTTTGCTATTA +2463
         *** *  ***    * ** **     ***  * * *       ****
Human  TGATACCAAGGTTTTTAGCTTAAGCAACTAGAG------------------TTGTCATCT +1932
Mouse  TGTAATCAAGACGGCAAATGTCAGCAACTAAAAATAAAGTTAAGCCTGCCTCTGTCCTTG +2523
       **  * ****      *   * ******** *                    **** *
Human  GAGATGG------GGATG---ACCTTGGAAG----------------------------- +1954
Mouse  GAGTTGGCTTCAGGGACACACACGCTGCAAGACACACGCCTGTGTGTGTGTGTGTATTAC +2583
       *** ***      ***     **  ** ***
Human  --GGGAAAA-------TCAG--------------CAAGA---GTTTGCCTTTGCACATA- +1987
Mouse  AAGAGAAGAAATGGCTTCAGGGACACACCCGCTGCAAGACACACACACCTCTGTATGTGT +2643
         * *** *       ****              *****        *** ** *  *
Human  ------GTCTTA-------------GGTGCCTATT------AGACATTGAA--------- +2013
Mouse  GTGTGTGTATTACAAGAGAAGAACTGGAGCCTGGTCTGCAGAGTTGTTGAGTTCCAGAAT +2703
             ** ***             ** ****  *      **   ****
Human  ----------------------AAAGAAA------------------TGGCAAGTAGGCA +2033
Mouse  TCCAGGATGCCCAGGGATGCACAAAGAAACCATCTCACAACCCATTTTAGAAAGGATCTA +2763
                             *******                 * * *** *   *
Human  GTAGACAGC-----AGAGTCTGAA--GTTCTGGAAGAGGTCCAGA-----CTGGAAATG- +2080
Mouse  GAAAAGGGCTAGGAGGAGTTAGAAAGGATCTAGAGAGGGGCTAGGAGGAGTTAGAAAGGA +2823
       * * *  **      ****  ***  * *** **   ** * **       * **** *
Human  --TACA------TTTGGAGGATGTCAGC-----CCTGTGGGAATGGAGTTAGGAAAATGC +2127
Mouse  TCTAGAGAGGGGCTAGGAGGA-GTTAGAAAGGATCTA-GAGAA--GGGCTAGGAGGAGGC +2879
         ** *       * ****** ** **       **  * ***  * * *****  * **
Human  TA------------TGATTTGTTCCCTTCCCTGTAGTTT---AG-------------TTT +2159
Mouse  TGGAGGTAAAGGACTGTTTTTTCCTTTTCTCCACAGTGTTCCAGAAGGAAGTGCATCTTC +2939
       *              ** *** * *  *** *   *** *   **           **
Human  TTACCCTGGCAGATTTGA--------------GGCC------------------------ +2181
Mouse  ATACACCACCACACCTGAAAGCAGGTAATCTTGGCCACCCTCTCAGTCAGCTGCGAATGC +2999
        *** *   ** *  ***               ****
Human  ---------TGCTTTG--------GATTTAGAGAAAGC--TGAGTTGGCCAGGACTTTAC +2222
Mouse  TGCTCATGTTGCTTTGCTGGGGGAGAGTTAGACAAGGCCTTCATCTGAACAAGCTTTTGC +3059
                *******        ** ***** ** **  * *  **  ** *  *** *
Human  TATTA-------------TGTAACC---------------AGGACTA-----CAAATGTC +2249
Mouse  TGTCAGACCATGTCTTTCTCTGACCCCATAATGTTGTTTGAGAGCTGGCTTTCGAA-GTC +3118
       * * *             * * ***               **  **      * ** ***
Human  AGC---AAC--TAAAAAT--------------AA-----AG--------AAAGTCAGGCC +2277
Mouse  AGCCTCAACAATGGCAATTGGTTTGTCTTCCCAACTCTCAGTCCACACCAAGATTAGACC +3178
       ***   ***  *   ***              **     **        **  * ** **
Human  C------TCTTCTGCCC----TTC-------------GAAATGGCTACAGG-GACCAAGT +2313
Mouse  CAAAGGACCTTTTGCCCAAGCTTCCCACACGAGAGAAAAAAAGAGTACAAATGGCCTGGT +3238
       *       *** *****    ***             *** *  ****   * **  **
Human  A--TGCA---------TACC----------CCACAAGACCAGAA---------------- +2336
Mouse  AATTGCCCCTGGAAATTACCAGTAGTGTTCCCAAGAGAGTTGAATACTTTTACTGTAATC +3298
       *  ***          ****          ***  ***   ***
Human  --GTAAGGA---------------AGGACCAGT------------------------AG +2354
Mouse  CTGTAAGAATATATATGTATAGCCAAGCCCAGTGACTGTTCCTCTCTCAGAACTTGAGAG +3358
         ***** *               * * *****                        **
Human  GAGGCTGGAGGTA---AAAGAAAA---------ATAAGGG----------CCCAGCACGG +2392
Mouse  GATCCTGAAGTTATCTGTAGTAAATCCTTCTCAATAAAGGGTATGTTCTATCAGGTGTAG +3418
       **  *** ** **     ** ***         **** **          *  *    *
Human  TAGCTCATGCCTATAATCCCAGCACTTTGGGAAGCGATGGATCACAA--GGTTAAGAGAT +2450
Mouse  TGGTGCATACCTTTAGTCCCAGCACTT-GGGAGGCAGAGGAAGGTAAATGTCTGAGTCAA +3477
       * *  *** *** ** ********** **** **   ***    **  *  * **  *
Human  GG--AGACCATCCTG-------------------GCCA---------ACATAGTGAAACC +2480
Mouse  AGCCAGCCTATTTTGCAGAGTGAGTTCCAGGGAAGCCAGAACTATATATACAGAGAAACC +3537
        *  ** * **  **                    ****         * * ** ******
Human  CTATCTCTGCTAAAAACACAA------------AAATT-----------AGCTGGGC--- +2514
Mouse  CTTTCT----TGAAAATACACCCCCCACCCTCCAAGTTTTGTTTCCAGGAGCTAGAGAGA +3593
       ** ***    * **** ***          ** **          **** *
Human  -------GTGGT----GGCACGCGCC-----TGTAGT---CCCAGCT--ACTCGGGAGGC +2553
Mouse  TGACTCAGTGGTTAAGAGCACGTGCTCTTCTTGTAGAGGATCTAGTCTAACTCCCAGTAC +3653
              *****     ***** **      *****     * **    ****      *
Human  CGA---GGCAGA--AGAATCACTT--GAACCGAGGAGGCAGAGGTTGCA---------GT +2597
Mouse  CCAAATGGCAGTTCAAAACCATCTATGACTCTAGTTCCCAGGGAATCCATTCCCTCTTGT +3713
       * *   *****   * ** **  *  **  * **    *** *  * **         **
Human  GA-----------GCCGAGATCGCAC-CACTGCAC---TTCAG-------CCT------- +2628
Mouse  GGCCTCCATGTCTACCAGGAACACACACACAGCACACATTCAGGCACTCACTTATATATG +3773
       *             **  ** * *** *** ****   *****       * *
```

```
Human  ----GGCAACAGAGCAAGACTTGGTCTCAAAAAAAAAAAAAGA-----AAG--------- +2670
Mouse  CATAGATAATAAAATAAATATATCTTTGGGAAAAAAAAAAAGATATTTAAGGTTAGGTAG +3833
           *  ** * *  **   *   * *   *************     ***
Human  -----------------------------------AAA--AAAAGAAAAAGAAAAGT--- +2690
Mouse  CCAGCCTGGATTAAGCTTGGTAGTGACCAGCATATAAATGAAAACAAAACAAAAAGTTGG +3893
                                         ***  **** ****  ******
Human  -AAGTTGC----------------CTCTC---CCC--CTTCCAAAAATGGCTGA--CA-- +2724
Mouse  AAAGCTGTGTGGGGGTGGTGCATACTTTTAATCCCAGCCTTCAGGA--GGCTGAGGCAGG +3951
        *** **                 ** *    ***  * * **  *  ******  **
Human  TTTCTCTTTGTTGCCCACA-GTGTTCAAGAA--GGAAGTG----------------TATC +2765
Mouse  TTGATCTCTGAGGCCAGTGTGAGTTCTAGGACAGGCAGGGCTACACAGAGAGACCCTGTC +4011
       **  *** **  ***     * **** ** *  ** ** *                * **
Human  TT---CATACATCACCA----CACC--TGAAAGC---AGGTAAACTTA----------AC +2803
Mouse  TTGAACAAACACCAAAAAGAATGGCAATGAGAGCCCGGAGAAAGCCTATCAGTTCCACAC +4071
       **   ** *** **  *       *  *** ***     * ** * **          **
Human  CTACCCT-------------------------TTTCCA----------AAAAT--TTTAA +2826
Mouse  CCATGCTGCCTGTGTGCCGTACCTGAGTCAGGTTTCCAGCAGCCACAGAAGGTGGCTCAC +4131
       * *  **                         ******          **  *   * *
Human  ACGGC----------------AGGA----CAGTAAATATT--------TTAGATGTTAAA +2858
Mouse  ATGGCCTGGACCTCCAGCTCCAGGAGAGCCAATGAATGCTGCTGGCCCCCAGACACTGAA +4191
       * ***                ****    ** * ***  *          ***   * **
Human  A-------GTCCTATAGTCTC-----TAGCGTGACTCT--TCATCTCTGCCACTGT--AG +2902
Mouse  TTACATCCGTTTCAGGGTCCTGGCCATGGTGTGCATGTGATCATCTGGACAACTTTTGAG +4251
              **   *  ***       * * ***  * *  ******   * *** *  **
Human  CACCAAAGCAGCCATAAACAATATGTAAA----TAAAC---AGATGTGGCTGT------A +2949
Mouse  AGTTGGATCTGGCAGGGTCAAAGTCAAGGCTGCTAGGCTTGAGAGGCAGCCATCTCCCCA +4311
         * * * **    ***  *  *      **  *   *** *  **  *      *
Human  TTCCAGTACAACTTTACC--TACAAAAACAGGCATCAGACCAGCTTGC------CAACTT +3001
Mouse  TCCCGACACACCATCATTAGTGTGTGTGCAGGTCAGAGAACAACTTGTGCGAGTTGACTC +4371
       * **   *** * * *    *       ****    *** ** ****         ***
Human  GTGGCATAGACTGTTTGCTACATGGAGCTT-------GT-----TCCA-GCCACTCCCCA +3059
Mouse  TTCACCTCCACCCTCTGCCA-ATGTAGCCTTCAAGGAGTGACAACCCATGCCCTTACCTA +4430
        *  * *  **  * *** * *** *** *       **      *** ***  * ** *
Human  TT----------------------ATCCTGC-----AGA---------------------- +3071
Mouse  TCGTGCAAGACCAGTAAATTTTAAATTCTACGTGTTAGAAAAGGGACAAGGTCAGCTCAC +4490
       *                       ** ** *     ***
Human  ----TGTG-----------------CTTTTCCAGA--CTGATCCAACTGCAGAGATGGCA +3105
Mouse  CGACTGTGGTGAATGGAATGTATGTCCTTTCCAGAACCTGGTCCACGTGCAGTCATGGCA +4544
           ****                 * ********  *** ****  *****  ******
Human  GCTGAGTCATTGCCTTTCTCCTTCGGGACACTGTCCAGCTGGGAGCTGGAAGCCTGGTAT
Mouse  GCTGAGTCCCTGCCTTTCACCTTGGAGACGGTGTCCAGCTGGGAGCTGGAAGCCTGGTAT
       ********  ******** **** * ***  ****************************
```

Supplementary sequence 3: Sequences and BLAST analysis of the human and mouse *CHOP* gene promoter are illustrate

Mouse and human *CHOP* promoter sequences. Homologous sequences are marked with stars.
The potential binding sites for transcription factors are marked with name of transcription factor. Transcription start site (*ATG*) is indicated in red.

7 References

1. Todd, N.W., I.G. Luzina, and S.P. Atamas, *Molecular and cellular mechanisms of pulmonary fibrosis.* Fibrogenesis Tissue Repair, 2012. **5**(1): p. 11.
2. Kendall, R.T. and C.A. Feghali-Bostwick, *Fibroblasts in fibrosis: novel roles and mediators.* Front Pharmacol, 2014. **5**: p. 123.
3. Travis, W.D., et al., *An official American Thoracic Society/European Respiratory Society statement: Update of the international multidisciplinary classification of the idiopathic interstitial pneumonias.* Am J Respir Crit Care Med, 2013. **188**(6): p. 733-48.
4. Raghu, G., et al., *An official ATS/ERS/JRS/ALAT statement: idiopathic pulmonary fibrosis: evidence-based guidelines for diagnosis and management.* Am J Respir Crit Care Med, 2011. **183**(6): p. 788-824.
5. Barkauskas, C.E. and P.W. Noble, *Cellular mechanisms of tissue fibrosis. 7. New insights into the cellular mechanisms of pulmonary fibrosis.* Am J Physiol Cell Physiol, 2014. **306**(11): p. C987-96.
6. Fernandez, I.E. and O. Eickelberg, *New cellular and molecular mechanisms of lung injury and fibrosis in idiopathic pulmonary fibrosis.* Lancet, 2012. **380**(9842): p. 680-8.
7. Lynch, J.P., 3rd, et al., *Usual interstitial pneumonia.* Semin Respir Crit Care Med, 2006. **27**(6): p. 634-51.
8. Marshall, R.P., et al., *Adult familial cryptogenic fibrosing alveolitis in the United Kingdom.* Thorax, 2000. **55**(2): p. 143-6.
9. Steele, M.P. and D.A. Schwartz, *Molecular mechanisms in progressive idiopathic pulmonary fibrosis.* Annu Rev Med, 2013. **64**: p. 265-76.
10. Lai, C.K., W.D. Wallace, and M.C. Fishbein, *Histopathology of pulmonary fibrotic disorders.* Semin Respir Crit Care Med, 2006. **27**(6): p. 613-22.
11. Ask, K., et al., *Targeting genes for treatment in idiopathic pulmonary fibrosis: challenges and opportunities, promises and pitfalls.* Proc Am Thorac Soc, 2006. **3**(4): p. 389-93.
12. Crystal, R.G., et al., *Future research directions in idiopathic pulmonary fibrosis: summary of a National Heart, Lung, and Blood Institute working group.* Am J Respir Crit Care Med, 2002. **166**(2): p. 236-46.
13. Renzoni, E., V. Srihari, and P. Sestini, *Pathogenesis of idiopathic pulmonary fibrosis: review of recent findings.* F1000Prime Rep, 2014. **6**: p. 69.
14. Keane, M.P., et al., *Inflammation and angiogenesis in fibrotic lung disease.* Semin Respir Crit Care Med, 2006. **27**(6): p. 589-99.
15. Davies, H.R., L. Richeldi, and E.H. Walters, *Immunomodulatory agents for idiopathic pulmonary fibrosis.* Cochrane Database Syst Rev, 2003(3): p. CD003134.
16. Richeldi, L., et al., *Corticosteroids for idiopathic pulmonary fibrosis.* Cochrane Database Syst Rev, 2003(3): p. CD002880.
17. Idiopathic Pulmonary Fibrosis Clinical Research, N., et al., *Prednisone, azathioprine, and N-acetylcysteine for pulmonary fibrosis.* N Engl J Med, 2012. **366**(21): p. 1968-77.
18. Kim, K.K., et al., *Alveolar epithelial cell mesenchymal transition develops in vivo during pulmonary fibrosis and is regulated by the extracellular matrix.* Proc Natl Acad Sci U S A, 2006. **103**(35): p. 13180-5.
19. Arase, Y., et al., *Hepatitis C virus enhances incidence of idiopathic pulmonary fibrosis.* World J Gastroenterol, 2008. **14**(38): p. 5880-6.
20. Gahl, W.A., et al., *Genetic defects and clinical characteristics of patients with a form of oculocutaneous albinism (Hermansky-Pudlak syndrome).* N Engl J Med, 1998. **338**(18): p. 1258-64.
21. Oh, J., et al., *Positional cloning of a gene for Hermansky-Pudlak syndrome, a disorder of cytoplasmic organelles.* Nat Genet, 1996. **14**(3): p. 300-6.

22. Mason, P.J. and M. Bessler, *The genetics of dyskeratosis congenita.* Cancer Genet, 2011. **204**(12): p. 635-45.
23. Nogee, L.M., et al., *A mutation in the surfactant protein C gene associated with familial interstitial lung disease.* N Engl J Med, 2001. **344**(8): p. 573-9.
24. Maitra, M., et al., *Surfactant protein A2 mutations associated with pulmonary fibrosis lead to protein instability and endoplasmic reticulum stress.* J Biol Chem, 2010. **285**(29): p. 22103-13.
25. Wang, Y., et al., *Genetic defects in surfactant protein A2 are associated with pulmonary fibrosis and lung cancer.* Am J Hum Genet, 2009. **84**(1): p. 52-9.
26. Korfei M, R.C., Mahavadi P, Henneke I, Markart P, Koch M, Lang G, Fink L, Bohle RM, Seeger W, Weaver TE, Guenther A., *Epithelial endoplasmic reticulum stress and apoptosis in sporadic idiopathic pulmonary fibrosis.* Am J Respir Crit Care Med., 2008. **178**(8): p. 838-46.
27. Lawson WE, C.P., Polosukhin VV, Roldan J, Cheng DS, Lane KB, Blackwell TR, Xu C, Markin C, Ware LB, Miller GG, Loyd JE, Blackwell TS., *Endoplasmic reticulum stress in alveolar epithelial cells is prominent in IPF: association with altered surfactant protein processing and herpesvirus infection.* Am J Physiol Lung Cell Mol Physiol, 2008. **294**(6): p. L1119-26.
28. Hawkins, A., et al., *A non-BRICHOS SFTPC mutant (SP-CI73T) linked to interstitial lung disease promotes a late block in macroautophagy disrupting cellular proteostasis and mitophagy.* Am J Physiol Lung Cell Mol Physiol, 2015. **308**(1): p. L33-47.
29. Cronkhite, J.T., et al., *Telomere shortening in familial and sporadic pulmonary fibrosis.* Am J Respir Crit Care Med, 2008. **178**(7): p. 729-37.
30. Armanios, M.Y., et al., *Telomerase mutations in families with idiopathic pulmonary fibrosis.* N Engl J Med, 2007. **356**(13): p. 1317-26.
31. Alder, J.K., et al., *Short telomeres are a risk factor for idiopathic pulmonary fibrosis.* Proc Natl Acad Sci U S A, 2008. **105**(35): p. 13051-6.
32. Heiss, N.S., et al., *X-linked dyskeratosis congenita is caused by mutations in a highly conserved gene with putative nucleolar functions.* Nat Genet, 1998. **19**(1): p. 32-8.
33. Ron, D., *Translational control in the endoplasmic reticulum stress response.* J Clin Invest, 2002. **110**(10): p. 1383-8.
34. Lin, J.H., P. Walter, and T.S. Yen, *Endoplasmic reticulum stress in disease pathogenesis.* Annu Rev Pathol, 2008. **3**: p. 399-425.
35. Isler, J.A., A.H. Skalet, and J.C. Alwine, *Human cytomegalovirus infection activates and regulates the unfolded protein response.* J Virol, 2005. **79**(11): p. 6890-9.
36. Lee, A.S., *The ER chaperone and signaling regulator GRP78/BiP as a monitor of endoplasmic reticulum stress.* Methods, 2005. **35**(4): p. 373-81.
37. Lee, A.H., N.N. Iwakoshi, and L.H. Glimcher, *XBP-1 regulates a subset of endoplasmic reticulum resident chaperone genes in the unfolded protein response.* Mol Cell Biol, 2003. **23**(21): p. 7448-59.
38. Yoshida, H., et al., *XBP1 mRNA is induced by ATF6 and spliced by IRE1 in response to ER stress to produce a highly active transcription factor.* Cell, 2001. **107**(7): p. 881-91.
39. Shen, J., et al., *ER stress regulation of ATF6 localization by dissociation of BiP/GRP78 binding and unmasking of Golgi localization signals.* Dev Cell, 2002. **3**(1): p. 99-111.
40. Bertolotti, A., et al., *Dynamic interaction of BiP and ER stress transducers in the unfolded-protein response.* Nat Cell Biol, 2000. **2**(6): p. 326-32.
41. Schroder, M. and R.J. Kaufman, *The mammalian unfolded protein response.* Annu Rev Biochem, 2005. **74**: p. 739-89.
42. Gorman, A.M., et al., *Stress management at the ER: regulators of ER stress-induced apoptosis.* Pharmacol Ther, 2012. **134**(3): p. 306-16.
43. Liu, C.Y., M. Schroder, and R.J. Kaufman, *Ligand-independent dimerization activates the stress response kinases IRE1 and PERK in the lumen of the endoplasmic reticulum.* J Biol Chem, 2000. **275**(32): p. 24881-5.

44. Harding, H.P., et al., *Perk is essential for translational regulation and cell survival during the unfolded protein response.* Mol Cell, 2000. **5**(5): p. 897-904.
45. Novoa, I., et al., *Feedback inhibition of the unfolded protein response by GADD34-mediated dephosphorylation of eIF2alpha.* J Cell Biol, 2001. **153**(5): p. 1011-22.
46. Shen, J. and R. Prywes, *Dependence of site-2 protease cleavage of ATF6 on prior site-1 protease digestion is determined by the size of the luminal domain of ATF6.* J Biol Chem, 2004. **279**(41): p. 43046-51.
47. Yoshida, H., *ER stress and diseases.* FEBS J, 2007. **274**(3): p. 630-58.
48. Wang, X., *The expanding role of mitochondria in apoptosis.* Genes Dev, 2001. **15**(22): p. 2922-33.
49. Ashkenazi, A. and V.M. Dixit, *Death receptors: signaling and modulation.* Science, 1998. **281**(5381): p. 1305-8.
50. Earnshaw, W.C., L.M. Martins, and S.H. Kaufmann, *Mammalian caspases: structure, activation, substrates, and functions during apoptosis.* Annu Rev Biochem, 1999. **68**: p. 383-424.
51. Ma, Y., et al., *Two distinct stress signaling pathways converge upon the CHOP promoter during the mammalian unfolded protein response.* J Mol Biol, 2002. **318**(5): p. 1351-65.
52. Urano, F., et al., *Coupling of stress in the ER to activation of JNK protein kinases by transmembrane protein kinase IRE1.* Science, 2000. **287**(5453): p. 664-6.
53. Deegan, S., et al., *Stress-induced self-cannibalism: on the regulation of autophagy by endoplasmic reticulum stress.* Cell Mol Life Sci, 2013. **70**(14): p. 2425-41.
54. Hoyer-Hansen, M. and M. Jaattela, *Connecting endoplasmic reticulum stress to autophagy by unfolded protein response and calcium.* Cell Death Differ, 2007. **14**(9): p. 1576-82.
55. B'Chir, W., et al., *The eIF2alpha/ATF4 pathway is essential for stress-induced autophagy gene expression.* Nucleic Acids Res, 2013. **41**(16): p. 7683-99.
56. Zinszner H, K.M., Wang X, Batchvarova N, Lightfoot RT, Remotti H, Stevens JL, Ron D, *CHOP is implicated in programmed cell death in response to impaired function of the endoplasmic reticulum.* Genes Dev., 1998. **12**(7): p. 982-995.
57. Wang, X.Z., et al., *Identification of novel stress-induced genes downstream of chop.* EMBO J, 1998. **17**(13): p. 3619-30.
58. McCullough KD, M.J., Klotz LO, Aw TY, Holbrook NJ., *Gadd153 sensitizes cells to endoplasmic reticulum stress by down-regulating Bcl2 and perturbing the cellular redox state.* Mol Cell Biol., 2001. **21**(4): p. 1249-59.
59. Chiribau CB1, G.F., Huang CC, Yuan CL, Hatzoglou M., *Molecular symbiosis of CHOP and C/EBP beta isoform LIP contributes to endoplasmic reticulum stress-induced apoptosis.* Mol Cell Biol., 2010. **30**(14): p. 3722-31.
60. Danial, N.N. and S.J. Korsmeyer, *Cell death: critical control points.* Cell, 2004. **116**(2): p. 205-19.
61. Cheng, E.H., et al., *BCL-2, BCL-X(L) sequester BH3 domain-only molecules preventing BAX- and BAK-mediated mitochondrial apoptosis.* Mol Cell, 2001. **8**(3): p. 705-11.
62. Puthalakath, H., et al., *ER stress triggers apoptosis by activating BH3-only protein Bim.* Cell, 2007. **129**(7): p. 1337-49.
63. Santos, C.X., et al., *Mechanisms and implications of reactive oxygen species generation during the unfolded protein response: roles of endoplasmic reticulum oxidoreductases, mitochondrial electron transport, and NADPH oxidase.* Antioxid Redox Signal, 2009. **11**(10): p. 2409-27.
64. Endo M, M.M., Akira S, Gotoh T., *C/EBP homologous protein (CHOP) is crucial for the induction of caspase-11 and the pathogenesis of lipopolysaccharide-induced inflammation.* J Immunol, 2006. **176**(10): p. 6245-53.
65. Fu HY1, O.K., Liao Y, Tsukamoto O, Isomura T, Asai M, Sawada T, Okuda K, Asano Y, Sanada S, Asanuma H, Asakura M, Takashima S, Komuro I, Kitakaze M, Minamino T., *Ablation of C/EBP homologous protein attenuates endoplasmic reticulum-mediated*

apoptosis and cardiac dysfunction induced by pressure overload. Circulation, 2010. **122**(4): p. 361-9.

66. Marciniak, S.J., et al., *CHOP induces death by promoting protein synthesis and oxidation in the stressed endoplasmic reticulum.* Genes Dev, 2004. **18**(24): p. 3066-77.
67. Song B, S.D., Ron D, Pennathur S, Kaufman RJ., *Chop deletion reduces oxidative stress, improves beta cell function, and promotes cell survival in multiple mouse models of diabetes.* J Clin Invest., 2008. **118**(10): p. 3378-89.
68. Seimon, T.A., et al., *Combinatorial pattern recognition receptor signaling alters the balance of life and death in macrophages.* Proc Natl Acad Sci U S A, 2006. **103**(52): p. 19794-9.
69. Timmins, J.M., et al., *Calcium/calmodulin-dependent protein kinase II links ER stress with Fas and mitochondrial apoptosis pathways.* J Clin Invest, 2009. **119**(10): p. 2925-41.
70. Li, G., et al., *NADPH oxidase links endoplasmic reticulum stress, oxidative stress, and PKR activation to induce apoptosis.* J Cell Biol, 2010. **191**(6): p. 1113-25.
71. Soderling, T.R., B. Chang, and D. Brickey, *Cellular signaling through multifunctional Ca2+/calmodulin-dependent protein kinase II.* J Biol Chem, 2001. **276**(6): p. 3719-22.
72. Li, G., et al., *Role of ERO1-alpha-mediated stimulation of inositol 1,4,5-triphosphate receptor activity in endoplasmic reticulum stress-induced apoptosis.* J Cell Biol, 2009. **186**(6): p. 783-92.
73. Back, S.H., et al., *Translation attenuation through eIF2alpha phosphorylation prevents oxidative stress and maintains the differentiated state in beta cells.* Cell Metab, 2009. **10**(1): p. 13-26.
74. Zhan, Q., et al., *The gadd and MyD genes define a novel set of mammalian genes encoding acidic proteins that synergistically suppress cell growth.* Mol Cell Biol, 1994. **14**(4): p. 2361-71.
75. Connor, J.H., et al., *Growth arrest and DNA damage-inducible protein GADD34 assembles a novel signaling complex containing protein phosphatase 1 and inhibitor 1.* Mol Cell Biol, 2001. **21**(20): p. 6841-50.
76. Yamaguchi, H. and H.G. Wang, *CHOP is involved in endoplasmic reticulum stress-induced apoptosis by enhancing DR5 expression in human carcinoma cells.* J Biol Chem, 2004. **279**(44): p. 45495-502.
77. Ohoka, N., et al., *TRB3, a novel ER stress-inducible gene, is induced via ATF4-CHOP pathway and is involved in cell death.* EMBO J, 2005. **24**(6): p. 1243-55.
78. Rutkowski, D.T., et al., *Adaptation to ER stress is mediated by differential stabilities of pro-survival and pro-apoptotic mRNAs and proteins.* PLoS Biol, 2006. **4**(11): p. e374.
79. Ji, C., et al., *Role of CHOP in hepatic apoptosis in the murine model of intragastric ethanol feeding.* Alcohol Clin Exp Res, 2005. **29**(8): p. 1496-503.
80. Silva, R.M., et al., *CHOP/GADD153 is a mediator of apoptotic death in substantia nigra dopamine neurons in an in vivo neurotoxin model of parkinsonism.* J Neurochem, 2005. **95**(4): p. 974-86.
81. Namba T, T.K., Ito Y, Ishihara T, Hoshino T, Gotoh T, Endo M, Sato K, Mizushima T., *Positive role of CCAAT/enhancer-binding protein homologous protein, a transcription factor involved in the endoplasmic reticulum stress response in the development of colitis.* Am J Pathol., 2009. **174**(5): p. 1786-98.
82. Thorp E, L.G., Seimon TA, Kuriakose G, Ron D, Tabas I., *Reduced apoptosis and plaque necrosis in advanced atherosclerotic lesions of Apoe-/- and Ldlr-/- mice lacking CHOP.* Cell Metab, 2009. **9**(5): p. 474-81.
83. Lee, J.H., et al., *Induction of the unfolded protein response and cell death pathway in Alzheimer's disease, but not in aged Tg2576 mice.* Exp Mol Med, 2010. **42**(5): p. 386-94.
84. Prasanthi, J.R., et al., *Silencing GADD153/CHOP gene expression protects against Alzheimer's disease-like pathology induced by 27-hydroxycholesterol in rabbit hippocampus.* PLoS One, 2011. **6**(10): p. e26420.

85. Yukioka, F., et al., *Presenilin-1 mutation activates the signaling pathway of caspase-4 in endoplasmic reticulum stress-induced apoptosis.* Neurochem Int, 2008. **52**(4-5): p. 683-7.
86. Vassar, R., et al., *Beta-secretase cleavage of Alzheimer's amyloid precursor protein by the transmembrane aspartic protease BACE.* Science, 1999. **286**(5440): p. 735-41.
87. Marwarha, G., et al., *Gadd153 and NF-kappaB crosstalk regulates 27-hydroxycholesterol-induced increase in BACE1 and beta-amyloid production in human neuroblastoma SH-SY5Y cells.* PLoS One, 2013. **8**(8): p. e70773.
88. Oyadomari S, T.K., Takiguchi M, Gotoh T, Matsumoto M, Wada I, Akira S, Araki E, Mori M., *Nitric oxide-induced apoptosis in pancreatic beta cells is mediated by the endoplasmic reticulum stress pathway.* Proc Natl Acad Sci U S A, 2001. **98**(19): p. 10845-50.
89. Oyadomari S, K.A., Takeda K, Gotoh T, Akira S, Araki E, Mori M., *Targeted disruption of the Chop gene delays endoplasmic reticulum stress-mediated diabetes.* J Clin Invest., 2002. **109**(4): p. 525-532.
90. Li, S.Y., et al., *Aldehyde dehydrogenase-2 (ALDH2) ameliorates chronic alcohol ingestion-induced myocardial insulin resistance and endoplasmic reticulum stress.* J Mol Cell Cardiol, 2009. **47**(2): p. 247-55.
91. Morse, E., et al., *TRB3 is stimulated in diabetic kidneys, regulated by the ER stress marker CHOP, and is a suppressor of podocyte MCP-1.* Am J Physiol Renal Physiol, 2010. **299**(5): p. F965-72.
92. Liew, C.W., et al., *The pseudokinase tribbles homolog 3 interacts with ATF4 to negatively regulate insulin exocytosis in human and mouse beta cells.* J Clin Invest, 2010. **120**(8): p. 2876-88.
93. Dickhout, J.G., et al., *Peroxynitrite causes endoplasmic reticulum stress and apoptosis in human vascular endothelium: implications in atherogenesis.* Arterioscler Thromb Vasc Biol, 2005. **25**(12): p. 2623-9.
94. Thorp, E., et al., *Brief report: increased apoptosis in advanced atherosclerotic lesions of Apoe-/- mice lacking macrophage Bcl-2.* Arterioscler Thromb Vasc Biol, 2009. **29**(2): p. 169-72.
95. Kumar, R., et al., *Brain ischemia and reperfusion activates the eukaryotic initiation factor 2alpha kinase, PERK.* J Neurochem, 2001. **77**(5): p. 1418-21.
96. Kohno, K., et al., *Neuroprotective nitric oxide synthase inhibitor reduces intracellular calcium accumulation following transient global ischemia in the gerbil.* Neurosci Lett, 1997. **224**(1): p. 17-20.
97. Krishnamoorthy, T., et al., *Tight binding of the phosphorylated alpha subunit of initiation factor 2 (eIF2alpha) to the regulatory subunits of guanine nucleotide exchange factor eIF2B is required for inhibition of translation initiation.* Mol Cell Biol, 2001. **21**(15): p. 5018-30.
98. Bousette, N., et al., *Calnexin silencing in mouse neonatal cardiomyocytes induces Ca2+ cycling defects, ER stress, and apoptosis.* J Cell Physiol, 2014. **229**(3): p. 374-83.
99. Thomas, A.Q., et al., *Heterozygosity for a surfactant protein C gene mutation associated with usual interstitial pneumonitis and cellular nonspecific interstitial pneumonitis in one kindred.* Am J Respir Crit Care Med, 2002. **165**(9): p. 1322-8.
100. Beers, M.F., C.A. Lomax, and S.J. Russo, *Synthetic processing of surfactant protein C by alevolar epithelial cells. The COOH terminus of proSP-C is required for post-translational targeting and proteolysis.* J Biol Chem, 1998. **273**(24): p. 15287-93.
101. Mulugeta, S., et al., *Misfolded BRICHOS SP-C mutant proteins induce apoptosis via caspase-4- and cytochrome c-related mechanisms.* Am J Physiol Lung Cell Mol Physiol, 2007. **293**(3): p. L720-9.
102. Mulugeta, S., et al., *A surfactant protein C precursor protein BRICHOS domain mutation causes endoplasmic reticulum stress, proteasome dysfunction, and caspase 3 activation.* Am J Respir Cell Mol Biol, 2005. **32**(6): p. 521-30.

103. Bridges, J.P., et al., *Expression of a human surfactant protein C mutation associated with interstitial lung disease disrupts lung development in transgenic mice.* J Biol Chem, 2003. **278**(52): p. 52739-46.
104. Lawson WE, C.D., Degryse AL, Tanjore H, Polosukhin VV, Xu XC, Newcomb DC, Jones BR, Roldan J, Lane KB, Morrisey EE, Beers MF, Yull FE, Blackwell TS, *Endoplasmic reticulum stress enhances fibrotic remodeling in the lungs.* Proc Natl Acad Sci U S A. , 2011. **108**(26): p. 10562-7.
105. Lawson, W.E., et al., *Genetic mutations in surfactant protein C are a rare cause of sporadic cases of IPF.* Thorax, 2004. **59**(11): p. 977-80.
106. Yonemaru, M., et al., *Elevation of antibodies to cytomegalovirus and other herpes viruses in pulmonary fibrosis.* Eur Respir J, 1997. **10**(9): p. 2040-5.
107. Egan, J.J., et al., *Epstein-Barr virus replication within pulmonary epithelial cells in cryptogenic fibrosing alveolitis.* Thorax, 1995. **50**(12): p. 1234-9.
108. Stewart, J.P., et al., *The detection of Epstein-Barr virus DNA in lung tissue from patients with idiopathic pulmonary fibrosis.* Am J Respir Crit Care Med, 1999. **159**(4 Pt 1): p. 1336-41.
109. Baumgartner, K.B., et al., *Cigarette smoking: a risk factor for idiopathic pulmonary fibrosis.* Am J Respir Crit Care Med, 1997. **155**(1): p. 242-8.
110. Steele, M.P., et al., *Clinical and pathologic features of familial interstitial pneumonia.* Am J Respir Crit Care Med, 2005. **172**(9): p. 1146-52.
111. Hengstermann, A. and T. Muller, *Endoplasmic reticulum stress induced by aqueous extracts of cigarette smoke in 3T3 cells activates the unfolded-protein-response-dependent PERK pathway of cell survival.* Free Radic Biol Med, 2008. **44**(6): p. 1097-107.
112. Tagawa, Y., et al., *Induction of apoptosis by cigarette smoke via ROS-dependent endoplasmic reticulum stress and CCAAT/enhancer-binding protein-homologous protein (CHOP).* Free Radic Biol Med, 2008. **45**(1): p. 50-9.
113. Tagawa, Y., et al., *Induction of CCAAT/enhancer-binding protein-homologous protein by cigarette smoke through the superoxide anion-triggered PERK-eIF2alpha pathway.* Toxicology, 2011. **287**(1-3): p. 105-12.
114. Jorgensen, E., et al., *Cigarette smoke induces endoplasmic reticulum stress and the unfolded protein response in normal and malignant human lung cells.* BMC Cancer, 2008. **8**: p. 229.
115. Rice, W.R., et al., *Maintenance of the mouse type II cell phenotype in vitro.* Am J Physiol Lung Cell Mol Physiol, 2002. **283**(2): p. L256-64.
116. Carlson, S.G., et al., *Regulation of the C/EBP-related gene gadd153 by glucose deprivation.* Mol Cell Biol, 1993. **13**(8): p. 4736-44.
117. Ron, D. and J.F. Habener, *CHOP, a novel developmentally regulated nuclear protein that dimerizes with transcription factors C/EBP and LAP and functions as a dominant-negative inhibitor of gene transcription.* Genes Dev, 1992. **6**(3): p. 439-53.
118. Gossen, M. and H. Bujard, *Tight control of gene expression in mammalian cells by tetracycline-responsive promoters.* Proc Natl Acad Sci U S A, 1992. **89**(12): p. 5547-51.
119. Fornace, A.J., Jr., I. Alamo, Jr., and M.C. Hollander, *DNA damage-inducible transcripts in mammalian cells.* Proc Natl Acad Sci U S A, 1988. **85**(23): p. 8800-4.
120. Bruhat, A., et al., *Amino acid limitation induces expression of CHOP, a CCAAT/enhancer binding protein-related gene, at both transcriptional and post-transcriptional levels.* J Biol Chem, 1997. **272**(28): p. 17588-93.
121. Marten, N.W., et al., *Effect of amino acid limitation on the expression of 19 genes in rat hepatoma cells.* FASEB J, 1994. **8**(8): p. 538-44.
122. Choi, A.M., et al., *Cell growth inhibition by prostaglandin A2 results in elevated expression of gadd153 mRNA.* Exp Cell Res, 1992. **199**(1): p. 85-9.
123. Price, B.D. and S.K. Calderwood, *Gadd45 and Gadd153 messenger RNA levels are increased during hypoxia and after exposure of cells to agents which elevate the levels of the glucose-regulated proteins.* Cancer Res, 1992. **52**(13): p. 3814-7.

124. Sylvester, S.L., et al., *Induction of GADD153, a CCAAT/enhancer-binding protein (C/EBP)-related gene, during the acute phase response in rats. Evidence for the involvement of C/EBPs in regulating its expression.* J Biol Chem, 1994. **269**(31): p. 20119-25.
125. Wang, X.Z., et al., *Signals from the stressed endoplasmic reticulum induce C/EBP-homologous protein (CHOP/GADD153).* Mol Cell Biol, 1996. **16**(8): p. 4273-80.
126. Chen, Q., et al., *Activation of the growth arrest and DNA damage-inducible gene gadd 153 by nephrotoxic cysteine conjugates and dithiothreitol.* J Biol Chem, 1992. **267**(12): p. 8207-12.
127. Ubeda, M., et al., *Stress-induced binding of the transcriptional factor CHOP to a novel DNA control element.* Mol Cell Biol, 1996. **16**(4): p. 1479-89.
128. Bartlett, J.D., et al., *Calcium ionophore A23187 induces expression of the growth arrest and DNA damage inducible CCAAT/enhancer-binding protein (C/EBP)-related gene, gadd153. Ca2+ increases transcriptional activity and mRNA stability.* J Biol Chem, 1992. **267**(28): p. 20465-70.
129. Gately, D.P. and S.B. Howell, *Paclitaxel activation of the GADD153 promoter through a cellular injury response element containing an essential Sp1 binding site.* J Biol Chem, 1996. **271**(34): p. 20588-93.
130. Bruhat, A., et al., *Amino acids control mammalian gene transcription: activating transcription factor 2 is essential for the amino acid responsiveness of the CHOP promoter.* Mol Cell Biol, 2000. **20**(19): p. 7192-204.
131. Yamazaki, T., et al., *Regulation of the human CHOP gene promoter by the stress response transcription factor ATF5 via the AARE1 site in human hepatoma HepG2 cells.* Life Sci, 2010. **87**(9-10): p. 294-301.
132. Gujuluva, C.N., et al., *Effect of UV-irradiation on cell cycle, viability and the expression of p53, gadd153 and gadd45 genes in normal and HPV-immortalized human oral keratinocytes.* Oncogene, 1994. **9**(7): p. 1819-27.
133. Zou, W., et al., *Coupling of endoplasmic reticulum stress to CDDO-Me-induced up-regulation of death receptor 5 via a CHOP-dependent mechanism involving JNK activation.* Cancer Res, 2008. **68**(18): p. 7484-92.
134. Calfon, M., et al., *IRE1 couples endoplasmic reticulum load to secretory capacity by processing the XBP-1 mRNA.* Nature, 2002. **415**(6867): p. 92-6.
135. Yoshida, H., et al., *ATF6 activated by proteolysis binds in the presence of NF-Y (CBF) directly to the cis-acting element responsible for the mammalian unfolded protein response.* Mol Cell Biol, 2000. **20**(18): p. 6755-67.
136. Shi, Y., et al., *Identification and characterization of pancreatic eukaryotic initiation factor 2 alpha-subunit kinase, PEK, involved in translational control.* Mol Cell Biol, 1998. **18**(12): p. 7499-509.
137. Yamaguchi, Y., et al., *Endoplasmic reticulum (ER) chaperone regulation and survival of cells compensating for deficiency in the ER stress response kinase, PERK.* J Biol Chem, 2008. **283**(25): p. 17020-9.
138. Hühn, M., *Endoplasmic Reticulum (ER)-stress signalling in the alveolar epithelium*, in *Faculties of Veterinary Medicine and Medicine*. 2012, Justus Liebig University Giessen Giessen. p. 191.
139. Averous, J., et al., *Induction of CHOP expression by amino acid limitation requires both ATF4 expression and ATF2 phosphorylation.* J Biol Chem, 2004. **279**(7): p. 5288-97.
140. Sawada, T., et al., *X-box binding protein 1 regulates brain natriuretic peptide through a novel AP1/CRE-like element in cardiomyocytes.* J Mol Cell Cardiol, 2010. **48**(6): p. 1280-9.
141. Olivares, S., R.M. Green, and A.S. Henkel, *Endoplasmic reticulum stress activates the hepatic activator protein 1 complex via mitogen activated protein kinase-dependent signaling pathways.* PLoS One, 2014. **9**(7): p. e103828.
142. Cho, H.K., et al., *HBx induces the proliferation of hepatocellular carcinoma cells via AP1 over-expressed as a result of ER stress.* Biochem J, 2015. **466**(1): p. 115-21.

143. Dong, L., et al., *Ets-1 mediates upregulation of Mcl-1 downstream of XBP-1 in human melanoma cells upon ER stress.* Oncogene, 2011. **30**(34): p. 3716-26.
144. Selimovic, D., et al., *Bortezomib/proteasome inhibitor triggers both apoptosis and autophagy-dependent pathways in melanoma cells.* Cell Signal, 2013. **25**(1): p. 308-18.
145. Guyton, K.Z., Q. Xu, and N.J. Holbrook, *Induction of the mammalian stress response gene GADD153 by oxidative stress: role of AP-1 element.* Biochem J, 1996. **314 (Pt 2)**: p. 547-54.
146. Seth, A., et al., *Regulation of the human stress response gene GADD153 expression: role of ETS1 and FLI-1 gene products.* Cell Death Differ, 1999. **6**(9): p. 902-7.
147. Bergelson, S., R. Pinkus, and V. Daniel, *Intracellular glutathione levels regulate Fos/Jun induction and activation of glutathione S-transferase gene expression.* Cancer Res, 1994. **54**(1): p. 36-40.
148. Bergelson, S. and V. Daniel, *Cooperative interaction between Ets and AP-1 transcription factors regulates induction of glutathione S-transferase Ya gene expression.* Biochem Biophys Res Commun, 1994. **200**(1): p. 290-7.
149. Bassuk, A.G. and J.M. Leiden, *A direct physical association between ETS and AP-1 transcription factors in normal human T cells.* Immunity, 1995. **3**(2): p. 223-37.
150. Logan, S.K., et al., *Synergistic transcriptional activation of the tissue inhibitor of metalloproteinases-1 promoter via functional interaction of AP-1 and Ets-1 transcription factors.* J Biol Chem, 1996. **271**(2): p. 774-82.
151. Barone, M.V., et al., *CHOP (GADD153) and its oncogenic variant, TLS-CHOP, have opposing effects on the induction of G1/S arrest.* Genes Dev, 1994. **8**(4): p. 453-64.
152. Matsumoto, M., et al., *Ectopic expression of CHOP (GADD153) induces apoptosis in M1 myeloblastic leukemia cells.* FEBS Lett, 1996. **395**(2-3): p. 143-7.
153. Friedman, A.D., *GADD153/CHOP, a DNA damage-inducible protein, reduced CAAT/enhancer binding protein activities and increased apoptosis in 32D c13 myeloid cells.* Cancer Res, 1996. **56**(14): p. 3250-6.
154. Eymin, B., et al., *Increased gadd153 messenger RNA level is associated with apoptosis in human leukemic cells treated with etoposide.* Cancer Res, 1997. **57**(4): p. 686-95.
155. Brenner, B., et al., *Fas- or ceramide-induced apoptosis is mediated by a Rac1-regulated activation of Jun N-terminal kinase/p38 kinases and GADD153.* J Biol Chem, 1997. **272**(35): p. 22173-81.
156. Oyadomari, S. and M. Mori, *Roles of CHOP/GADD153 in endoplasmic reticulum stress.* Cell Death Differ, 2004. **11**(4): p. 381-9.
157. Feng, B., et al., *The endoplasmic reticulum is the site of cholesterol-induced cytotoxicity in macrophages.* Nat Cell Biol, 2003. **5**(9): p. 781-92.
158. Devries-Seimon, T., et al., *Cholesterol-induced macrophage apoptosis requires ER stress pathways and engagement of the type A scavenger receptor.* J Cell Biol, 2005. **171**(1): p. 61-73.
159. Hagimoto, N., et al., *Induction of apoptosis and pulmonary fibrosis in mice in response to ligation of Fas antigen.* Am J Respir Cell Mol Biol, 1997. **17**(3): p. 272-8.
160. Uhal, B.D., et al., *Alveolar epithelial cell death adjacent to underlying myofibroblasts in advanced fibrotic human lung.* Am J Physiol, 1998. **275**(6 Pt 1): p. L1192-9.
161. Barbas-Filho, J.V., et al., *Evidence of type II pneumocyte apoptosis in the pathogenesis of idiopathic pulmonary fibrosis (IFP)/usual interstitial pneumonia (UIP).* J Clin Pathol, 2001. **54**(2): p. 132-8.
162. Plataki, M., et al., *Expression of apoptotic and antiapoptotic markers in epithelial cells in idiopathic pulmonary fibrosis.* Chest, 2005. **127**(1): p. 266-74.
163. Kuwano, K., et al., *Mitochondria-mediated apoptosis of lung epithelial cells in idiopathic interstitial pneumonias.* Lab Invest, 2002. **82**(12): p. 1695-706.
164. Kuwano, K., et al., *The involvement of Fas-Fas ligand pathway in fibrosing lung diseases.* Am J Respir Cell Mol Biol, 1999. **20**(1): p. 53-60.

165. Maeyama, T., et al., *Upregulation of Fas-signalling molecules in lung epithelial cells from patients with idiopathic pulmonary fibrosis.* Eur Respir J, 2001. **17**(2): p. 180-9.
166. Mahavadi, P., et al., *Epithelial stress and apoptosis underlie Hermansky-Pudlak syndrome-associated interstitial pneumonia.* Am J Respir Crit Care Med, 2010. **182**(2): p. 207-19.
167. Cha SI, R.C., Lee JS, Kukreja J, Barry SS, Jones KD, Elicker BM, Kim DS, Papa FR, Collard HR, Wolters PJ., *Cleaved cytokeratin-18 is a mechanistically informative biomarker in idiopathic pulmonary fibrosis.* Respir Res, 2012. **13**(105).
168. Korfei M, S.S., Ruppert C, Henneke I, Markart P, Loeh B, Mahavadi P, Wygrecka M, Klepetko W, Fink L, Bonniaud P, Preissner KT, Lochnit G, Schaefer L, Seeger W, Guenther A, *Comparative proteomic analysis of lung tissue from patients with idiopathic pulmonary fibrosis (IPF) and lung transplant donor lungs.* J Proteome Res, 2011. **10**(5): p. 2185-205.
169. Korfei M, v.d.B.D., Henneke I, Markart P, Ruppert C, Mahavadi P, Ghanim B, Klepetko W, Fink L, Meiners S, Krämer OH, Seeger W, Vancheri C, Guenther A., *Comparative proteome analysis of lung tissue from patients with idiopathic pulmonary fibrosis (IPF), non-specific interstitial pneumonia (NSIP) and organ donors.* J Proteomics., 2013. **24**.
170. Nakatani, Y., et al., *Interstitial pneumonia in Hermansky-Pudlak syndrome: significance of florid foamy swelling/degeneration (giant lamellar body degeneration) of type-2 pneumocytes.* Virchows Arch, 2000. **437**(3): p. 304-13.
171. Mahavadi, P., A. Guenther, and B.R. Gochuico, *Hermansky-Pudlak syndrome interstitial pneumonia: it's the epithelium, stupid!* Am J Respir Crit Care Med, 2012. **186**(10): p. 939-40.
172. Brush, M.H., D.C. Weiser, and S. Shenolikar, *Growth arrest and DNA damage-inducible protein GADD34 targets protein phosphatase 1 alpha to the endoplasmic reticulum and promotes dephosphorylation of the alpha subunit of eukaryotic translation initiation factor 2.* Mol Cell Biol, 2003. **23**(4): p. 1292-303.
173. Yagi, A., et al., *GADD34 induces p53 phosphorylation and p21/WAF1 transcription.* J Cell Biochem, 2003. **90**(6): p. 1242-9.
174. Shi, W., et al., *GADD34-PP1c recruited by Smad7 dephosphorylates TGFbeta type I receptor.* J Cell Biol, 2004. **164**(2): p. 291-300.
175. Akram, K.M., et al., *Alveolar epithelial cells in idiopathic pulmonary fibrosis display upregulation of TRAIL, DR4 and DR5 expression with simultaneous preferential over-expression of pro-apoptotic marker p53.* Int J Clin Exp Pathol, 2014. **7**(2): p. 552-64.
176. Gotoh, T., et al., *hsp70-DnaJ chaperone pair prevents nitric oxide- and CHOP-induced apoptosis by inhibiting translocation of Bax to mitochondria.* Cell Death Differ, 2004. **11**(4): p. 390-402.
177. Crapo, J.D., *Oxidative stress as an initiator of cytokine release and cell damage.* Eur Respir J Suppl, 2003. **44**: p. 4s-6s.
178. Griffith, B., et al., *NOX enzymes and pulmonary disease.* Antioxid Redox Signal, 2009. **11**(10): p. 2505-16.
179. Kinnula, V.L. and J.D. Crapo, *Superoxide dismutases in the lung and human lung diseases.* Am J Respir Crit Care Med, 2003. **167**(12): p. 1600-19.
180. Kinnula, V.L., et al., *Oxidative stress in pulmonary fibrosis: a possible role for redox modulatory therapy.* Am J Respir Crit Care Med, 2005. **172**(4): p. 417-22.
181. Cantin, A.M., et al., *Oxidant-mediated epithelial cell injury in idiopathic pulmonary fibrosis.* J Clin Invest, 1987. **79**(6): p. 1665-73.
182. Strausz, J., et al., *Oxygen radical production by alveolar inflammatory cells in idiopathic pulmonary fibrosis.* Am Rev Respir Dis, 1990. **141**(1): p. 124-8.
183. Waghray, M., et al., *Hydrogen peroxide is a diffusible paracrine signal for the induction of epithelial cell death by activated myofibroblasts.* FASEB J, 2005. **19**(7): p. 854-6.

184. Wallach-Dayan, S.B., et al., *Bleomycin initiates apoptosis of lung epithelial cells by ROS but not by Fas/FasL pathway.* Am J Physiol Lung Cell Mol Physiol, 2006. **290**(4): p. L790-L796.
185. Markart, P., et al., *Alveolar oxidative stress is associated with elevated levels of nonenzymatic low-molecular-weight antioxidants in patients with different forms of chronic fibrosing interstitial lung diseases.* Antioxid Redox Signal, 2009. **11**(2): p. 227-40.
186. Delaunay-Moisan, A. and C. Appenzeller-Herzog, *The antioxidant machinery of the endoplasmic reticulum: Protection and signaling.* Free Radic Biol Med, 2015. **83**: p. 341-51.
187. Palm, F. and L. Nordquist, *Renal oxidative stress, oxygenation, and hypertension.* Am J Physiol Regul Integr Comp Physiol, 2011. **301**(5): p. R1229-41.
188. Poli, G., *Pathogenesis of liver fibrosis: role of oxidative stress.* Mol Aspects Med, 2000. **21**(3): p. 49-98.
189. Cullinan, S.B., et al., *Nrf2 is a direct PERK substrate and effector of PERK-dependent cell survival.* Mol Cell Biol, 2003. **23**(20): p. 7198-209.
190. Harding, H.P., et al., *An integrated stress response regulates amino acid metabolism and resistance to oxidative stress.* Mol Cell, 2003. **11**(3): p. 619-33.
191. Hagimoto, N., et al., *TGF-beta 1 as an enhancer of Fas-mediated apoptosis of lung epithelial cells.* J Immunol, 2002. **168**(12): p. 6470-8.
192. Willis, B.C., et al., *Induction of epithelial-mesenchymal transition in alveolar epithelial cells by transforming growth factor-beta1: potential role in idiopathic pulmonary fibrosis.* Am J Pathol, 2005. **166**(5): p. 1321-32.
193. Kolb, M., et al., *Transient expression of IL-1beta induces acute lung injury and chronic repair leading to pulmonary fibrosis.* J Clin Invest, 2001. **107**(12): p. 1529-36.
194. Hoshino, T., et al., *Role of proinflammatory cytokines IL-18 and IL-1beta in bleomycin-induced lung injury in humans and mice.* Am J Respir Cell Mol Biol, 2009. **41**(6): p. 661-70.
195. Liu, X., et al., *The CC chemokine ligand 2 (CCL2) mediates fibroblast survival through IL-6.* Am J Respir Cell Mol Biol, 2007. **37**(1): p. 121-8.
196. Rath, E., et al., *Induction of dsRNA-activated protein kinase links mitochondrial unfolded protein response to the pathogenesis of intestinal inflammation.* Gut, 2012. **61**(9): p. 1269-78.
197. Endo M, O.S., Suga M, Mori M, Gotoh T., *The ER stress pathway involving CHOP is activated in the lungs of LPS-treated mice.* J Biochem, 2005. **138**(4): p. 501-7
198. Kayagaki N, W.S., Lamkanfi M, Vande Walle L, Louie S, Dong J, Newton K, Qu Y, Liu J, Heldens S, Zhang J, Lee WP, Roose-Girma M, Dixit VM., *Non-canonical inflammasome activation targets caspase-11.* Nature, 2011. **479**(7371): p. 117-21.
199. Kim SR, K.D., Kang MR, Lee KS, Park SY, Jeong JS, Lee YC., *Endoplasmic reticulum stress influences bronchial asthma pathogenesis by modulating nuclear factor κB activation.* J Allergy Clin Immunol., 2013. **132**(6): p. 1397-408.
200. Nakayama Y, E.M., Tsukano H, Mori M, Oike Y, Gotoh T., *Molecular mechanisms of the LPS-induced non-apoptotic ER stress-CHOP pathway.* J Biochem, 2010. **147**(4): p. 471-83.
201. Gao H, S.R., *C/EBPzeta (CHOP/Gadd153) is a negative regulator of LPS-induced IL-6 expression in B cells.* Mol Immunol, 2009. **47**(2-3): p. 390-7.
202. Tanaka, Y., et al., *The exacerbating roles of CCAAT/enhancer-binding protein homologous protein (CHOP) in the development of bleomycin-induced pulmonary fibrosis and the preventive effects of tauroursodeoxycholic acid (TUDCA) against pulmonary fibrosis in mice.* Pharmacol Res, 2015. **99**: p. 52-62.
203. Scotton, C.J. and R.C. Chambers, *Molecular targets in pulmonary fibrosis: the myofibroblast in focus.* Chest, 2007. **132**(4): p. 1311-21.
204. Klingberg, F., B. Hinz, and E.S. White, *The myofibroblast matrix: implications for tissue repair and fibrosis.* J Pathol, 2013. **229**(2): p. 298-309.

205. Ramos, C., et al., *Fibroblasts from idiopathic pulmonary fibrosis and normal lungs differ in growth rate, apoptosis, and tissue inhibitor of metalloproteinases expression.* Am J Respir Cell Mol Biol, 2001. **24**(5): p. 591-8.
206. Li, Y., et al., *Severe lung fibrosis requires an invasive fibroblast phenotype regulated by hyaluronan and CD44.* J Exp Med, 2011. **208**(7): p. 1459-71.
207. Xu, Y.D., et al., *Release of biologically active TGF-beta1 by alveolar epithelial cells results in pulmonary fibrosis.* Am J Physiol Lung Cell Mol Physiol, 2003. **285**(3): p. L527-39.
208. Bergeron, A., et al., *Cytokine profiles in idiopathic pulmonary fibrosis suggest an important role for TGF-beta and IL-10.* Eur Respir J, 2003. **22**(1): p. 69-76.
209. Cool, C.D., et al., *Fibroblast foci are not discrete sites of lung injury or repair: the fibroblast reticulum.* Am J Respir Crit Care Med, 2006. **174**(6): p. 654-8.
210. Kulasekaran, P., et al., *Endothelin-1 and transforming growth factor-beta1 independently induce fibroblast resistance to apoptosis via AKT activation.* Am J Respir Cell Mol Biol, 2009. **41**(4): p. 484-93.
211. Chauncey, J.B., M. Peters-Golden, and R.H. Simon, *Arachidonic acid metabolism by rat alveolar epithelial cells.* Lab Invest, 1988. **58**(2): p. 133-40.
212. Wilborn, J., et al., *Cultured lung fibroblasts isolated from patients with idiopathic pulmonary fibrosis have a diminished capacity to synthesize prostaglandin E2 and to express cyclooxygenase-2.* J Clin Invest, 1995. **95**(4): p. 1861-8.
213. Elias, J.A., et al., *Human alveolar macrophage inhibition of lung fibroblast growth. A prostaglandin-dependent process.* Am Rev Respir Dis, 1985. **131**(1): p. 94-9.
214. Huang, S., et al., *Prostaglandin E(2) inhibits collagen expression and proliferation in patient-derived normal lung fibroblasts via E prostanoid 2 receptor and cAMP signaling.* Am J Physiol Lung Cell Mol Physiol, 2007. **292**(2): p. L405-13.
215. White, E.S., et al., *Prostaglandin E(2) inhibits fibroblast migration by E-prostanoid 2 receptor-mediated increase in PTEN activity.* Am J Respir Cell Mol Biol, 2005. **32**(2): p. 135-41.
216. Garrison, G., et al., *Reversal of myofibroblast differentiation by prostaglandin E(2).* Am J Respir Cell Mol Biol, 2013. **48**(5): p. 550-8.
217. Moore, B.B., et al., *Alveolar epithelial cell inhibition of fibroblast proliferation is regulated by MCP-1/CCR2 and mediated by PGE2.* Am J Physiol Lung Cell Mol Physiol, 2003. **284**(2): p. L342-9.
218. Lama, V., et al., *Prostaglandin E2 synthesis and suppression of fibroblast proliferation by alveolar epithelial cells is cyclooxygenase-2-dependent.* Am J Respir Cell Mol Biol, 2002. **27**(6): p. 752-8.
219. Maher, T.M., et al., *Diminished prostaglandin E2 contributes to the apoptosis paradox in idiopathic pulmonary fibrosis.* Am J Respir Crit Care Med, 2010. **182**(1): p. 73-82.
220. Mercer, P.F., et al., *Pulmonary epithelium is a prominent source of proteinase-activated receptor-1-inducible CCL2 in pulmonary fibrosis.* Am J Respir Crit Care Med, 2009. **179**(5): p. 414-25.
221. Scotton, C.J., et al., *Increased local expression of coagulation factor X contributes to the fibrotic response in human and murine lung injury.* J Clin Invest, 2009. **119**(9): p. 2550-63.
222. Ayala, P., et al., *Attenuation of endoplasmic reticulum stress using the chemical chaperone 4-phenylbutyric acid prevents cardiac fibrosis induced by isoproterenol.* Exp Mol Pathol, 2012. **92**(1): p. 97-104.
223. Kassan, M., et al., *Endoplasmic reticulum stress is involved in cardiac damage and vascular endothelial dysfunction in hypertensive mice.* Arterioscler Thromb Vasc Biol, 2012. **32**(7): p. 1652-61.
224. Heazlewood, C.K., et al., *Aberrant mucin assembly in mice causes endoplasmic reticulum stress and spontaneous inflammation resembling ulcerative colitis.* PLoS Med, 2008. **5**(3): p. e54.

225. Lund, P.K. and R.J. Rigby, *What are the mechanisms of fibrosis in IBD?* Inflamm Bowel Dis, 2008. **14 Suppl 2**: p. S127-8.
226. Cybulsky, A.V., et al., *Complement C5b-9 membrane attack complex increases expression of endoplasmic reticulum stress proteins in glomerular epithelial cells.* J Biol Chem, 2002. **277**(44): p. 41342-51.
227. Kimura, K., et al., *Dysfunction of the ER chaperone BiP accelerates the renal tubular injury.* Biochem Biophys Res Commun, 2008. **366**(4): p. 1048-53.
228. Mimura, N., et al., *Aberrant quality control in the endoplasmic reticulum impairs the biosynthesis of pulmonary surfactant in mice expressing mutant BiP.* Cell Death Differ, 2007. **14**(8): p. 1475-85.
229. Ohse, T., et al., *Albumin induces endoplasmic reticulum stress and apoptosis in renal proximal tubular cells.* Kidney Int, 2006. **70**(8): p. 1447-55.
230. Pallet, N., et al., *Cyclosporine-induced endoplasmic reticulum stress triggers tubular phenotypic changes and death.* Am J Transplant, 2008. **8**(11): p. 2283-96.
231. Pfaffenbach, K.T., et al., *Linking endoplasmic reticulum stress to cell death in hepatocytes: roles of C/EBP homologous protein and chemical chaperones in palmitate-mediated cell death.* Am J Physiol Endocrinol Metab, 2010. **298**(5): p. E1027-35.
232. Tamaki, N., et al., *CHOP deficiency attenuates cholestasis-induced liver fibrosis by reduction of hepatocyte injury.* Am J Physiol Gastrointest Liver Physiol, 2008. **294**(2): p. G498-505.
233. Castriotta, R.J., et al., *Workshop on idiopathic pulmonary fibrosis in older adults.* Chest, 2010. **138**(3): p. 693-703.
234. Selman, M., et al., *Aging and interstitial lung diseases: unraveling an old forgotten player in the pathogenesis of lung fibrosis.* Semin Respir Crit Care Med, 2010. **31**(5): p. 607-17.
235. Naidoo, N., et al., *Aging impairs the unfolded protein response to sleep deprivation and leads to proapoptotic signaling.* J Neurosci, 2008. **28**(26): p. 6539-48.
236. Torres-Gonzalez, E., et al., *Role of endoplasmic reticulum stress in age-related susceptibility to lung fibrosis.* Am J Respir Cell Mol Biol, 2012. **46**(6): p. 748-56.
237. van der Vlies, D., J. Woudenberg, and J.A. Post, *Protein oxidation in aging: endoplasmic reticulum as a target.* Amino Acids, 2003. **25**(3-4): p. 397-407.
238. Puzianowska-Kuznicka, M. and J. Kuznicki, *The ER and ageing II: calcium homeostasis.* Ageing Res Rev, 2009. **8**(3): p. 160-72.
239. Citrin, D.E., et al., *Role of type II pneumocyte senescence in radiation-induced lung fibrosis.* J Natl Cancer Inst, 2013. **105**(19): p. 1474-84.
240. Colavitti, R. and T. Finkel, *Reactive oxygen species as mediators of cellular senescence.* IUBMB Life, 2005. **57**(4-5): p. 277-81.
241. Shivshankar, P., et al., *Caveolin-1 deficiency protects from pulmonary fibrosis by modulating epithelial cell senescence in mice.* Am J Respir Cell Mol Biol, 2012. **47**(1): p. 28-36.
242. Aoshiba, K., T. Tsuji, and A. Nagai, *Bleomycin induces cellular senescence in alveolar epithelial cells.* Eur Respir J, 2003. **22**(3): p. 436-43.
243. Driscoll, B., et al., *Telomerase in alveolar epithelial development and repair.* Am J Physiol Lung Cell Mol Physiol, 2000. **279**(6): p. L1191-8.
244. Waisberg, D.R., et al., *Abnormal expression of telomerase/apoptosis limits type II alveolar epithelial cell replication in the early remodeling of usual interstitial pneumonia/idiopathic pulmonary fibrosis.* Hum Pathol, 2010. **41**(3): p. 385-91.
245. Mondello, C. and A.I. Scovassi, *Telomeres, telomerase, and apoptosis.* Biochem Cell Biol, 2004. **82**(4): p. 498-507.

8 Declaration

“I declare that I have completed this dissertation single-handedly without the unauthorized help of a second party and only with the assistance acknowledged therein. I have appropriately acknowledged and referenced all text passages that are derived literally from or are based on the content of published or unpublished work of others, and all information that relates to verbal communications. I have abided by the principles of good scientific conduct laid down in the charter of the Justus Liebig University of Giessen in carrying out the investigations described in the dissertation.”

Place and Date

Signature

9 Acknowledgements

In the last chapter of my thesis, I would like to express my sincere acknowledgements to all those who have encouraged me with their support and suggestions during my PhD.

I would like to thank Prof. Dr. Werner Seeger for his insight into science and life areas, which, in his eyes, essentially exist together in a very productive and friendly relationship and also for accepting me into “Molecular Biology and Medicine of the Lung” programme. I would like to thank Dr. Rory Morty for teaching me of so many new technics of molecular biology as well as lung biology.

I would like to express my sincere gratitude to my supervisor, Prof. Dr. Andreas Guenther for giving me the opportunity to work in his laboratory. I thank him especially for his expertise and research insights. I am eternally grateful for his guidance, encouragement, and patience throughout my PhD project. During this time, Prof. Dr. Andreas Guenther has given me the opportunity to participate in various international conferences. Moreover, thanks to him I gained invaluable knowledge and experience not only how to deal with experiments but also how to deal with people in various situations.

My deep gratitude goes to Dr. Martina Korfei, without her and her ideas my project would not exist. Thanks to Dr. Martina Korfei I managed to develop scientific thinking and I learned how to work in a team and absolutely independently. Thank you for helping me during my work as well as motivating me learn more in scientific field. I will never forget all scientific and social experience which I got from Dr. Martina Korfei.

I want to thank all the members of my laboratory. You created a group, which was wonderful because of diversity, sometimes this diversity created problems, nevertheless in hard times we were able to solidarize.

Finally, I would like to thank my friends and family for their great support. Without them, my life in Giessen would not be possible. Especially I want to say many thanks to my the best friend Dr. Maryna Balvinska for her understanding, motivation and support in difficult situations.

Der Lebenslauf wurde aus der elektronischen Version der Arbeit entfernt.

The curriculum vitae was removed from the electronic version of the paper.